ÇUKUROVA UNIVERSITY
INSTITUTE OF NATURAL APPLIED SCIENCES

PhD THESIS

Mehmet BİLGİLİ

PREDICTIONS OF WIND SPEED AND WIND POWER POTENTIAL USING ARTIFICIAL NEURAL NETWORKS

DEPARTMENT OF MECHANICAL ENGINEERING

ADANA, 2007

ÇUKUROVA ÜNİVERSİTESİ
FEN BİLİMLERİ ENSTİTÜSÜ

PREDICTIONS OF WIND SPEED AND WIND POWER POTENTIAL USING ARTIFICIAL NEURAL NETWORKS

Mehmet BİLGİLİ

DOKTORA TEZİ

MAKİNA MÜHENDİSLİĞİ ANABİLİM DALI

Bu tez …/…/2007 Tarihinde Aşağıdaki Jüri Üyeleri Tarafından Oybirliği ile Kabul Edilmiştir.

İmza:……………….	İmza:………………	İmza:……………………………..
Prof.Dr.Beşir ŞAHİN	Prof.Dr.Erdem KOÇ	Prof.Dr.Ertuğrul BALTACIOĞLU
DANIŞMAN	ÜYE	ÜYE

İmza:……………………	İmza:……………………….
Doç.Dr.Hüseyin AKILLI	Doç.Dr.Ahmet PINARBAŞI
ÜYE	ÜYE

Bu Tez Enstitümüz Makine Mühendisliği Anabilim Dalında Hazırlanmıştır.
Kod No:

Prof. Dr. Aziz ERTUNÇ
Enstitü Müdürü
İmza Mühür

Bu çalışma Ç. Ü. Araştırma Projeleri Birimi tarafından desteklenmiştir.
Proje No: MMF2006D18

Not: Bu tezde kullanılan özgün ve başka kaynaktan yapılan bildirişlerin, çizelge, şekil ve fotoğrafların kaynak gösterilmeden kullanımı, 5846 sayılı Fikir v Sanat Eserleri Kanunundaki hükümlere tabidir.

ABSTRACT

PhD THESIS

PREDICTIONS OF WIND SPEED AND WIND POWER POTENTIAL USING ARTIFICIAL NEURAL NETWORKS

Mehmet BİLGİLİ

DEPARTMENT OF MECHANICAL ENGINEERING
INSTITUTE OF NATURAL APPLIED SCIENCES
ÇUKUROVA UNIVERSITY

Supervisor : Prof.Dr. Beşir ŞAHİN
Year : 2007, Pages: 193
Jury : Prof.Dr. Erdem KOÇ
Prof.Dr. Ertuğrul BALTACIOĞLU
Assoc.Prof.Dr. Hüseyin AKILLI
Assoc.Prof.Dr. Ahmet PINARBAŞI

In this study, wind power density in the southern and southwestern region of Turkey was determined by using the Weibull and Rayleigh probability density functions and the Wind Atlas Analysis and Application Program (WAsP). Moreover, wind speed of a target station was predicted using wind speeds of reference stations and other meteorological parameters with the artificial neural networks (ANNs) method. ANNs were also applied to predict the long term monthly temperature and rainfall at any specific point of Turkey based on the use of the neighboring measuring stations data. The wind data taken with an interval of one hour were measured by the General Directorate of Electrical Power Resources Survey Administration (EIE) at 9 measuring stations such as Akhisar, Belen, Datça, Gelendost, Söke, Gökçeada, Foca, Gelibolu and Bababurnu. The long-term wind data, containing hourly wind speeds and directions, cover the period from the year 1998 to 2003. Wind speeds of reference stations and other meteorological parameters were used as an input neurons in the ANN architecture, while the target station wind speed was used as an output neuron in the ANN architecture. In MATLAB, different artificial neural network learning algorithms have been used to establish the ANN models. The results obtained with these models were compared with the actual data. Comparisons have shown that there was a good agreement between predicted and measured data. Errors obtained in these models are well within acceptable limits.

Keywords: Artificial neural networks, Meteorological parameters, Reference station, Target station, Wind speed.

ÖZ

DOKTORA TEZİ

YAPAY SİNİR AĞLARI İLE RÜZGAR HIZI VE RÜZGAR GÜCÜ POTANSİYELİ TAHMİNLERİ

Mehmet BİLGİLİ

ÇUKUROVA ÜNİVERSİTESİ
FEN BİLİMLERİ ENSTİTÜSÜ
MAKİNA MÜHENDİSLİĞİ ANABİLİM DALI

Danışman : Prof.Dr. Beşir ŞAHİN
Yıl : 2007, Sayfa: 193
Jüri : Prof.Dr. Erdem KOÇ
Prof.Dr. Ertuğrul BALTACIOĞLU
Doç.Dr. Hüseyin AKILLI
Doç.Dr. Ahmet PINARBAŞI

Bu çalışmada, Türkiye'nin güney ve güneybatı bölgesindeki rüzgar gücü potansiyeli, Weibull ve Rayleigh olasılık yoğunluğu fonksiyonları ve "Wind Atlas Analysis and Application" Programı (WAsP) kullanılarak hesaplanmıştır. Ayrıca, bir hedef istasyonun rüzgar hızı, etrafını çevreleyen referans istasyonların rüzgar hızlarından ve diğer meteorolojik parametrelerinden faydalanılarak yapay sinir ağları (YSA) yöntemi ile tahmin edilmiştir. Bundan başka, YSA, Türkiye'nin herhangi bir özel noktasındaki ortalama sıcaklık ve yağmur parametrelerini, etrafını çevreleyen referans istasyonların değerlerinden faydalanarak tahmin etmek için uygulanmıştır. Bir saat aralıklarla alınan rüzgar hızı dataları, Elektrik İşleri Etüt İdaresi (EİE) tarafından Akhisar, Belen, Datça, Gelendost, Söke, Gökçeada, Foca, Gelibolu ve Bababurnu gibi 9 ayrı rüzgar ölçüm istasyonlarından elde edilmiştir. Saatlik rüzgar hızları ve yön bilgilerini içeren datalar 1998 ile 2003 yılları arasını kapsamaktadır. Referans istasyonlar olarak kabul edilen istasyonların rüzgar hızı dataları ve diğer meteorolojik parametreler oluşturulan yapay sinir ağının giriş katmanında kullanılırken, hedef istasyon olarak kabul edilen istasyonun rüzgar hızı değeri yapay sinir ağının çıkış katmanında kullanılmıştır. MATLAB programında, farklı yapay sinir ağı öğrenme algoritmaları kullanılarak bir tahmin modeli oluşturulmuş ve elde edilen sonuçlar ile gerçek değerler karşılaştırılmıştır. Bunun sonucunda bulunan hata değerlerinin kabul edilebilir sınırlar içerisinde olduğu görülmüştür.

Anahtar Kelimeler: Hedef istasyon, Meteorolojik parametreler, Referans istasyon, Rüzgar hızı, Yapay sinir ağları.

ACKNOWLEDGEMENTS

The list is endless if I have to thank all the people that made possible this work. My first and sincere thanks goes to my advisor Prof. Dr. Beşir ŞAHİN for his support, guidance and encouragement. He showed me what I thought nobody could really do: that there are no limits on what we can achieve. Thanks, from the bottom of my heart.

I would like to thank Prof. Dr. Erdem KOÇ for his technical support, guidance, and dedication throughout the preparation of this thesis. Knowing and feeling his support during my PhD thesis helped me a lot to my self-confidence.

I am grateful to Assist. Prof. Dr. Hüseyin AKILLI for his continues support, help, friendship and encouragement.

On a personal level many thanks go to Lecturer Yılmaz KOÇAK, Erdoğan ŞİMŞEK and Yusuf POLAT for their continuous moral support, motivation and friendship.

In addition, I would like to thank all the staff of Department of Mechanical Engineering at Çukurova University.

At last, but not least, I would like to thank my wife, Ferhunde. Finally, I would like to thank my daughter and son.

NOMENCLATURE

EIE	: Elektrik İşleri Etüd İdaresi
IEA	: International Energy Agency
TEK	: Türkiye Elektrik Kurumu
MENR	: Ministry of Energy and Natural Sources (Enerji ve Tabii Kaynaklar Bakanlığı)
TEAS	: Türkiye Elektrik Üretim-Iletim A.S.
TEDAS	: Türkiye Elektrik Dagitim A.S.
TEIAS	: Turkiye Elektrik Iletim A.S.
EUAS	: Elektrik Uretim A.S.
EPDK	: Enerji Piyasasi Duzenleme Kurumu
MTA	: Maden Tetkik ve Arama
BOTAŞ	: Boru Hatları ile Petrol Taşıma A.Ş.
ANN	: Artificial Neural Network
SCG	: Scaled Conjugate Gradient
LM	: Levenberg-Marquardt
CGP	: Pola-Ribiere Conjugate Gradient
RBFN	: Radial Basis Function Network
HFM	: Hopfield Model
MLP	: Multi-Layered Perceptron
ERNN	: Elman Recurrent Neural Network
SCCF	: Sample Cross Correlation Function
ARMA	: Aautoregressive moving average
ANFIS	: Adaptive Neuro-Fuzzy Inference Systems
SVM	: Support Vector Machines
PCA	: Principal Component Analysis
WAsP	: Wind Atlas Analysis and Application Program
TSMS	: Turkish State Meteorological Service
LMS	: Least Mean Square
RP	: Resilient Propagation

MLR	: Multiple Linear Regression
RPE	: Recursive Prediction Error
RMSE	: Root Mean Squared Error
MAPE	: Mean Absolute Percentage Error
MAE	: Mean Absolute Error
RSP	: Respirable Suspended Particulates
MATLAB	: Matris Laboratuarı
GWh	: Gigawatt hour
GW	: Gigawaat
MW	: Megawatt
p	: Total number of inputs
y	: Input signals
w	: Synaptic weights
u	: Linear combiner output
θ	: Threshold
$\varphi(.)$	: Activation function
$f(x)$	: Transfer function
n	: Iteration number
$d(n)$	: Desired response or target output
$e(n)$	: Error signal
$y(n)$	: Function signal appearing at the output of neuron
$E(n)$	: Instantaneous sum of squared errors of the network
$v(n)$	: Net internal activity level
$\Delta w_{ji}(n)$	: Correction
$\partial E(n)/\partial w_{ji}(n)$	: Instantaneous gradient
η	: Learning-rate parameter
$\delta_j(n)$	: Local gradient
a	: Unknown coefficient
y	: Dependent value
x	: Independent value

A	: Area (m^2)
c	: Weibull scale parameter (m/s)
$f(v)$	: Probability of measured wind speed
$f_W(v)$	: Weibull probability function
$f_R(v)$	: Rayleigh probability function
$F_W(v)$	: Cumulative Weibull probability function
$F_R(v)$	: Cumulative Rayleigh probability function
k	: Weibull shape parameter (dimensionless)
n	: Number of observations
$P(v)$	: Mean wind power density (W/m^2)
P_W	: Weibull mean wind power density (W/m^2)
P_R	: Rayleigh mean wind power density (W/m^2)
R	: Correlation coefficient
v	: Wind speed (m/s)
v_m	: Mean wind speed (m/s)
$\Gamma()$	: Gamma function
ρ	: Air density (kg/m^3)
σ	: Standard deviation (m/s)

TABLE OF CONTENTS **PAGE**

LIST OF TABLES **PAGE**

LIST OF FIGURES **PAGES**

1. INTRODUCTION

Turkey's geographical location stands as a natural land bridge connecting Europe to Asia. Therefore, it has increasingly important role to play as an "energy corridor" between the major oil and natural gas producing countries in the Middle East, Caspian Sea and the Western energy markets (IEA, 2005). Furthermore, Turkey, with a population of 65,311,000 in the year of 2000, has the highest population increasing rate, 1.4% among the Organization for the Economic Cooperation and Development (OECD) countries. In addition, Turkey's energy demand grows rapidly due to the social and economic development of the country and is expected to continue to grow in the near future (Kaya, 2006).

Energy is one of the most significant components in the economic development of countries. It is also certain that energy is the most important necessity of human life and hence there is an increasing relation between the level of development and amount of energy consumption. It is inevitably essential for the economic and social growths and an improved quality of life in Turkey, as in other countries. This situation makes energy resources significantly important for the whole world (Yılmaz and Uslu, 2007; Sözen and Arcaklıoğlu, 2007). Out of various energy sources, an electric power is considered to be a kind of energy source which can be used in variety of industry. In general, electricity is generated from the hydropower, thermal and nuclear power plants. It is known that the hydropower plants generate electricity by using generators driven by water turbines, operating by means of falling water from a certain elevation with a high rate of volume flow rate. Coal, oil or natural gas are used in the thermal power plants for generating electricity. Atomic fuels like uranium, thorium and plutonium are used in nuclear power plants. Other types energy production sources are wind, wave, sun and biomass (Demirbaş and Bakış, 2004). Supplies of energy resources such as fossil fuels (coal, oil, natural gas) and nuclear fuels (uranium and thorium) are generally known to be finite; but other energy sources, such as solar, hydro, biomass, and wind energies, are generally considered to be renewable and therefore sustainable over the relatively long term. In addition, energy generation from the fossil fuels burned in the thermal power plants causes to pollutions in the environment (Demirbaş, 2002).

A rapid increase of energy demand in the world is due to the rate of population growth, the high rate of industrialization, social and economical development of Turkey. But, thermal power plants based on fossil fuels degrade the quality of environment in large scale in fact; there is growing evidence of environmental problems due to a combination of several factors. The environmental impact of human activities worldwide has also grown dramatically because of the rate of world population growth, social development, energy consumption, improving condition of life, industrial activities, etc. Demirbaş (2002) stated that achieving solutions to the environmental problems that we face today requires long-term potential actions for sustainable development. In this regard, renewable energy resources appear to be one of the most efficient and effective solutions.

1.1. Development of Electricity Generation in Turkey

Turkey is located between Europe and Asia. It is situated in Anatolia and southeastern Europe bordering the Black Sea, the Aegean Sea and the Mediterranean Sea. Turkey extends more than 1,600 kilometers from west to east but generally less than 800 kilometers from north to south. Its total land area is about 779,452 square kilometers, of which 755,688 square kilometers are in Asia and 23,764 square kilometers in Europe. From the point of view of this geographical location, Turkey is situated bridge-like between southeastern Europe and Asia. Moreover, the economy and population of Turkey grow rapidly. As a developing country, Turkey’s population is estimated to be over 100 million by the year of 2020 (Yüksek et al., 2006). For this reason, demands for energy and particularly for electricity have been growing rapidly. Electricity energy is a vital input for the technological, social and economic development of Turkey (Hamzaçebi, 2007).

Electricity in Turkey is generated from the thermal, hydro, wind and the geothermal power plants. The development of Turkey’s installed capacity in electricity generation between 1923 and 2005 is illustrated in Figure 1.1. In addition, the development of Turkey's electricity generation between 1923 and 2005 is presented in Figure 1.2. Turkey's electricity supply industry dates back to 1902, when a 2 kW dynamo was connected to a water mill in Tarsus. Although this power plant was the first experience of Turkey in electricity production, the first larger-scale power plant was built in Istanbul in 1913. When the Republic of Turkey was founded in 1923, its installed capacity of electricity production and total electricity production were 33 MW and 45 GWh, respectively (IEA, 2001; Yılmaz and Uslu, 2007). In 1935, the Electrical Power Resources Survey and Development Administration (Elektrik Isleri Etut Idaresi, EIE) was established for the purpose of carrying out surveys and preparatory work to assess hydro potential and prepare a hydro power plant projects. Construction of power plants began on a larger scale, by both private and publicly-owned entities in the 1950s. At the beginning of the decade, installed capacity was about 408 MW (IEA, 2001).

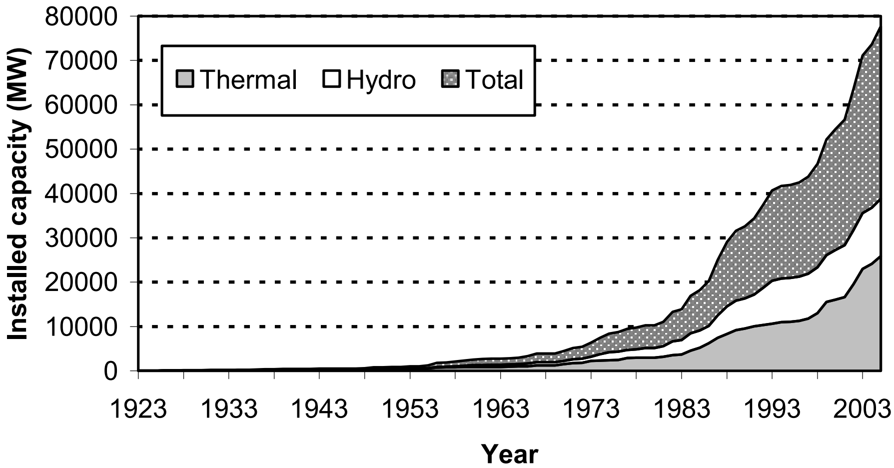

Figure 1.1. The development of Turkey's installed capacity in electricity generation between 1923 and 2005

By 1970, installed capacity of electricity was increased to about 2,235 MW, and both growing power consumption and the government's electrification plans required more coherent organization of the power industry. At the time, only 7% of all villages were electrified. As a consequence, the government established the

Turkish Electricity Authority (Türkiye Elektrik Kurumu, TEK) as a fully state-owned and state run entity that year. In 1993, TEK was split into 2 separate state-owned electric companies called as the Ministry of Energy and Natural Sources (MENR): The Turkish Electricity Generation Transmission Corporation (Türkiye Elektrik Üretim-Iletim A.S., TEAS) and Turkish Electricity Distribution Corporation (Türkiye Elektrik Dagitim A.S., TEDAS). In 1999, Turkey's installed power generation capacity reached 26,117 MW, and 99.9% of its population was connected to the electricity grid (IEA, 2001; Kıncay and Ozturk, 2003).

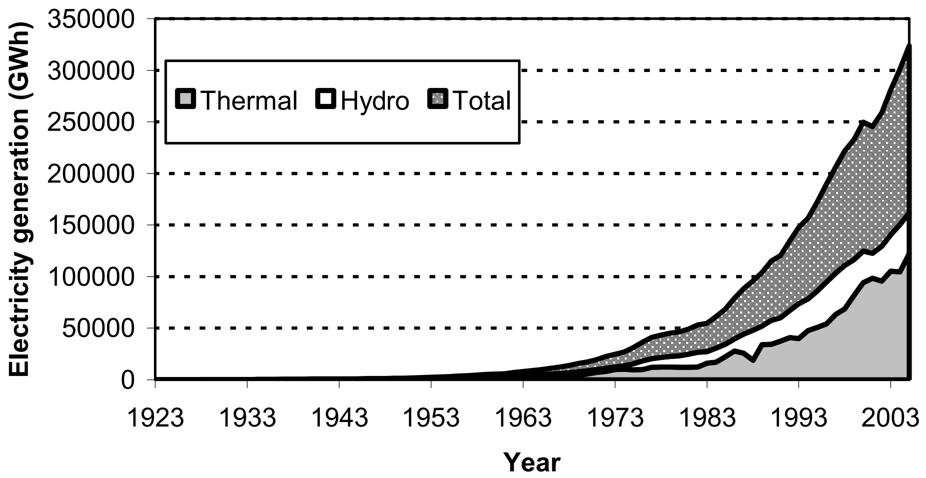

Figure 1.2. The development of Turkey's electricity generation between 1923 and 2005

Figure 1.3 shows the installed capacity and annual electricity production of Turkey's electric power plants in 2005. As reported by the Turkish Electricity Transmission Company (Turkiye Elektrik Iletim A.S., TEIAS), the installed capacity of Turkey's electric power plants was 38,843.5 MW with the annual electricity production of 161,956.2 GWh in 2005 (TEIAS, 2005). Of the total electricity generation, 75.48% came from the thermal power plants, while 24.43% came from the hydro power plants. In addition, the wind power plants and the geothermal power plants met 0.04% and 0.06% of Turkey's electric power generation, respectively. In this year, 122,242.3 GWh of this energy was produced by operating the thermal power plants. On the other hand, the annual electricity productions of the hydro power plants and the wind power plants were 39,560.5 GWh and 59 GWh, respectively. During the next 20 years, the electric power plants installed capacity is expected to reach 109,227 MW and the annual electricity production is going to be 623,835 GWh (Kenisarin et al., 2006).

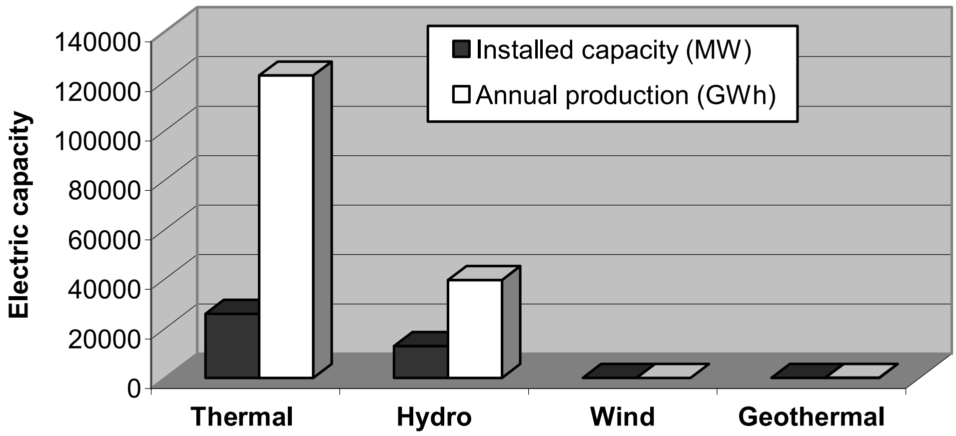

Figure 1.3. The installed capacity and annual electricity production of Turkey's electric power plants in 2005

1.2. Energy Resources in Turkey's Electricity Generation

The demand for energy in the world grows rapidly and is expected to continue to grow in the near future as a result of the social, economical and industrial developments, and a high level of population growth. In parallel with this development, renewable energy sources have received increasing attention from the world due to the limited reserves of fossil fuels and their negative impacts on the environment. In this regard, the utilization of the renewable energy resources, such as solar, geothermal, and wind energy appears to be one of the effective solutions (Hepbasli and Ozgener, 2004; Bilgili et al., 2007).

Turkey's electricity generation is based on the solid-fired resources (hard coal, lignite and imported coal), the liquid-fired resources (fuel-oil, diesel oil, LPG, Naphtha), natural gas, hydro, and others such as renewable energy and wastes sources. The solid-fired and hydraulic resources being the basic; oil and natural gas resources are main primary energy resources of Turkey in electricity generation. Figure 1.4 shows the development of Turkey's electricity generation used the primary energy resources between 1940 and 2005. By 1950s, the thermal power plants were used commonly in the electricity production. In the following years, the hydroelectric power plants were put into operation in order to use the considerable amount of water resources of the country. After 1960s, oil as an imported resource, was replaced with the national resources due to the petroleum crises. Therefore, the proportion of use of lignite in the energy field increased. During the period 1985-2003, the share of lignite-fired power plants in electricity production decreased from 42% to 16.8%. On the other hand, in the same period, the share of the natural gas-fired power plants increased from 17% to 45.2%. The share of electricity produced by the hydroelectric power plants reduced from 35% to 25.1%. As seen in Figure 1.4, the natural gas consumption became the fastest growing primary energy source in the country. Turkey's natural gas consumption was 735 million m^3 in 1987, but this consumption reached 27,314 million m^3 in 2005.

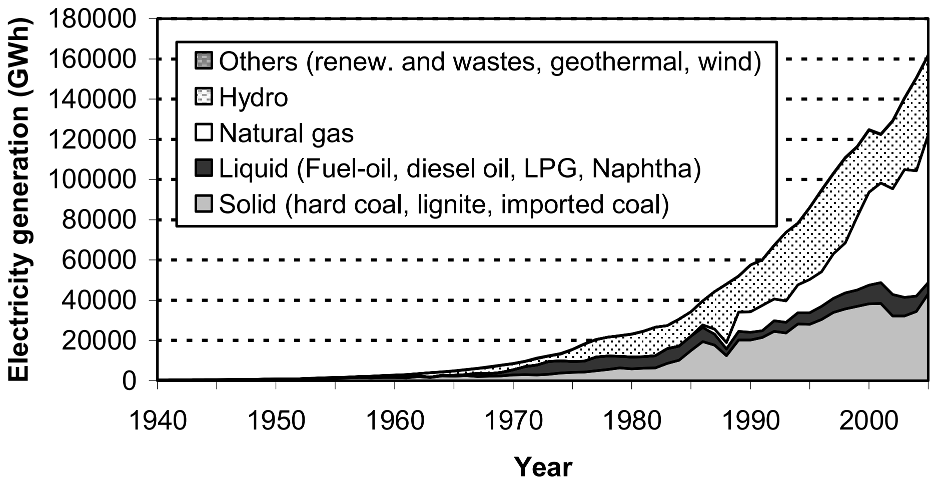

Figure 1.4. The development of Turkey's electricity generation by primary energy resources between 1940 and 2005

Turkey's electricity generation by primary energy resources in 2004 and 2005 is illustrated in Figure 1.5. The annual electricity productions in 2004 and 2005 were 150,698.3 GWh and 161,956.2 GWh, respectively. In this electricity generation, the share of the natural gas was 45.35% (73,444.9 GWh) in 2005. The solid-fired resources accounted for 26.67% (43,192.5 GWh), hydro for 24.43% (39,560.5 GWh), oil for 3.39% (5,482.5 GWh), and others such as renewable energy and wastes sources for 0.17% (275.8 GWh).

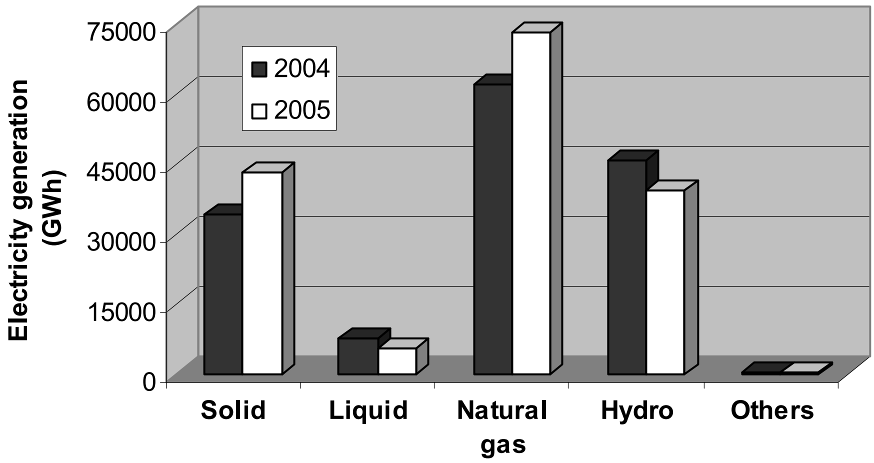

Figure 1.5. Turkey's electricity generation by primary energy resources in 2004 and 2005

Although Turkey has a wide range of energy resources, these resources are limited. Turkey does not possess huge fossil fuel reserves. Almost all types of oil and natural gas are imported from neighboring countries. Excluding lignite; coal, oil and natural gas reserves capacities in the country are low and far from being able to meet the projected domestic demand. Coal is a major fuel source for Turkey. Domestically produced coal accounted for about 24% of the country's total energy consumption, used primarily for power generation, steel manufacturing and cement production. Turkey is a large producer of lignite (Kaya, 2006). The richest lignite deposits which spread out all over the country are concentrated in Kangal, Orhaneli, Tufanbeyli, Soma, Tunçbilek, Seyitömer, Çan, Muğla, Beypazarı, and Afşin-Elbistan basins. As per the latest findings, the total lignite reserve estimation is 8,374 million tons, of which 7,339 million tons (88%) are proven. The most promising lignite deposits are in Afşin-Elbistan basin which accounts for 43% of the total deposits of Turkey. This reserve is assumed to be sufficient for existing and upcoming units of Afşin-Elbistan

Thermal Power Plants. However, low calorific value lignite below 1,500 kCal/kg accounts for approximately 58% of our lignite reserves. Share of better quality lignite over 3,000 kCal/kg is very low (8.5%) (EUAS, 2005). Turkey has substantial reserves of renewable energy resources. Main renewable energy resources are; hydro, biomass, wind, biogas, geothermal, and solar in Turkey (Kaya, 2006).

1.3. Thermal Power Plants in Turkey

Thermal power plants are the most important option in electricity generation of Turkey. In thermal power plants, mechanical power is produced by a heat engine, which transforms thermal energy, often from combustion of a fuel, into rotational energy. Most thermal power stations produce steam, and these are sometimes called steam power stations. In comparison with hydro power, thermal power plants take less time to design, obtain approval, build and recover investment. However, they have higher operating costs, typically shorter operating lives (about 25 years) (Yüksek et al., 2006). Furthermore, thermal power plants increase local pollution through SO_x, NO_x, volatile organic compounds, and oils containing primarily particulates and increase global pollution through CO_2, the greenhouse gas that causes global worming. These strong pollutants have harmful effects on living organisms and the entire ecosystem (Cicek and Koparal, 2006).

As of the end of 2005, thermal power plants in Turkey supply approximately 66.7% of Turkey's total installed capacity for electric power generation, while 75.5% of total electricity is generated from thermal power plants. Turkey's thermal electric capacity by the electricity utilities is given in Table 1.1. Turkey has 458 thermal power plants with a total installed capacity of 25,902.3 MW generating an average of 122,242.3 GWh/year. In 2005, sixteen thermal power plants belonging to the Electricity Generation Company (Elektrik Uretim A.S., EUAS) produced 26,489.3 GWh of electric power, corresponding to 21.67% of total thermal electricity generation capacity. Moreover, 56 thermal power plants belonging to the production companies produced 62,737.7 GWh of electric power, corresponding to 51.32% of total thermal electricity generation capacity, followed by the power plants of autoproducers with a 13.29% capacity, the private entities with a 5.34% capacity, the

EUAS's affiliated partnerships with a 4.34% capacity, by the transfer of operational rights with a 3.32% capacity, and the mobile power plants with a 0.72% capacity (TEIAS, 2005). As of the end of 2005, the locations of 22 thermal power plants and their capacities belonging to the EUAS, affiliated partnerships of EUAS and private entities are illustrated in Figure 1.6 and Table 1.2.

Table 1.1. Turkey's thermal electric capacity by the electricity utilities

Electricity utilities	Number of power plants		Installed capacity		Electricity generation	
		%	MW	%	GWh	%
EUAS	16	3.49	7625.9	29.44	26489.3	21.67
Affiliated partnerships of EUAS	3	0.66	2154.0	8.32	5301.4	4.34
Private entities	3	0.66	1680.0	6.49	6531.0	5.34
Autoproducers	367	80.13	3496.7	13.50	16246.9	13.29
Production companies	56	12.23	9576.0	36.97	62737.7	51.32
Mobile power plants	11	2.40	749.7	2.89	877.7	0.72
Transfer of operational R.	2	0.44	620.0	2.39	4058.3	3.32
Termal total	458	100	25902.3	100	122242.3	100

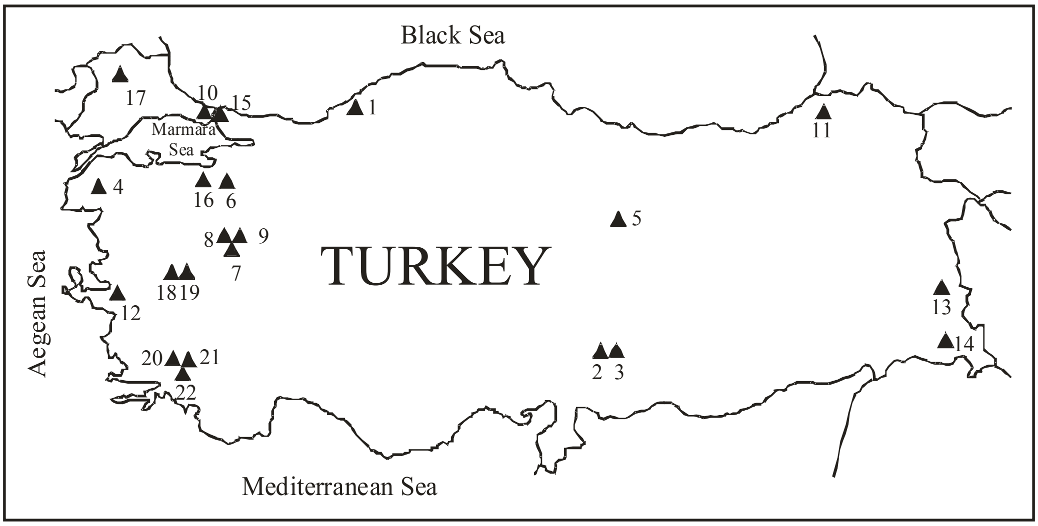

Figure 1.6. Locations of thermal power plants of the EUAS, affiliated partnerships of the EUAS and private entities in Turkey

Table 1.2. Thermal power plants of the EUAS, affiliated partnerships of EUAS and private entities in Turkey

Utilities	Item no of TPPs[a]	Name of power plant	Location	Fuel type	Installed capacity (MW)	Generation (GWh)
EUAS	1	Çatalağzı	Zonguldak	Hard coal	300	1856.7
	2	Afşin-Elbistan	K.Maraş	Lignite	1355	2512.9
	3	Afşin-Elbistan	K.Maraş	Lignite	360	4431.3
	4	Çan	Çanakkale	Lignite	320	824.4
	5	Kangal	Sivas	Lignite	457	2049.8
	6	Orhaneli	Bursa	Lignite	210	634
	7	Seyitömer	Kütahya	Lignite	600	3455.1
	8	Tunçbilek A	Kütahya	Lignite	65	1210.4
	9	Tunçbilek B	Kütahya	Lignite	300	-
	10	Ambarlı	İstanbul	Fuel oil	630	854.8
	11	Hopa	Artvin	Fuel oil	50	-

[a] Numbers represent in Figure 1.6

Table 1.2. (Continued) Thermal power plants of the EUAS, affiliated partnerships of EUAS and private entities in Turkey

Utilities	Item no of TPPs[a]	Name of power plant	Location	Fuel type	Installed capacity (MW)	Generation (GWh)
EUAS	12	Aliağa	İzmir	Diesel oil	180	-
	13	Engil	Van	Diesel oil	15	-
	14	Çukurca	Hakkari	Diesel oil	1	0.2
	15	Ambarlı	İstanbul	N. Gas	1350.9	6275.5
	16	Bursa	Bursa	N. Gas	1432	2384.2
Affiliated partnerships of EUAS	17	Hamitabat	Kırklareli	N. Gas	1120	1416.7
	18	Soma A	Manisa	Lignite	44	74
	19	Soma B	Manisa	Lignite	990	3810.7
Private entities	20	Kemerköy	Muğla	Lignite	630	1488.6
	21	Yatağan	Muğla	Lignite	630	3344
	22	Yeniköy	Muğla	Lignite	420	1698.4

[a] Numbers represent in Figure 1.6

Turkey's electricity generation by thermal energy resources in 2004 and 2005 is presented in Figure 1.7. Electricity generation produced by the thermal energy resources increased from 104,463.7 GWh in 2004 to 122,242.3 GWh in 2005. Of the total thermal generation in the year of 2005, the share of natural gas was 60.1% (73,444.9 GWh). Lignite accounted for 24.5% (29,946.3 GWh), imported coal for 8.4% (10,281.1 GWh), fuel-oil for 4.2% (5,120.7 GWh), and hard coal for 2.4% (2,965.1 GWh). According to these results, natural gas is the most important energy resources for the thermal power plants in Turkey. Turkey has small proven natural gas reserves. Turkey's indigenous gas production corresponds to 3% of the total gas demand making the country almost fully dependent on gas imports. Presently, BOTAŞ is the sole natural gas importer (IEA, 2005).

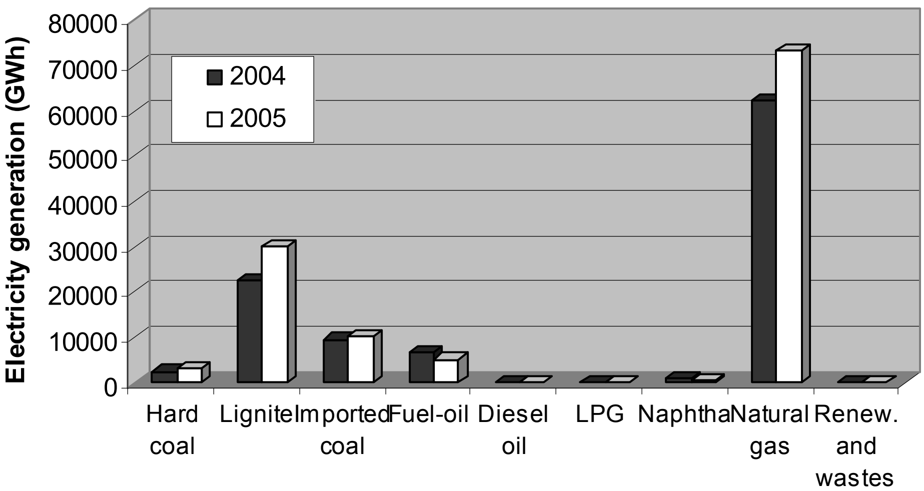

Figure 1.7. Turkey's electricity generation by thermal energy resources in 2004 and 2005

1.4. Hydro Power Plants in Turkey

Hydro power plants are the most important option as a renewable, clean and economical energy sources for Turkey (Demirbaş and Bakış, 2004). In hydro power plants, hydro-turbines convert water pressure into mechanical shaft power, which can be used to drive an electricity generator, or other machinery. The power available is proportional to the product of pressure head and water discharge. Hydroelectric plants tend to have longer lives than fuel-fired generation. The major advantage of hydroelectricity is elimination of the cost of fuel. Since no fossil fuel is consumed, emission of carbon dioxide from burning such fuels is eliminated. In addition, reservoirs created by hydroelectric schemes provide a lot of facilities such as secure water supply, irrigation for agricultural production and flood control, and societal benefits such as increased recreational opportunities, improved navigation, the development of fisheries, cottage industries, etc (Yüksek et al., 2006).

Table 1.3. Turkey’s hydro electric capacity by the electricity utilities in 2005

Electricity utilities	Number of power plants		Installed capacity		Electricity generation	
		%	MW	%	GWh	%
EUAS	108	75.00	11109.7	86.08	35045.8	88.59
Autoproducers	7	4.86	562.8	4.36	834.5	2.11
Production companies	28	19.44	1203.5	9.33	3617.9	9.15
Transfer of operational rights	1	0.69	30.1	0.23	62.3	0.16
Hydro total	144	100	12906.1	100	39560.5	100

As of the end of 2005, the hydro power plants in Turkey supply approximately 33.2% of Turkey’s total installed capacity for electric power generation, while 24.4% of total electricity is generated from the hydro power plants. Turkey’s hydro electric capacity by the electricity utilities is given in Table 1.3. Turkey has 144 hydro power plants with a total installed capacity of 12,906.1 MW generating an average of 39,560.5 GWh of electric power per year. In 2005, 108 hydro power plants belonging to the Electricity Generation Company (EUAS) produced 35,045.8 GWh of electric power, corresponding to 88.59% of the total hydro electricity generation capacity. Also, 28 hydro power plants belonging to the production companies produced 3,617.9 GWh of electric power, corresponding to 9.15% of the total hydro electricity generation capacity, followed by the power plants of autoproducers with a 2.11% capacity, and the transfer of operational rights with a

0.16% capacity (TEIAS, 2005). As of the end of 2005, locations of 44 hydro power plants and their capacities belonging to the EUAS are illustrated in Figure 1.8 and Table 1.4.

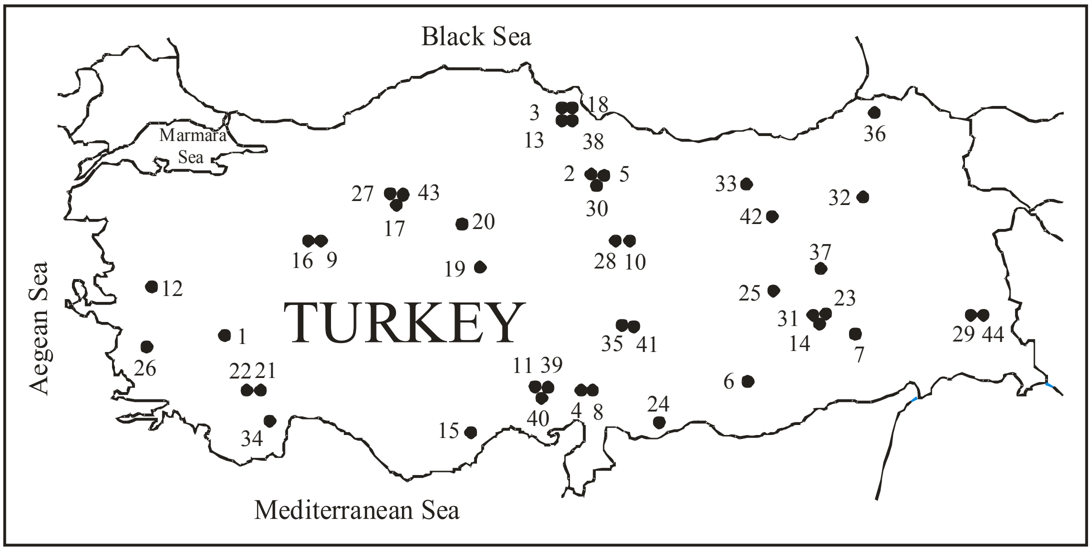

Figure 1.8. Locations of hydro power plants with dam of the EUAS in Turkey

The installed capacity of the hydropower plants owned by the General Directorate of Electrical Power Resources Survey and Development Administration (EIE) are presented in Table 1.5. As of February 2007, Turkey has 142 hydroelectric power plants in operation with a total installed capacity of 12,788 MW generating an average of 45,930 GWh electric powers per year. Forty-one hydroelectric power plants are currently under construction with a 4,397 MW of installed capacity to generate an average 14,351 GWh electricity energy annually. Furthermore, 589 more hydroelectric power plants will be constructed in the near future to be able to utilize maximum use of the remaining 69,173 GWh/year of economically viable hydropower energy potential. Consequently, a total of 772 hydroelectric power plants with the installed capacity of 36,544 MW will be in use in coming years (EIE, 2007).

Table 1.4. Hydro power plants with dam of the EUAS in Turkey

Item no of TPPs[a]	Name of power plant	Location	Installed capacity (MW)	Generation (GWh)
1	Adıgüzel	Denizli	62.00	142.80
2	Almus	Tokat	27.00	95.30
3	Altınkaya	Samsun	702.55	653.40
4	Aslantaş	Adana	138.00	599.10
5	Ataköy	Tokat	5.53	8.70
6	Atatürk	Ş.Urfa	2405.00	7846.10
7	Batman	Batman	198.00	354.60
8	Berke	Adana	510.00	1587.80
9	Beyköy	Eskişehir	16.80	57.40
10	Çamlıgöze	Sivas	32.00	101.20
11	Çatalan	Adana	168.90	340.00
12	Demirköprü	Manisa	69.00	102.40
13	Derbent	Samsun	56.40	155.40
14	Dicle	Diyarbakır	110.00	148.90
15	Gezende	İçel	159.37	361.30
16	Gökçekaya	Eskişehir	278.40	364.70
17	H.Polatkan/Sarıyar	Ankara	160.00	275.40
18	H.Uğurlu	Samsun	500.00	1372.90
19	Hirfanlı	Kırşehir	128.00	74.30
20	Kapulukaya	Kırıkkale	54.00	44.40
21	Karacaören I	Burdur	32.00	104.70
22	Karacaören II	Burdur	47.20	152.00
23	Karakaya	Diyarbakır	1800.00	7480.60
24	Karkamış	G.Antep	189.00	390.20
25	Keban	Elazığ	1330.00	6694.90

[a] Numbers represent in Figure 1.8

Table 1.4. (Continued) Hydro power plants with dam of the EUAS in Turkey

Item no of TPPs[a]	Name of power plant	Location	Installed capacity (MW)	Generation (GWh)
26	Kemer	Aydın	48.00	56.20
27	Kesikköprü	Ankara	76.00	50.00
28	Kılıçkaya	Sivas	120.00	378.50
29	Koçköprü	Van	8.80	23.20
30	Köklüce	Tokat	90.00	474.50
31	Kralkızı	Diyarbakır	94.50	94.60
32	Kuzgun	Erzurum	20.90	20.90
33	Kürtün	Gümüşhane	85.00	200.10
34	Manavgat	Antalya	48.00	109.50
35	Menzelet	K.Maraş	124.00	512.30
36	Muratlı	Artvin	115.00	251.50
37	Özlüce	Bingöl	170.00	489.60
38	S.Uğurlu	Samsun	69.00	358.70
39	Seyhan I	Adana	60.00	176.70
40	Seyhan II	Adana	7.20	2.90
41	Sır	K.Maraş	283.50	728.90
42	Tercan	Erzincan	15.00	52.10
43	Yenice	Ankara	37.90	91.60
44	Zernek (Hoşap)	Van	3.50	9.10

[a] Numbers represent in Figure 1.8

Table 1.5. Potential of hydro power plants in Turkey as of February 2007

Status of economically viable potential	Number of hydro-electric plants	Total installed capacity (MW)	Average annual generation (GWh/year)
In operation	142	12788	45930
Under construction	41	4397	14351
In program	589	19359	69173
Total potential	772	36544	129454

1.5. Wind Power Plants in Turkey

One of the main renewable energy resources all over the world is wind which has played a long and important role in the history of human civilization. Wind power has been harnessed by mankind for thousands of years. Since earliest recorded history, wind power has been used to move ships, grind grain and pump water (Hepbasli and Ozgener, 2004). The last decade was characterized by rough development of wind power engineering all over the world. Leading positions are taken by Germany, Spain and USA. The rates of growth of this branch of power engineering exceed 39% annually. No other branch of power engineering developed with such higher rates (Kenisarin et al., 2006).

Turkey is surrounded by the Black Sea in the North, the Marmara and Aegean Sea in the West and the Mediterranean Sea in the South with a very long seashores. The regions of Aegean and Marmara have higher wind energy potential comparing to the other regions (Hepbasli and Ozgener, 2004). In addition, the rate of wind energy potential in Antakya and İskenderun regions is high enough to produce electricity (Bilgili et al., 2004; Sahin et al., 2005). But, all regions of Turkey are not suitable for the installation of wind turbines due to a topographic structure and a low level of wind energy potential. Although Turkey has sufficient wind energy potentials, the present utilization of wind energy is limited by an installed capacity of 131.35 MW as of May 2007 (EPDK, 2007).

In 2005, wind power plants in Turkey produced 59 GWh of electric power with a total installed capacity of 20.1 MW. They provided approximately 0.05% of

Turkey's total installed capacity of the electric power generation, while 0.04% of total electricity is generated from the wind power plants. As of May 2007, the wind power plants in Turkey and their locations are illustrated in Figure 1.9 and Table 1.6 (EPDK, 2007). Although the first Turkish wind turbine was constructed in Çeşme by Vestas company in 1985 (55 kW), the development of modern Turkish wind power engineering began from 21st of November 1998 when the first 3 Enercon E-40 model wind turbines of 500 kW each began to operate at Alaçatı, İzmir. Then, the wind farm consisting of 12 Vestas V44/600 turbines was constructed at the same region in November 1998 and the third wind farm with a total installed capacity of 10.2 MW started to operate in June 2000 at Bozcaada Island (Hepbasli and Ozgener, 2004; Kenisarin et al., 2006). The wind farm consisting of 20 General Electric GE/1.5 MW turbines were constructed at Bandırma, Balıkesir in September 2006. According to the projection of the Energy Market Regulatory Authority (Enerji Piyasasi Duzenleme Kurumu, EPDK), as of May 2007, Turkey has 9 wind power plants in operation with a total installed capacity of 131.35 MW. Fourteen wind power plants are currently under construction with a total installed capacity of 610.76 MW. Consequently, a total of 23 wind power plants with the installed capacity of 742.11 MW will be in use by the year 2009 (EPDK, 2007).

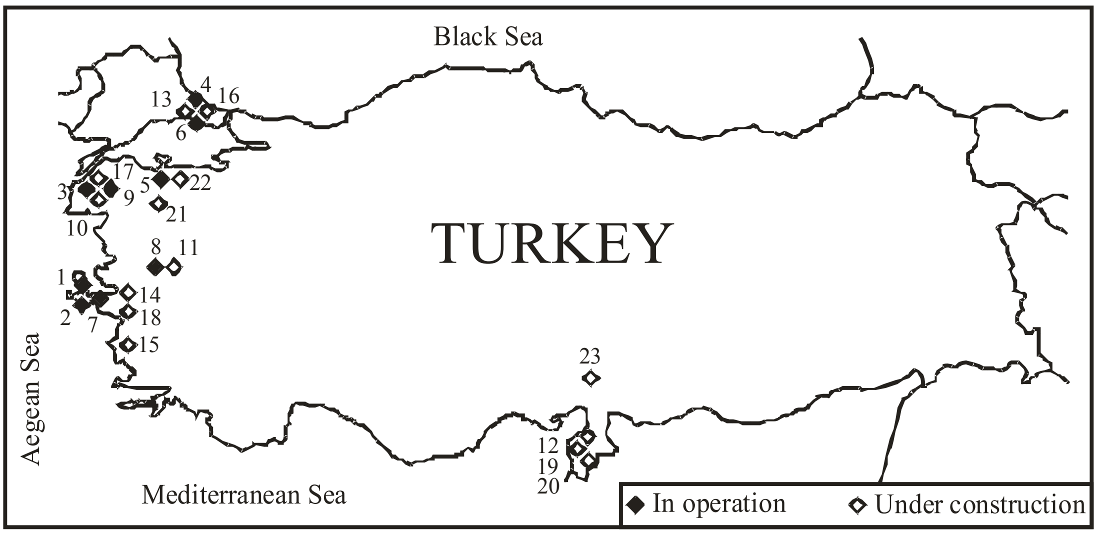

Figure 1.9. Locations of wind power plants in Turkey

Table 1.6. Distribution of Turkey's wind energy installations by regional as of May 2007 (*: In operation, others: Under construction)

Item no of WPPs[a]	Place	Company	Date of commis sioning	Installed capacity (MW)	Cum. installed capacity (MW)
1	Izmir-Çesme*	Demirer A.Ş.	1998	1.5	1.5
2	Izmir-Çesme*	Güçbirliği A.Ş.	1998	7.2	8.7
3	Çanakkale-Bozcaada*	Demirer-Enercon	2000	10.2	18.9
4	İstanbul-Hadımköy*	Sunjüt A.Ş.	2003	1.2	20.1
5	Balıkesir-Bandırma*	Bares A.Ş.	I/2006	30.0	50.1
6	İstanbul-Silivri*	Ertürk A.Ş.	II/2006	0.85	50.95
7	İzmir-Çeşme*	Mare A.Ş.	I/2007	39.2	90.15
8	Manisa-Akhisar*	Deniz A.Ş.	I/2007	10.8	100.95
9	Çanakkale-İntepe*	Anemon A.Ş.	I/2007	30.4	131.35
10	Çanakkale-Gelibolu	Doğal A.Ş.	II/2007	15.2	146.55
11	Manisa-Sayalar	Doğal A.Ş.	II/2007	30.4	176.95
12	Hatay-Samandağ	Deniz A.Ş.	II/2007	30.0	206.95
13	İstanbul-G.O.Paşa	Lodos A.Ş.	I/2008	24.0	230.95
14	İzmir-Aliağa	İnnores A.Ş.	I/2008	42.5	273.45
15	Aydın-Çine	Sabaş A.Ş.	I/2008	19.5	292.95
16	İstanbul-Çatalca	Ertürk A.Ş.	I/2008	60.0	352.95
17	Çanakkale	As Mak. T. A.Ş.	II/2008	30.0	382.95
18	İzmir-Kemalpaşa	Ak-El A.Ş.	II/2008	66.6	449.61
19	Hatay-Samandağ	Ezse Ltd. Şti.	II/2008	35.0	484.61
20	Hatay-Samandağ	Ezse Ltd. Şti.	II/2008	22.5	507.11
21	Balıkesir-Şamlı	Baki A.Ş.	II/2008	90.0	597.11
22	Balıkesir-Bandırma	Bangüç A.Ş.	II/2008	15.0	612.11
23	Osmaniye-Bahçe	Rotor A.Ş.	I/2009	130.0	742.11

[a] Numbers represent in Figure 1.9

1.6. Geothermal Power Plants in Turkey

Geothermal energy is one of the most promising alternative energy sources. It is also environmentally advantageous energy source which produces for less air pollution than fossil-fuel sources. It can be utilized in various forms such as electricity generation, direct use, space heating, heat pumps, greenhouse heating, and industrial usage in Turkey (Etemoglu and Can, 2007; Balat, 2006).

Turkey is the 7th richest country in the world in the geothermal energy potential with the capacity of 38,000 MW for its direct use and for electricity generation (Ocak et al., 2004). Approximately, 88% of this potential is appropriate for thermal use with the temperature less than 473 K and the remain is capable of producing electricity with the temperature more than 473 K (Demirbaş et al., 2004).

The first geothermal researches and investigations in Turkey were started by the Turkey Mineral Research and Exploration Institute (Maden Tetkik ve Arama, MTA) in the 1960s. Upon this, 170 geothermal fields have been discovered by MTA, where 95% of them are low-medium enthalpy fields, which are suitable mostly for the direct-use applications. Denizli-Kızıldere (473-515 K), Aydın- Germencik (505 K), Çanakkale-Tuzla (447 K), Aydın-Salavatlı (444 K), Kütahya-Simav (435 K), Manisa-Salihli (423 K), and İzmir-Seferihisar (426 K) are high enthalpy fields, which are suitable for the electrical energy production (Balat, 2006).

Figure 1.10 shows the development of Turkey's installed capacity and electricity generation in the geothermal power plants. The first geothermal power plant was put in operation in 1984 in Denizli-Sarayköy. In 2005, geothermal power plants in Turkey provided approximately 0.04% of Turkey's total installed capacity for electric power generation, while 0.06% of total electricity was generated from the geothermal power plants. As of May 2007, the geothermal power plants in Turkey and their locations are illustrated in Figure 1.11 and in Table 1.7 (EPDK, 2007). According to the projection of the Energy Market Regulatory Authority (EPDK), Turkey has 2 geothermal power plants in operation with a total installed capacity of 22.95 MW. Three geothermal power plants are currently under construction with a 38.2 MW of installed capacity. Consequently, a total of 5 geothermal power plants with the installed capacity of 61.15 MW will be in use in coming years (EPDK, 2007).

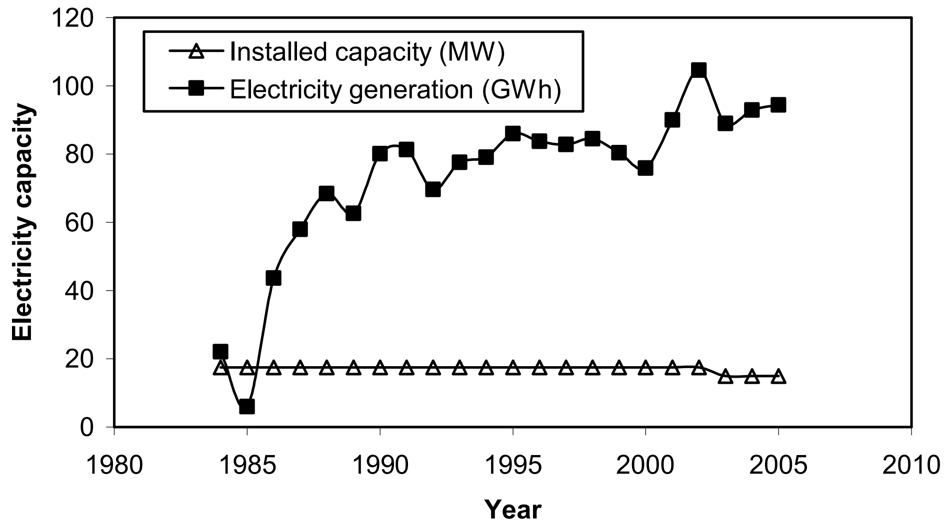

Figure 1.10. The development of Turkey's installed capacity and electricity generation in the geothermal power plants

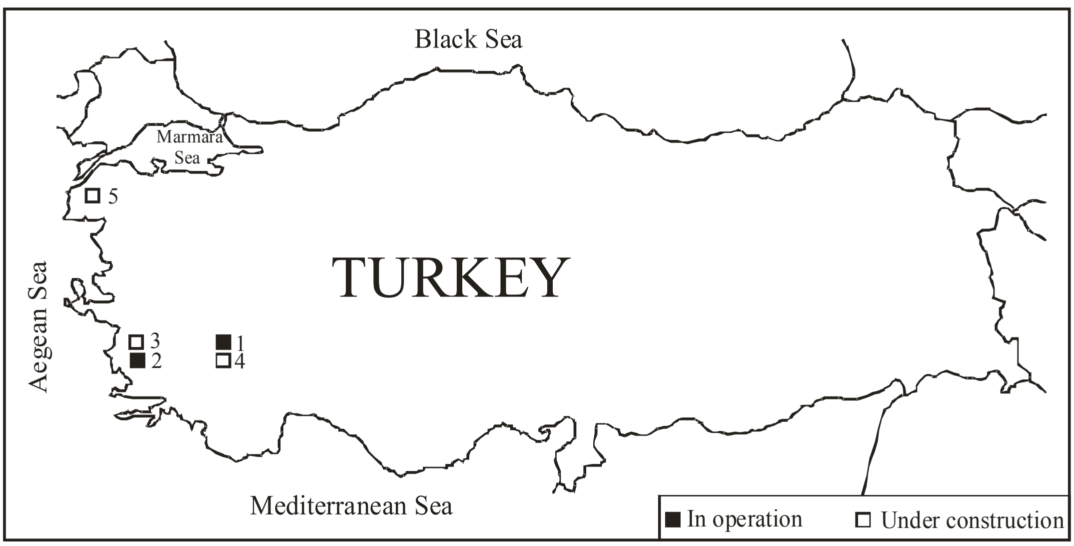

Figure 1.11. Locations of geothermal power plants in Turkey

Table 1.7. Geothermal power plants in Turkey

Item no of WPPs[a]	Place	Company	Installed capacity (MW)	Generation (GWh)
1	Denizli-Sarayköy*	EUAS	15.0	82.5
2	Aydın-Sultanhisar*	Menderes A.Ş.	7.951	56.0
3	Aydın-Germencik	Gürmat A.Ş.	25.2	178.704
4	Denizli-Sarayköy	Bereket A.Ş.	5.5	38.0
5	Çanakkale-Ayvacık	Dardanel A.Ş.	7.5	63.0

*: In operation, others: under construction, [a]: Numbers represent in Figure 1.11

1.7. Aim and Outline of the Study

One of the most suitable areas of Turkey for wind power generation is some locations of the eastern Mediterranean region. Along the Mediterranean Sea coast, valleys and mountains are not perpendicularly formed and besides the Taurous Mountains are situated away from the sea coast in many regions. Therefore, these regions are exposed to southerly winds that are not as strong as the northerly winds that occur over the Black Sea. Especially, at the vicinity of İskenderun bay there are suitable locations for wind power generation (Durak and Şen, 2002). Beside, deciding the most suitable site for a wind turbine and defining the necessary parameters about turbines such as size, blade shape, total capacity, direction etc., it is also required feasibility report on the fundamental properties of the site such as wind behavior, availability, continuity, and probability in the proposed region. In order to use those properties, statistical and dynamic characteristics of wind of the site should be obtained using wind observations and statistical wind data (Karsli and Geçit, 2003).

Nowadays, renewable energy such as wind energy is one of the most attractive sources of energy. Resources may need to prepare an inventory on the availability of wind energy an area where there is no measured wind speed data. For this type of situation, it seems useful to predict the wind energy potential using artificial neural network (ANN) method. Kalogirou et al. (1999) stated that the predicted variations of meteorological parameters such as wind speed, relative humidity, solar radiation, air temperature, etc. are needed in the industry of renewable energy for design purposes, performance analysis and running cost estimation of renewable energy systems. In addition, they reported that for proper and efficient utilization of wind power, it is very important to know the statistical characteristics, persistence, availability, diurnal variation and prediction of wind speed. The values of wind power distributions are needed for site selection, performance prediction and planning of wind turbines. Moreover, prediction of wind speed is needed for any regional inventory wind energy studies in advance. In this sense, the establishment of a model for wind speed correlation in a region is of great importance in the management of wind energy resources for power generation as well as in other research fields related to energy conservation (Bechrakis et al., 2004).

The amount of heat energy that is absorbed varies spatially as well as temporally because of roughness of the earth surface. This creates temperature, pressure and density (specific mass) differences that, in turn, create forces that move air from one place to another. It is evident that depending on the surface features of the earth, some areas are preferable to others for extracting kinetic energy from the wind in the atmospheric boundary layer (Öztopal, 2006). Because of the fact that this kinetic energy varies directly proportional to the third grade power of the wind speed, the prediction of the wind energy is usually obtained using estimated wind speeds. Wind estimation is difficult due to the complex structures of parameters which affect wind strongly such as topographical properties of the earth, the rotation of the world, temperature and pressure difference.

When the atmospheric air cools down, the density of the air increases and hence the dense air collapse down due to the gravitational force. So, dense air causes a high rate of pressure in close region of the earth surface. On the contrary, under warm weather condition, atmospheric air expends, the rate of density decays down and hence a low level of pressure region occurs along the earth surface. For this reason, there is a pressure differences between cold and warm air regions. Air movements attempt to balance the instability and finally, from a higher pressure region to lower pressure region air movement occurs which is called wind speed (Erol, 1999). The main parameters for the cause of air movement called wind are atmospheric temperature, atmospheric pressure, air density and environmental conditions. As a result, in order to predict wind speed one can use these meteorological parameters using artificial neural network method.

In this study, wind characteristics in various locations of the Marmara, Aegean and Mediterranean region of Turkey were investigated using computer package program called WAsP. Before the construction of the wind turbine generator in these sites (Akhisar, Bababurnu, Belen, Datça, Foca, Gelendost, Gelibolu, Gökçeada, Söke, Antakya, İskenderun, Karataş, Yumurtalık, Dörtyol, Samandağ, Mersin and Adana), several fundamental properties such as wind behavior, availability, continuity, and probability were carried out in order to provide the necessary information to the potential investors about cost and economical aspects of the planning wind energy project. Wind direction frequency distribution, probability distribution, Weibull parameters, mean wind speed and power potential variations were determined. All of these wind characteristics were studied according to the wind directions, hours of day and months, separately.

To evaluate the mean wind speed and potential of any region, it is necessary to calculate the values of Weibull parameters (k and c) of long-term wind speeds using several methods and program such as the commonly used graphical method, the maximum likelihood method, the modified maximum likelihood method and WAsP (Wind Atlas Analysis and Application Program) package program. In this study, firstly, neural network methodology was applied in order to estimate the mean wind power potential in Antakya, İskenderun, Karataş and Samandağ districts, located in the south-eastern region of Turkey. Frequency values of each observed wind speed range were used in the input layer of the network, while mean wind power potential was used in the output layer of the network.

Secondly, a model was developed to predict the mean monthly wind speed of any pivot station using the mean monthly wind speeds of neighboring stations which are referred to as the reference. Spatial modeling of wind speeds in the Mediterranean region of Turkey has been investigated using artificial neural networks. The relation amongst the stations was defined and the reference stations were determined to predict any pivot stations, because the accuracy of the results is basically dependent on the correlation coefficient level between the two stations' wind speed. The mean monthly wind speeds of neighboring stations and corresponding month were used in the input layer of the network; on the other hand, the mean monthly wind speed of pivot station was used in the output layer of the network.

Furthermore, the aim of this work is to apply Multiple Linear Regression and Artificial Neural Network models for wind speed prediction with using various meteorological variables of Antakya, Mersin and Samandağ meteorological stations, located in the south-eastern region of Turkey. By providing meteorological data such as pressure, density, temperature and humidity, wind speed was predicted using artificial neural networks. Here, meteorological data such as pressure, density, temperature and humidity were utilized in the input layer of the network; in addition to this, the mean wind speed will also be utilized in the output layer of the network.

In addition, the aim of the present study is to apply artificial neural networks (ANNs) method for regional daily, weekly and monthly wind speed prediction in some parts of the Aegean and Marmara region of Turkey. The wind data taken with an interval of one hour were measured by the General Directorate of Electrical Power Resources Survey Administration (EIE) at 4 measuring stations such as Gökçeada, Foca, Gelibolu and Bababurnu. The long-term wind data, containing hourly wind speeds and directions, cover the period from the year 1998 to 2003. Daily, weekly and monthly wind data were obtained by using the averages of hourly wind data. The wind speeds of three different stations were used as input neurons in the ANN architecture, while wind speed of target station was used as an output neuron in the ANN architecture.

Lastly, Artificial Neural Networks (ANNs) were applied to predict the long term monthly temperature and rainfall at any specific point of Turkey based on the use of the neighboring measuring stations data. For this purpose, meteorological data measured by the Turkish State Meteorological Service (TSMS) between the years 1975 and 2006 from 76 measuring stations were used as a training (59 stations) and testing (17 stations) data. Four neurons which receive input signals of latitude, longitude, altitude and month were used in the input layer of the network. Two neurons which produce corresponding output signals of the long term monthly temperature and rainfall were utilized in the output layer of the network

2. LITERATURE REVIEW

Artificial neural network approach to spatial estimation of wind velocity data was reviewed by Öztopal (2006). In his study, weighting factors of surrounding stations necessary for the prediction of a pivot station were presented by an artificial neural network technique. Daily wind velocity measurements in the Marmara region from 1993 to 1997 were considered for application of the ANN methodology. Wind velocity measurements in the nearest nine stations were used for pivot station estimation. Nine station wind velocities were used as input neurons in the ANN architecture. The hidden layer neurons number and learning rate were adopted as 10 and 0.3, respectively. In the wind velocity regional estimation procedure, 15,000 iterations were used, and the delta error step was considered as 0.045. From the results of his study can be found that this methodology gives better regional estimations during the winter months, and regionally, at continental stations. Under and over estimation problems in objective analysis can be avoided by the ANN approach.

Kalogirou et al. (1999) investigated wind speed prediction using artificial neural networks. In their study, a multilayered artificial neural network has been used for predicting the mean monthly wind speed in regions of Cyprus where data are not available. Data for the period 1986-1996 have been used to train a neural network, whereas data for the year 1997 were used for validation. Both learning and prediction were performed with adequate accuracy. Two network architectures of the similar type have been tried. One with eleven neurons in the input layer and one with five. The second one proved to be more accurate in predicting the mean wind speed. The month of the year and the mean monthly values of wind speed at two levels (2m and 7m) for two control stations were used in the input layer of the network. On the other hand, the mean monthly values of wind speed of a third station called target station were used in the output layer of the network. The maximum percentage difference for the validation set was confined to less than 1.8% on an annual basis, which is considered by the domain expert as adequate.

Bechrakis and Sparis (2004) presented a method for establishing wind speed correlation between neighboring measuring stations. The aim of their study is to develop a model, in which given the wind speed at a particular site to simulate the wind speed at another, nearby site, in order to estimate the wind power of an area. This method takes into account the evolution of the sample cross correlation function (SCCF) of wind speed in time domain and uses an artificial neural network to perform the wind speed simulation. The data, which has been used in their study, were acquired from two different locations in South and Northern Greece. Tests in their study showed that the higher the SCCF value between two sites, the better simulation achieved.

Çam et al. (2005) investigated the estimations of average wind speed and wind power values using artificial neural networks in seven regions of Turkey. They applied this method for predicting average wind speed at the different heights of various regions, speeding up the evaluation and helping us to determine possible wind farm sites. To start with, a network has been set up and trained with the data set obtained from several stations–each station gather data from five different heights–from each region; one randomly selected height value of a station has been used as test data. In the input layer, longitude, latitude, altitude and height are used, while wind speeds and related power values correspond to output layer. The network has successfully predicted the required output values for the test data and the mean error levels for regions varied between 3 % and 6 %.

Sfetsos (2000) investigated a comparison of various forecasting techniques applied to mean hourly wind speed time series. In his study, a comparison of various forecasting approaches was presented on mean hourly wind speed data using time series analysis. In addition to the traditional linear (ARMA) models and the commonly used feed forward and recurrent neural networks, other approaches were also examined including the Adaptive Neuro-Fuzzy Inference Systems (ANFIS) and Neural Logic Networks. The data used in the study are mean hourly wind speed values measured on the location of Odigitria of the Greek island of Crete. They cover a period of 1 month, March 1996, 744 h in total. As a result of his study, the artificial intelligence based models that were used outperformed the respective linear ones and all nonlinear models exhibited comparable root mean squared (RMS) error. The model with the least error was identified as a Neural Logic Network that incorporated Logic Rules, which produced an RMS error 4.9% lower than of the persistent approach.

A novel method for the forecasting of mean hourly wind speed data using time series analysis was presented by Sfetsos (2002). In his study, two different data sets were examined. The first consists of one month worth of data, March 1998, measured at a site near the monastery of Odigitria in the southern part of the Greek island of Crete. The second data set contains meteorological data from the wind test site of the Rutherford Appleton Laboratory in Oxfordshire, Uk. From the results of his study can be found that the RMS error of the iterative approach is approximately 19.2% better than the persistent, which is much higher compared to the 4.67% of the ANN model.

A neural networks approach for wind speed prediction was investigated by Mohandes et al. (1998). Their study introduced neural networks technique for wind speed prediction and compares its performance with an autoregressive model. The statistical characteristics of mean monthly and daily wind speed in Jeddah, Saudi Arabia were studied. The autocorrelation coefficients were computed and the correlogram was found compatible with the real diurnal variation of mean wind speed. The results on their testing data indicated that the neural network approach outperforms the AR model as indicated by the prediction graph and by the root mean squire errors.

More and Deo (2003) employed the technique of neural networks in order to forecast daily, weekly as well as monthly wind speeds at two coastal locations in India. In their study, both feed forward as well as recurrent networks were used. Wind speeds data, collected by India Meteorological Department between 1989 and 2000 years, were used. The data pertaining to the first 10 years was used for training, while the observations of the last 2 years were reserved for testing of the network. Finally, it was concluded that the network forecasting was fairly close to the corresponding measurements with average errors restricted to 4.3 %, 5.4 % and 6.3

%, respectively; in the case of monthly, weekly and daily forecasts when adequately trained networks were involved.

Application of a control algorithm for wind speed prediction and active power generation was reviewed by Flores et al. (2005). The main objective of their study is to offer a new method of prediction of wind speeds. The algorithm presented in their study is based on an artificial neural network and two types of wind data have been used to test the algorithm. In the first, data was collected from a not very windy area; in the second data was collected from a real wind farm located in Navarre (North of Spain), and the values vary from very low to high speeds. It can be concluded from the first set of results presented in their study that the algorithm is valid for estimating average speed values.

Bechrakis et al. (2004) investigated wind resource assessment of an area using short term data correlated to a long term data set. In their study, concurrent measurements from target and reference sites over periods of 1-month and 2-month were used to train the artificial neural network. All measurements were used place in Country Cork, a region in southwest Ireland. The ANN method was applied for the prediction of the wind speed of target station using neighboring measuring station. The maximum cross-correlation coefficient was obtained for each pair wind speed time series of all stations in order to expect a reasonable result. They stayed that the cross-correlation coefficient in each pair wind speed time series must be higher than 0.6 in order to expect a reasonable result and, the accuracy of the results is basically dependent on the cross-correlation level between the two stations' wind speed, which is related to the morphology of the surrounding area.

Sözen et al. (2005) investigated solar-energy potential in Turkey using artificial neural networks. In their study, scaled conjugate gradient and Levenberg-Marquardt learning algorithms were used in the network. Meteorological data for four years (2000-2003) from 18 cities (Bilecik, Kırşehir, Akhisar, Bingöl, Batman, Bodrum, Uzunköprü, Şile, Bartın, Yalova, Horasan, Polatlı, Malazgirt, Köyceğiz, Manavgat, Dörtyol, Karataş and Birecik) spread over Turkey were used as data in order to train the neural network. Meteorological and geographical data (latitude, longitude, altitude, month, mean sunshine duration and mean temperature) were used in the input layer of the network. Solar radiation was the output layer. It has been found that the maximum mean absolute percentage error was 3.448 %. Finally, it was concluded that the ANN model seems promising for evaluating solar-resource potential at places where there are no monitoring stations in Turkey.

Forecasting based on neural network approach of solar potential in Turkey was investigated by Sözen et al. (2005). The main focus of their study was put forward to solar energy potential in Turkey using artificial neural networks. Scaled conjugate gradient (SCG), Pola-Ribiere conjugate gradient (CGP), and Levenberg-Marquardt (LM) learning algorithms and logistic sigmoid transfer function were used in the network in their study. In order to train the neural network, meteorological data for last 4 years (2000-2003) from 12 cities (Çanakkale, Kars, Hakkari, Sakarya, Erzurum, Zonguldak, Balıkesir, Artvin, Çorum, Konya, Siirt, Tekirdağ) spread over Turkey were used as training (nine stations) and testing (three stations) data. Meteorological and geographical data (latitude, longitude, altitude, month, mean sunshine duration and mean temperature) were used as input to the network. Solar radiation was the output. The maximum mean absolute percentage error was found to be less than 6.78% and R^2 values to be about 99.7768% for the testing stations.

Maqsood et al. (2005) studied an application of computing models to hourly weather analysis in southern Saskatchewan, Canada. In their study, the model was trained and tested using hourly weather data of temperature, wind speed and relative humidity in 2001. The performance of the radial basis function network (RBFN) was compared with those of multi-layered perceptron (MLP) network, Elman recurrent neural network (ERNN) and Hopfield model (HFM) to examine their applicability for weather analysis. Inputs, output and context neurons have linear activation functions; while hidden neurons have sigmoid activation function. Reliabilities of the models were then evaluated by a number of statistical measures. The results indicated that the RBFN produces the most accurate forecasts compared to the MLP, ERNN and HFM.

Li et al. (2001) investigated comparative analysis of regression and artificial neural network models for wind turbine power curve estimation. Their paper examined and compared regression and artificial neural network models used for the estimation of wind power curves. First, characteristics of wind turbine power generation were investigated. Then, models for turbine power curve estimation using both regression and neural network methods were presented and compared. The performances of the two models were studied. The regression model was shown to be function dependent, and the neural network model was found to possess better performance than the regression model for turbine power curve estimation under complicated influence factors.

Support vector machines for wind speed prediction were studied by Mohandes et al. (2004). Their study introduced support vector machines (SVM), the latest neural network algorithm, to wind speed prediction and compared their performance with the multilayer perceptron (MLP) neural networks. Mean daily wind speed data from Madina city, Saudi Arabia, was used for building and testing both models in their study. To find the best order, systems of orders from 1 to 11 were studied. The order of the system determined the number of previous wind speed days used as inputs to predict the wind speed of the next day. The Levenberg-Marquardt optimization method was used in implementing the back-propagation algorithm due to its proven performance. The activation function of the hidden layer was the tansing function, while the activation function of the output layer was linear function. Results indicated that SVM compare favorably with the MLP model based on the root mean square errors between the actual and the predicted data.

Kalogirou (2001) investigated a review of artificial neural networks in renewable energy systems applications. His study presents various applications of neural networks mainly in renewable energy problems in a thematic rather than a chronological or any other order. In his study, artificial neural networks were used in the field of solar energy; for modeling and design of a solar steam generating plant, for the estimation of a parabolic through collector intercept factor and local concentration ratio and for the modeling and performance prediction of solar water heating systems. In all those models a multiple hidden layer architecture was used. Errors obtained in these models were well within acceptable limits.

Perez-Llera et al. (2002) studied local short-term prediction of wind speed. In their study, neural network methodology was applied to construct a meteorological forecasting tool which predicts the local short-term wind speed. The values of 12 meteorological variables (wind speed, gust wind, wind direction, air temperature, relative humidity, air pressure, visibility, sunshine duration, net atmospheric radiation, water temperature) were used for neural network model. The lineal correlation between all the variables was studied taking them two by two. At the end of their study, the best network model was obtained for wind speed prediction. The past wind speed, atmospheric pressure and air temperature were used as input neurons in the ANN architecture. On the other hand, the wind speed in a near future was used as output neuron in the ANN architecture.

Locally recurrent neural networks for long-term wind speed and power prediction were investigated by Barbounis and Theocharis (2006). In their study, local recurrent network structure was presented along with the respective notation. The global and the three local versions of the recursive prediction error (RPE) algorithm were investigated. The computational and storage costs of the learning schemes were discussed. Their experimental results demonstrated that the recurrent forecast models provide better multistep ahead forecasts compared to the persistent method, the atmospheric and time-series models.

Lu et al. (2004) studied a neural network model with principal component analysis (PCA)/radial basis function (RBF) approach for forecasting pollutant trends in Mong Kok urban air, Hong Kong. In their study, the PCA was presented and used to reduce and orthogonolize the input variables of a multilayer feed-forward neural network implemented for air pollutant prediction. A combined PCA/RBF network was proposed and used to forecast the respirable suspended particulates (RSP), nitrogen oxides (NO_x), and nitrogen dioxide (NO_2) concentrations in hourly time series based on the practical air pollutant database compiled from monitoring in the Mong Kok downtown area.

Yalcintas (2006) studied an energy benchmarking model based on the artificial neural network method with a case example for tropical climates. Yalcintas and Akkurt (2005) investigated artificial neural networks applications in building energy predictions and a case study for tropical climates. Artificial neural networks were applied for thermopiezoelectric systems by Sunar (1999). Al-Shehri (1999) studied the artificial neural network method for forecasting residential electrical energy. Bator and Sieniutycz (2006) investigated application of artificial neural network for emission prediction of dust pollutants.

3. MATERIAL AND METHOD

3.1. Artificial Neural Networks

Artificial neural networks are effective and reliable algorithms capable of performing functional input/output mappings. Their parallel, multi-parametric characters, and computing speed, make them a powerful computational tool especially when the underlying physical-mathematical models are complicated. ANNs are also known as universal approximators. Information is processed in a non-algorithmic way. Knowledge is acquired through learning, which means that ANNs can be used to model complex systems for which mathematical descriptions are not available (Rajpal et al., 2006).

A simplified model of a neural network is machine that is designed to model the way in which the brain performs a particular task or function of interest; the network is usually implemented using electronic components or simulated in software on a digital computer (Haykin, 1994). During the past 15 years there has been a substantial increase in the interest on artificial neural networks. ANNs have been applied successfully in a various fields of mathematics, engineering, medicine, economics, meteorology, psychology, and many others (Kalogirou, 2001). They have been used in a wide range of applications including pattern classification, function approximation, optimization, prediction and automatic control and many other engineering problems (Mohandes et al., 2004). This method learns from given examples by constructing an input-output mapping in order to perform predictions. In other words, to train and test a neural network, input data and corresponding output values are necessary (Çam et al., 2005). ANNs can be trained to overcome the limitations of the conventional approaches to solve complex problems that are difficult to model analytically (Sözen et al., 2005).

3.1.1. Biological and Artificial Neurons

A biological neuron is shown in Figure 3.1 (Kalogirou, 2001). In the brain there is a flow of coded information (using electrochemical media, the so-called neurotransmitters) from the synapse towards the axon. The axon of each neuron transmits information to a number of other neurons. The neuron receives information at the synapses from a large number of other neurons. It is estimated that each neuron may receive stimuli from as many as 10,000 other neurons. Groups of neurons are organised into subsystems and the integration of these subsystems forms the brain. It is estimated that the human brain has around 100 billion interconnected neurons.

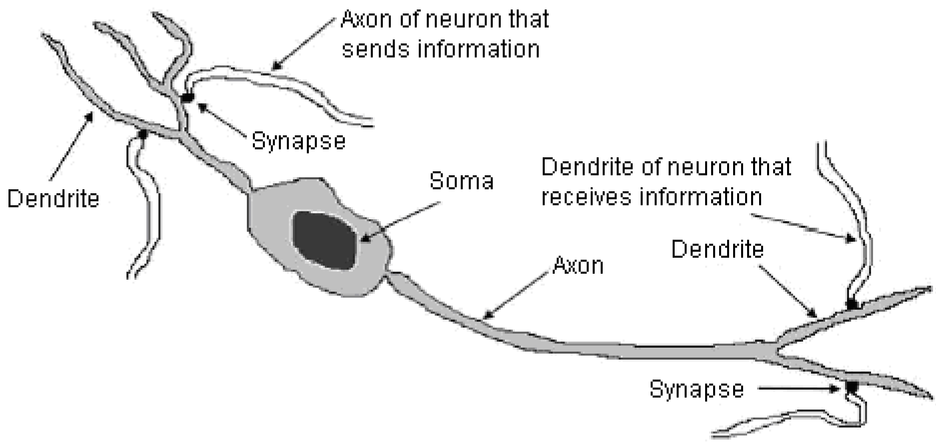

Figure 3.1. A simplified model of a biological neuron

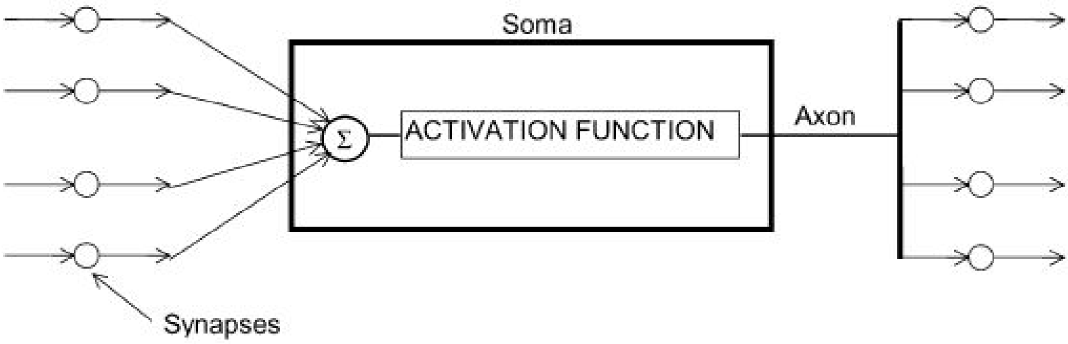

Figure 3.2. A simplified model of an artificial neuron

Figure 3.2 shows a highly simplified model of an artificial neuron, which may be used to simulate some important aspects of the real biological neuron (Kalogirou, 2001). An ANN is a group of interconnected artificial neurons, interacting with one another in a concerted manner. In such a system, excitation is applied to the input of the network. Following some suitable operation, it results in a desired output. At the synapses, there is an accumulation of some potential, which in the case of the artificial neurons is modeled as a connection weight. These weights are continuously modified, based on suitable learning rules.

3.1.2. Models of a Neuron

Fundamental processing element of a neural network is a neuron. The network usually consists of an input layer, some hidden layers and an output layer (Sözen et al., 2005). The model of a neuron is shown in Figure 3.3 (Haykin, 1994).

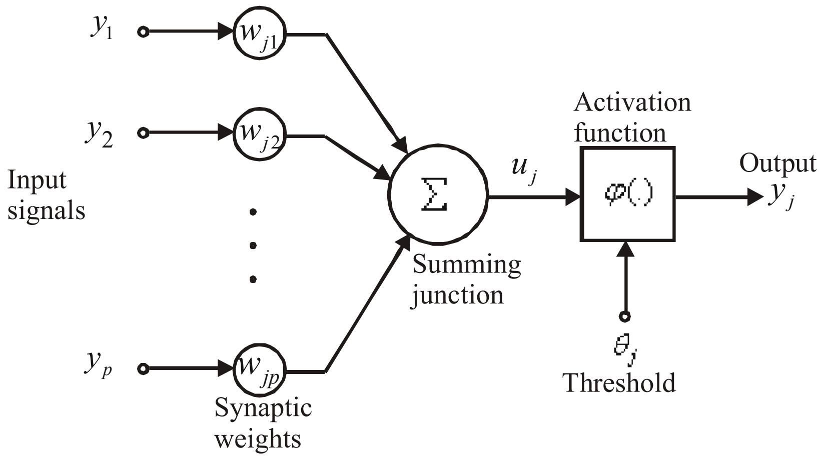

Figure 3.3. Nonlinear model of a neuron

A neuron j may be mathematically described with the following pair of equations (Haykin, 1994);

$$u_j = \sum_{i=0}^{p} w_{ji} y_i \tag{3.1.1}$$

and

$$y_j = \varphi(u_j - \theta_j) \qquad (3.1.2)$$

Haykin (1994) described that the nonlinear model of a neuron that p is the total number of inputs applied to neuron j; y_1, y_2,…..,y_p are the input signals; w_{j1}, w_{j2},......w_{jp} are the synaptic weights of neuron j; u_j is the linear combiner output; θ_j is the threshold; $\varphi(.)$ is the activation function; and y_j is the output signal of the neuron. The use of threshold θ_j has the effect of applying *an affine transformation* to the output u_j of the linear combiner in the model of Figure 3.3 as given by,

$$v_j = u_j - \theta_j \qquad (3.1.3)$$

3.1.3. Types of Transfer Function

Activation or transfer function, denoted by $\varphi(.)$, defines the output of a neuron in terms of activity level its input. Each neuron of ANN has an associated transfer function that determines its output. Transfer functions used in MATLAB software are presented in Table 3.1 (Demuth and Beale, 2004).

Log-Sigmoid transfer function (Logsig) takes input values between plus and minus infinity and squashes the output into the range between 0 and 1 as shown below (Rajpal et al., 2006);

$$f(x) = \frac{1}{1+e^{-x}} \qquad (3.1.4)$$

Hyperbolic Tangent Sigmoid function (Tansig) is another important transfer function. The input can vary from plus to minus infinity. The output of the function varies from -1 to +1 as shown below;

$$f(x) = \frac{e^{x} - e^{-x}}{e^{x} + e^{-x}} \qquad (3.1.5)$$

Table 3.1. Transfer functions and graphs

Transfer function	Graph
Competitive	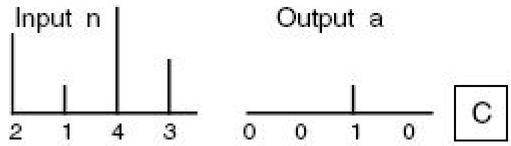 $a = softmax(n)$
Hard-Limit	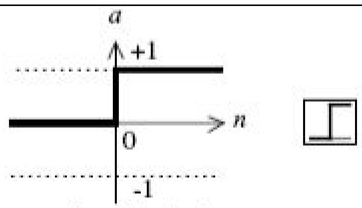 $a = hardlim(n)$
Symmetric Hard-Limit	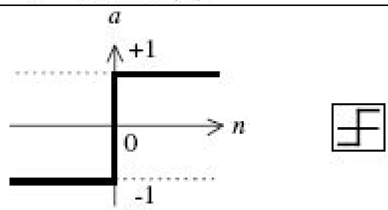 $a = hardlims(n)$
Log-Sigmoid	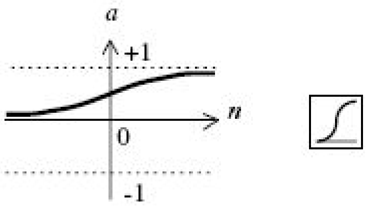 $a = logsig(n)$
Positive linear	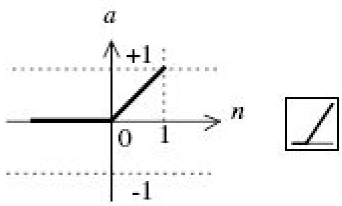 $a = poslin(n)$
Linear	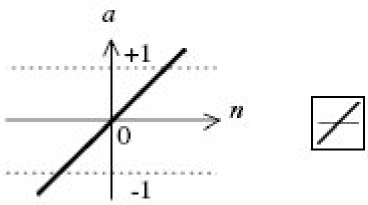 $a = purelin(n)$

Table 3.1. (Continued) Transfer functions and graphs

Transfer function	Graph
Radial Basis	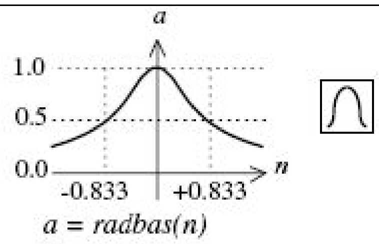
Satlin	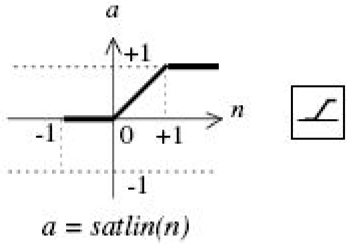
Satlins	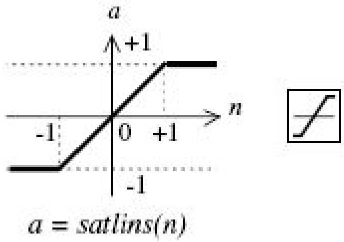
Softmax	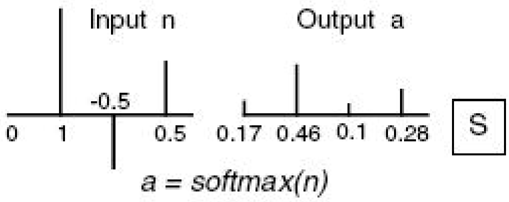
Tan-Sigmoid	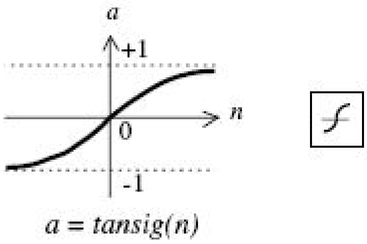
Triangular Basis	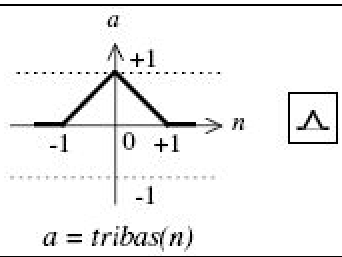

A linear function (Purelin) whose output is equal to its input is usually used at the output stage of the neural network as shown below;

$$f(x) = x \tag{3.1.6}$$

3.1.4. Derivation of the Back-Propagation Algorithm

In the case of neuron j is an output node, Figure 3.4 shows signal-flow graph highlighting the details of output neuron j (Haykin, 1994). The error signal at the output of neuron j at iteration n is defined as;

$$e_j(n) = d_j(n) - y_j(n) \tag{3.1.7}$$

where the symbol $d_j(n)$ refers to the desired response or target output for neuron j and is used to compute $e_j(n)$, the symbol $y_j(n)$ refers to the function signal appearing at the output of neuron j at iteration n (Haykin, 1994).

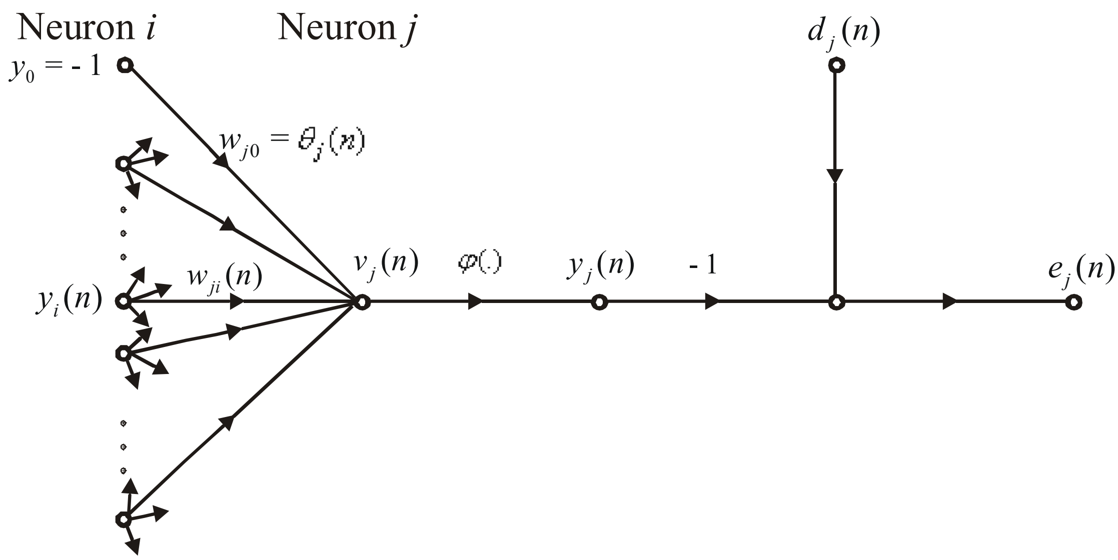

Figure 3.4. Signal-flow graph highlighting the details of output neuron j.

The instantaneous sum of squared errors of the network is written as;

$$E(n)=\frac{1}{2}\sum e_j^2(n) \tag{3.1.8}$$

As shown in Figure 3.4, the net internal activity level $v_j(n)$ produced at the input of the nonlinearity associated with neuron j is therefore presented as;

$$v_j(n)=\sum_{i=0}^{p} w_{ji}(n)y_i(n) \tag{3.1.9}$$

Where p is the total number of inputs (excluding the threshold) applied to neuron j. The synaptic weight w_{j0} (corresponding to the fixed input y_0=-1) equals the threshold θ applied to neuron j. The function signal $y_j(n)$ appearing at the output of neuron j at iteration n is,

$$y_j(n)=\varphi_j(v_j(n)) \tag{3.1.10}$$

The back-propagation algorithm applies a correction $\Delta w_{ji}(n)$ to the synaptic weight $w_{ji}(n)$, which is proportional to the instantaneous gradient $\partial E(n)/\partial w_{ji}(n)$. This gradient may be expressed as follows (Haykin, 1994);

$$\frac{\partial E(n)}{\partial w_{ji}(n)}=\frac{\partial E(n)}{\partial e_j(n)}\frac{\partial e_j(n)}{\partial y_j(n)}\frac{\partial y_j(n)}{\partial v_j(n)}\frac{\partial v_j(n)}{\partial w_{ji}(n)} \tag{3.1.11}$$

Differentiating both sides of Eq. (3.1.8) with respect to $e_j(n)$, we get;

$$\frac{\partial E(n)}{\partial e_j(n)}=e_j(n) \tag{3.1.12}$$

Differentiating both sides of Eq. (3.1.7) with respect to $y_j(n)$, we get;

$$\frac{\partial e_j(n)}{\partial y_j(n)} = -1 \tag{3.1.13}$$

Next, differentiating both sides of Eq. (3.1.10) with respect to $v_j(n)$, leads to;

$$\frac{\partial y_j(n)}{\partial v_j(n)} = \varphi_j'(v_j(n)) \tag{3.1.14}$$

Finally, differentiating Eq. (3.1.9) with respect to $w_{ji}(n)$ yields;

$$\frac{\partial v_j(n)}{\partial w_{ji}(n)} = y_i(n) \tag{3.1.15}$$

Hence, the use of Eqs. (3.1.12) and (3.1.15) in (3.1.11) gives;

$$\frac{\partial E(n)}{\partial w_{ji}(n)} = -e_j(n)\varphi_j'(v_j(n))y_j(n) \tag{3.1.16}$$

The correction $\Delta w_{ji}(n)$ applied to $w_{ji}(n)$ is defined by the delta rule;

$$\Delta w_{ji}(n) = -\eta \frac{\partial E(n)}{\partial w_{ji}(n)} \tag{3.1.17}$$

where η is a constant that determines the rate of learning; it is called the learning-rate parameter of the back-propagation algorithm. The use of Eq. (3.1.16) in (3.1.17) yields;

$$\Delta w_{ji}(n) = \eta\delta_j(n)y_i(n) \tag{3.1.18}$$

where the local gradient $\delta_j(n)$ is defined as;

$$\delta_j(n) = -\frac{\partial E(n)}{\partial e_j(n)} \frac{\partial e_j(n)}{\partial y_j(n)} \frac{\partial y_j(n)}{\partial v_j(n)} \tag{3.1.19}$$

$$\delta_j(n) = e_j(n)\varphi_j^{'}(v_j(n)) \tag{3.1.20}$$

The local gradient points require changes in synaptic weights. According to Eq. (3.1.20), the local gradient $\delta_j(n)$ for output neuron *j* is equal to the product of the corresponding error signal $e_j(n)$ and the derivate $\varphi_j^{'}(v_j(n))$ of the associated activation function.

From Eqs. (3.1.18) and (3.1.20) we note that a key factor involved in the calculation of the weight adjustment $\Delta w_{ji}(n)$ is the error signal $e_j(n)$ at the output of neuron *j*. In this context, we may identify two distinct cases, depending on where in the network neuron *j* is located. In case I, neuron *j* is an output node. This case is simple to handle, because each output node of the network is supplied with a desired response of its own, making it a straightforward matter to calculate the associated error signal. In case II, neuron *j* is a hidden node. Even though hidden neurons are not directly accessible, they share responsibility for any error made at the output of the network.

Case I: Neuron j is an output node

When neuron *j* is located in the output layer of the network, it would be supplied with a desired response of its own. Hence we may use Eq. (3.1.7) to compute the error signal $e_j(n)$ associated with this neuron as seen Figure 3.4. Having determined $e_j(n)$, it is a straightforward matter to compute the local gradient $\delta_j(n)$ using Eq. (3.1.20).

Case II: Neuron j is a hidden node

When neuron j is located in a hidden layer of the network, there is no specified desired response for that neuron. Accordingly, the error signal for a hidden neuron would have to be determined recursively in terms of the error signals of all the neurons to which that hidden neuron is directly connected; this is where the development of the back-propagation algorithm gets complicated. Consider the situation depicted in Figure (3.5), which depicts neuron j is a hidden node of the network. According to Eq. (3.1.20), we may redefine the local gradient $\delta_j(n)$ for hidden neuron j as;

$$\delta_j(n) = -\frac{\partial E(n)}{\partial y_j(n)} \frac{\partial y_j(n)}{\partial v_j(n)} \tag{3.1.21}$$

$$\delta_j(n) = -\frac{\partial E(n)}{\partial y_j(n)} \varphi_j^{'}(v_j(n)), \qquad \text{neuron j is hidden} \tag{3.1.22}$$

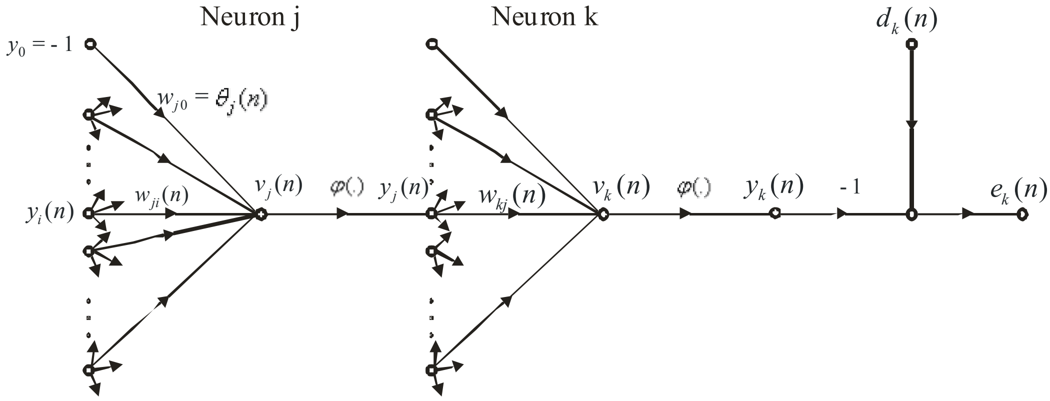

Figure 3.5. Signal-flow graph highlighting the details of output neuron k connected to hidden neuron j

Where, in the second line, we have made use of Eq. (3.1.14). To calculate the partial derivative $\partial E(n)/\partial y_j(n)$, we may proceed as follows. From Figure (3.5) we see that,

$$E(n) = \frac{1}{2}\sum_{k \in C} e_k^2(n), \quad \text{neuron } k \text{ is an output node} \tag{3.1.23}$$

which is a rewrite of Eq. (3.1.8) except for the use of index k in place of index j. We have done so in order to avoid confusion with the use of index j that refers to a hidden neuron under case II. In any event, differentiating Eq. (3.1.23) with respect to the function signal $y_j(n)$, we get,

$$\frac{\partial E(n)}{\partial y_j(n)} = \sum_k e_k \frac{\partial e_k(n)}{\partial y_j(n)} \tag{3.1.24}$$

Next, we use the chain rule for the partial derivative $\partial e_k(n)/\partial y_j(n)$, and thus rewrite Eq. (3.1.24) in the equivalent form,

$$\frac{\partial E(n)}{\partial y_j(n)} = \sum_k e_k \frac{\partial e_k(n)}{\partial v_k(n)} \frac{\partial v_k(n)}{\partial y_j(n)} \tag{3.1.25}$$

However, from Figure 3.5, we note that

$$e_k(n) = d_k(n) - y_k(n) \tag{3.1.26}$$

$$e_k(n) = d_k(n) - \varphi_k(v_k(n)), \quad \text{neuron } k \text{ is an output node} \tag{3.1.27}$$

Hence,

$$\frac{\partial e_k(n)}{\partial v_k(n)} = -\varphi_k^{'}(v_k(n)) \tag{3.1.28}$$

We also note from Figure 3.5 that for neuron k, the net internal activity level is

$$v_k(n) = \sum_{j=0}^{q} w_{kj}(n) y_j(n) \tag{3.1.29}$$

where q is the total number of inputs (excluding the threshold) applied to neuron k. Here again, the synaptic weight $w_{k0}(n)$ is equal to the threshold $\theta_k(n)$ applied to neuron k and the corresponding input y_0 is fixed at the value -1. In any event, differentiating Eq. (3.1.29) with respect to $y_j(n)$ yields,

$$\frac{\partial v_k(n)}{\partial y_j(n)} = w_{kj}(n) \tag{3.1.30}$$

Thus, using Eqs. (3.1.28) and (3.1.30) in (3.1.25), we get the desired partial derivative;

$$\frac{\partial E(n)}{\partial y_j(n)} = -\sum_k e_k(n) \varphi_k^{'}(v_k(n)) w_{kj}(n) \tag{3.1.31}$$

$$\frac{\partial E(n)}{\partial y_j(n)} = -\sum_k \delta_k(n) w_{kj}(n) \tag{3.1.32}$$

where, in the second line, we have used the definition of the local gradient $\delta_j(n)$ given in Eq. (3.1.20) with the index k substituted for j. Finally, using Eq. (3.1.32) in (3.1.22), we get the local gradient $\delta_j(n)$ for hidden neuron j, after rearranging terms, as follows;

$$\delta_j(n) = \varphi_j^{'}(v_j(n)) \sum_k \delta_k(n) w_{kj}(n), \qquad \text{neuron } j \text{ is hidden} \tag{3.1.33}$$

We may now summarize the relations that we have derived for the back-propagation algorithm. First, the correction $\Delta w_{ji}(n)$ applied to the synaptic weight connecting neuron i to neuron j is defined by the delta rule;

$$\begin{pmatrix} Weight \\ correction \\ \Delta w_{ji}(n) \end{pmatrix} = \begin{pmatrix} learning \\ rate\ parameter \\ \eta \end{pmatrix} . \begin{pmatrix} local \\ gradient \\ \delta_j(n) \end{pmatrix} . \begin{pmatrix} input\ signal \\ of\ neuron\ j \\ y_i(n) \end{pmatrix} \tag{3.1.34}$$

According to the method of steepest descent, given the old value of the jith weight $w_{ji}(n)$ at iteration n, the updated value of this weight at the next iteration $n+1$ is computed as;

$$w_{ji}(n+1) \quad w_{ji}(n) + \Delta w_{ji}(n) \tag{3.1.35}$$

3.1.5. Basic Learning Laws

Many learning laws are in common use. Most of these laws are some sort of variation of the best known and oldest learning law, Hebb's Rule (Anderson and McNeil, 1992). Research into different learning functions continues as new ideas routinely show up in trade publications. Some researchers have the modeling of biological learning as their main objective. Others are experimenting with adaptations of their perceptions of how nature handles learning. Either way, man's understanding of how neural processing actually works is very limited. Learning is certainly more complex than the simplifications represented by the learning laws currently developed.

3.1.5.1. Hebb's Rule

The first, and undoubtedly the best known, learning rule was introduced by Donald Hebb (Anderson and McNeil, 1992). His basic rule is: If a neuron receives an input from another neuron, and if both are highly active (mathematically have the same sign), the weight between the neurons should be strengthened.

3.1.5.2. Hopfield Law

It is similar to Hebb's rule with the exception that it specifies the magnitude of the strengthening or weakening. It states, "if the desired output and the input are both active or both inactive, increment the connection weight by the learning rate, otherwise decrement the weight by the learning rate."

3.1.5.3. The Delta Rule

This rule is a further variation of Hebb's Rule (Anderson and McNeil, 1992). It is one of the most commonly used. This rule is based on the simple idea of continuously modifying the strengths of the input connections to reduce the difference (the delta) between the desired output value and the actual output of a processing element. This rule changes the synaptic weights in the way that minimizes the mean squared error of the network. This rule is also referred to as the Widrow-Hoff Learning Rule and the Least Mean Square (LMS) Learning Rule. The way that the Delta Rule works is that the delta error in the output layer is transformed by the derivative of the transfer function and is then used in the previous neural layer to adjust input connection weights. In other words, this error is back-propagated into previous layers one layer at a time. The process of back-propagating the network errors continues until the first layer is reached. The network type called Feedforward, Back-propagation derives its name from this method of computing the error term. When using the delta rule, it is important to ensure that the input data set is well randomized. Well ordered or structured presentation of the training set can lead to a network which can not converge to the desired accuracy. If that happens, then the network is incapable of learning the problem.

3.1.5.4. The Gradient Descent Rule

This rule is similar to the Delta Rule in that the derivative of the transfer function is still used to modify the delta error before it is applied to the connection weights (Anderson and McNeil, 1992). Here, however, an additional proportional constant tied to the learning rate is appended to the final modifying factor acting upon the weight. This rule is commonly used, even though it converges to a point of stability very slowly.

It has been shown that different learning rates for different layers of a network help the learning process converge faster. In these tests, the learning rates for those layers close to the output were set lower than those layers near the input. This is especially important for applications where the input data is not derived from a strong underlying model.

3.1.5.5. Kohonen's Learning Law

This procedure, developed by Teuvo Kohonen, was inspired by learning in biological systems (Anderson and McNeil, 1992). In this procedure, the processing elements compete for the opportunity to learn, or update their weights. The processing element with the largest output is declared the winner and has the capability of inhibiting its competitors as well as exciting its neighbors. Only the winner is permitted an output, and only the winner plus its neighbors are allowed to adjust their connection weights.

Further, the size of the neighborhood can vary during the training period. The usual paradigm is to start with a larger definition of the neighborhood, and narrow in as the training process proceeds. Because the winning element is defined as the one that has the closest match to the input pattern, Kohonen networks model the distribution of the inputs. This is good for statistical or topological modeling of the data and is sometimes referred to as self-organizing maps or self-organizing topologies.

3.1.6. Training Algorithms

There are several different back-propagation training algorithms. They have a variety of different computation and storage requirements, and no one algorithm is best suited to all locations. Table 3.2 summarizes the training algorithms included in MATLAB software (Demuth and Beale, 2004).

Table 3.2. Training algorithms

Function	Description
traingd	Basic gradient descent. Slow response, can be used in incremental mode training.
traingdm	Gradient descent with momentum. Generally faster than traingd. Can be used in incremental mode training.
traingdx	Adaptive learning rate. Faster training than traingd, but can only be used in batch mode training.
trainrp	Resilient back-propagation. Simple batch mode training algorithm with fast convergence and minimal storage requirements.
traincgf	Fletcher-Reeves conjugate gradient algorithm. Has smallest storage requirements of the conjugate gradient algorithms.
traincgp	Polak-Ribiere conjugate gradient algorithm. Slightly larger storage requirements than traincgf. Faster convergence on some problems.
traincgb	Powell- Beale conjugate gradient algorithm. Slightly larger storage requirements than traincgp. Generally faster convergence.
trainscg	Scaled conjugate gradient algorithm. The only conjugate gradient algorithm that requires no line search. A very good general purpose training algorithm.
trainbfg	BFGS quasi-Newton method. Requires storage of approximate Hessian matrix and has more computation in each iteration than conjugate gradient algorithms, but usually converges in fewer iterations.
trainoss	One step secant method. Compromise between conjugate gradient methods and quasi-Newton methods.
trainlm	Levenberg-Marquardt algorithm. Fastest training algorithm for networks of moderate size. Has memory reduction feature for use when the training set is large.
trainbr	Bayesian regularization. Modification of the Levenberg-Marquardt training algorithm to produce networks that generalizes well. Reduces the difficulty of determining the optimum network architecture.

3.1.6.1. Resilient Back-propagation (trainrp)

Multilayer networks typically use sigmoid transfer functions in the hidden layers. These functions are often called “squashing” functions, since they compress an infinite input range into a finite output range. Sigmoid functions are characterized by the fact that their slope must approach zero as the input gets large. This causes a problem when using steepest descent to train a multilayer network with sigmoid functions, since the gradient can have a very small magnitude; and therefore, cause small changes in the weights and biases, even though the weights and biases are far from their optimal values. The purpose of the resilient back-propagation training algorithm is to eliminate these harmful effects of the magnitudes of the partial derivatives.

3.1.6.2. Scaled Conjugate Gradient (trainscg)

Each of the conjugate gradient algorithms that we have discussed so far requires a line search at each iteration. This line search is computationally expensive, since it requires that the network response to all training inputs be computed several times for each search. The scaled conjugate gradient algorithm (SCG) was designed to avoid the time-consuming line search. This algorithm is too complex to explain in a few lines, but the basic idea is to combine the model-trust region approach with the conjugate gradient approach.

3.1.6.3. Levenberg-Marquardt (trainlm)

The Levenberg-Marquardt algorithm was designed to approach second-order training speed without having to compute the Hessian matrix. When the performance function has the form of a sum of squares (as is typical in training feedforward networks), then the Hessian matrix is approximated and the gradient is computed with the Jacobian matrix that is computed through a standard back-propagation technique.

3.1.7. Benefits of Neural Networks in This Study

It is apparent that a neural network derives its computing power through, first, its massively parallel distributed structure and, second, its ability to learn and therefore generalize; generalization refers to the neural network producing reasonable outputs for inputs not encountered during training. These two information-processing capabilities make it possible for neural networks to solve complex (large-scale) problems that are currently intractable. In practice, however, neural networks cannot provide the solution working by themselves alone. Rather, they need to be integrated into a consistent system engineering approach. The use of neural networks offers the following useful properties and capabilities (Haykin, 1994):

1. Nonlinearity: Weibull distribution function is utilized for evaluating the mean wind speed and potential of any region. This function must be considered a linear form to obtain weibull parameters. Therefore analytical calculation of weibull parameters is possible with the help of the least squares method. On the other hand, a neuron is basically a nonlinear device. Consequently, a neural network, made up of an interconnection of neurons, is itself nonlinear. Nonlinearity is a highly important property, particularly if the underlying physical mechanism responsible for the generation of an input signal is inherently nonlinear.

2. Input-Output Mapping: A popular paradigm of learning called supervised learning involves the modification of the synaptic weights of a neural network by applying a set of labeled training samples or task examples. Each example consists of a unique input signal and the corresponding desired response. The training of the network is repeated for many examples in the set until the network reaches a steady state, where there are no further significant changes in the synaptic weights. Thus the network learns from the examples by constructing an input-output mapping for the problem at hand. In this study, an input-output mapping has been constructed between the input signal and the corresponding desired response to estimate wind speed and wind power potential.

3. Adaptivity: Neural networks have a built-in capability to adapt their synaptic weights to changes in the surrounding environment. In particular, a neural network trained to operate in a specific environment can be easily retrained to deal with minor changes in the operating environmental conditions. Moreover, when it is operating in a nonstationary environment, a neural network can be designed to change its synaptic weights in real time. The natural architecture of a neural network for pattern classification, signal processing and control applications, coupled with the adaptive capability of the network, make it an ideal tool for use in adaptive pattern classification, adaptive signal processing and adaptive control.

4. VLSI Implementability: A neural network is a machine that is designed to model the way in which the brain performs a particular task or function of interest; the network is usually implemented using electronic components or simulated in software on a digital computer. The massively parallel nature of a neural network makes it potentially fast for the computation of certain tasks. This same feature makes a neural network ideally suited for implementation using *very-large-scale-integrated* (VLSI) technology. The particular virtue of VLSI is that it provides a means of capturing truly complex behavior in a highly hierarchical fashion, which makes it possible to use a neural network as a tool for real-time applications.

5. Neurobiological Analogy: The design of a neural network is motivated by analogy with the brain, which is a living proof that fault-tolerant parallel processing is not only physically possible but also fast and powerful. Neurobiologists look to (artificial) neural networks as a research tool for the interpretation of neurobiological phenomena. On the other hand, engineers look to neurobiology for new ideas to solve problems more complex than those based on conventional hard-wired design techniques. In this study, the method of artificial neural network will be applied to predict wind speed which is often considered as one of the most difficult meteorological parameters to forecast due to the result of the complex interactions between large scale forcing mechanisms such as pressure and temperature differences, the rotation of the earth and local characteristics of the surface.

3.1.8. Computer Program Used in MATLAB

MATLAB simulations were performed to estimate mean wind speed using artificial neural networks. This program was performed as,

```
p=ogren;
t1=hedef;
net = newff(minmax(p),[6 1],{'logsig' 'purelin'},'trainscg');
net.trainParam.epochs = 1000;
net.trainParam.goal = 0.0005;
net = train(net,p,t1);
y1 = sim(net,p);
p=test;
t2=gercek;
y2=sim(net,p);
x1=1:509;
x2=1:204;
plot(x1,t1,x1,y1)
plot(x2,t2,x2,y2)
end
final_hidden_layer_weights=net.iw{1,1}
final_output_layer_weights=net.lw{2,1}
final_hidden_bias_weights=net.b{1}
final_output_bias_weights=net.b{2}
```

3.2. Multiple Linear Regression Analysis

Multiple regression analysis is one of the most widely used methodologies for expressing the dependence of a response variable on several independent variables (Abdul-Wahab et al., 2005). The first step in regression analysis is to select independent variables for constructing a model. Here, the important peculiarity is;

1. to pick out adequate dependent variables,
2. to discover linear correlations of cause and effect between dependent and independent variables, and
3. to include only related independent variables to the model.

If there are too many independent variables, the variables which provide substantial contribution to the interpretation of the variations of dependent variables must be selected (Sahinler, 2000).

Multiple linear regression is presently formulated for the case of two variables as (Chapra and Canale, 1985);

$$y = a_0 + a_1 x_1 + a_2 x_2 + e \tag{3.2.1}$$

Where the coefficients that minimize the sum of the squares of the residuals are determined by solving,

$$\begin{bmatrix} n & \sum x_{1i} & \sum x_{2i} \\ \sum x_{1i} & \sum x_{1i}^2 & \sum x_{1i} x_{2i} \\ \sum x_{2i} & \sum x_{1i} x_{2i} & \sum x_{2i}^2 \end{bmatrix} \begin{bmatrix} a_0 \\ a_1 \\ a_2 \end{bmatrix} = \begin{bmatrix} \sum y_i \\ \sum x_{1i} y_i \\ \sum x_{2i} y_i \end{bmatrix} \tag{3.2.2}$$

Where n is input number of data points, a_0, a_1 and a_2 are unknown coefficients, e is the error or residual between the model and the observations, y is the dependent value and, x_1 and x_2 are the independent values.

3.3. WAsP Program

In this study, Wind Atlas Analysis and Application Program (WAsP) was also used to investigate wind characteristics of sites. WAsP program and associated software has been developed by Riso National Laboratory, Denmark. WAsP is a PC-program for the vertical and horizontal extrapolation of wind climate statistics. It contains several models to describe the wind flow over different terrains and close to sheltering obstacles. WAsP consists of five main calculation blocks such as analysis of raw data, generation of wind atlas data, wind climate estimation, estimation of wind power potential and calculation of wind farm production (Mortensen et al., 2001).

Four basic data are considered necessary for WAsP packet program that is used in the determination of wind power potential. These are hourly wind speed and direction, sheltering obstacles, surface roughness changes and orographic data (terrain height). Obstacles have an impact on the wind speed and alter the wind direction particularly for lower level of height. If there are obstacles around measurement station, wind speeds must be reconsidered again by taking the effect of these parameters into account (Bilgili et al., 2004). In deciding about the effectiveness of the wind speed measurement around a site, the topographic and climatic conditions must be taken into consideration. Especially, any method of wind speed predictions should consider the topographic and climatologic features. The wind speed measured at a site is determined mainly by two factors; the overall weather systems (which usually have an extent of several hundred kilometers) and the nearby topography within few kilometers of the station. The collective effect of the terrain surface and obstacles, leading to an overall retarding of the wind near the ground, is referred to as the roughness of the terrain. Orographic elements such as hills, cliffs, ridges, and escarpments exert an additional influence on the wind. s and orography are amongst the main factors that affect the wind speed (Durak and Şen, 2002).

3.4. Weibull and Rayleigh Distribution Function

Generally, previously measured wind data are used for the estimation of wind power potential of any area. First of all, at any locations, hourly wind speeds and wind directions are first observed and monitored. These results are used for frequency and probability modeling. Wind speed data in time-series format is usually arranged in the frequency distribution format since it is more convenient for statistical analysis. Therefore, the available time-series data were translated into frequency distribution format. The wind speed probability distributions and the functions representing them mathematically are the main tools used in the wind-related literature. Their use includes a wide range of applications, from the techniques used to identify the parameters of the distribution functions to the use of such functions for analyzing the wind speed data and wind energy economics (Çelik, 2003).

There are various methods to establish an adequate statistical model for obtaining the wind speed frequency distribution, which may later be used for predicting the wind energy potential. The Weibull distribution has been accepted to give a good fit to wind data wind energy applications (Incecik and Erdoğmuş, 1995). The Weibull distribution is a two-parameter distribution. This distribution is expressed as;

$$f_W(v) = \left(\frac{k}{c}\right)\left(\frac{v}{c}\right)^{k-1} \exp\left[-\left(\frac{v}{c}\right)^k\right] \tag{3.4.1}$$

Where $f_W(v)$ is the probability of observing wind speed v, k is the Weibull shape parameter (dimensionless) and c is the Weibull scale parameter, which has a reference value in the units of wind speed (Akpinar and Akpinar, 2004). Besides, the cumulative probability function of the Weibull distribution is calculated as below.

$$F_W(v) = 1 - \exp\left[-\left(\frac{v}{c}\right)^k\right] \tag{3.4.2}$$

There are several methods of determining Weibull k and c parameters, such as least-square fit to observed distribution method, mean wind speed-standard deviation method, the maximum likelihood method (Genc et al., 2005; Çelik, 2004; Gökçek et al., 2007; Seguro and Lambert, 2000). In this study, the two parameters k and c, are obtained using mean wind speed-standard deviation method. According to this method, Weibull k and c parameters are expressed with Eq. (3.4.3) and Eq. (3.4.4), respectively (Gökçek et al., 2007).

$$k = \left(\frac{\sigma}{v_m}\right)^{-1.086} \qquad (1 \le k \le 10) \tag{3.4.3}$$

$$c = \frac{v_m}{\Gamma(1+1/k)} \tag{3.4.4}$$

Where v_m is the mean wind speed and is calculated using Eq. (3.4.5). σ is the standard deviation and is calculated using Eq. (3.4.6). $\Gamma()$ is the Gamma function. For any y value, it is usually written as Eq. (3.4.7) (Gökçek et al., 2007).

$$v_m = \frac{1}{n}\left[\sum_{i=1}^{n} v_i\right] \tag{3.4.5}$$

$$\sigma = \left[\frac{1}{n-1}\sum_{i=1}^{n}\left(v_i - v_m\right)^2\right]^{1/2} \tag{3.4.6}$$

$$\Gamma(y) \quad \int_0^\infty \exp\left(-x\right)x^{y-1}dx \tag{3.4.7}$$

Where n is the number of hours in the period of the considered time such as month, season or year.

The Rayleigh function is a special and simplified case of the Weibull function. It is obtained when the shape factor c of the Weibull function is assumed to be equal to 2. The Rayleigh probability density function and cumulative density function are given by (Gökçek et al., 2007),

$$f_R(v) = \frac{\pi v}{2v_m^2}\exp\left[-\left(\frac{\pi}{4}\right)\left(\frac{v}{v_m}\right)^2\right] \tag{3.4.8}$$

$$F_R(v) = 1 - \exp\left[-\left(\frac{\pi}{4}\right)\left(\frac{v}{v_m}\right)^2\right] \tag{3.4.9}$$

The two significant parameters k and c are closely related to the mean value of the wind speed v_m as (Akpinar and Akpinar, 2004),

$$v_m = c\Gamma\left(1+\frac{1}{k}\right) \tag{3.4.10}$$

It is well known that the power of the wind that flows at speed v through a blade sweep area A increases as the cube of its velocity and is given by (Çelik, 2003)

$$P(v) = \frac{1}{2}\rho A v^3 \tag{3.4.11}$$

The wind power density of the considered site per unit area based on any probability density function can be expressed as (Akpinar and Akpinar, 2004),

$$P(v) = \frac{1}{2}\rho\int_0^\infty v^3 f(v)dv \tag{3.4.12}$$

Where ρ =1.225 kg/m^3 is the air density. Wind power density per unit area of a site based on a Weibull probability density function can be expressed as follows,

$$P_W = \frac{1}{2}\rho c^3\Gamma\left(1+\frac{3}{k}\right) \tag{3.4.13}$$

Setting k equal to 2, the mean wind speed and the power density for the Rayleigh density function is found to be (Çelik, 2003; Akpinar and Akpinar; 2006)

$$v_m = c\sqrt{\pi/4} \tag{3.4.14}$$

$$P_R = \frac{3}{\pi}\rho v_m^3 \tag{3.4.15}$$

4. RESULTS AND DISCUSSION

4.1. Wind Power Potential of the Eastern Mediterranean Region of Turkey

4.1.1. Wind Data

Hourly measured wind speeds and directions gathered from eight stations, located in the south-eastern region of Turkey, were used to investigate wind power potential of this region. The long-term wind data, containing hourly wind speed and direction information, covers the period between 1992 and 2001. The information about the location of the stations and the elevations above the sea level are given in Table 4.1. Besides, the map of the region, the locations of the stations and the dominant prevailing wind direction for each station; and topographical map of the region are presented in Figure 4.1 and Figure 4.2, respectively. Except Adana and Antakya; all stations are located on the costal site.

Table 4.1. Locations of stations

Station	Latitude	Longitude	Altitude (m)	Height of Anemometer (m)
Antakya	$36^0.12'$	$36^0.10'$	100	10
İskenderun	$36^0.35'$	$36^0.10'$	4	10
Karataş	$36^0.34'$	$35^0.23'$	22	10
Yumurtalık	$36^0.46'$	$35^0.47'$	27	10
Dörtyol	$36^0.51'$	$36^0.13'$	28	10
Samandağ	$36^0.05'$	$35^0.58'$	4	10
Adana	$36^0.59'$	$35^0.18'$	28	10

The direction of the wind is crucially important for the evaluation of the possibilities of utilizing wind power. Table 4.2 shows the sectoral frequencies of wind direction at the given meteorological stations. According to this table, the dominant prevailing wind directions for Antakya, Samandağ and Karataş

Meteorological Stations are 210^{o}, on the other hand for Adana, Yumurtalık, Dörtyol and İskenderun are 0^{0}, 30^{0}, 120^{0} and 300^{0}, respectively.

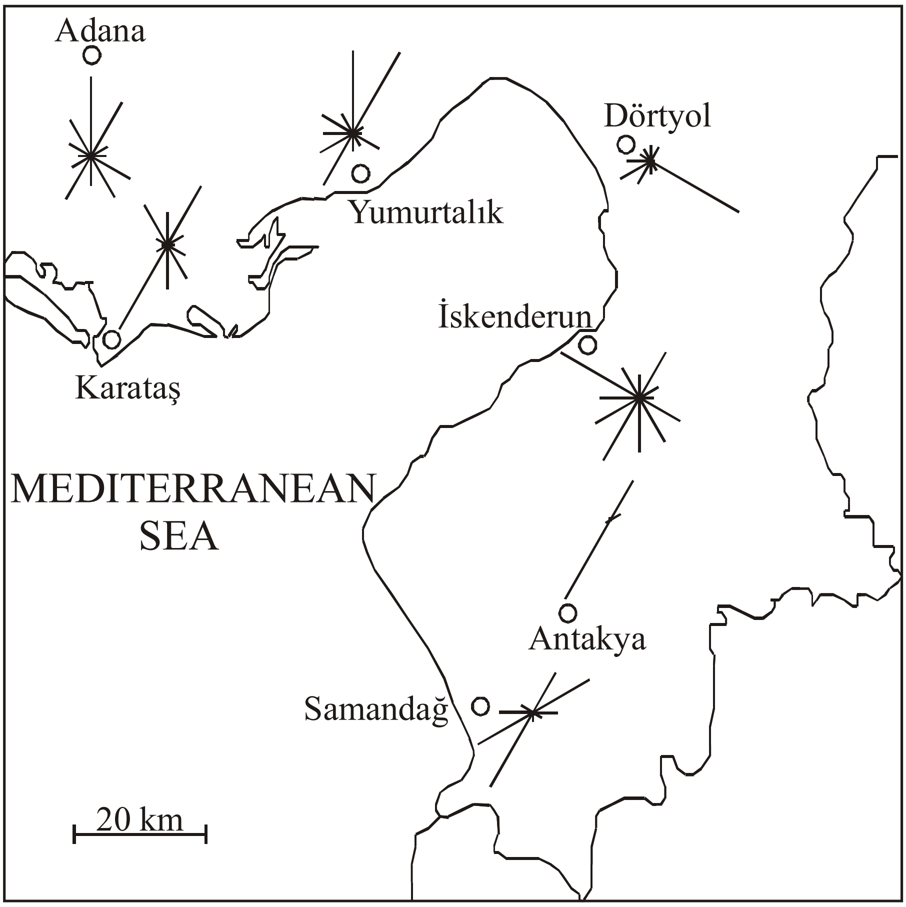

Figure 4.1. The map of the region, location and dominant wind direction of the stations

The Weibull parameters (*k* and *c*) of hourly wind speeds observed at the stations and the values of the mean wind speed and potential are given in Table 4.3. The values of the shape parameter (*k*) and scale parameter (*c*) have been found to be slightly dependent on the condition of stations. Parameter scale values are near to the average wind speeds, which mean that the Weibull distribution is a reasonable fit to the present data. The mean wind speed varies mainly from 0.8 m/s to a maximum 4.0 m/s as seen in this table.

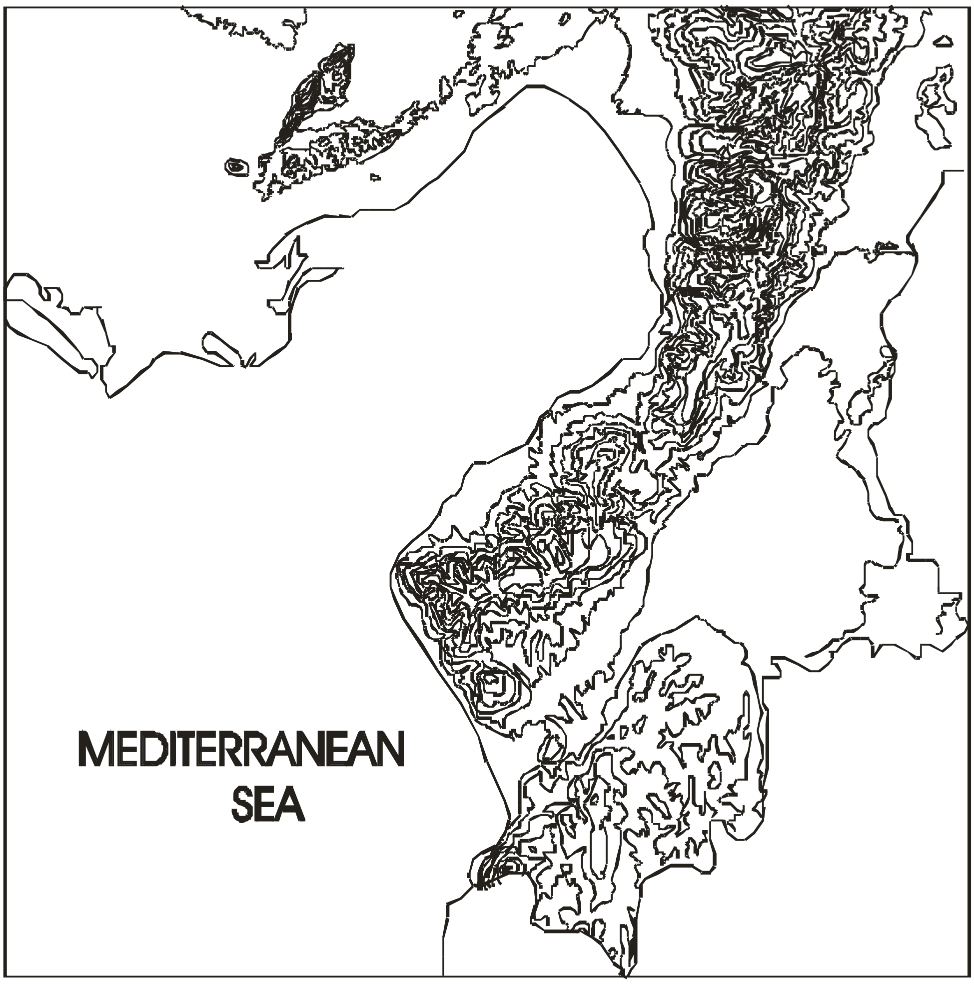

Figure 4.2. Topographical map of the region

Figures 4.3-9 show the frequency distribution of wind speeds for meteorological stations. The frequency distribution of the wind speeds help towards answering questions such as: How long is a wind power plant out of action in the case of lack of wind, which is the range of the most frequent wind speeds? How often does the wind power plant achieve its rated output? The hourly wind speed is higher than 3 m/s 41% of occasions at the Antakya meteorological station. The hourly wind speed is higher than 3 m/s 31% of the time at the İskenderun meteorological station. Similarly, hourly wind speed is higher than 3 m/s 72% of the time at the Samandağ meteorological station.

Table 4.2. The sectoral frequencies of wind direction at meteorological stations

Direction	Frequency(%)						
	Antakya	İskenderun	Karataş	Yumurtalık	Dörtyol	Samandağ	Adana
N(0^0)	2.0	4.2	8.1	18.6	5.7	0,2	17,7
NE(30^0)	27.6	9.5	16.8	21.0	5.8	12,9	13,9
EN(60^0)	7.3	4.0	4.6	2.7	0.9	18,4	4,2
E(90^0)	0.5	2.7	1.8	1.9	1.4	6,8	3,3
ES(120^0)	0.4	8.5	5.0	6.9	36.6	2,8	10,1
SE(150^0)	0.2	9.1	9.6	3.2	4.0	0,8	10,6
S(180^0)	0.7	9.9	10.8	4.0	4.8	2,5	6,5
SW(210^0)	55.1	13.2	24.0	13.3	9.5	24,1	11,1
WS(240^0)	3.4	9.1	3.2	8.6	12.8	17,8	4,8
W(270^0)	0.8	7.2	1.3	6.6	8.7	9,5	2,9
WN(330^0)	0.6	16.4	3.3	8.1	4.6	3,8	5,6
NW(330^0)	1.3	6.3	11.6	5.0	5.0	0,5	9,3

Table 4.3. Hourly wind data at meteorological stations

Station	Period (year)	Weibull parameter (c) (m/s)	Weibull parameter (k)	Mean wind speed (m/s)	Mean energy density (W/m^2)
Antakya	1997-2001	3.1	1.70	2.8	29
İskenderun	"	2.7	1.21	2.6	37
Karataş	"	3.1	1.94	2.7	25
Yumurtalık	"	2.1	1.27	1.9	15
Dörtyol	"	1.1	1.34	0.9	2
Samandağ	"	4.6	2.18	4.0	71
Adana	"	0.9	0.98	0.8	3

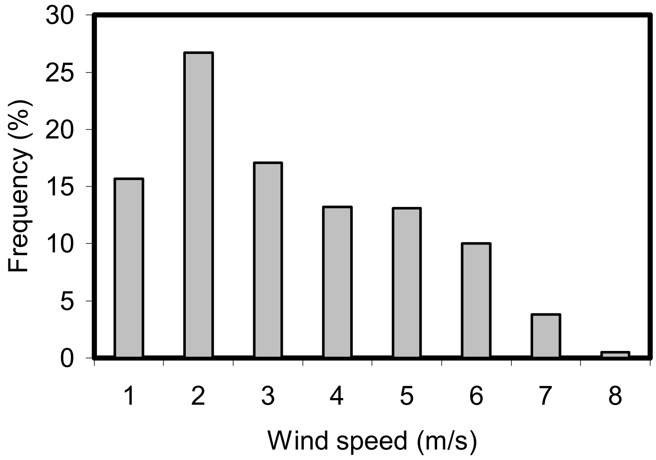

Figure 4.3. Frequency distribution of wind speeds for Antakya meteorological station

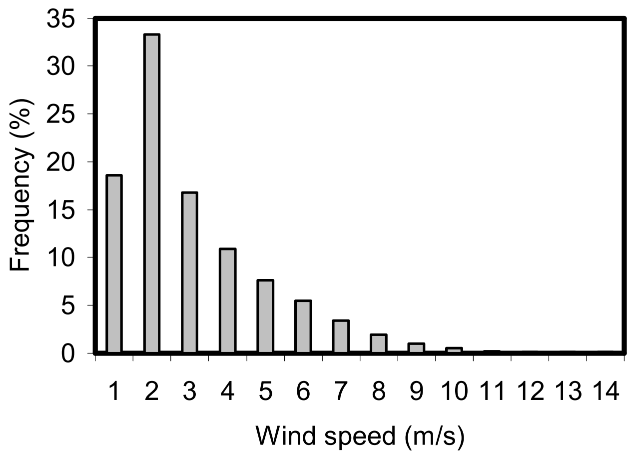

Figure 4.4. Frequency distribution of wind speeds for İskenderun meteorological station

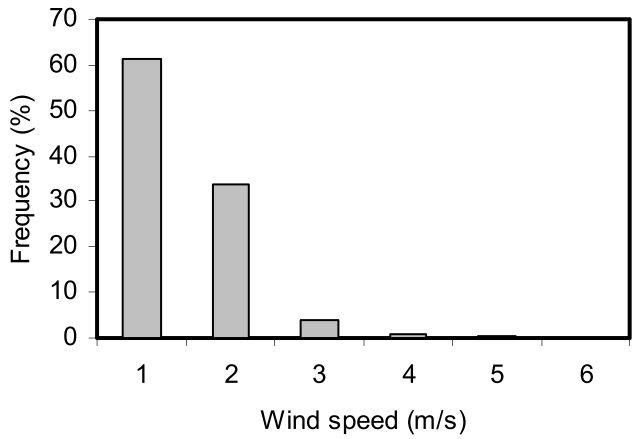

Figure 4.5. Frequency distribution of wind speeds for Dörtyol meteorological station

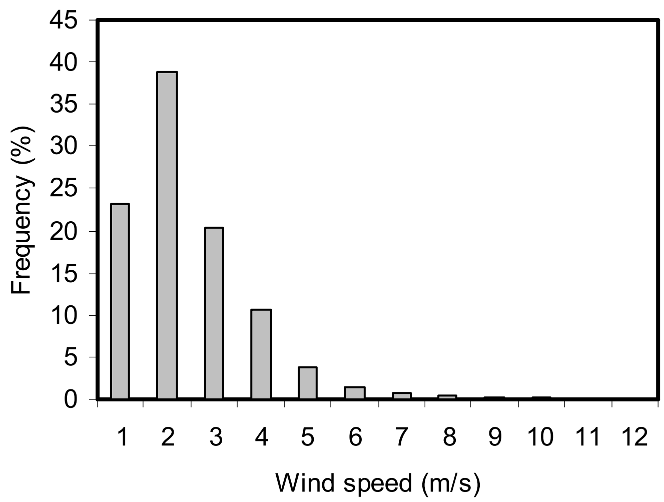

Figure 4.6. Frequency distribution of wind speeds for Yumurtalık meteorological station

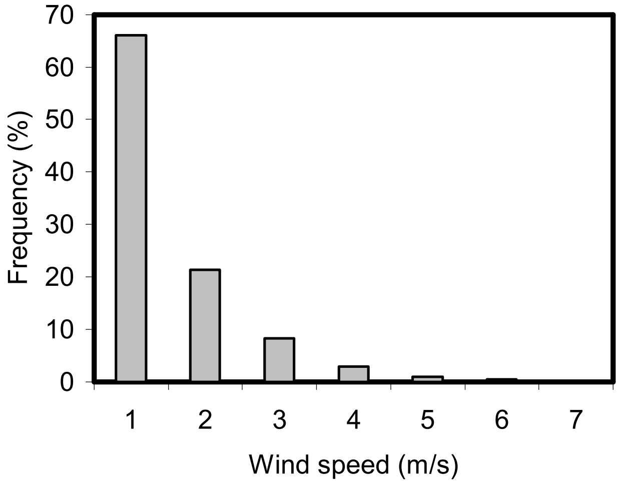

Figure 4.7. Frequency distribution of wind speeds for Adana meteorological station

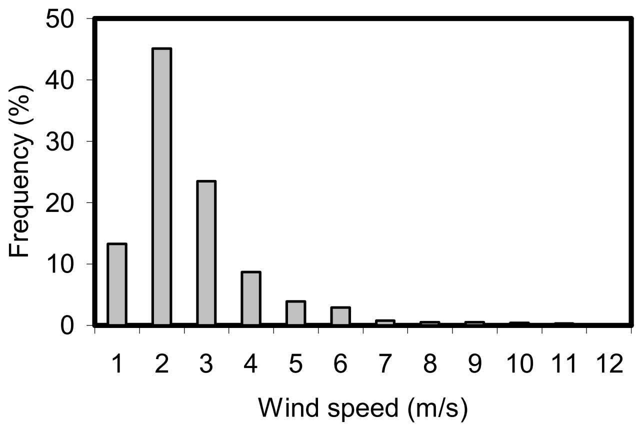

Figure 4.8. Frequency distribution of wind speeds for Karataş meteorological station

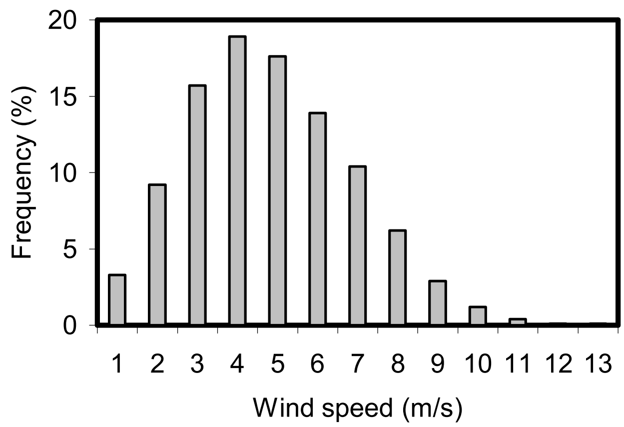

Figure 4.9. Frequency distribution of wind speeds for Samandağ meteorological station

Figure 4.10 shows the time variation of the hourly mean wind speed on a daily basis for 10 years between 1992 and 2001. As a result, for all regions the lowest wind speeds appear generally in the morning around 07:00. However, the highest wind speeds appear in the afternoon between 12:00 and 18:00. The daily time-evolution of wind speed is quite important for the integration of wind power into the overall energy supply.

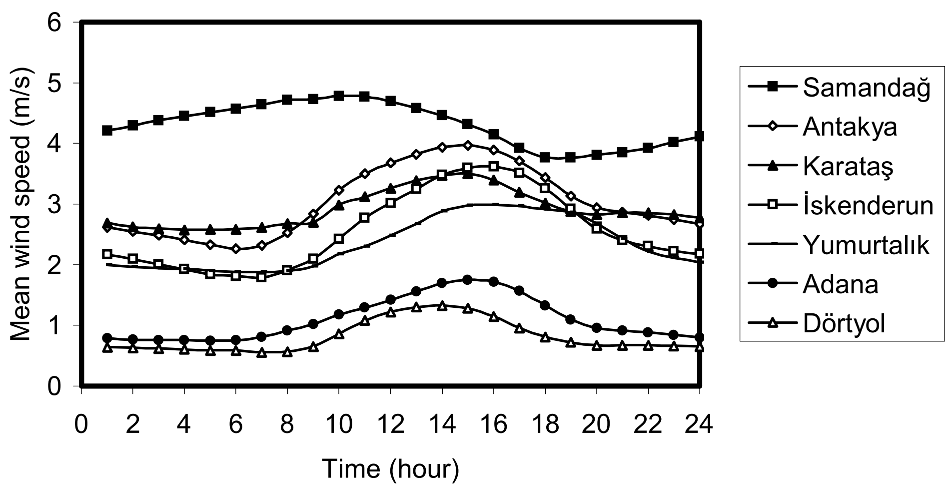

Figure 4.10. Daily time variation of the mean hourly wind speeds for meteorological stations

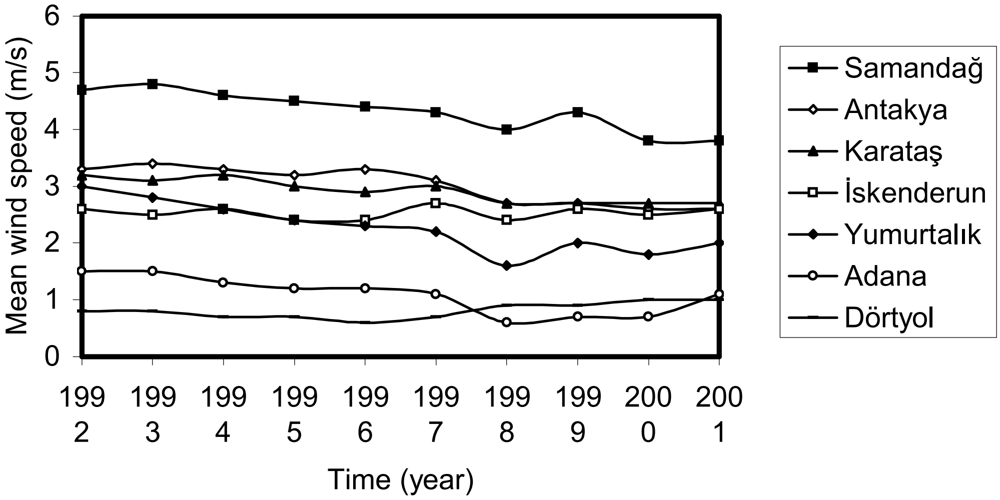

Figure 4.11. Variation of the yearly mean wind speeds for meteorological stations

The yearly wind characteristics provide basic information about the wind strength and consequently about the supply of wind power. The variations of the yearly mean wind speeds measured at these stations are shown in Figure 4.11. The wind speeds appears to decrease occurs during the 10-year period. The wind speeds indicate that a substantial decrease occurs during 10-year especially at Antakya and Samandağ meteorological stations. In 1992, the mean wind speed was 3.3 m/s and the mean wind energy potential was 42 W/m^2, while in 2001, the mean wind speed decreased to 2.6 m/s and the mean wind energy potential was 26 W/m^2 in Antakya. We suspect that the reason for this decrease in the wind speed is that the terrain surface around the meteorological station changes substantially during the period of 10 years. In the present study, the roughness of the terrain was examined for all stations in order to consider the effect of obstacles, orography and roughness on the measured wind speed. This result suggests that meteorological stations have to be moved from their present places to suitable places where the height of roughness and other parameters which affect the speed of wind at the meteorological stations, are negligible. The differences of wind speeds for 10 years between 1992 and 2001 are not significant at İskenderun meteorological station. In 1992, the mean wind speed was 2.6 m/s and the mean wind energy potential was 44 W/m^2. On the other hand, in

2001, the mean wind speed was 2.6 m/s and the mean wind energy potential was 36 W/m^2.

The monthly variations of the mean wind speeds derived from the time-series data at seven stations are shown in Figures 4.12-18. A dramatic variation in monthly mean wind speed occurs during a year at these meteorological stations. The highest monthly mean wind speed appears in July and August and; the lowest wind speed occurs in November and December approximately at all meteorological stations.

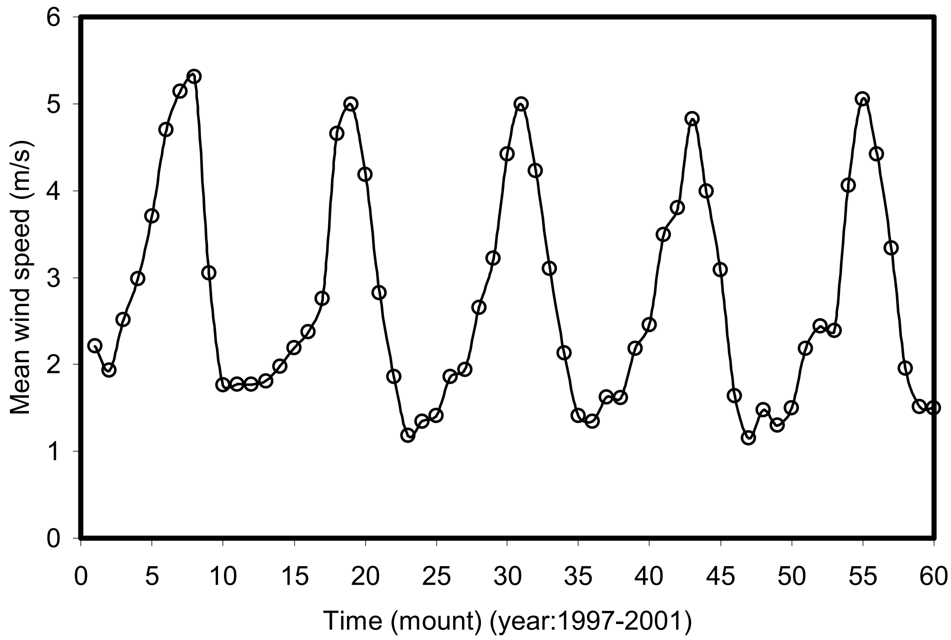

Figure 4.12. Monthly variation of mean wind speeds for Antakya meteorological station

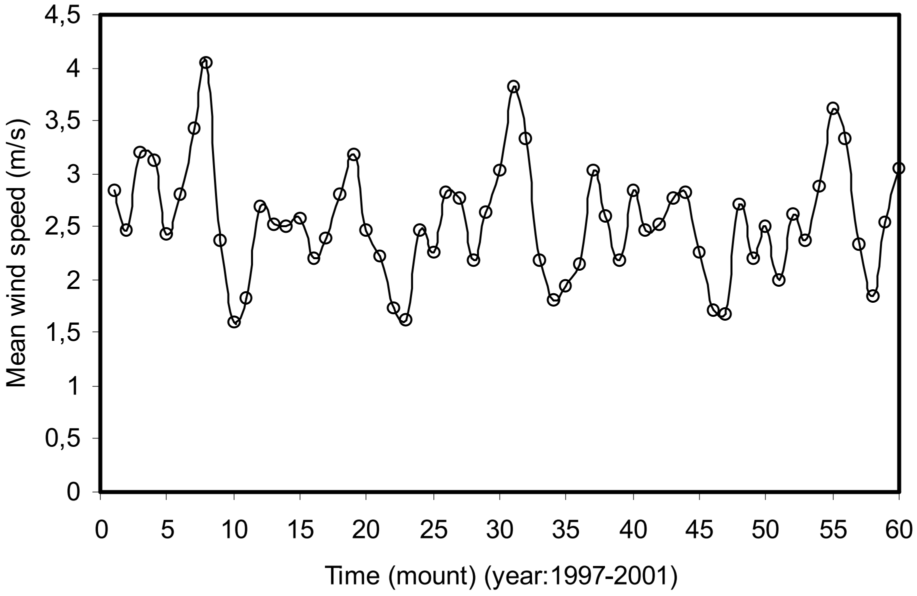

Figure 4.13. Monthly variation of mean wind speeds for İskenderun meteorological station

Figure 4.14. Monthly variation of mean wind speeds for Dörtyol meteorological station

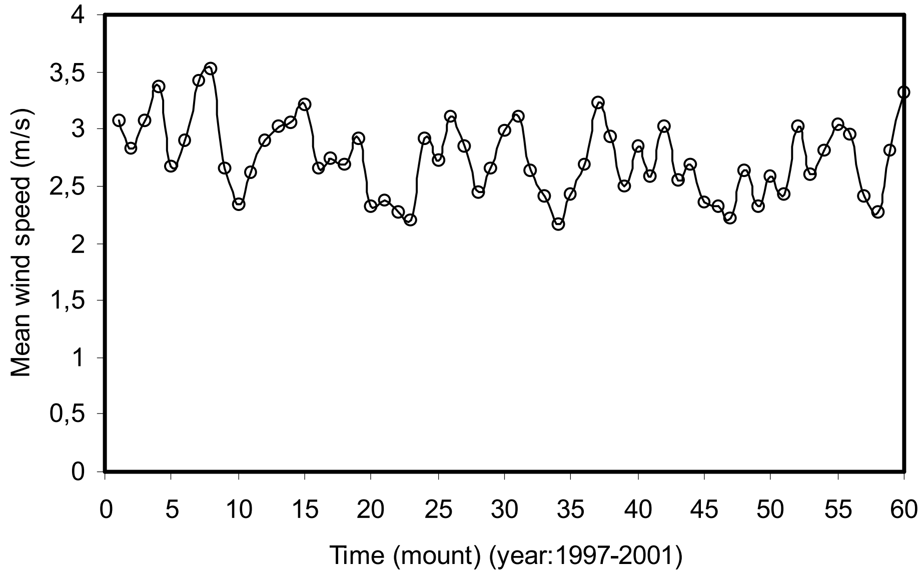

Figure 4.15. Monthly variation of mean wind speeds for Karataş meteorological station

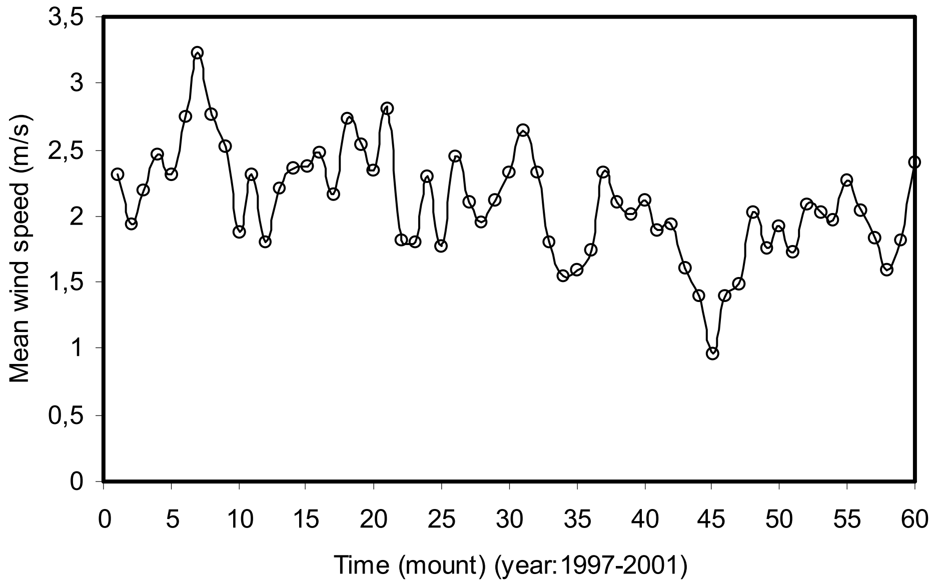

Figure 4.16. Monthly variation of mean wind speeds for Yumurtalık meteorological station

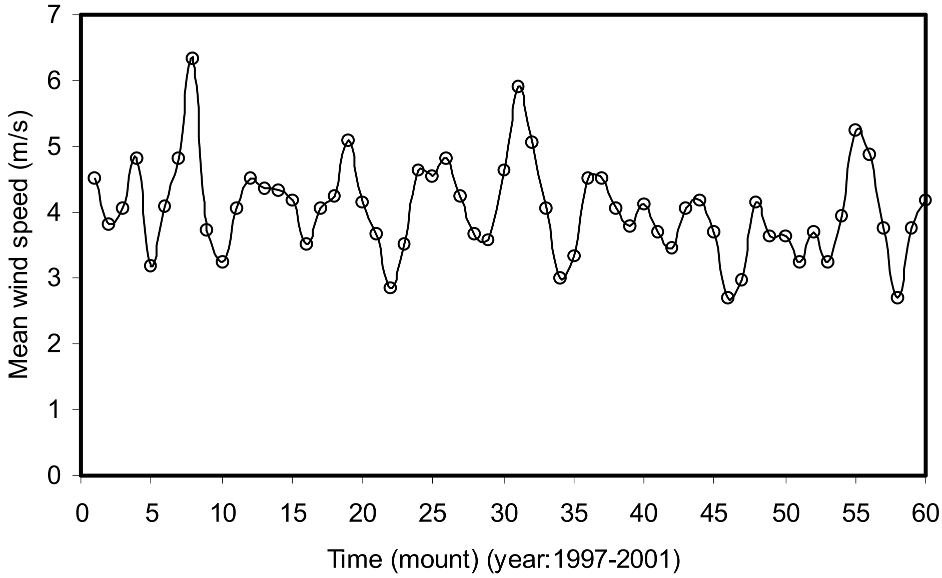

Figure 4.17. Monthly variation of mean wind speeds for Samandağ meteorological station

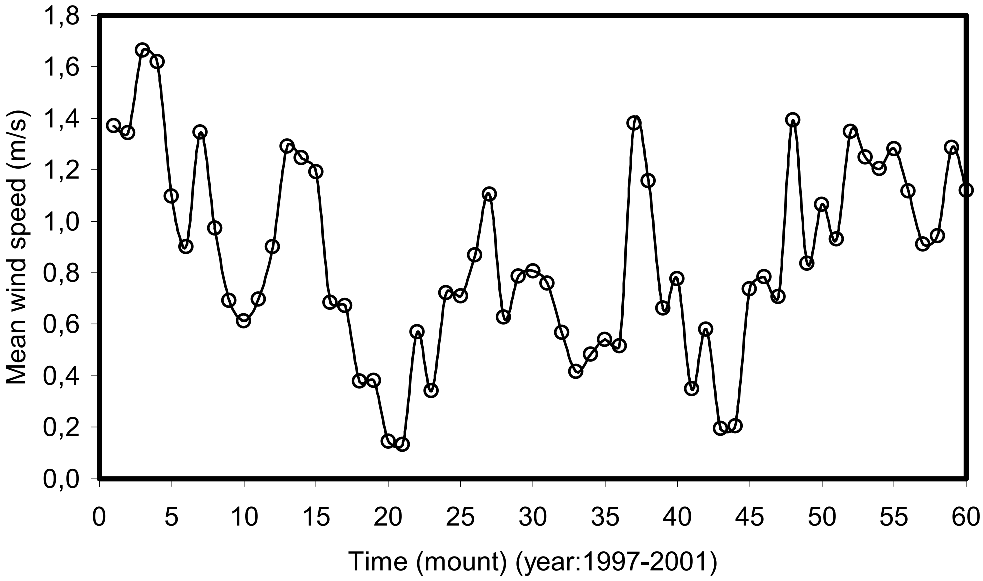

Figure 4.18. Monthly variation of mean wind speeds for Adana meteorological station

4.1.2. The Results of Corrected Values of Wind Data

Along the Mediterranean Sea coast, valleys and mountains are not perpendicular formed and the Taurous Mountains are situated away from the sea cost in many regions. Therefore, these regions are exposed to southerly winds that are not as strong as the northerly winds that occur over the Black Sea. However, in the eastern Mediterranean region, which is in the vicinity of İskenderun Bay, receives satisfactory wind power which is convenient for power generation (Durak and Şen, 2002).

In deciding about the effectiveness of the wind speed measurement around a site, the topographic and climatic conditions must be taken into consideration. Especially, any method of wind speed prediction should consider the topographic and climatologic features. The wind speed measured at a site is determined mainly by two factors; the overall weather systems (which usually have an extent of several hundred kilometers) and the nearby topography within few kilometers of the station. The collective effect of the terrain surface and obstacles, leading to an overall retarding of the wind near the ground, is referred to as the roughness of the terrain. Orographic elements such as hills, cliffs, ridges, and escarpments exert an additional influence on the wind. Roughness and orography are amongst the main factors that affect the wind speed (Durak and Şen, 2002).

Firstly, in the analysis made for the wind speed measuring point, all of shelter behind obstacles, roughness and topographical data which affect the wind speed and direction were not eliminated. Obstacles have an impact on the wind speed and alter the wind direction particularly for lower level of height. Secondly, the wind speeds were reconsidered again by taking the effect of these parameters into account. With WASP packet program, wind speeds and potentials including corrected wind speeds and potentials were obtained for standard heights by taking the effect of these parameters into account and using hourly wind data. Using the resource file formed by WASP, the maps of wind potential were drawn for the heights of 10 and 25 m. These maps are shown in Figures 4.19 and 20. The wind potential can be seen on these maps directly at each point. The present investigations showed that at 25 m height above the ground level, the mean wind energy potentials reach to 500 W/m^2 in many areas of this region. These areas seem to be very convenient for wind turbines installation. The most promising locations are İskenderun, Antakya and Samandağ.

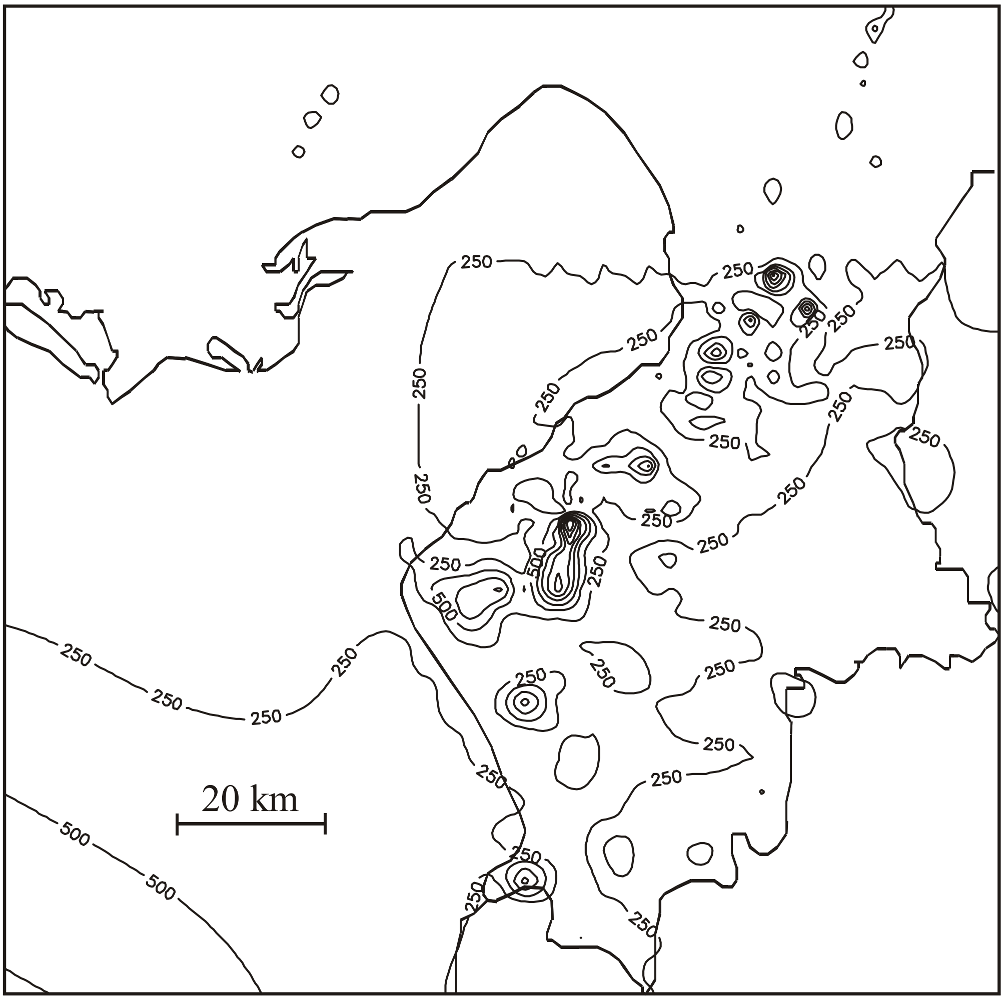

Figure 4.19. Regional distribution of mean wind energy potential (W/m^2) in the south-east region of Mediterranean for 10 m above the ground level (minimum contour: 250 W/m^2, increment: 250 W/m^2).

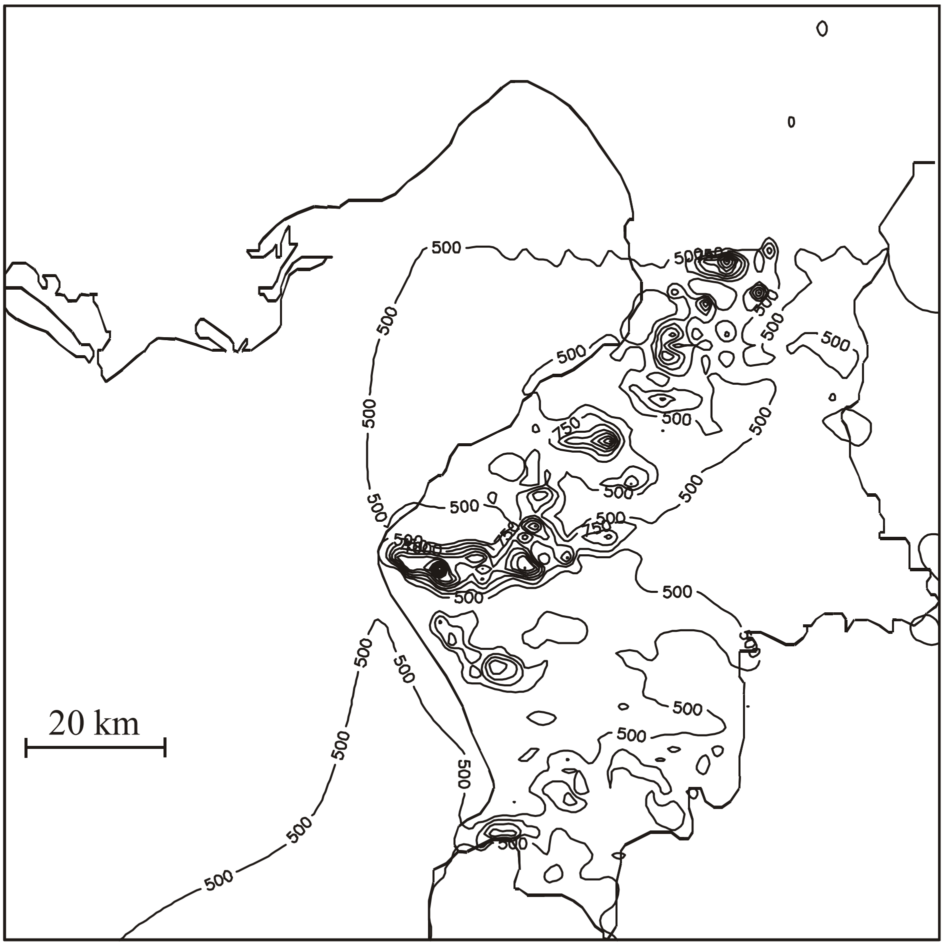

Figure 4.20. Regional distribution of mean wind energy potential (W/m^2) in the south-east region of Mediterranean for 25 m above the ground level (minimum contour: 500 W/m^2, increment: 250 W/m^2).

4.2. Wind Characteristics in Belen-Hatay, Turkey

4.2.1. Location of the Site

The data used in this study were collected from Belen-Hatay station located in the eastern Mediterranean region of Turkey. This station has been set up by the General Directorate of Electrical Power Resources Survey Administration (EIE). The map of the region and the location of the station are presented in Figure 4.21. Adana and Hatay are two of the industrialized provinces in the eastern Mediterranean region of Turkey, with population of around 3.2 millions. With the neighboring provinces the population goes up to approximately 6 millions according to population census done in 2004. Estimated population of Adana and Antakya combined is presently 4.2 millions and with neighboring provinces the population goes up to 7.8 millions. Electricity production from the wind power should be locally preferred over thermal power plants (Sahin et al., 2005).

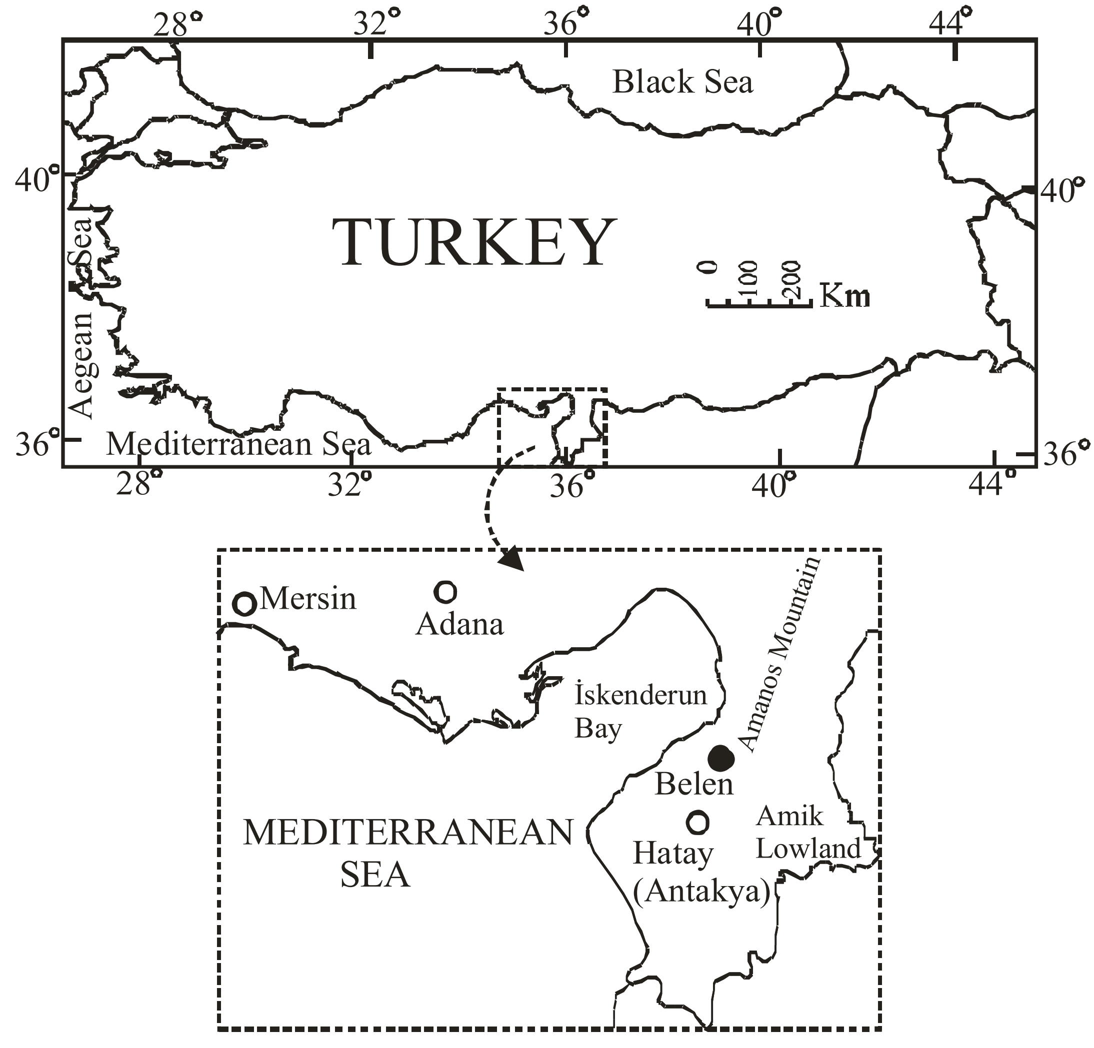

Figure 4.21. The map of the region and the location of the station

Two most important mountain pass such as Gülek mountain pass and Belen mountain pass provide high way route between Europe and Middle East. More specifically, Belen mountain pass is situated along wide spread valley between east of Mediterranean region and Amik lowland, on the Amanos mountain in the provision of Belen. In this region, there is a wide range of land which is suitable for wind turbine farm. Belen has a fairly high wind speeds which varies proportional to the altitude. Mediterranean climate is dominant in this region, usually hot and dry in summer, lukewarm and rainy in winter. But, climate properties vary depending on the level of the height above the sea level. On the slope of a mountain looking at the sea, an increase of terrestrial effects on climate is observed. However, the weather in this region does not show intense terrestrial climate due to the Mediterranean Sea effect.

The long-term wind data, containing hourly wind speeds and directions, cover the period from the year 2004 to 2005. The mean monthly, annual and diurnal wind speeds were calculated from these hourly wind speed data. Height of anemometer of the station is 10 m above the ground level. Geographical coordinates and measurement period of this station are given in Table 4.4. The wind observation station is situated at the coordinates of $36^0$12'00"N latitude and $38^0$28'01"E longitude. The height of the station is 474 meter above the sea level. Around the measurement area, there were no obstacles which cause an impact on the wind speeds and directions.

Table 4.4. Geographical coordinate and measurement period of Belen station

Station	Latitude	Longitude	Altitude (m)	Period	Anemometer height (m)
Belen	36^0 12' 00" N	38^0 28' 01" E	474	2004-2005	10

4.2.2. Wind Speed Probability Distribution

Generally, previously measured wind data are used for the estimation of wind power potential of any area. First of all, at any locations, hourly wind speeds and wind directions are first observed and monitored. These results are used for frequency and probability modeling. Wind speed data in time-series format is usually arranged in the frequency distribution format since it is more convenient for statistical analysis. Therefore, the available time-series data were translated into frequency distribution format. The wind speed probability distributions and the functions representing them mathematically are the main tools used in the wind-related literature. Their use includes a wide rage of applications, from the techniques used to identify the parameters of the distribution functions to the use of such functions for analyzing the wind speed data and wind energy economics (Celik, 2003). The frequency distribution and probability density of the wind speeds help towards answering questions of how long is a wind power plant out of action in the case of lack of wind, which is the range of the most frequent wind speeds, and how often does the wind power plant achieve its rated output (Pashardes and Christofides, 1995).

Yearly cumulative distributions derived from the long term wind speed data of Belen-Hatay are presented in Figure 4.22. It is also clear from the figure that the three curves show the same variation according to each other. This figure indicates that the hourly wind speeds in Belen-Hatay are higher than 5 m/s in about 70% of occasions. Seasonal cumulative distributions for the year 2004 are presented in Figure 4.23. It is interesting to note that the wind speeds of summer months in Belen-Hatay are higher than the others.

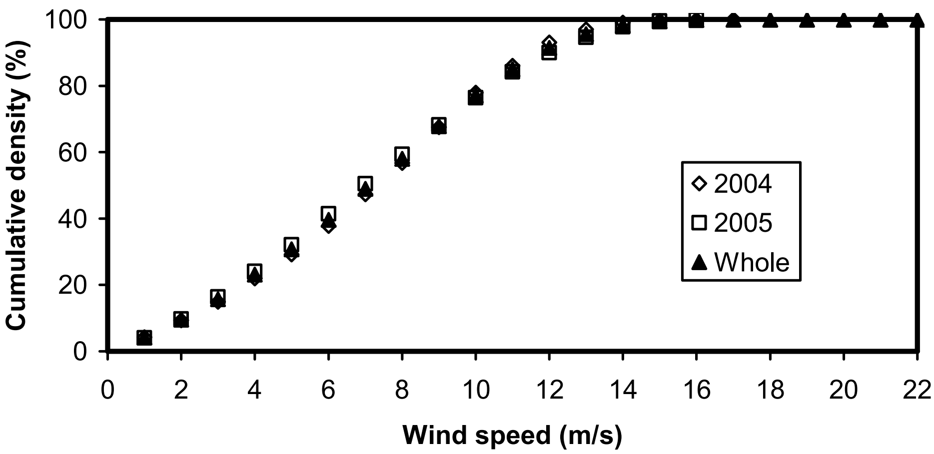

Figure 4.22. Yearly cumulative probability distributions of wind speeds

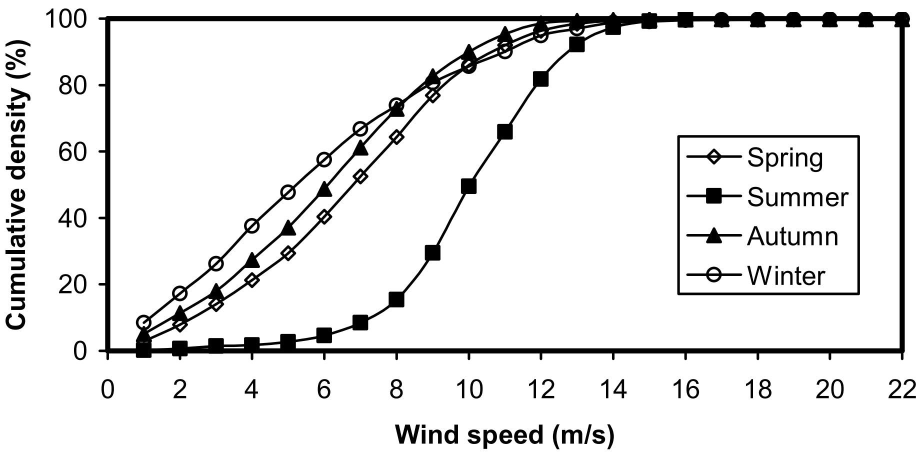

Figure 4.23. Seasonal cumulative probability distributions of wind speeds for the year 2004

4.2.3. Wind Direction Frequency Distribution

There are two important aspects in the selection of the type of orientation of the wind turbines and their location. These are the wind speed distribution in each direction and the most frequent wind directions (Torres et al., 1999). Besides the level and structure of wind speeds, the direction of the wind is of decisive significance for the evaluation of the possibilities of utilizing wind power. The direction statistics play an important role in optimal positioning of a wind turbine farm in a given area (Pashardes and Christofides, 1995). Wind directions and speeds are also affected by topography (Matsui et al., 2002). Yearly wind direction frequency distribution of Belen-Hatay station is presented in Figure 4.24. It is also clearly seen from the figure that the three curves show the same variation. The data of the wind direction show that the maximum frequency occurs at the west-north (WN) direction. In this region, northwestern winds are effective and the winds from WN direction continuously blow during 42.5% of the time for the year 2004 with a speed of 9.23 m/s. The effect of wind that is observed at the lowest degree is in the direction of south (S), south-west (SW) and west-south (WS) with a speed of 2.21 m/s, 2.06 m/s and 2.69 m/s, respectively. Seasonal wind direction with frequency distribution of Belen-Hatay station for 2004 is presented in Figure 4.25. It is also clear from the figure that during spring, summer and autumn, wind speeds at the west-north (WN) direction are effective, on the other hand during winter, wind speeds at the south-east (SE) direction are effective.

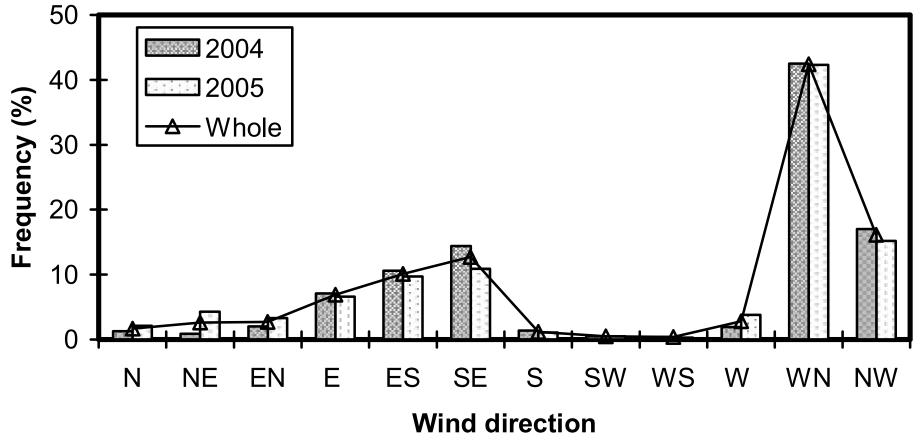

Figure 4.24. Yearly wind direction frequency distribution

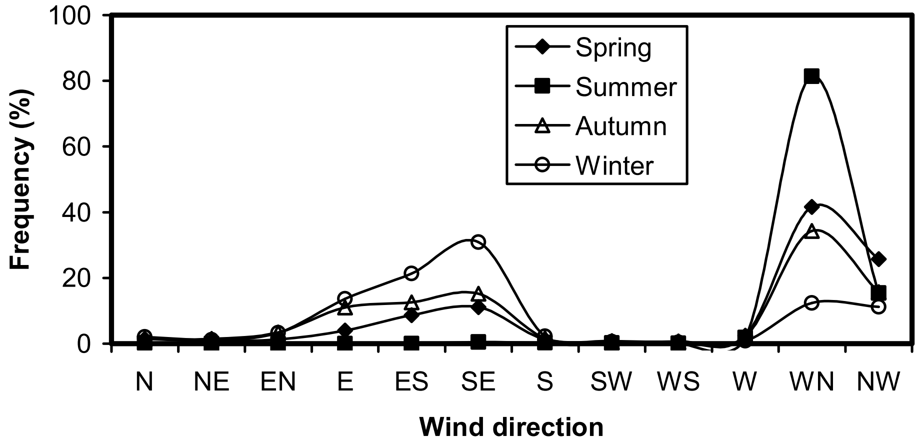

Figure 4.25. Seasonal wind direction frequency distribution for the year 2004

4.2.4. Variation of Weibull Parameters

It is known that there are several efforts to construct an adequate statistical model for describing the wind speed frequency distribution, which may be used for predicting the energy output. The Weibull distribution has been accepted to give a good fit to wind data wind energy applications (Incecik and Erdoğmuş, 1995). The Weibull distribution is a two-parameter distribution.

Table 4.5. The Weibull parameters according to the wind directions

Wind direction	2004		2005		Whole	
	c (m/s)	k	c (m/s)	k	c (m/s)	k
0^0 (N)	2.7	1.29	2.8	1.52	2.8	1.44
30^0 (NE)	1.6	1.75	3.5	1.54	3.1	1.4
60^0 (EN)	6.3	1.43	4.7	1.47	5.1	1.35
90^0 (E)	8.9	3.17	7.6	2.73	8.3	2.85
120^0 (ES)	5.7	1.81	5.3	1.69	5.5	1.74
150^0 (SE)	4.9	1.8	5.2	2.2	5.1	1.95
180^0 (S)	2.5	1.54	2.1	1.54	2.3	1.54
210^0 (SW)	2.3	1.84	2.0	2.03	2.2	1.86
240^0 (WS)	3.0	2.58	3.3	1.39	3.2	1.74
270^0 (W)	6.7	1.81	10.7	4.32	9.6	2.97
300^0 (WN)	10.2	3.92	10.4	3.72	10.3	3.81
330^0 (NW)	7.8	2.85	7.0	2.32	7.4	2.61

For the years 2004 and 2005, the Weibull parameters according to the wind directions in Belen-Hatay station are given in Table 4.5. The Weibull shape parameters (k) are within the range 1.35-3.81 for the whole year. The Weibull scale parameters (c) also vary between 2.2 m/s and 10.3 m/s. It can be seen that the maximum c parameter appears in the direction of WN with 10.3 m/s. On the other hand, the minimum c parameter is in the direction of SW with 2.2 m/s. The highest k parameter for the whole year is in the direction of WN with 3.81, while the lowest appears in the direction of EN with 1.35. The monthly Weibull parameters of Belen-Hatay station are given in Table 4.6. It is seen from the table that the monthly Weibull shape parameters (k) for the whole year range from a low of 1.82 in

December to a high of 5.84 in July. While the highest monthly Weibull scale parameter (*c*) value is determined as 11.4 m/s in July, the lowest monthly *c* value is found as 5.3 m/s in December.

Table 4.6. The monthly Weibull parameters

Month	2004		2005		Whole	
	c (m/s)	k	c (m/s)	k	c (m/s)	k
January	6.4	1.65	6.9	2.02	6.7	1.84
February	7.1	2.00	6.4	1.98	6.8	1.99
March	7.1	2.70	6.0	2.4	6.6	2.55
April	7.2	2.04	7.4	2.27	7.3	2.16
May	8.9	3.64	8.8	2.97	8.9	3.31
June	10.3	5.09	10.4	3.81	10.4	4.45
July	10.8	4.90	12.0	6.78	11.4	5.84
August	11.5	4.59	12.2	5.36	11.9	4.98
September	8.6	3.78	8.8	5.36	8.7	4.57
October	6.0	2.36	5.8	2.24	5.9	2.3
November	6.1	1.96	5.6	2.26	5.9	2.11
December	6.1	1.65	4.5	1.98	5.3	1.82

4.2.5. Variation of Wind Speeds

The production of wind energy is essentially dependent on the magnitude and regularity of wind speeds (Pashardes and Christofides, 1995). Wind speed is the most important parameter in the design and study of wind energy conversion systems (Akpinar and Akpinar, 2005). A detailed knowledge of the wind speed distribution and the most frequent wind directions are substantially important when choosing wind turbines and locations (Torres et al., 1999). For this purpose, yearly mean wind speeds according to the wind directions, monthly mean wind speeds and daily variation of wind speeds of Belen-Hatay station were determined by using the WAsP program. The variation of yearly mean wind speeds according to the wind directions of Belen-Hatay station is presented in Figure 4.26. It is also clear from the figure that the three curves show the same variation according to each other. The highest yearly mean wind speed for the whole year is in the direction of WN with 9.3 m/s, while the lowest appears in the direction of SW with 1.92 m/s. In this region, wind speeds observed in the direction of WN are effective and strong. The variation of seasonal mean wind speeds of Belen-Hatay station for the year 2004 is presented in Figure 4.27. It is also clear from the figure that during spring, winter and autumn, wind speeds at the west-north (WN) and east (E) directions are strong, on the other hand, during the summer season; wind speeds at the west (W) and west-north (WN) directions are strong.

The monthly variation of mean wind speeds of Belen-Hatay station for the year 2004 and 2005 is presented in Figure 4.28. The highest monthly mean wind speeds for whole year occur mainly in July and August with 10.5 m/s and 11.0 m/s respectively, and the lowest wind speed occur in December and March with 4.7 m/s and 5.6 m/s respectively. It is apparent from the figure that monthly mean wind speed data of 2004 and 2005 agree well with the each other. The variation of diurnal wind speeds of Belen-Hatay station for the year 2004 and 2005 is presented in Figure 4.29. It is also clear from the figure that the three curves show the same variation. Diurnal wind speed for the whole year varies between 6.05 m/s and 7.76 m/s. The diurnal wind speed has its minimum value during the morning hours and its maximum value during the afternoon hours. In other words, in this region, the wind speed is higher during the day and lower during the night. This is due to the high level of solar intensity during the day. Figure 4.30 shows the variation of diurnal mean wind speeds for the seasons of winter, spring, summer and autumn in the year 2005. From the graph it reveals that diurnal wind speeds during the summer are higher than diurnal wind speeds during the winter, spring and autumn.

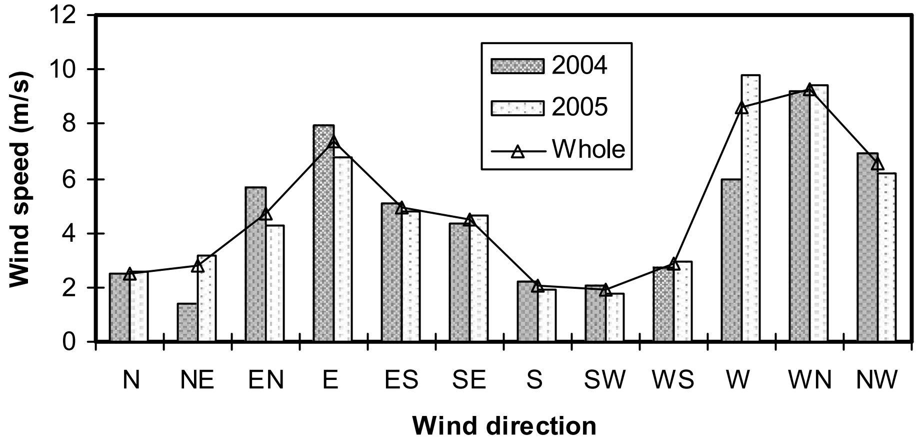

Figure 4.26. The variation of yearly mean wind speeds according to the wind directions

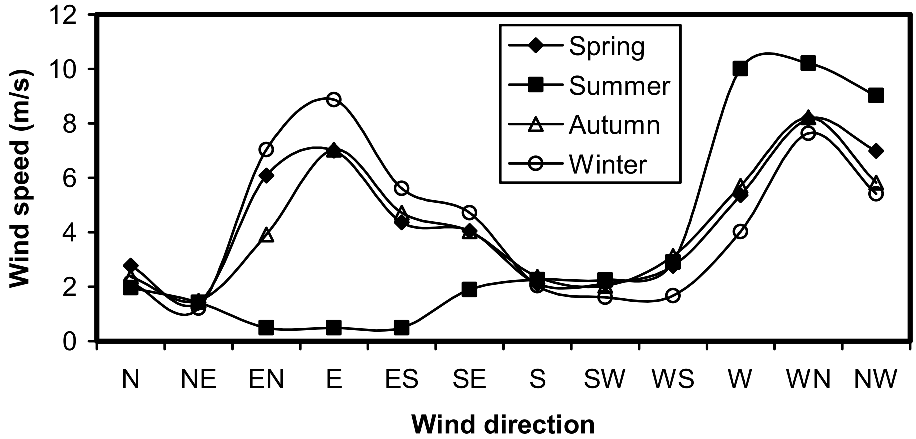

Figure 4.27. The variation of seasonal mean wind speeds according to the wind directions for the year 2004

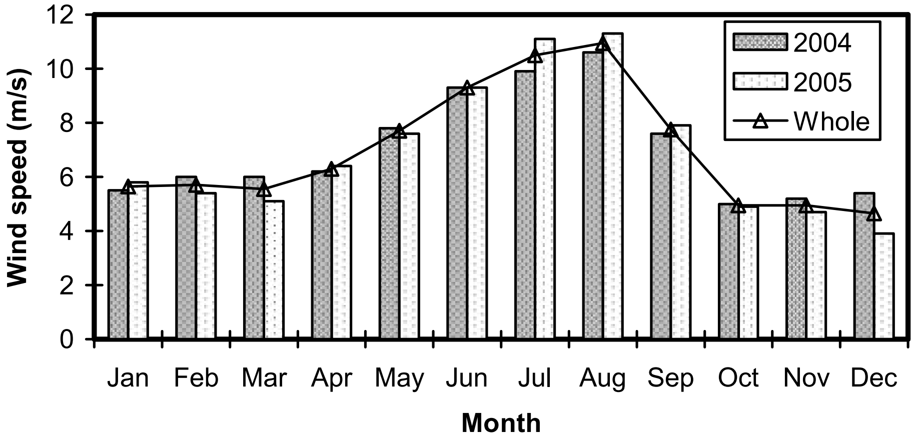

Figure 4.28. The monthly variation of mean wind speeds for the year 2004 and 2005

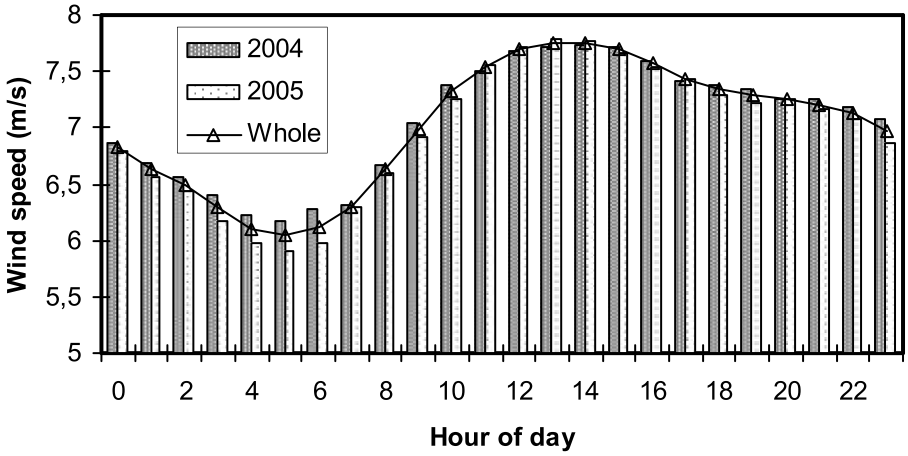

Figure 4.29. The variation of diurnal wind speeds for the year 2004 and 2005

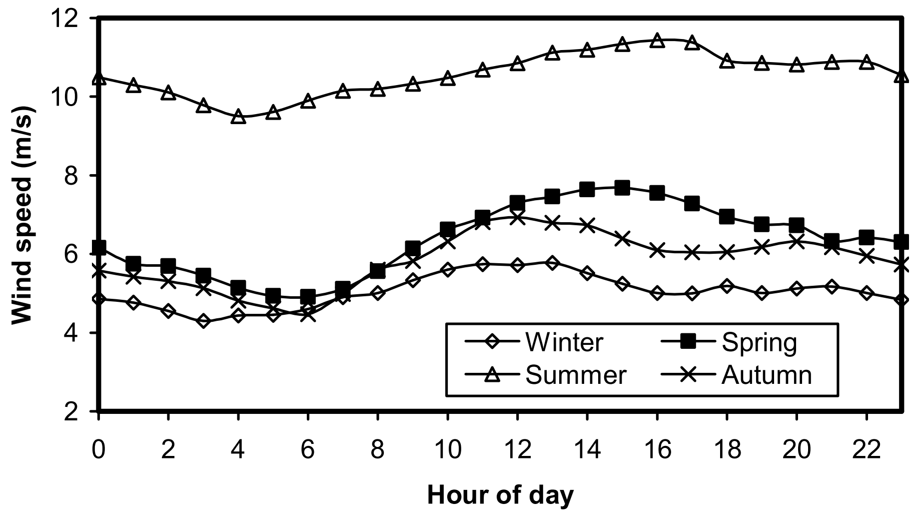

Figure 4.30. The variation of diurnal mean wind speeds for the seasons in the year 2005

4.2.6. Variation of Wind Power Potential

The variation of yearly mean wind power potential according to the wind directions of Belen-Hatay station is presented in Figure 4.31. It is also clear from the figure that the three curves show the same variation according to each other. The highest yearly mean wind power potential for the whole year is in the direction of WN with 620 W/m^2, while the lowest appears in the direction of SW with 9 W/m^2. In this region, wind power potential determined in the direction of WN is effective and fairly strong. The variation of seasonal mean wind power potential of Belen-Hatay station for the year 2004 is presented in Figure 4.32. It is also clear from the figure that during spring, winter and autumn, wind power potentials at the west-north (WN) and east (E) directions are fairly strong, on the other hand during summer; wind power potential at the west (W) and west-north (WN) directions are fairly strong.

The monthly variation of mean wind power potential of Belen-Hatay station for the year 2004 and 2005 is presented in Figure 4.33. The highest monthly mean wind power potential for whole year occurs mainly in July and August with 797.5 W/m^2 and 903 W/m^2 respectively, and the lowest in October and November with 143 W/m^2 and 154 W/m^2 respectively. It is apparent that monthly mean wind power potential data of 2004 and 2005 agree well with each other. The variation of diurnal wind power potential of Belen-Hatay station for the year 2004 and 2005 is presented in Figure 4.34. It is also clear that the three curves show the same variation with a good agreement. Diurnal wind power potential for the whole year varies between 291.5 W/m^2 and 448 W/m^2. The diurnal wind power potential has its minimum value during the morning hours and its maximum value during the afternoon hours. In other words, in this region, the wind power potential is higher during the day and lower during the night.

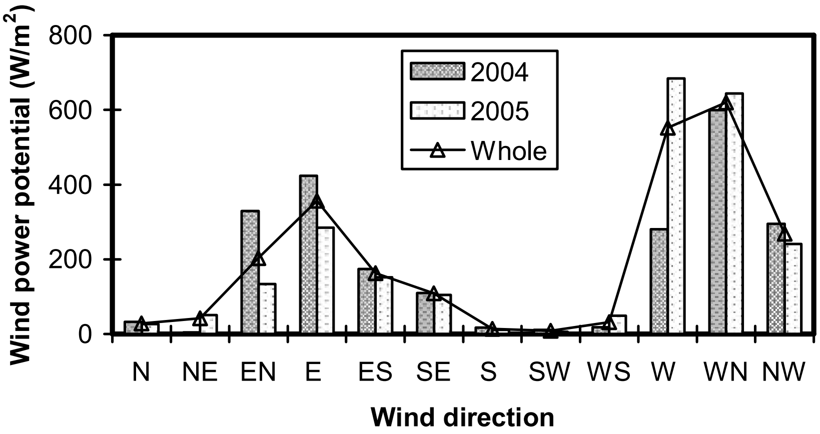

Figure 4.31. The variation of yearly mean wind power potential according to the wind directions

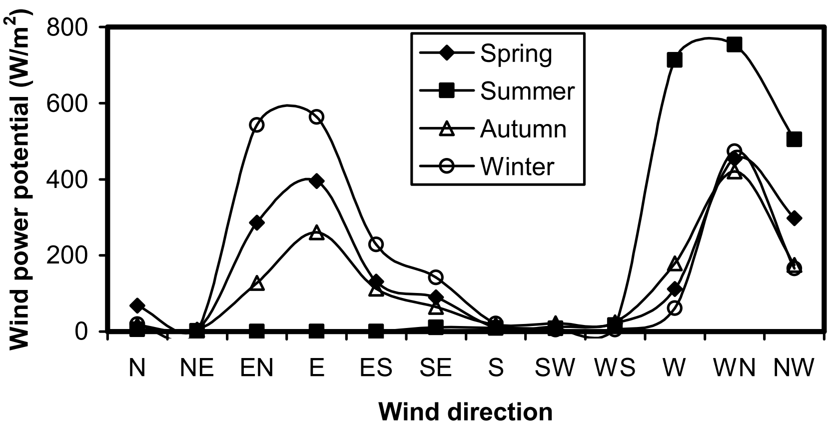

Figure 4.32. The variation of seasonal mean wind power potential for the year 2004

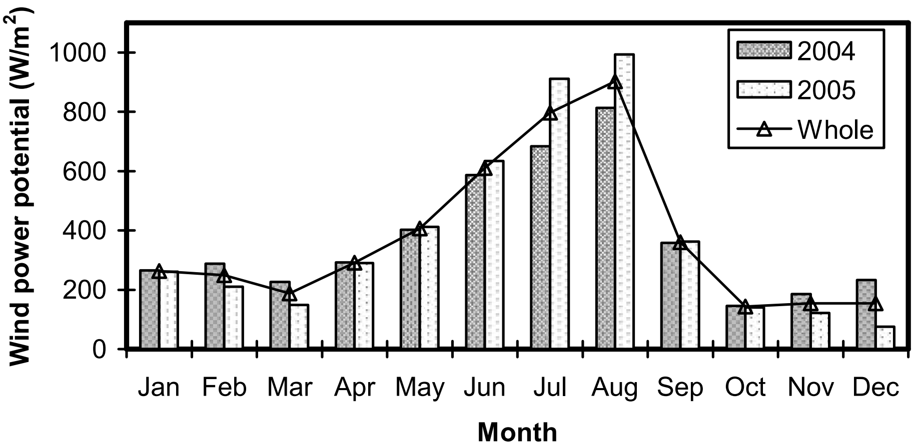

Figure 4.33. The monthly variation of mean wind power potential for the year 2004 and 2005

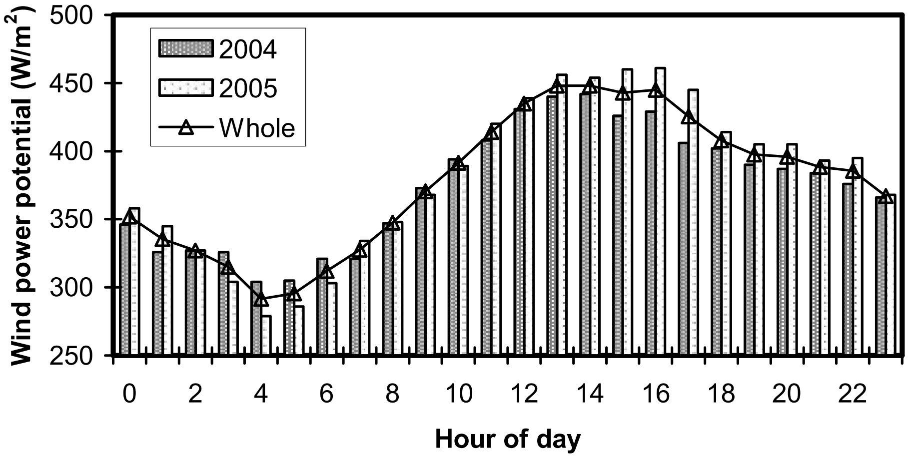

Figure 4.34. The variation of diurnal wind power potential for the year 2004 and 2005

Turkey's energy demand is growing rapidly and expected to continue grow in the near future. The annual increase in energy consumption is 6-8%, except for recession years. The installed capacity of electric power plants in the year 2005 was 38,843.5 MW with annual electricity production of 161,983.3 GWh. Presently, 66.68% of this energy is produced in operating thermal power plants. The combustion of coal, lignite, petroleum, wood, agricultural and animal waste, environmental pollution will be a serious problem in the future. In this regard, renewable energy resources appear to be one of the most efficient and effective solutions for sustainable energy development and environmental pollution prevention in Turkey (Ocak et al., 2004).

The Belen-Hatay region has a reasonably well wind power potential. In this region, the hourly wind speeds are higher than 5 m/s in about 70% of occasions at 10 m height above the ground level. The monthly mean wind speeds are higher than 5 m/s during 9 months of the year; on the other hand the monthly mean wind power potentials are higher than 200 W/m^2 during 8 months of the year. While a wind generator is being installed in this region, the yearly wind characteristics should be provided basic information about the wind strength and consequently about the supply of wind power. The variations of the yearly mean wind characteristics measured in the year of 2004 and 2005 are given in Table 4.7. It can be seen from this table that in 2004, the mean wind speed is 7.1 m/s and the mean wind power potential is 374 W/m^2. On the other hand in 2005, the mean wind speed is 7.0 m/s and the mean wind power potential is 382 W/m^2. According to the critical values of mean wind speed, having wind speed of 7.1 m/s is well for the utilization of the wind energy potential.

Table 4.7. The yearly mean wind characteristics measured in the year of 2004 and 2005

Wind characteristics	2004	2005	Whole
Weibull parameter (c) (m/s)	8.30	8.20	8.30
Weibull parameter (k)	2.63	2.31	2.46
Wind speed (m/s)	7.10	7.00	7.00
Standard deviation of wind speeds (m/s)	3.50	3.66	3.58
Wind power potential (W/m^2)	374	382	378

4.3. Investigation of Wind Power Density in the Southern and Southwestern Region of Turkey

4.3.1. Location of the Sites

The data used in this study were collected from Belen, Datça, Foca, Gelendost, and Söke stations located in the southern and southwestern region of Turkey. These wind speed measuring stations were set up by the General Directorate of Electrical Power Resources Survey Administration (EIE). The map of the region and location of the stations are presented in Figure 4.35. The height of anemometer of all stations is 10 m above the ground level. Geographical coordinates and measurement years of these stations are given in Table 4.8. Region of stations extends from latitude $36^0$12'00" to $38^0$39'25" north and longitude $26^0$46'22" to $36^0$28'01" east, while the height of stations above the sea level varies between 6 meter and 474 meter. Around the wind speed measuring stations, there are no obstacles which cause an impact on the wind speeds and directions.

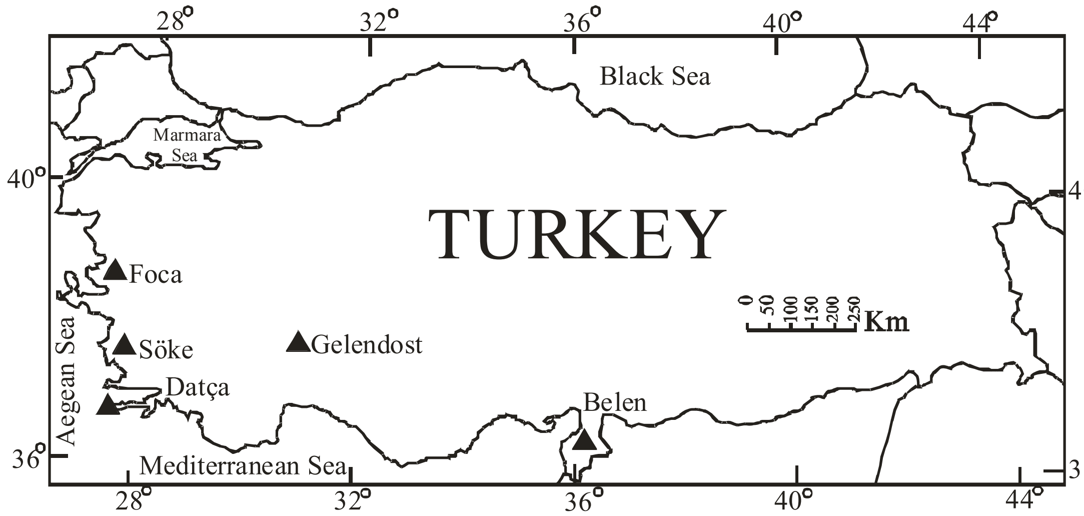

Figure 4.35. Map of the region and location of the stations

Table 4.8. Geographical coordinates and measurement years of stations

Station	Latitude	Longitude	Altitude (m)	Measurement year	Anemometer height (m)
Belen	36^0 12' 00" N	36^0 28' 01" E	474	2005	10
Datça	36^0 46' 04" E	27^0 37' 08" N	20	2001	10
Foca	38^0 39' 25" N	26^0 46' 22" E	175	2001	10
Gelendost	38^0 08' 27" N	30^0 50' 06" E	973	2001	10
Söke	37^0 41' 56" N	27^0 23' 13" E	6	2001	10

4.3.2. Wind Data Analysis

There are two important aspects in the selection of the type of orientation of the wind turbines and their location. These are the level and probability of wind speed distributions in each direction and the most frequent wind directions (Torres et al., 1999). Besides the level and structure of wind speeds, the direction of the wind is of decisive significance for the evaluation of the possibilities of utilizing wind power. The direction statistics play an important role in optimal positioning of a wind turbine farm in a given area (Pashardes and Christofides, 1995). Wind directions and speeds are also affected by topography (Matsui et al., 2002). For this purpose, the wind direction frequency distributions were determined by using the WAsP program. Variations of the wind direction frequency distributions for all stations are presented in Figure 4.36. These figures indicate that the dominant wind directions of 4 stations are the same. The dominant wind direction of Belen, Datça, Gelendost and Söke stations are in the direction of WN (300^0).

Variation of diurnal wind speeds for all stations is presented in Figure 4.37. It is also clear from this figure that the diurnal wind speed varies between 3.27 m/s and 7.79 m/s. The diurnal wind speed has its minimum value during the morning hours and its maximum value during the afternoon hours. In other words, in these regions, the wind speed is higher during the day and lower during the night. This is due to the high level of solar intensity during the day. In addition, the diurnal wind speeds of Belen are higher than the other stations. The diurnal wind speeds of this station vary between 5.91 m/s and 7.79 m/s. This level of wind speed is considerably high for the utilization of wind energy conversion systems. Unluckily, there is no any wind turbine installation in these regions yet for the electricity generations. The minimum diurnal wind speed appears in Söke and Gelendost stations.

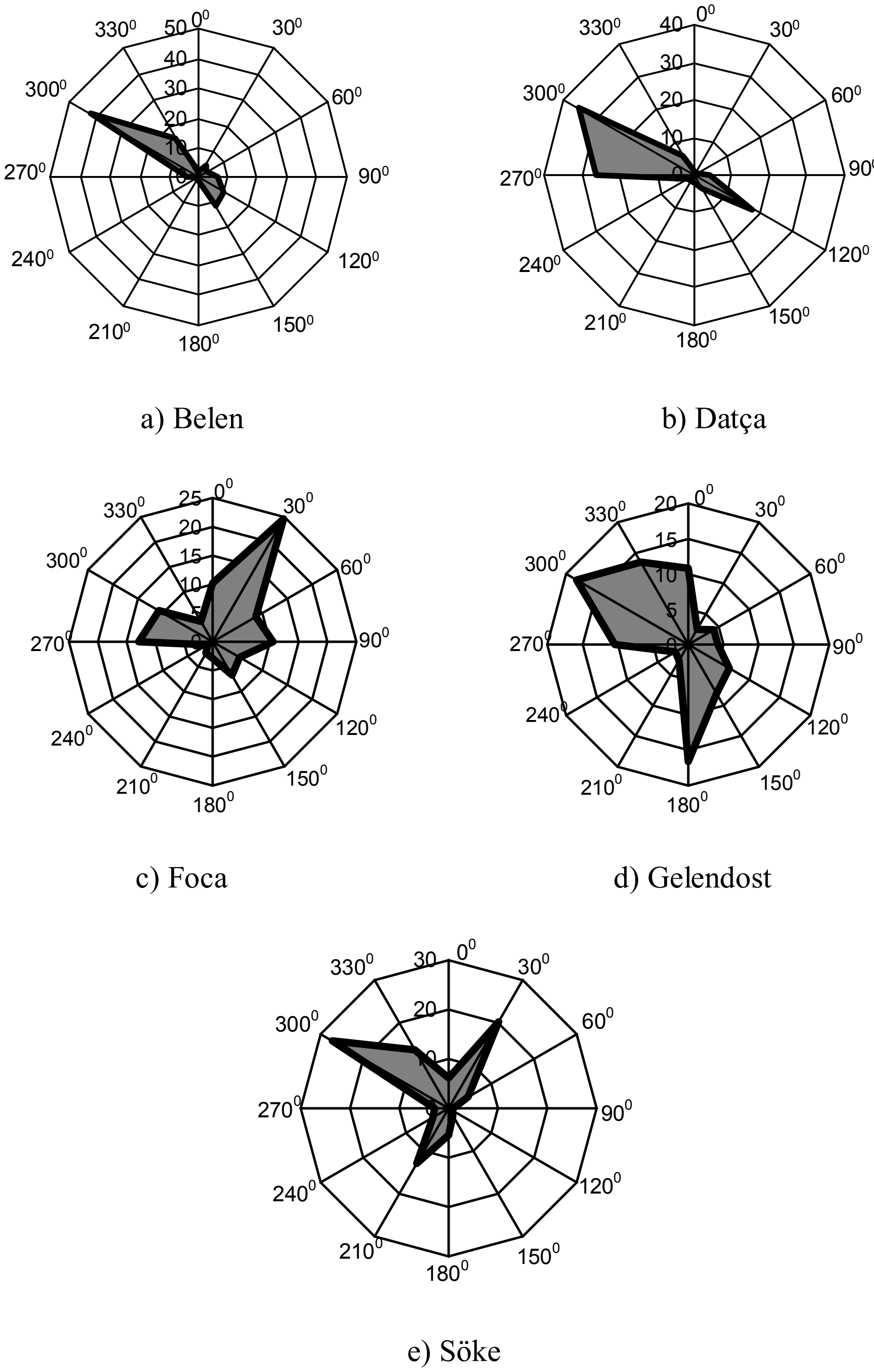

Figure 4.36. Wind direction frequency distributions of the stations

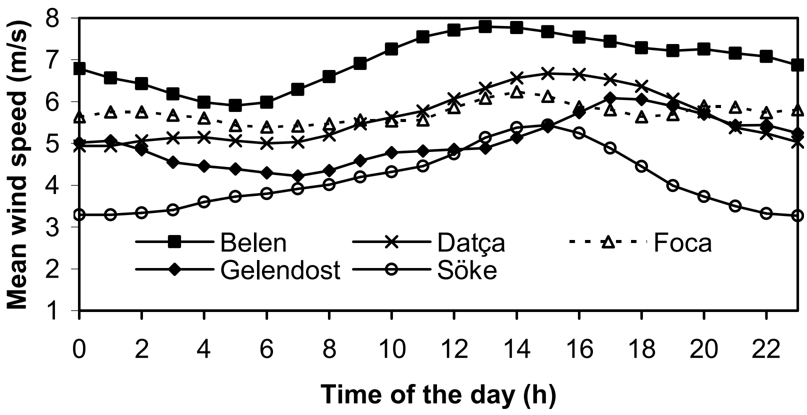

Figure 4.37. Hourly variation of the mean wind speed

The production of wind energy is essentially dependent on the magnitude and regularity of wind speeds (Pashardes and Christofides, 1995). Wind speed is the most important parameter in the design and study of wind energy conversion systems (Akpinar and Akpinar, 2005). A detailed knowledge of the wind speed distribution and the most frequent wind directions are substantially important when choosing the suitable wind turbines and locations (Matsui et al., 2002). For this purpose, monthly mean wind speed (v_m) and standard deviation of wind speeds (σ) in Belen, Datça, Foca, Gelendost, and Söke stations were determined from observed data. Monthly and annual mean wind speed and standard deviation for all stations are presented in Table 4.9. There is a significant difference in the mean wind speeds among stations and between the summer and winter months. The lowest value of the wind speed is 3.12 m/s in March at Söke station, while the highest value is 11.32 m/s in August at Belen station. It is apparent from the table that the wind speeds of Belen, Datça and Söke have its maximum value during the months of July and August. On the other hand, the wind speeds of Foca and Gelendost have its maximum value during the month of December. It is another significant point that Belen presents higher wind speeds value than the others. Annual mean wind speeds range from a low level of 4.10 m/s in Söke station to a high level of 6.97 m/s at Belen station. The standard deviation of wind speeds varies mainly from a low level of 2.53 m/s to a maximum level of 3.66 m/s.

Table 4.9. Monthly and annual mean wind speed and standard deviation for all stations

Station	Parameters	Jan.	Feb.	Mar.	Apr.	May	Jun.	Jul.	Aug.	Sep.	Oct.	Nov.	Dec.	Annual
Belen	v_m (m/s)	5.78	5.44	5.12	6.38	7.59	9.30	11.11	11.32	7.95	4.91	4.68	3.92	6.97
	σ (m/s)	3.54	3.23	2.60	3.29	3.26	2.90	1.92	2.29	1.99	2.65	2.58	2.22	3.66
Datça	v_m (m/s)	4.56	5.14	4.70	4.48	6.49	5.63	7.99	5.95	6.26	5.54	5.32	5.39	5.63
	σ (m/s)	3.19	3.87	3.31	3.29	3.07	3.54	2.65	2.55	3.10	3.25	4.05	3.61	3.44
Foca	v_m (m/s)	5.58	5.53	5.65	5.36	4.87	5.48	5.82	6.28	4.74	5.83	6.06	7.45	5.73
	σ (m/s)	2.80	2.90	2.63	2.53	2.32	2.05	1.90	2.05	2.41	2.83	3.41	2.97	2.68
Gelendost	v_m (m/s)	3.79	6.04	4.79	5.98	5.30	5.20	4.92	4.46	4.27	4.28	5.55	6.17	5.05
	σ (m/s)	3.00	4.81	3.65	4.56	3.12	2.94	2.49	2.40	3.01	2.37	4.33	4.76	3.63
Söke	v_m (m/s)	3.24	3.54	3.12	3.14	4.55	4.94	6.03	5.11	3.78	4.51	3.55	3.62	4.10
	σ (m/s)	1.85	2.18	2.25	2.15	2.66	2.67	2.45	2.49	2.48	2.34	2.27	2.48	2.53

Table 4.10. Monthly and annual Weibull parameters for all stations

Station	Parameters	Jan.	Feb.	Mar.	Apr.	May	Jun.	Jul.	Aug.	Sep.	Oct.	Nov.	Dec.	Annual
Belen	*k*	1.7	1.76	2.09	2.05	2.5	3.54	6.73	5.67	4.5	1.95	1.91	1.85	2.01
	c (m/s)	6.48	6.11	5.78	7.2	8.55	10.33	11.9	12.24	8.71	5.54	5.27	4.41	7.87
Datça	*k*	1.47	1.36	1.46	1.4	2.25	1.66	3.32	2.51	2.15	1.78	1.34	1.55	1.71
	c (m/s)	5.04	5.61	5.19	4.91	7.33	6.3	8.91	6.71	7.07	6.23	5.8	5.99	6.31
Foca	*k*	2.11	2.02	2.29	2.26	2.24	2.91	3.37	3.37	2.08	2.19	1.87	2.71	2.28
	c (m/s)	6.3	6.24	6.38	6.05	5.5	6.14	6.48	6.99	5.35	6.58	6.83	8.38	6.47
Gelendost	*k*	1.29	1.28	1.34	1.34	1.78	1.86	2.1	1.96	1.46	1.9	1.31	1.33	1.43
	c (m/s)	4.1	6.52	5.22	6.51	5.96	5.86	5.55	5.03	4.71	4.82	6.02	6.71	5.56
Söke	*k*	1.84	1.69	1.43	1.51	1.79	1.95	2.66	2.18	1.58	2.04	1.63	1.51	1.69
	c (m/s)	3.65	3.97	3.43	3.48	5.12	5.57	6.78	5.77	4.21	5.09	3.97	4.01	4.59

4.3.3. Probability Density Distributions

The frequency distribution and probability density of the wind speeds help answering the following questions: i) How long is a wind power plant out of production in the case of lack of wind? ii) Which is the range of the most frequent wind speeds? iii) How often does the wind power plant achieve its rated output? In this study, firstly, shape (*k*) and scale (*c*) parameters of the Weibull function were calculated. Monthly and annual Weibull parameters for all stations are given in Table 4.10. As seen in this table, the shape parameters are within the range of $1.28 \leq k \leq 6.73$ for all stations. The scale parameters also vary between 3.43 m/s and 12.24 m/s. Then, wind speed frequency distributions for all stations were determined by using the Weibull and Rayleigh probability density functions.

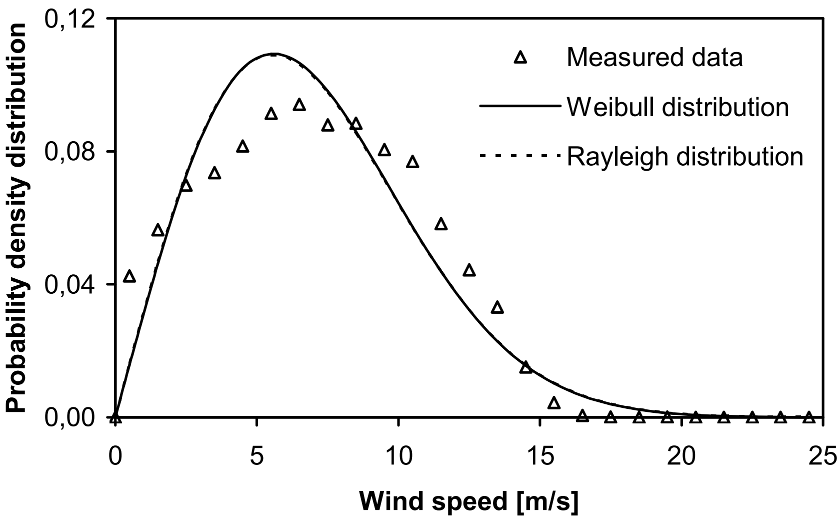

Figure 4.38. Wind speed frequency distributions in Belen station

Figures 4.38-42 present the wind speed frequency distributions of all stations. As seen in this figures, the top point of the curve is the most frequent wind speed. Moreover, in whole regions, the Weibull distribution is a better fit measured probability density distributions than the Rayleigh distribution. The Weibull, Rayleigh and observed probability distribution of the wind speeds in Belen for the year 2005 is given in Table 4.11. Annual cumulative probability distributions of all stations determined by Weibull model are presented in Figures 4.43. It is also clear from this figure that the hourly wind speeds in Belen are higher than the others. This region looks considerably promising for the electricity generation according to the others.

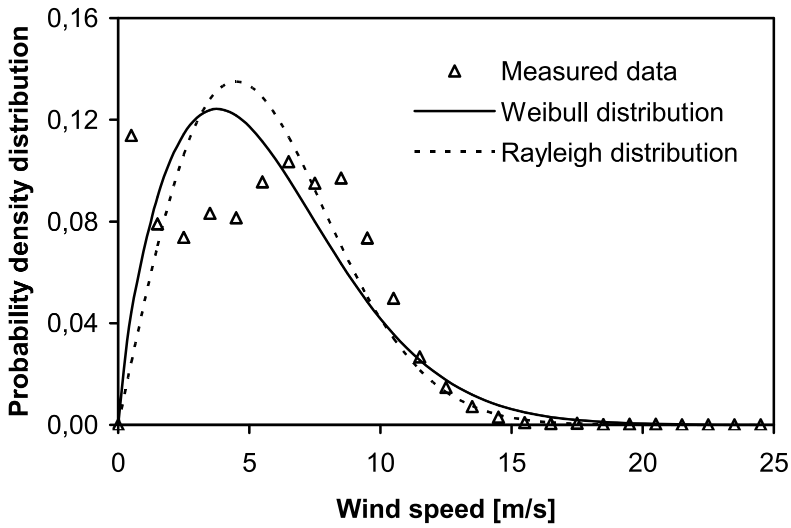

Figure 4.39. Wind speed frequency distributions in Datça station

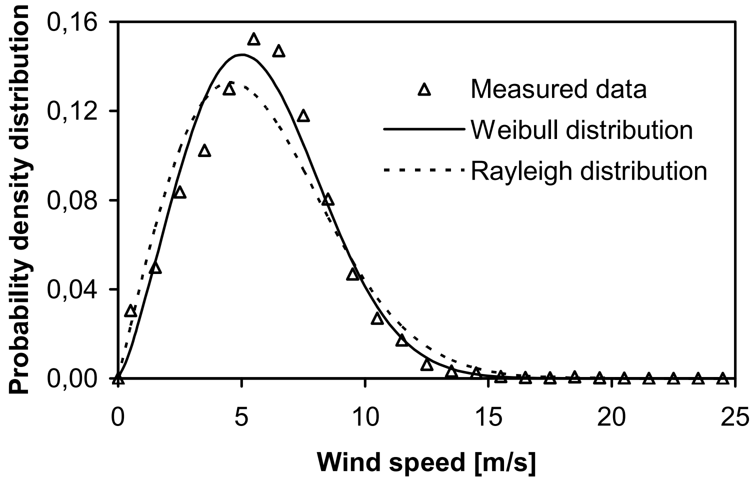

Figure 4.40. Wind speed frequency distributions in Foca station

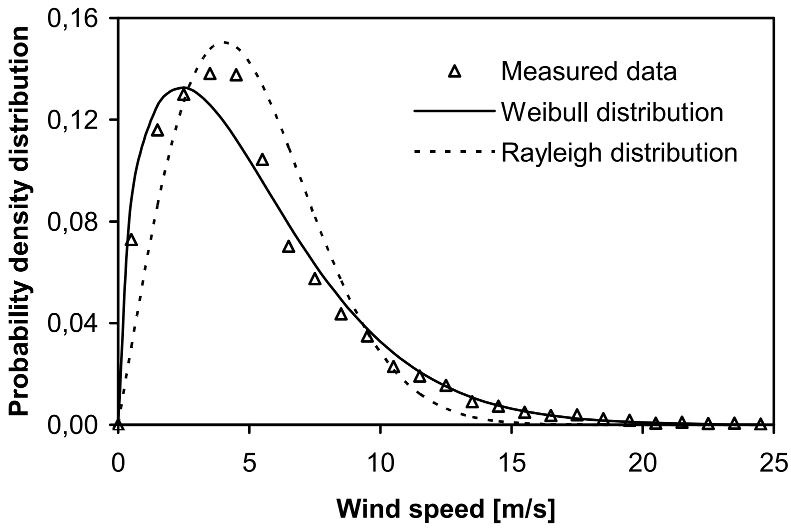

Figure 4.41. Wind speed frequency distributions in Gelendost station

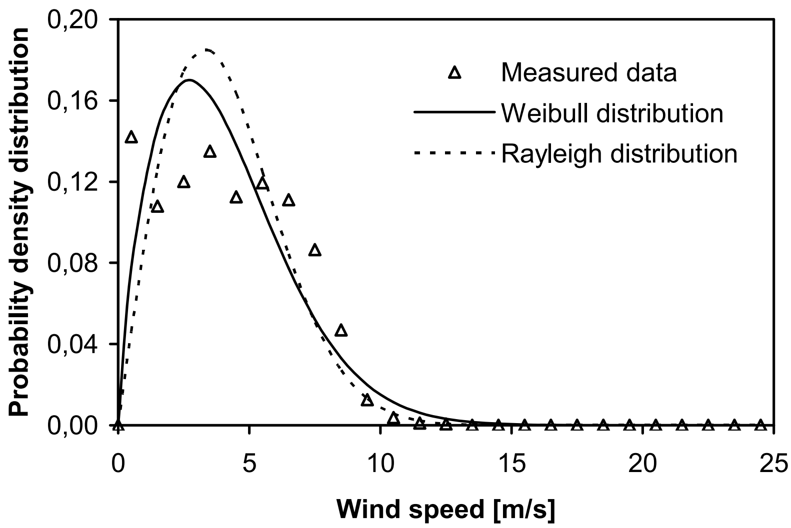

Figure 4.42. Wind speed frequency distributions in Söke station

Table 4.11. Weibull, Rayleigh and measured probability distribution of the wind speeds in Belen for the year 2005

i	Speed class v_i (m/s)	Mean wind speed v_{mi} (m/s)	Frequency of occurrence f_i	Probability distribution		
				Measured data $f(v_i)$	Weibull model $f_W(v_i)$	Rayleigh model $f_R(v_i)$
1	0-1	0.5	373	0.0426	0.0157	0.0161
2	1-2	1.5	494	0.0564	0.0462	0.0468
3	2-3	2.5	612	0.0699	0.0726	0.0731
4	3-4	3.5	645	0.0736	0.0926	0.0928
5	4-5	4.5	715	0.0816	0.1049	0.1049
6	5-6	5.5	801	0.0914	0.1093	0.1091
7	6-7	6.5	825	0.0942	0.1066	0.1062
8	7-8	7.5	771	0.0880	0.0981	0.0977
9	8-9	8.5	775	0.0885	0.0859	0.0855
10	9-10	9.5	706	0.0806	0.0717	0.0714
11	10-11	10.5	674	0.0769	0.0573	0.0571
12	11-12	11.5	510	0.0582	0.0439	0.0438
13	12-13	12.5	389	0.0444	0.0323	0.0323
14	13-14	13.5	291	0.0332	0.0229	0.0229
15	14-15	14.5	133	0.0152	0.0156	0.0157
16	15-16	15.5	39	0.0045	0.0102	0.0103
17	16-17	16.5	5	0.0006	0.0064	0.0065
18	17-18	17.5	1	0.0001	0.0039	0.004
19	18-19	18.5	0	0.0000	0.0023	0.0024
20	19-20	19.5	1	0.0001	0.0013	0.0013
21	20-21	20.5	0	0.0000	0.0007	0.0007
22	21-22	21.5	0	0.0000	0.0004	0.0004
23	22-23	22.5	0	0.0000	0.0002	0.0002
24	23-24	23.5	0	0.0000	0.0001	0.0001
25	24-25	24.5	0	0.0000	0.0000	0.0000

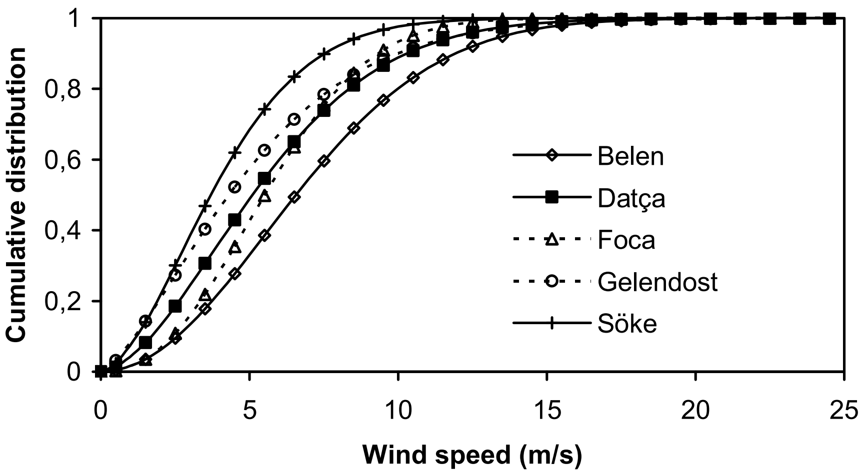

Figure 4.43. Weibull cumulative probability distributions for all stations

4.3.4. Power Density Distributions

The monthly variations of the mean power densities, which are calculated using measured data, WAsP program, Weibull and Rayleigh model, are presented in Figures 4.44-48. It is apparent from the figures that the power densities vary rapidly from month to month for all stations. It is another significant point that Belen present higher wind power potential than the others. In this region, the monthly mean wind power potentials are higher than 200 W/m^2 during 8 months of the year at 10 m height above the ground level. The maximum monthly mean wind power potential calculated using the measured probability density distribution appears at Belen station with 1,000.6 W/m^2 during the month of August. It is interesting to note that the Weibull distribution is better in fitting the observed monthly probability density distributions than the Rayleigh distribution for all stations. But, in general, the WAsP program provides better power density estimations for all stations than the Weibull and Rayleigh model.

The performance values for all stations, such as MAPE and R are given in Table 4.12. The MAPE values ranged from 0.59% to 47.88% differ from the observed data for all stations. The maximum MAPE was found to be 47.88% for Gelendost station in the Rayleigh model, while the best result was found to be 0.59% for Gelendost station in the WAsP program. The maximum correlation coefficient was found to be 0.99995at Belen station by the WAsP program, while the minimum correlation coefficient was found as 0.88092 using Rayleigh model for Datça station.

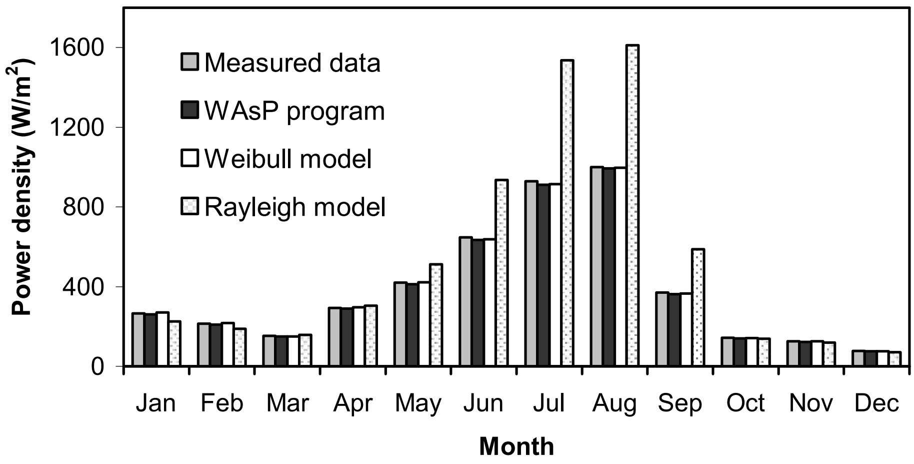

Figure 4.44. Monthly variation of the mean power densities in Belen

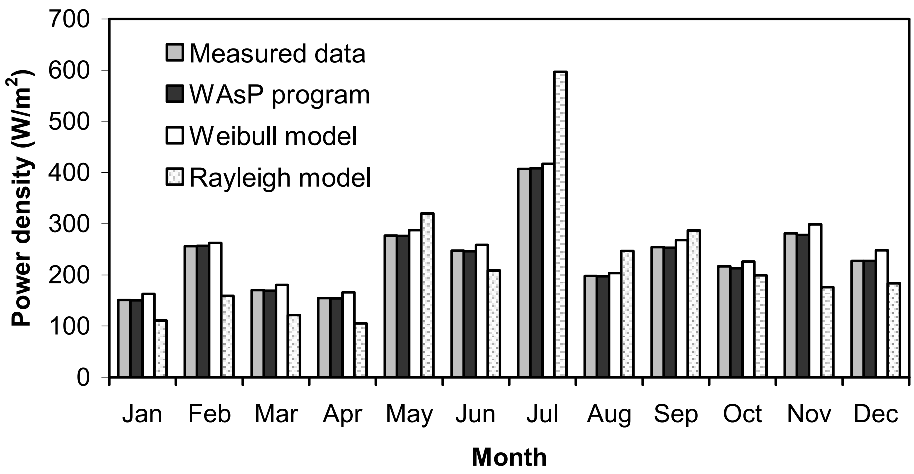

Figure 4.45. Monthly variation of the mean power densities in Datça

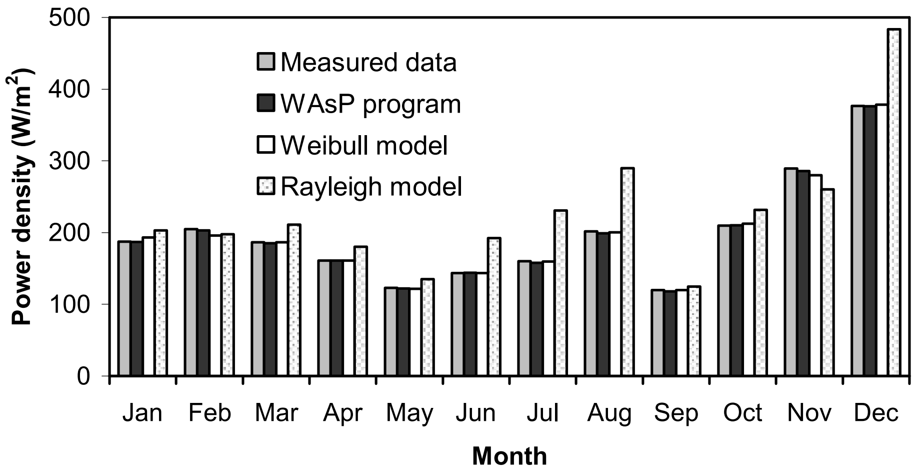

Figure 4.46. Monthly variation of the mean power densities in Foca

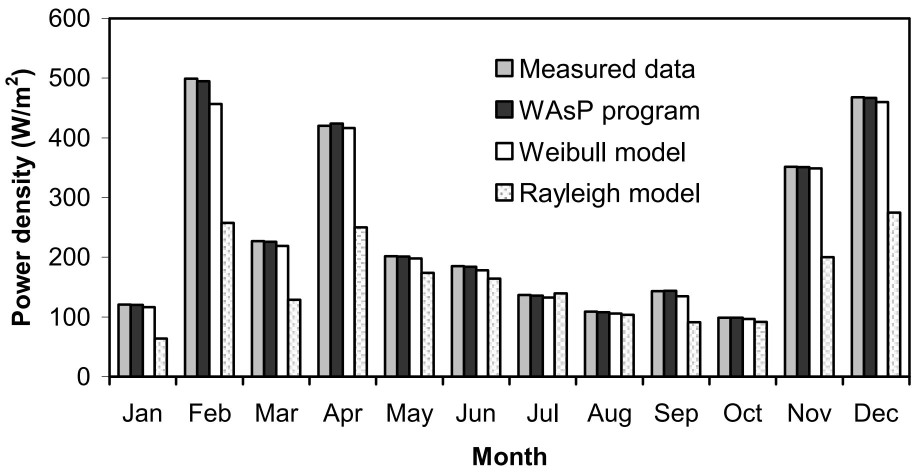

Figure 4.47. Monthly variation of the mean power densities in Gelendost

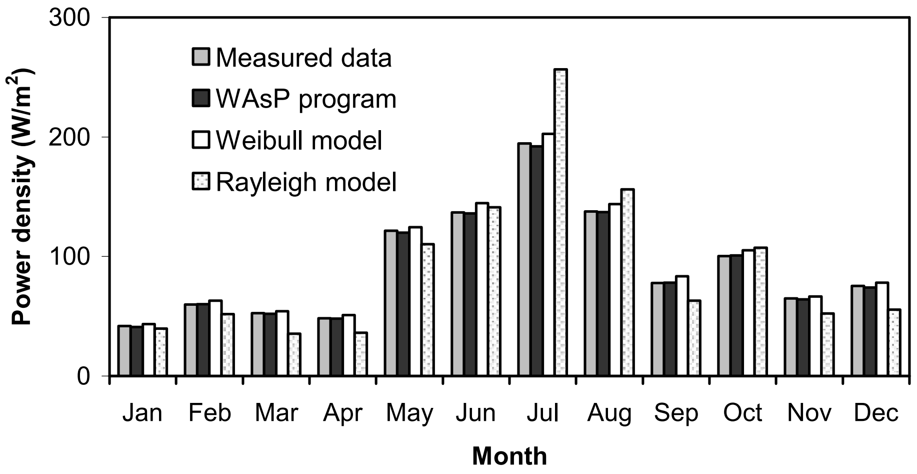

Figure 4.48. Monthly variation of the mean power densities in Söke

Table 4.12. Performance values for all stations

Station	WAsP program		Weibull model		Rayleigh Model	
	MAPE	R	MAPE	R	MAPE	R
Belen	2.00150	0.99995	1.1021	0.99990	18.141	0.99319
Datça	0.59131	0.99985	5.3631	0.99809	35.427	0.88092
Foca	0.71853	0.99987	1.2313	0.99823	14.633	0.91253
Gelendost	0.58815	0.99992	3.4718	0.99795	47.875	0.94197
Söke	0.98962	0.99988	4.1645	0.99969	20.086	0.98119

The variation of the annual wind power density distribution obtained from the Weibull model for all stations are shown in Figure 4.49. It is clear from the figure that, the annual wind power density of Belen station is higher than the other stations. The maximum energy production at this station is obtained at the wind speed of about 11.5 m/s. Although this wind speed is available 5% time period of one year during this period of wind speed 10% of the total wind energy can be produced for this one year period of time.

The annual wind power potentials for all stations are given in Table 4.13. It is clear from the table that the WAsP program and the Weibull model provide better power density estimations than Rayleigh model for all stations. According to the measured data, the highest annual wind power potential value is determined as 383.72 W/m^2 at Belen station while the lowest annual wind power potential value is found as 93.05 W/m^2 at Söke station. The annual wind power potential values of Datça, Foca, and Gelendost stations are determined as 236.55 W/m^2, 197.19 W/m^2 and 244.47 W/m^2, respectively.

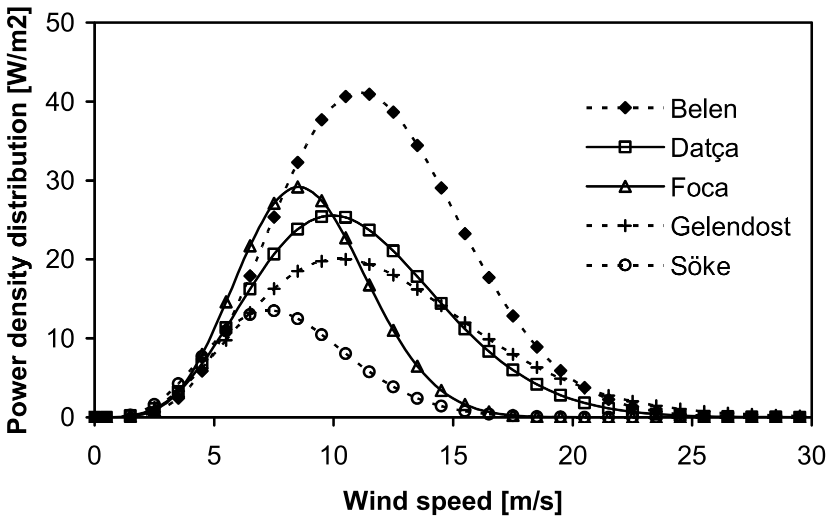

Figure 4.49. Annual wind power density distribution obtained from the Weibull model for all stations

Table 4.13. Annual wind power potentials (W/m^2) for all stations

Station	Measured data	WAsP program	Weibull model	Rayleigh Model
Belen	383.72	387.00	394.81	396.09
Datça	236.55	238.00	248.38	208.75
Foca	197.19	199.00	195.40	220.08
Gelendost	244.47	246.00	230.60	150.65
Söke	93.05	95.00	97.26	80.623

4.4. Prediction of Wind Power Potential

4.4.1. Preparation of Input and Output Data

In this study, hourly wind speed data, collected by the Turkish State Meteorological Service (TSMS) from 4 measuring stations (Antakya, Karataş, İskenderun and Samandağ) during 1994-2001 periods, were used. This data was divided into two sections. The first section of the data which covers the years between 1994 and 1999 was supplied to the ANN for training process. The second section of the data which covers the years of 2000 and 2001 was supplied to the ANN for testing process. Frequency values of each observed wind speed range were utilized in the input layer of the network, while mean wind power potential was used in the output layer of the network. Wind Atlas Analysis and Application Program (WAsP) was applied in the preparation of input and output data. Frequency values of wind speeds and mean wind power potential were calculated as monthly. As an example, frequency values of wind speeds of the 2000 were given for Karataş in Table 4.14. Frequency distribution of wind speeds for Karataş (February 2000) is shown in Figure 4.50. In the second column of Table 4.14, each observed wind speed range is given. Frequency values of each observed wind speed range are also provided in between third and fourteenth columns of Table 4.14. In response to the input frequencies, output values of the network or mean values of monthly wind power potential are given in Table 4.15.

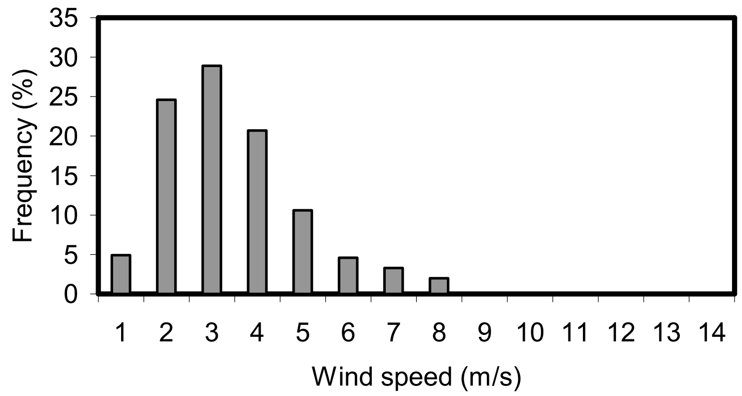

Figure 4.50. Frequency distribution of wind speeds for Karataş (February 2000)

Table 4.14. Frequency values used in the input layer of the network for Karataş (year 2000)

No i	Wind speed range v_i (m/s)	Frequency values of wind speeds f_i (per thousand)											
		Jan.	Feb.	March	Apr.	May	June	July	Aug.	Sep.	Oct.	Nov.	Dec.
1	0-1	35	49	86	97	120	67	145	125	118	71	76	36
2	1-2	161	246	360	279	234	169	210	194	317	344	424	226
3	2-3	285	289	293	245	290	247	249	249	263	331	297	395
4	3-4	234	207	133	167	208	269	250	265	203	187	150	246
5	4-5	151	106	55	97	95	165	126	126	78	53	18	68
6	5-6	90	46	20	46	31	54	20	28	19	11	7	20
7	6-7	28	33	25	25	14	25	0	11	1	4	14	8
8	7-8	12	20	14	25	7	3	0	3	0	0	7	0
9	8-9	3	1	11	11	1	0	0	0	0	0	3	0
10	9-10	1	1	3	4	0	0	0	0	1	0	3	0
11	10-11	0	1	0	1	0	0	0	0	0	0	1	0
12	11-12	0	0	0	1	0	0	0	0	0	0	0	0
13	12-13	0	0	0	1	0	0	0	0	0	0	0	0
14	13-14	0	0	0	0	0	0	0	0	0	0	0	0

Table 4.15. Mean wind power potential used in the output layer of the network for Karataş (year 2000)

Station	Mean wind power potential P (W/m^2)											
	Jan.	Feb.	Mar.	Apr.	May	Jun.	Jul.	Aug.	Sep.	Oct.	Nov.	Dec.
Karataş	36	32	25	38	22	28	18	22	16	13	17	18

4.4.2. Artificial Neural Network Architecture

Artificial neural network architecture used in this study is shown in Figure 4.51. This network consists of an input layer, two hidden layers and an output layer. Frequency values of each observed wind speeds were used in the input layer of the network, while mean wind power potential was used in the output layer of the network. Layers of neurons other than the input and output layer are called hidden layers. Resilient propagation (RP), scaled conjugate gradient (SCG) and Levenberg-Marquardt (LM) learning algorithms were used in the present simulation. Neurons in the input layer have no transfer function. Logistic sigmoid transfer function (logsig) was used in the hidden layers and output layer of the network as an activation function. The values used in the input and output layers were normalized as $v_N = [v_R - v_{\min}]/[v_{\max} - v_{\min}]$ in the range of (0-1). MATLAB simulations were performed to estimate mean wind power potential. The number of neurons in each layer of the network for all stations is given in Table 4.16.

In each layer, every neuron is connected to a neuron of adjacent layer having different weights. Each neuron as indicated in Figure 4.51 receives signals from the neurons of the previous layer weighted by the interconnect values between neurons except input layer. Neurons then produce an output signals by passing the summed signals through sigmoid function (Maqsood et al., 2005). The weights of the connections between neurons are adjusted during the training process in order to achieve the desired input/output relation of the network (Mohandes et al., 2004). The difference between the predicted output of the network and the desired output that defined during the training process is used in order to adjust the weights. This procedure continuous until the difference between actual output of the network and the desired output is equal with a specified remainder value. Here, the criterion is that the network output should be closer to the value of desired output. This training process has to be repeated for the rest of the input-output pairs which exist in the training data. The back-propagation algorithm is used to minimize an error function defined by the average of sum of their square difference between the output of each neuron in the output layer and the desired output (Mohandes et al., 2004).

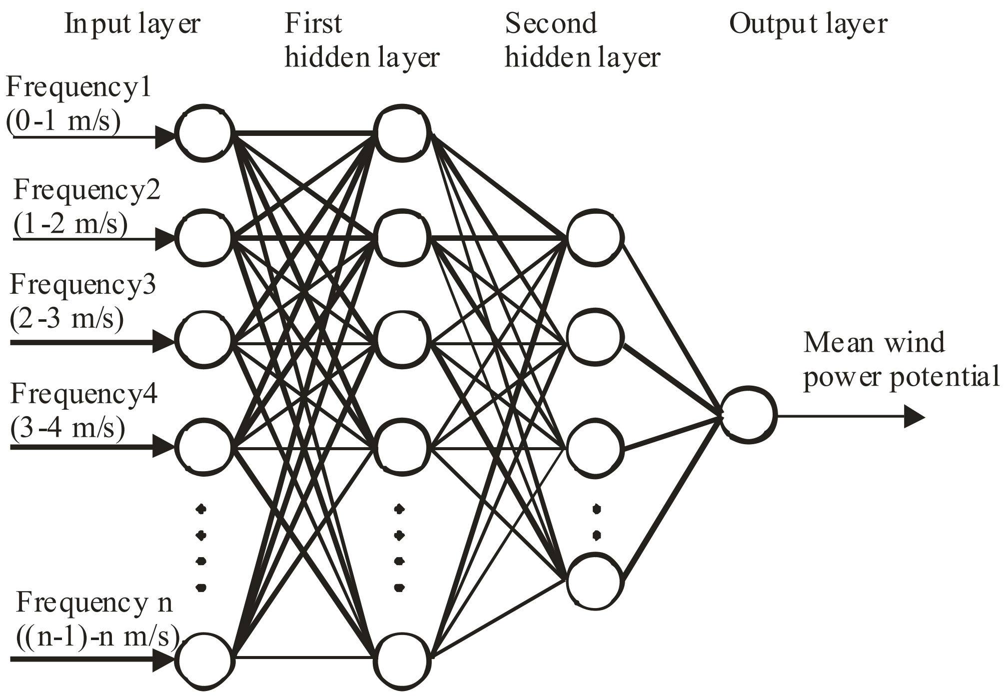

Figure 4.51. ANN architecture

Table 4.16. The number of neurons in each layer of network

Station	Number of neurons in the input layer	Number of neurons in the first hidden layer	Number of neurons in the second hidden layer	Number of neurons in the output layer
Antakya	14	28	28	1
İskenderun	17	34	17	1
Karataş	14	28	28	1
Samandağ	14	28	14	1

4.4.3. Results and Discussion

Application of ANN is wide spread particularly in engineering problems. But there is not much work done on the prediction of the wind energy using ANN. In the present study, it is realized that artificial neural network is easy to apply for the prediction of the wind power potential.

The root mean squared error (RMSE) and the mean absolute percentage error (MAPE) were used to see the convergence between the target value and the output value. These two parameters are defined as follows respectively (Melesse and Hanley, 2005),

$$RMSE = \left[\frac{1}{n} \sum_{i=1}^{n} \left(t_i - o_i \right)^2 \right]^{1/2} \tag{4.4.1}$$

$$MAPE = \frac{1}{n} \sum_{i=1}^{n} abs\left(\frac{o_i - t_i}{o_i} \right).100 \tag{4.4.2}$$

In addition, the absolute fraction of variance (R^2) is defined as follows (Sözen et al., 2005),

$$R^2 = 1 - \left[\frac{\sum_{i=1}^{n} (t_i - o_i)^2}{\sum_{i=1}^{n} o_i^{\,2}} \right] \tag{4.4.3}$$

Where, t is the target value, o is the output value and n is the total number of months.

ANN has two operating modes, called training and testing process. Firstly, training process is applied to design the model. Then, testing process is applied to evaluate the performance of the network. ANN can give different results for each test using algorithm constructed in the present work. Therefore, 20 tests were performed for each meteorological station separately and for the most appropriate result, average value of these tests was taken. The performance values for all stations, such as RMSE, MAPE and R^2 for testing process are given in Table 4.17. Results indicate that the RP learning algorithm provides better results compared to the SCG and LM learning algorithm. The MAPE values ranged from 2.90% to 7.84% differ from the actual value for all stations and learning algorithms. The maximum MAPE was found as 7.84% for Antakya in the SCG learning algorithm, while the best result was found as 2.90% for Karataş in the RP learning algorithm.

Table 4.17. Statistical errors for different learning algorithms

Station	RP learning algorithm			SCG learning algorithm			LM learning algorithm		
	RMSE	R^2	MAPE	RMSE	R^2	MAPE	RMSE	R^2	MAPE
Antakya	0.84	0.99	6.28	1.79	0.99	7.84	0.98	0.99	7.21
Karataş	0.89	0.99	2.90	1.01	0.99	3.80	0.93	0.99	3.53
İskenderun	2.29	0.99	3.85	3.58	0.99	7.52	3.61	0.99	7.54
Samandağ	3.21	0.99	4.04	5.00	0.99	6.92	3.88	0.99	5.30

In the present study, 2 years i.e. 24 months of hourly wind speed data from the year 2000 to 2001 were taken for comparison. As seen in Figures 4.52-55 prediction of ANN (RP, SCG and LM) follows the variation of actual data exactly. Here, the results of WAsP are taken as an actual data. In the case of Antakya meteorological station, there are two sharp points with a level of 80 W/m^2 which correspond to the month of July, where as the lowest level of wind power potential with a level of 10 W/m^2 corresponding to the months of January and February as indicated in Figure 4.52 occurs. Even though, the prediction of ANN agrees well with the actual value. On the other hand, the actual mean wind power potential of İskenderun meteorological station presented in Figure 4.54 varies rapidly from month to month. Even though, the prediction of ANN for most of the months agrees well with the actual values. It seems that as long as the necessary data are utilized for learning and testing process of the ANN method. It is possible to estimate an accurate result. It can be concluded that the ANN looks promising in predicting the wind energy potential. The performance of the ANN method is examined and its data are presented in Figures 4.56-59. From beginning month to the last month, most of the results agreed well. Only a few point scattered from a linear line for İskenderun meteorological station.

Obstacles situated around meteorological stations reduce the actual value of wind speed dramatically. Unfortunately, there are many buildings exist around these meteorological stations. With is in mind, Şahin et al. (2005) considered the effect of obstacles, orography and roughness on the measured wind speed in order to obtain the corrected wind speed values. Hence, Şahin et al. (2005) reported that the mean wind energy potentials reach 500 W/m^2 at 25 m height above the ground level in many areas of these regions. In the present work, measured wind speed data were only used to see the capability of the ANN. For this reason, the mean value of wind energy potential that predicted by WAsP and ANN is low because of using uncorrected wind speed data.

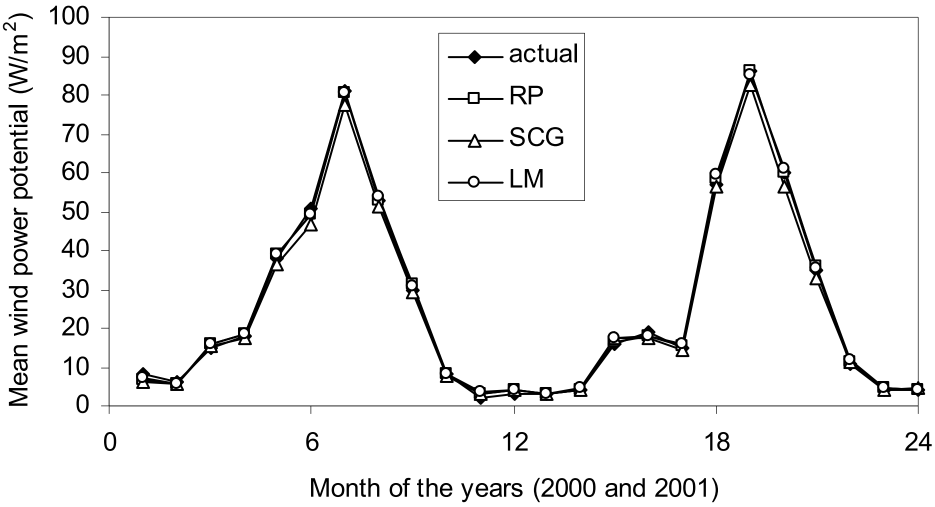

Figure 4.52. Comparison between prediction of artificial neural network (RP, SCG and LM) and actual results for Antakya meteorological station

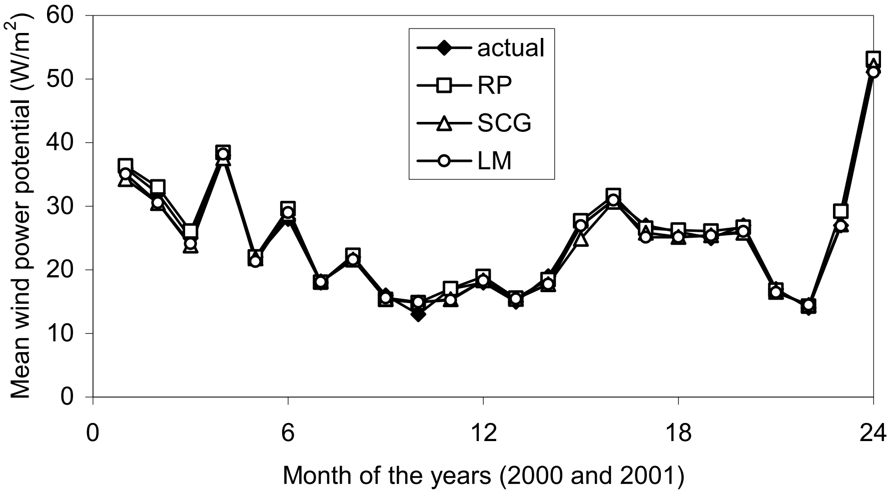

Figure 4.53. Comparison between prediction of artificial neural network (RP, SCG and LM) and actual results for Karataş meteorological station

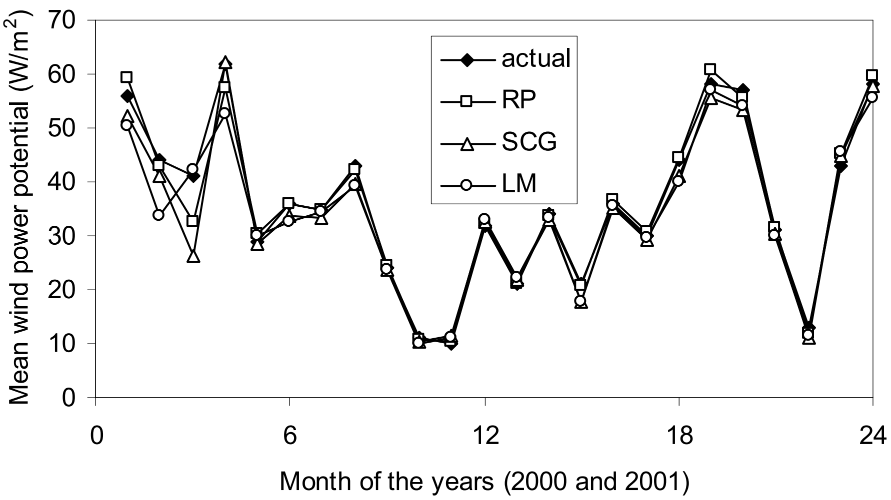

Figure 4.54. Comparison between prediction of artificial neural network (RP, SCG and LM) and actual results for İskenderun meteorological station

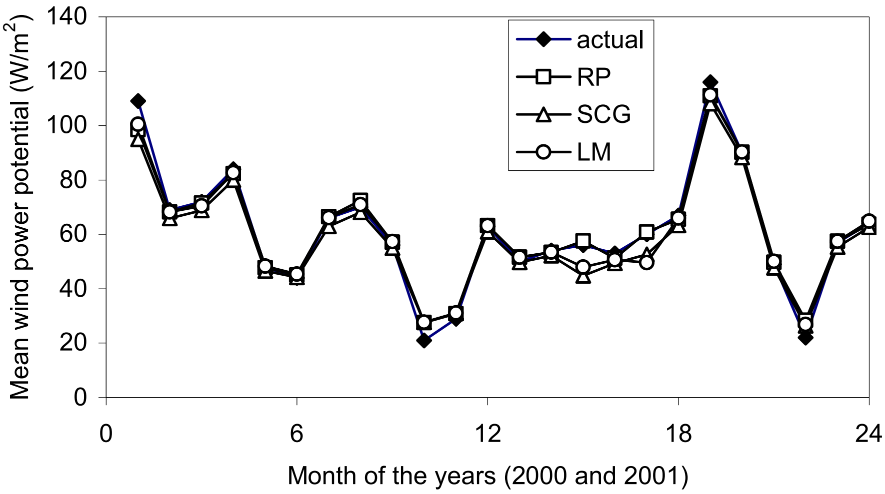

Figure 4.55. Comparison between prediction of artificial neural network (RP, SCG and LM) and actual results for Samandağ meteorological station

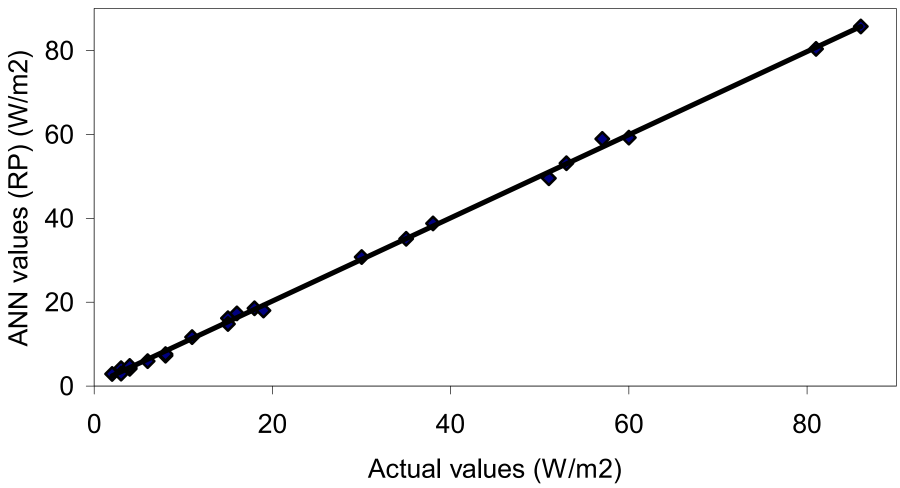

Figure 4.56. Actual mean wind power potentials and network predictions for testing process of Antakya meteorological station

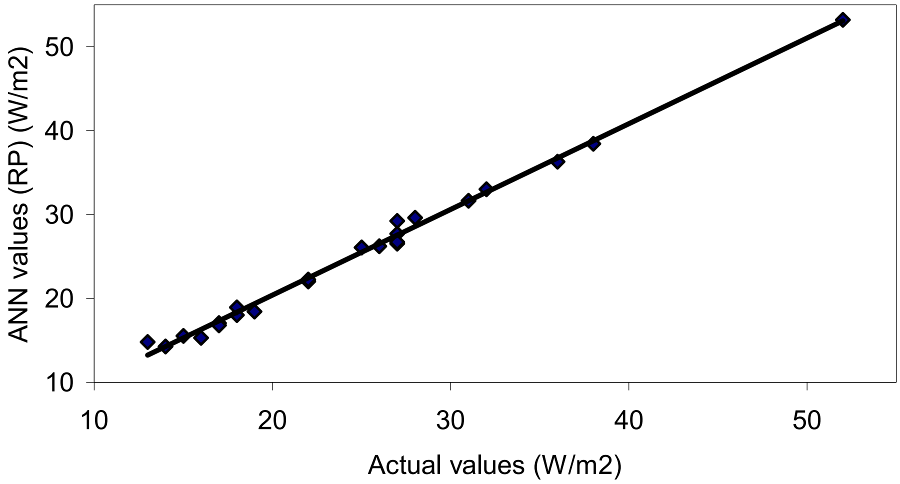

Figure 4.57. Actual mean wind power potentials and network predictions for testing process of Karataş meteorological station

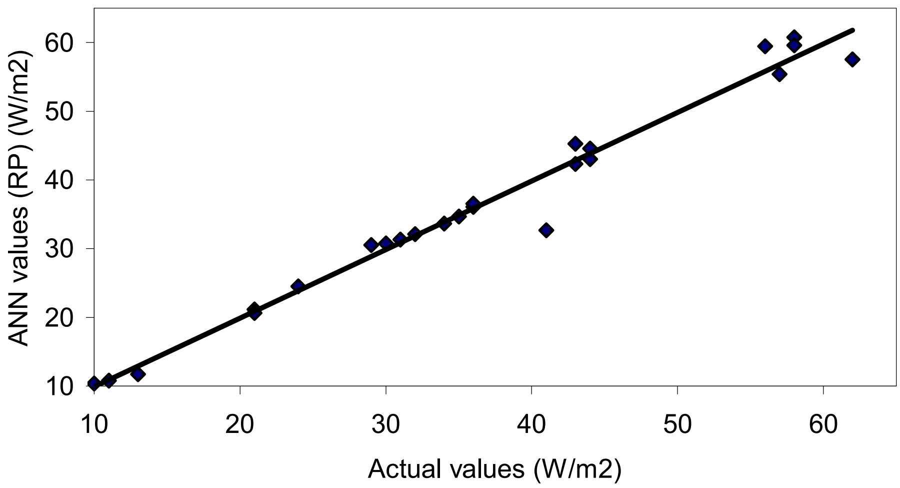

Figure 4.58. Actual mean wind power potentials and network predictions for testing process of İskenderun meteorological station

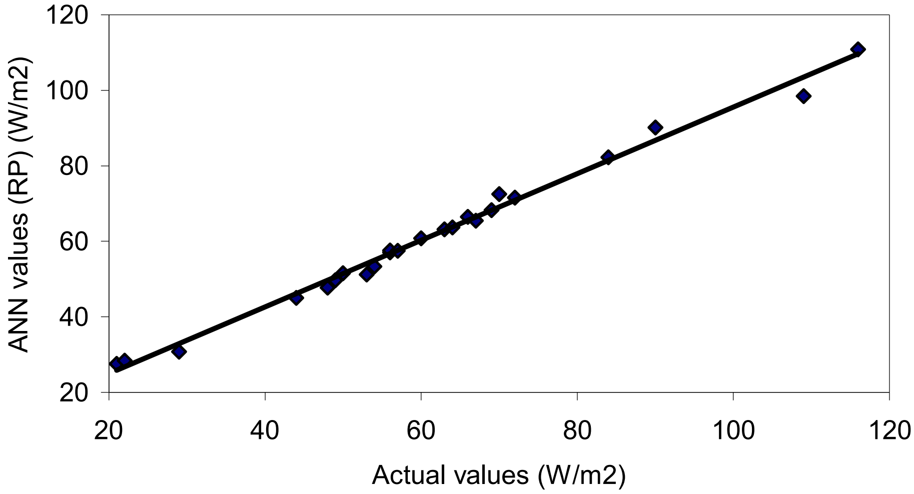

Figure 4.59. Actual mean wind power potentials and network predictions for testing process of Samandağ meteorological station

4.5. Application of Artificial Neural Networks for the Wind Speed Prediction of Target Station Using Reference Stations Data

4.5.1. Preparation of Input and Output Data

In this study, hourly wind speed data, collected by the Turkish State Meteorological Service (TSMS) at 8 measuring stations such as Antakya, İskenderun, Samandağ, Dörtyol, Karataş, Yumurtalık, Adana and Mersin stations in the eastern Mediterranean region of Turkey, were used. The long-term wind data, containing hourly wind speeds, directions and related information, cover the period from the year 1992 to 2001. The mean monthly wind speeds were calculated from these hourly wind speed data. These data were divided into two parts. The first part of the data which covers the years between 1992 and 1999 was used for training procedure. The second part of the data which covers the years of 2000 and 2001 was utilized for testing procedure. The map of the region, the location of the stations and the dominant prevailing wind directions for each station are presented in Figure 4.60. Stations are located between 36^0.05” and 36^0.59” north latitude, while the heights of stations above the sea level vary between 3 meter and 100 meter. Except Adana and Antakya; all stations are located on the coastal site of the eastern Mediterranean region of Turkey. Dominant prevailing wind directions for Antakya, Samandağ and Karataş meteorological stations are 210^0 (SW). In these regions, southwestern winds are effective. For Adana, Yumurtalık, Dörtyol, İskenderun and Mersin, dominant prevailing wind directions are 0^0 (N), 30^0 (NE), 120^0 (ES), 300^0 (WN) and 330^0 (NW), respectively. The mean wind speeds and dominant prevailing wind directions of all stations are presented in Table 4.18. As seen in this table, the mean wind speed varies mainly from 0.8 m/s to a maximum of 4.0 m/s. Height of anemometer of all stations is 10 m above the ground level. Mediterranean climate is dominant in this region, usually hot and dry in summer, lukewarm and rainy in winter. But, climate properties vary depending on the level of the height above the sea level. On the slope of a mountain looking at the sea, an increase of terrestrial effects on climate is observed. However, the weather in this region does not show intense terrestrial climate due to the Mediterranean Sea effect.

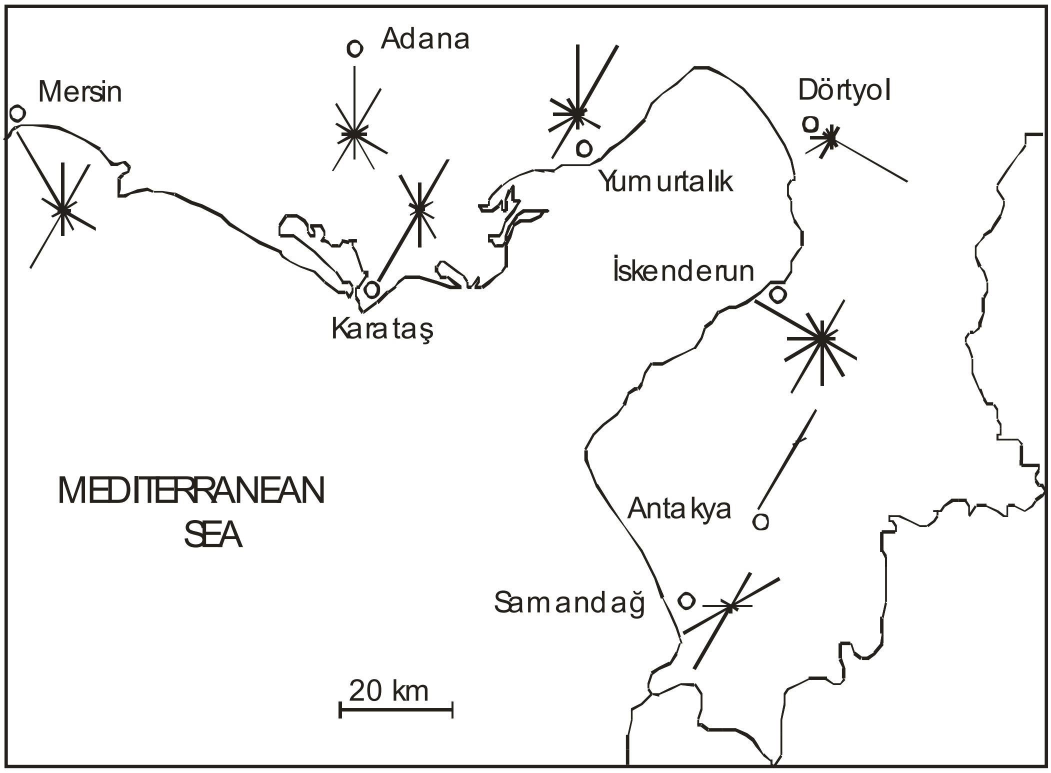

Figure 4.60. Map of the region, location of the stations and dominant wind directions

Table 4.18. Mean wind speeds and dominant prevailing wind directions of all stations

Station	Latitude	Longitude	Altitude (m)	Mean wind speed (m/s)	Dominant prevailing wind direction
Antakya	36^0.12’’	36^0.10’’	100	2.8	SW(210^0), NE(30^0)
İskenderun	36^0.35’’	36^0.10’’	4	2.6	WN(300^0), SW(210^0)
Karataş	36^0.34’’	35^0.23’’	22	2.7	SW(210^0), NE(30^0)
Yumurtalık	36^0.46’’	35^0.47’’	27	1.9	NE(30^0), N(0^0)
Dörtyol	36^0.51’’	36^0.13’’	28	0.9	ES(120^0), WS(240^0)
Samandağ	36^0.05’’	35^0.58’’	4	4.0	SW(210^0), EN(60^0)
Adana	36^0.59’’	35^0.18’’	28	0.8	N(0^0), NE(30^0)
Mersin	36^0.49’’	34^0.36’’	3	2.3	NW(330^0), SW(210^0)

Table 4.19. Correlation coefficients of wind speeds amongst stations

Station	Mersin	Adana	Yumurtalık	İskenderun	Karataş	Samandağ	Antakya	Dörtyol
Dörtyol	1	0.04	0.1	0.02	0.24	0.06	0.18	0.25
Antakya	0.04	1	0.46	0.4	**0.66**	0.44	0.14	**0.91**
Samandağ	0.1	0.46	1	**0.76**	**0.74**	**0.69**	0.41	0.31
Karataş	0.02	0.4	**0.76**	1	**0.72**	**0.85**	**0.67**	0.36
İskenderun	0.24	**0.66**	**0.74**	**0.72**	1	**0.59**	0.29	**0.59**
Yumurtalı	0.06	0.44	**0.69**	**0.85**	**0.59**	1	**0.76**	0.43
Adana	0.18	0.14	0.41	**0.67**	0.29	**0.76**	1	0.15
Mersin	0.25	**0.91**	0.31	0.36	**0.59**	0.43	0.15	1

In this study, a model was developed to estimate wind speed of any target station utilizing wind speeds of the reference measuring stations. Firstly, the mean monthly wind speed obtained at 8 measuring stations in the eastern Mediterranean region of Turkey were compared with each other and the correlation coefficients between them two by two were determined. The accuracy of the results is basically depended on the cross-correlation level between the two stations' wind speed, which is related to the morphology of the surrounding area (Bechrakis and Sparis, 2004). Thus, the relation amongst stations was defined and reference stations were determined for any target station. For the mean monthly wind speed between 1992 and 2001 the correlation coefficients of wind speeds amongst stations are presented in Table 4.19. As seen in this table, Antakya, İskenderun, Karataş, Mersin, Samandağ and Yumurtalık were defined as target stations sequentially except Adana and Dörtyol stations due to a high rate of correlation factors.

4.5.2. Artificial Neural Network Architecture

Artificial neural network architecture used in this study for Karataş meteorological station which is selected as a target station is shown in Figure 4.61. This network consists of an input layer, two hidden layers and an output layer. The mean monthly wind speeds of reference stations and corresponding month were used in the input layer of the network. İskenderun, Yumurtalık, Adana and Samandağ stations were selected as a reference stations. The most significant point in the selection of these reference stations is that there is a good relation with high correlation coefficient between the target station and reference station. The mean monthly wind speed of Karataş which is target station was used in the output layer of the network. For other target stations, the reference stations in the input layer of the network, the number of the neurons in the hidden layers of the network and the number of patterns in the training and testing procedure are given in Table 4.20. Resilient propagation (RP) learning algorithm was used in the present simulation. Neurons in the input layer have no transfer function. Logistic sigmoid transfer function (logsig) and linear transfer function (purelin) were used in the hidden layers and output layer of the network as an activation function, respectively. Simulations were performed to estimate the mean monthly wind speed of target station. In each layer, every neuron is connected to a neuron of adjacent layer having different weights. Each neuron as indicated in Figure 4.61, receives signals from the neurons of the previous layer weighted by the interconnect values between neurons except input layer. Neurons then produce an output signal by passing the summed signal through an activation function (Maqsood et al., 2005). Mohandes et al. (2004) stated that during the training procedure, the weights of the connections between neurons are adjusted in order to achieve the desired input/output relation of the network. This procedure goes on until the difference between the actual output of the network and the desired output is equal with a specified remainder value. Here, the criterion is put forward as the network output which should be closer to the value of desired output. This training procedure has to be repeated for the rest of the input-output pairs existing in the training data.

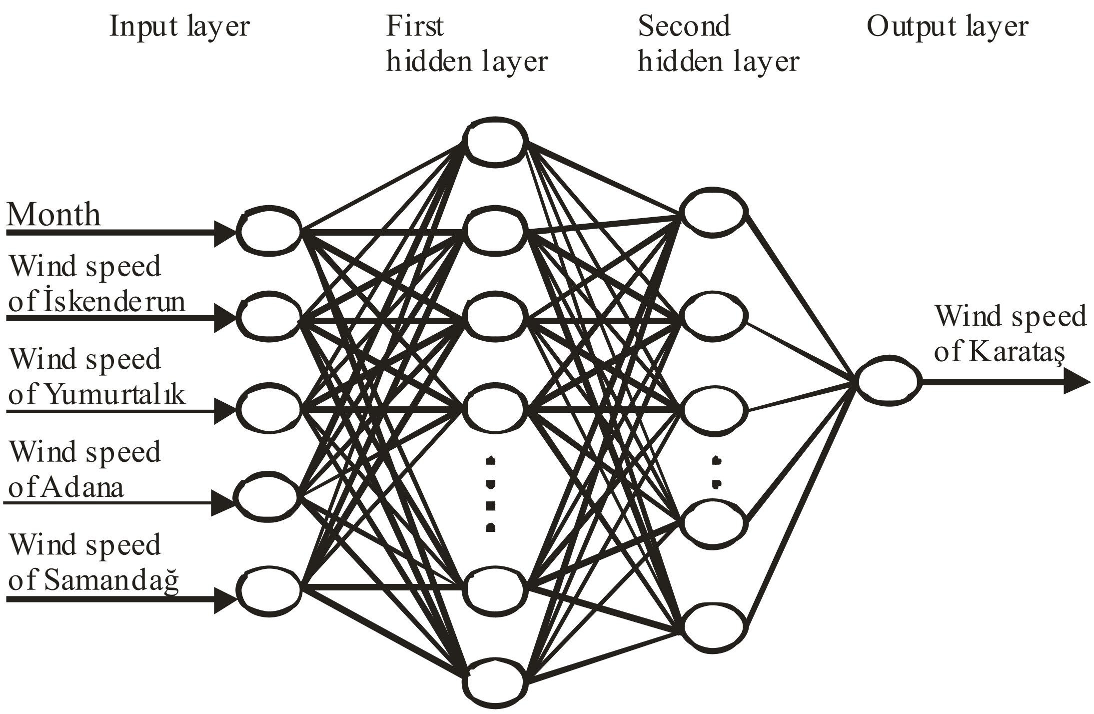

Figure 4.61. ANN architecture

Table 4.20. Reference stations and number of neurons in the hidden layers of the network for target stations

Target station	Reference stations	Number of neurons in hidden layers	Number of patterns in training	Number of patterns in testing
Antakya	İskenderun, Mersin	6-6	95	24
İskenderun	Yumurtalık, Mersin, Antakya, Samandağ, Karataş	12-6	75	24
Karataş	İskenderun, Yumurtalık, Adana, Samandağ	10-5	73	24
Mersin	Antakya, İskenderun	6-3	95	24
Samandağ	Karataş, İskenderun, Yumurtalık	8-4	75	24
Yumurtalık	Adana, Samandağ, Karataş, İskenderun	10-5	73	24

4.5.3. Results and Discussion

In the present study, it is realized that artificial neural network is convenient method to apply for the prediction of the wind speed. The mean absolute percentage error (MAPE) was used to see the convergence between the target value and the output value. In addition, the coefficient of correlation between the target value and output value is defined as follows (Perez-Llera et al., 2002),

$$R = \frac{\overline{t.o} - \bar{t}.\bar{o}}{\sqrt{\left[\overline{t^2} - \left(\bar{t}\right)^2\right].\left[\overline{o^2} - \left(\bar{o}\right)^2\right]}} \tag{4.5.1}$$

Where, t is the target value, o is the output value, n is the total number of months, $\bar{t}$ is the mean of the t_i's, $\bar{o}$ is the mean of o_i's and $\overline{t.o}$ is the mean of the $t_i.o_i$'s.

ANNs have two step procedure; these are called training and testing procedure. They are initially trained and then their accuracy is checked with the testing database. ANN can give different results for each test using algorithm constructed in the present work. Therefore, 10 tests were performed for each meteorological station separately and for the most appropriate result, average values of these tests were taken. The performance values for all stations, such as MAPE and R for training and testing procedure are given in Table 4.21. The MAPE values ranged from 4.49% to 14.13% differ from the actual value for all stations and testing procedure. The maximum MAPE was found to be 14.13% for Antakya station in the testing procedure, while the best result was found to be 4.49% for Mersin station in the testing procedure. The maximum correlation coefficient between the target value and output value was found to be 0.97 for testing procedure of Mersin station, while the minimum correlation coefficient was found as 0.67 for Yumurtalık station. Moreover, another significant point in this table, the performance values of the training procedure are better than the performance values of the testing procedure.

Table 4.21. The performance values for training and testing procedure

Station	Training procedure		Testing procedure	
	MAPE	R	MAPE	R
Antakya	5.53	0.97	14.13	0.96
İskenderun	1.48	0.99	9.97	0.87
Karataş	1.7	0.97	6.66	0.72
Mersin	3.44	0.96	4.49	0.97
Samandağ	3.07	0.95	8.83	0.83
Yumurtalık	2.56	0.97	13.25	0.67

In the present study, 2 years i.e. 24 months of hourly wind speed data from the year 2000 to 2001 were taken for comparison. As seen in Figures 4.62-67, prediction of ANN follows the variation of actual data exactly. In the case of Antakya meteorological station, there are two sharp points with a level of 5 m/s which correspond to the month of July, where as the lowest level of wind speed with a level of 1.1 m/s which corresponds to the months of November and December as indicated in Figure 4.62. Even though, the prediction of ANN agrees well with the actual value. On the other hand, actual mean wind speed of İskenderun meteorological station presented in Figure 4.63 varies rapidly from month to month, though, the prediction of ANN for most of the months agrees well with the actual values. It seems that as long as the necessary data are utilized for training and testing procedure of the ANN method, it is possible to estimate an accurate result. It can be concluded that the ANN looks promising in predicting the wind speed of a target station depending on the selection of the reference measuring stations.

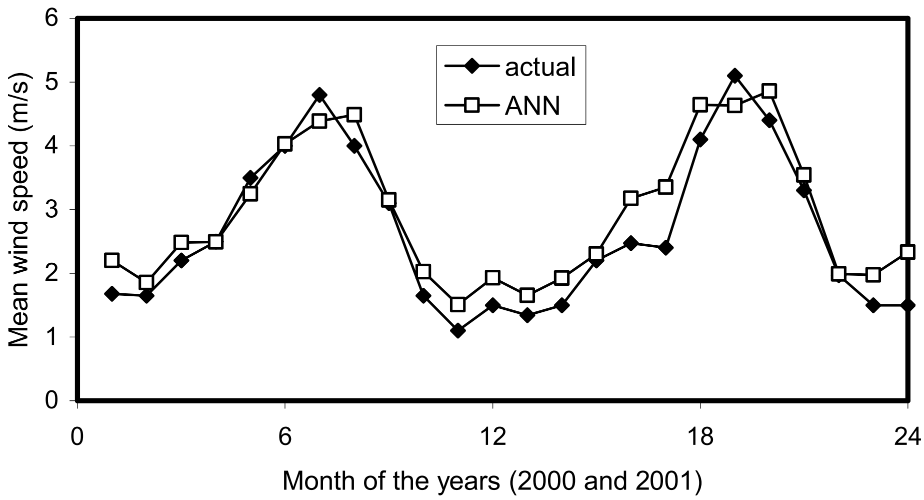

Figure 4.62. Comparison between prediction of ANN and actual results for Antakya meteorological station

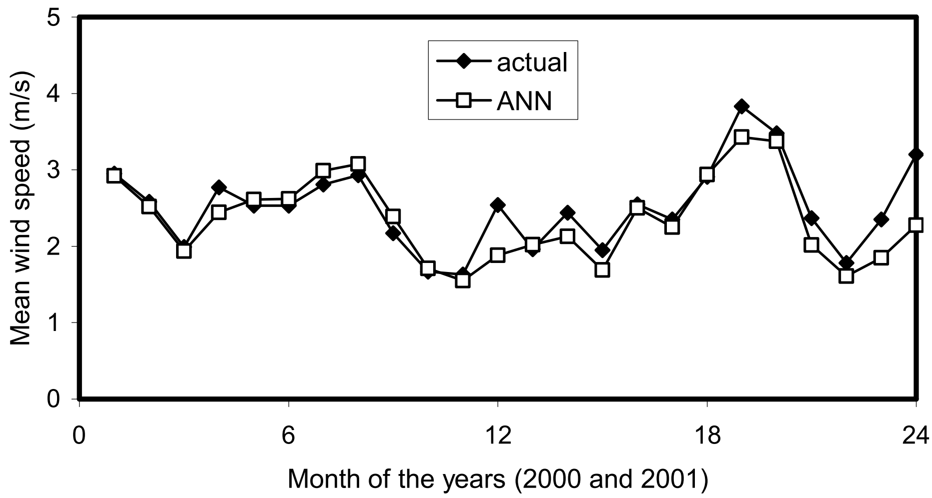

Figure 4.63. Comparison between prediction of ANN and actual results for İskenderun meteorological station

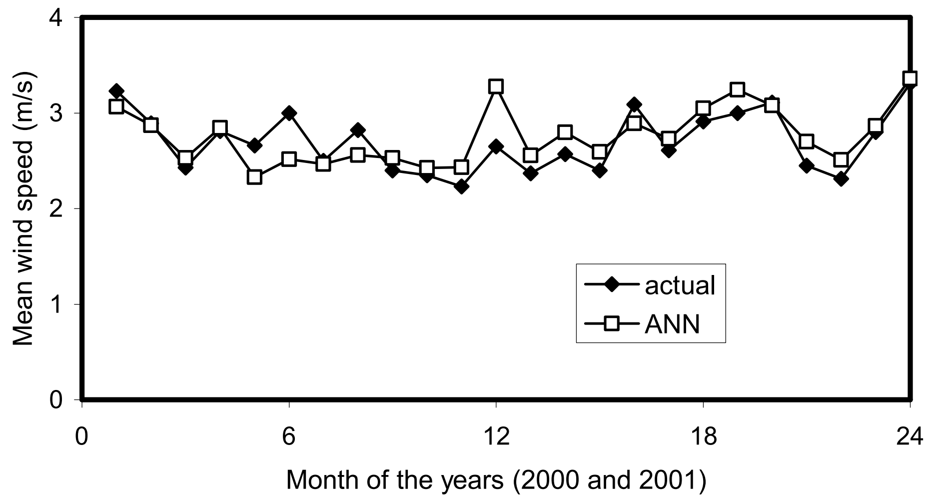

Figure 4.64. Comparison between prediction of ANN and actual results for Karataş meteorological station

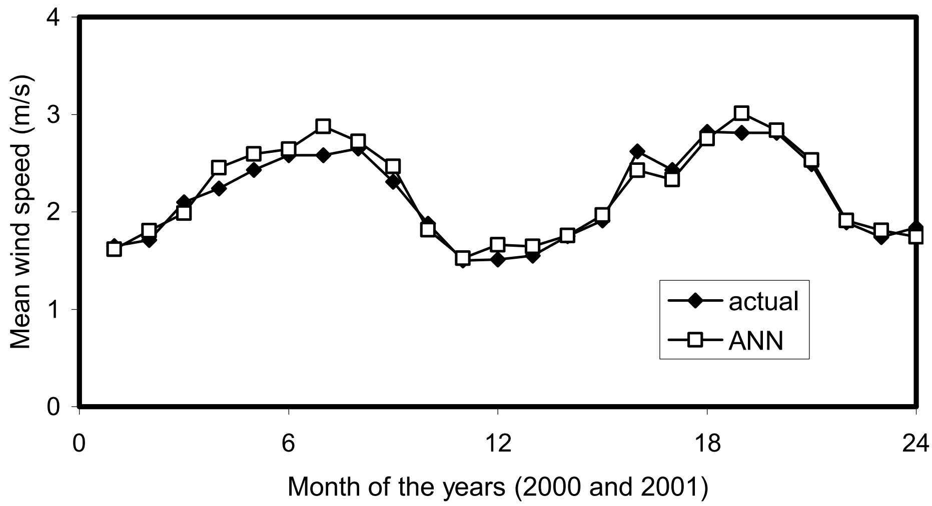

Figure 4.65. Comparison between prediction of ANN and actual results for Mersin meteorological station

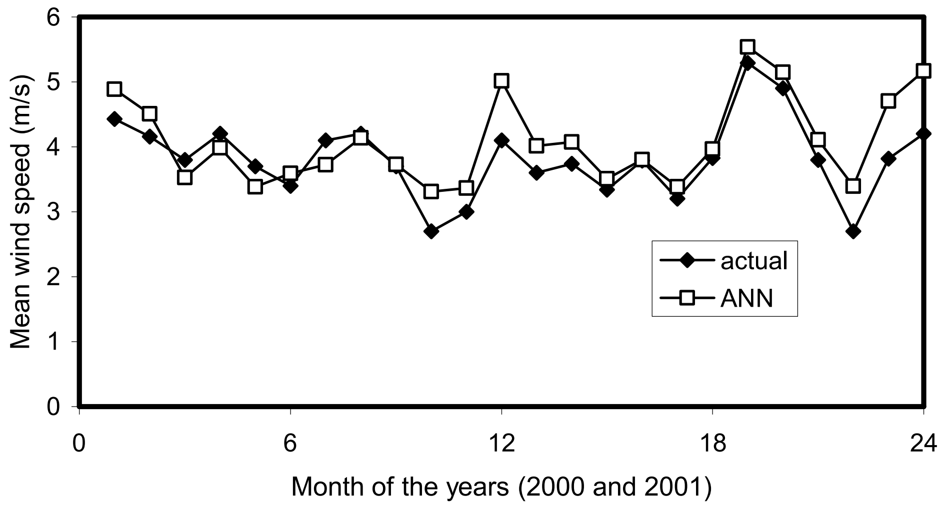

Figure 4.66. Comparison between prediction of ANN and actual results for Samandağ meteorological station

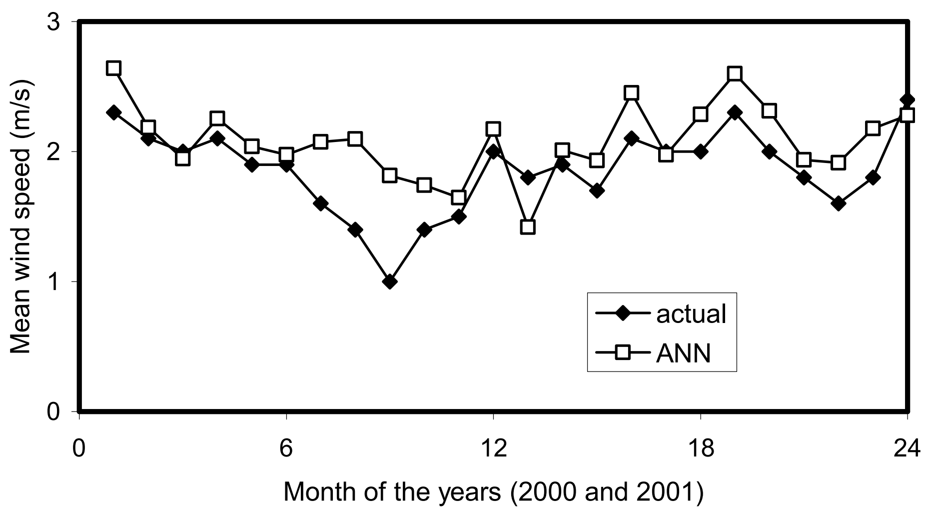

Figure 4.67. Comparison between prediction of ANN and actual results for Yumurtalık meteorological station

4.6. Wind Speed Prediction Using Other Meteorological Variables

The amount of heat energy that is absorbed varies spatially as well as temporally because of roughness of the earth surface. This creates ambient temperature, atmospheric pressure and air density (specific mass) differences on the earth. When the atmospheric air cools down, the density of the air increases and hence the dense air collapse down due to the gravitational force. So, dense air causes a high rate of pressure in close region of the earth surface. On the contrary, under warm weather condition, atmospheric air expends, the rate of density decays down and hence a low level of pressure region occurs along the earth surface. For this reason, there is a pressure differences between cold and warm air regions. Air movements attempt to balance the instability and finally, from a higher pressure region to lower pressure region air movement occurs which is called wind speed (Erol, 1999). The main parameters for the cause of air movement called wind are atmospheric temperature, atmospheric pressure, air density and environmental conditions. As a result, in order to predict wind speed one can use these meteorological parameters.

Nowadays, renewable energy such as wind energy is one of the most attractive sources of energy. Researches may need to prepare an inventory on the availability of wind energy an area where the wind speed data are not available. For this type of situation, it seems useful to predict the wind energy potential using ANN method. Kalogirou et al. (1999) stated that the predicted variations of meteorological parameters such as wind speed, relative humidity, solar radiation, air temperature, etc. are needed in the industry of renewable energy for design purposes, performance analysis and running cost of renewable energy systems. In addition, they reported that for proper and efficient utilization of wind power, it is very important to know the statistical characteristics, persistence, availability, diurnal variation and prediction of wind speed. The values of wind power distributions are needed for site selection, performance prediction and planning of wind turbines. Moreover, prediction of wind speed is needed for any regional inventory wind energy studies in advance. In this sense, the establishment of a model for wind speed correlation in a region is of great importance in the management of wind energy resources for power generation as well as in other research fields related to energy conservation (Bechrakis et al., 2004).

The aim of this work is to apply Multiple Linear Regression and Artificial Neural Network models for wind speed prediction with using various meteorological variables of Antakya, Mersin and Samandağ meteorological stations, located in the south-eastern region of Turkey.

4.6.1. Analysis of meteorological variables

In this study, monthly meteorological variables, collected by the Turkish State Meteorological Service (TSMS) at 3 measuring stations which are located in Antakya, Mersin and Samandağ districts were presently used. These meteorological variables measured during the years of 1996-2005 include wind speed, dominant wind direction, ambient temperature, atmospheric pressure, relative humidity and rainfall. Stations are located between $36^0.05"$ and $36^0.49"$ north latitude in the eastern Mediterranean region of Turkey. Heights of meteorological stations of Antakya, Mersin and Samandağ above the sea level are 100 meter, 3 meter and 4 meter respectively. Except Antakya; Mersin and Samandağ meteorological stations are located on the coastal site of the eastern Mediterranean region. Mediterranean climate is dominant in this region, usually hot and dry in summer season, lukewarm and rainy in winter season. But, climate properties vary depending on the level of the height above the see level. On the slope of a mountain looking at the sea, an increase of terrestrial effects on climate is observed. However, the weather in this region does not show intensed terrestrial climate due to the Mediterranean See effect (Bilgili et al., 2007).

Figures 4.68-70 present average monthly variation of meteorological parameters such as wind speed, ambient temperature, atmospheric pressure, relative humidity and rainfall for Antakya, Mersin and Samandağ meteorological stations, respectively. As seen in these figures, the atmospheric temperature and the wind speed increase, on the other hand, the atmospheric pressure and rainfall decrease for Antakya and Mersin meteorological stations. For Samandağ meteorological station, there is no relationship at all between the wind speed and other meteorological parameters. For Antakya meteorological station, as seen in Figure 4.68, mean monthly wind speed varies drastically between 1.7 and 5.2 m/s with an average value of 3.0 m/s. The maximum monthly wind speed occurs in summer season, while the minimum monthly wind speed occurs in winter season. It is shown that atmospheric temperature varied between 8.4 ^{0}C and 27.9 ^{0}C with an average value of 18.4 ^{0}C. It is obvious that, the maximum monthly atmospheric temperature occurs in summer season, while the minimum monthly atmospheric temperature occurs in winter season, as expected. This situation indicates that there is a good relationship between the monthly wind speed and monthly atmospheric temperature. Furthermore, monthly wind speeds are negatively correlated with atmospheric pressure.

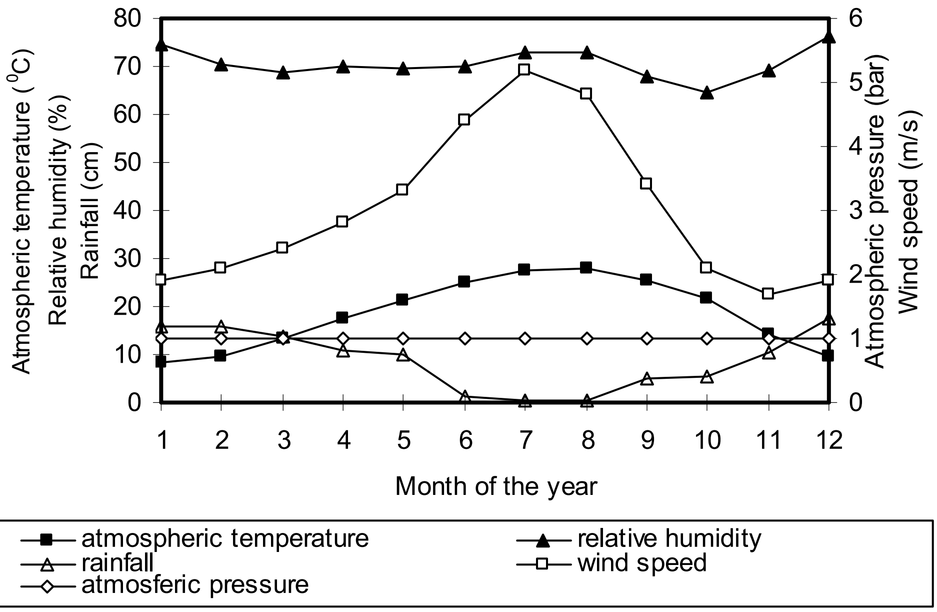

Figure 4.68. Average monthly variation of meteorological parameters for Antakya meteorological station

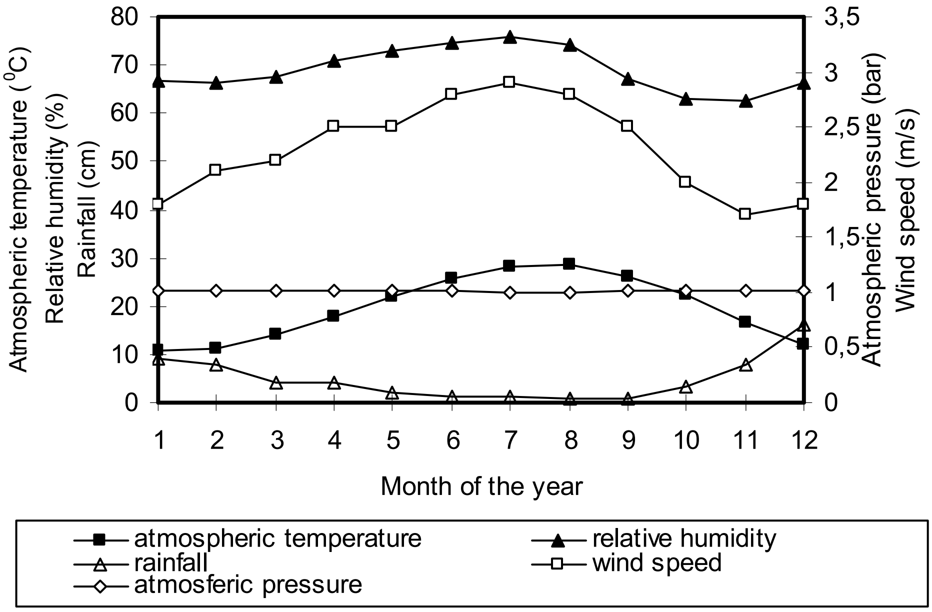

Figure 4.69. Average monthly variation of meteorological parameters for Mersin meteorological station

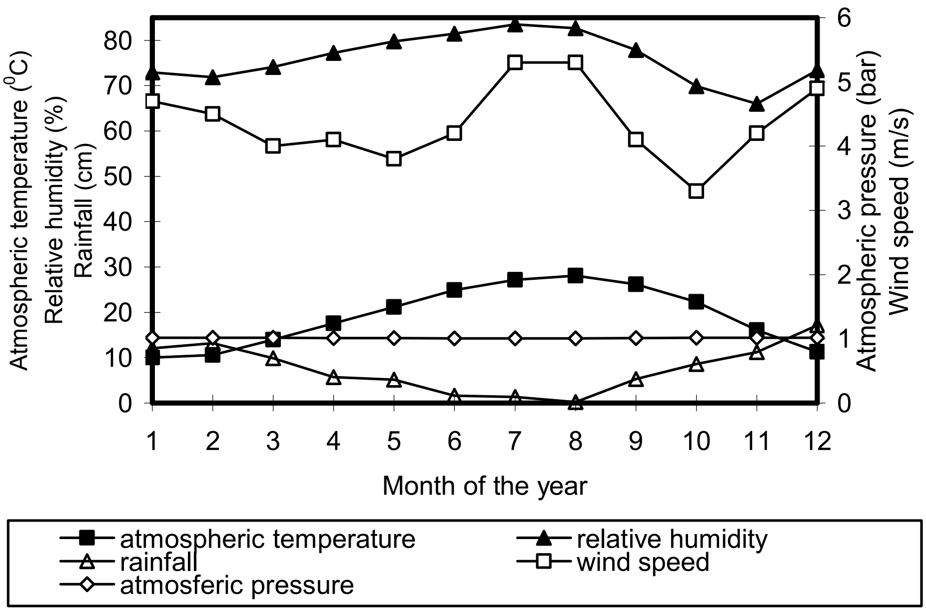

Figure 4.70. Average monthly variation of meteorological parameters for Samandağ meteorological station

In order to obtain models of prediction for wind speed with various meteorological variables using MLR and ANN methods, the first step in this analysis is the selection of the independent variables. Here, the most significant point is the fact that there is a high rate of correlation coefficient between the wind speed which is the dependent variable and the various meteorological variables which are the independent variables. Here, independent related variable must be only included to the model. Because, the regression model must be established in a way that the best estimation should be performed using a few independent variables as much as possible (Sahinler, 2000). For this purpose, the diagrams of measured wind speeds of each meteorological station are constructed against other meteorological data and the correlation coefficients between all variables were calculated by taking them two by two. The results obtained for Antakya, Mersin and Samandağ meteorological stations are shown in Tables 4.22-24, respectively. An adequate value of the cross correlation function for an accurate simulation must be higher than 0.6 (Bechrakis et al., 2004). Therefore, as it is shown in these tables, significant correlation coefficients were indicated in bold. This means that these parameters have a strong correlation with each other. There is a high rate of correlation coefficient between the wind speed and various meteorological variables such as atmospheric temperature and pressure for Antakya and Mersin meteorological stations. Wind speeds are positively correlated with atmospheric temperature in these meteorological stations, while wind speeds are negatively correlated with atmospheric pressure. Because of the fact that, in order to obtain prediction models for wind speed of Antakya and Mersin meteorological stations, it can be selected atmospheric temperature and pressure as independent (predictor) variables. In addition, for Samandağ meteorological station, there is no high rate of correlation coefficient between the wind speed and various meteorological variables. Because of inconsistency between the wind speed and other meteorological variables, simulations of prediction models may provide misleading results.

Table 4.22. Correlation coefficients between all meteorological variables for Antakya meteorological station

	Wind speed	Wind direction	Atm. temperature	Atm. pressure	Relative humidity	Rainfall
Wind speed	1	**0.68**	**0.83**	**-0.91**	-0.07	-0.52
Wind direction		1	**0.81**	**-0.77**	-0.17	-0.35
Atm. temperature			1	**-0.90**	-0.18	-0.55
Atm. pressure				1	0.09	0.41
Relative humidity					1	0.23
Rainfall						1

Table 4.23. Correlation coefficients between all meteorological variables for Mersin meteorological station

	Wind speed	Wind direction	Atm. temperature	Atm. pressure	Relative humidity	Rainfall
Wind speed	1	-0,44	**0.74**	**-0.85**	0.55	-0.40
Wind direction		1	-0.37	0.52	-0.53	-0.22
Atm. temperature			1	**-0.88**	0.52	-0.48
Atm. pressure				1	**-0.69**	0.39
Relative humidity					1	-0.01
Rainfall						1

Table 4.24. Correlation coefficients between all meteorological variables for Samandağ meteorological station

	Wind speed	Wind direction	Atm. temperature	Atm. pressure	Relative humidity	Rainfall
Wind speed	1	0.04	0.10	-0.30	0.34	-0.13
Wind direction		1	**0.78**	**-0.74**	**0.65**	**-0.62**
Atm. temperature			1	**-0.88**	0.59	**-0.60**
Atm. pressure				1	**-70**	0.55
Relative humidity					1	-0.27
Rainfall						1

4.6.2. Results for Multiple Regression Analysis

It is also well known that wind speed is related to various meteorological variables in the atmosphere such as atmospheric temperature, atmospheric pressure, air density and other air variables in the environment (Erol, 1999). As it is stated in Tables 4.22 and 23, wind speeds are correlated wit atmospheric temperature and pressure for Antakya and Mersin meteorological stations as expected. In the multiple regression method, the most significant point is to select the predictor variables that provide the best prediction equation for modeling of dependent variable. For instance, atmospheric temperature and pressure were selected as the independent variables in order to obtain predictive equation for modeling of wind speed. These two independent variables were then used as a predictor variable in the multiple regression analysis. By using the data between the years 1996 and 2001, the following model was obtained for Antakya, Mersin and Samandağ meteorological stations, respectively. Here, the dimensions of meteorological data such as wind speed, atmospheric temperature and pressure are taken as m/s, ^{0}C and mbar respectively.

$$\left[wind\ speed\right] = 221.39 + 0.00910\left[atm.temperature\right] - 0.21864\left[atm.\ pressure\right]$$

$$\left[wind\ speed\right] = 93.164 - 0.00230\left[atm.temperature\right] - 0.08977\left[atm.\ pressure\right]$$

$$\left[wind\ speed\right] = 151.30 - 0.07911\left[atm.temperature\right] - 0.14383\left[atm.\ pressure\right]$$

The monthly wind speeds between the years 2002 and 2005 were predicted using these equations for Antakya, Mersin and Samandağ meteorological stations, separately. The scatter diagrams of the regression predictions against the actual values were drawn for these meteorological stations in order to indicate the performance of the MLR model. Especially for Antakya and Mersin meteorological stations, as seen in Figures 4.71 and 72, the predicted results are as fairly close to the corresponding actual measurements. In addition, as seen in Figure 4.73, because of the low rate of correlation coefficient between the wind speed and other meteorological variables for Samandağ meteorological station, the predicted results are not in good agreement with the corresponding actual measurements as expected.

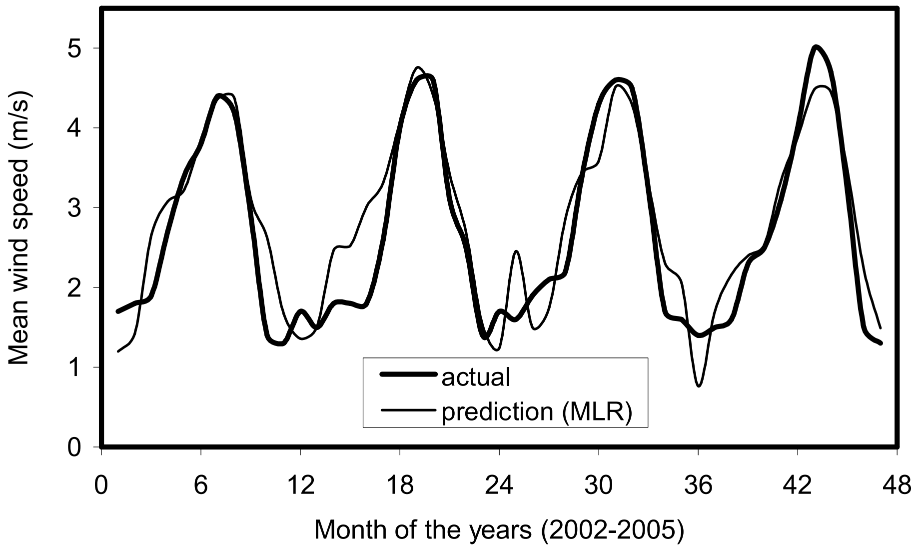

Figure 4.71. Comparison between prediction of MLR and actual results for Antakya meteorological station

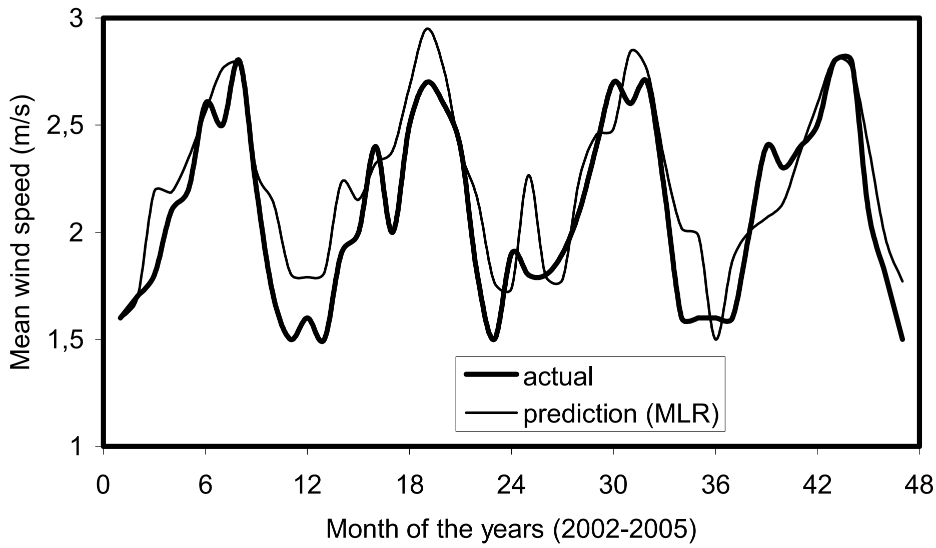

Figure 4.72. Comparison between prediction of MLR and actual results for Mersin meteorological station

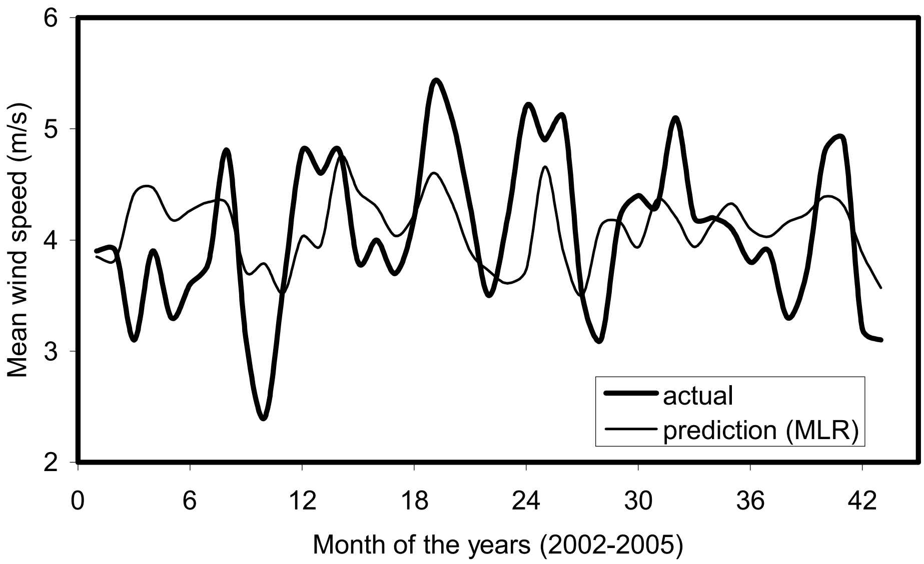

Figure 4.73. Comparison between prediction of MLR and actual results for Samandağ meteorological station

4.6.3. Results for Artificial Neural Networks

Artificial neural network architecture used in this study is shown in Figure 4.74. This network consists of an input layer, a hidden layer and an output layer. Monthly atmospheric temperature and pressure were used in the input layer of the network. In addition, monthly wind speed was used in the output layer of the network. Meteorological data measured during the period of 1996-2005 were divided into two sections. The first section of the data which covers the years between 1996 and 2001 was used for training process. The second part of the data which covers the years of 2002 and 2005 was utilized for testing process. Resilient propagation (RP), Scaled Conjugate Gradient (SCG) and Levenberg-Marquardt (LM) learning algorithm were applied in the present simulation. Neurons in the input layer have no transfer function. Logistic sigmoid transfer function (logsig) was used in the hidden layers and output layer of the network as an activation function. The values applied in the input and output layers were normalized by the following formula in the range of (0-1) (Krauss et al., 1997).

$$X_N = \frac{(X_R - X_{\min})}{(X_{\max} - X_{\min})} \tag{4.6.1}$$

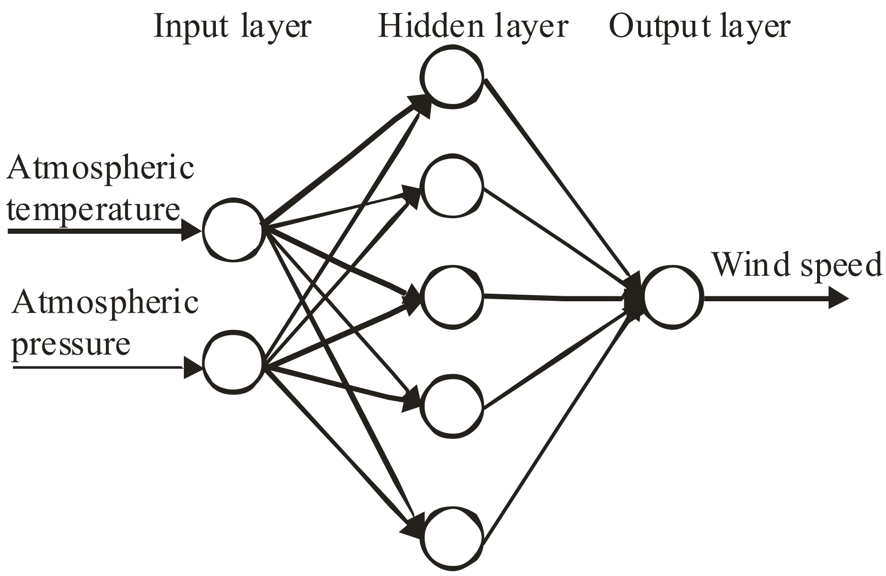

Figure 4.74. ANN architecture

Where, X_N is normalized value, X_R is real value, X_{min} is minimal value and X_{max} is maximal value. Normalizing of the training inputs generally improves the quality of the training (Krauss et al., 1997). Simulations were performed to estimate the mean monthly wind speed using atmospheric temperature and pressure. As Maqsood et al. (2005) reported that in each layer, every neuron is connected to a neuron of adjacent layer having different weights. Each neuron as indicated in Figure 4.74, receives signals from the neurons of the previous layer weighted by the interconnect values between neurons except input layer. Neurons then produce an output signal by passing the summed signal through an activation function. Mohandes et al. (2004) stated that during the training process, the weights of the connections between neurons are adjusted in order to achieve the desired input/output relation of the network. This procedure goes on until the difference between the actual output of the network and the desired output is equal with a specified remainder value. Here, the criterion is put forward as the network output which should be closer to the value of desired output. This training process has to be repeated for the rest of the input-output pairs existing in the training data. The scatter diagrams of the network predictions against the actual values were drawn for all meteorological stations in order to indicate the performance of the ANN method. As seen in Figures 4.75-77, the results of prediction have fairly close agreement with the corresponding actual measurements for all stations.

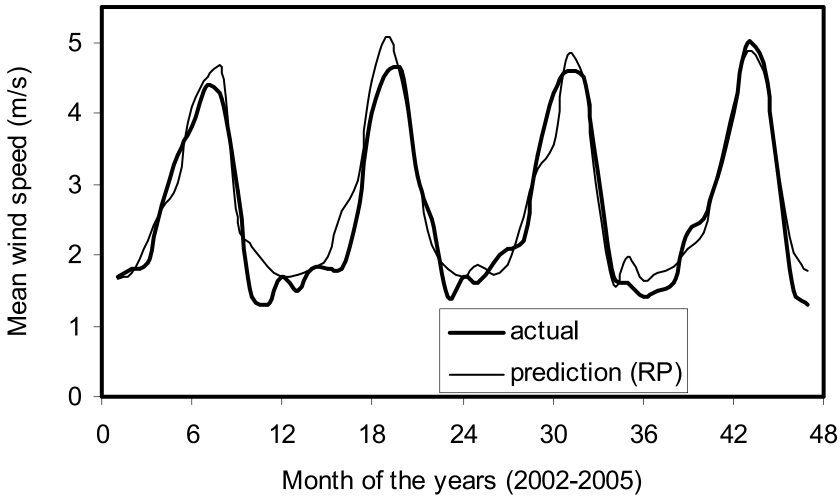

Figure 4.75. Comparison between prediction of RP and actual results for Antakya meteorological station

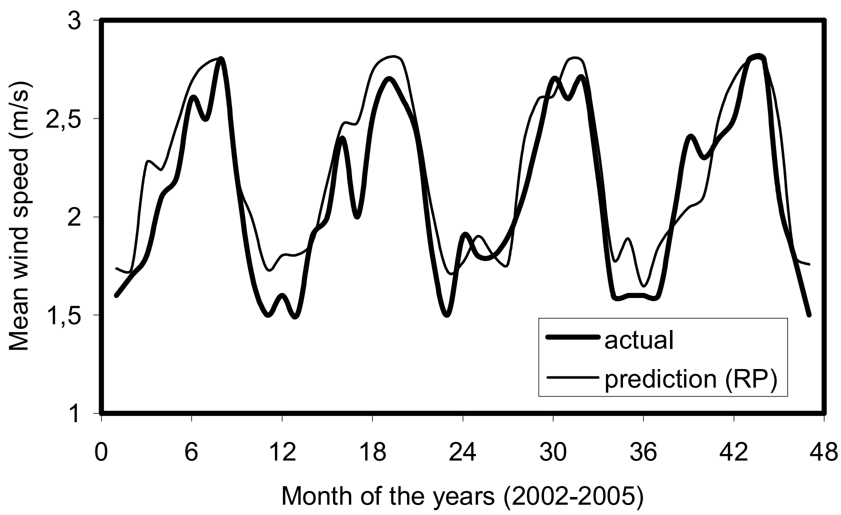

Figure 4.76. Comparison between prediction of RP and actual results for Mersin meteorological station

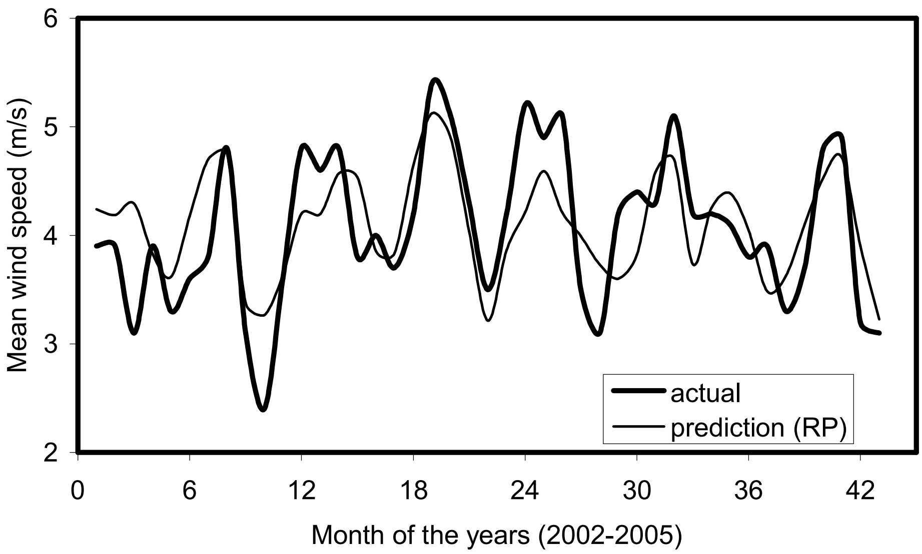

Figure 4.77. Comparison between prediction of RP and actual results for Samandağ meteorological station

4.6.4. Comparative Analysis of MLR model to ANN model

MLR and ANN models attempt to minimize sum squares of error between experimentally measured and predicted values. Regression requires an explicit function to be defined before the least squares parameter estimates, while a neural network depends further more on the training data and the learning algorithm (Li et al., 2001).

For comparative analysis of MLR model to ANN model, the mean absolute percentage error (MAPE) and the correlation coefficient (R) were used to see the convergence between the target values and the output values.

The performance values of MLR and ANNs methods (RP, SCG and LM learning algorithm), such as MAPE and the correlation coefficient, R are given in Table 4.25 for all stations. The MAPE values of MLR model differ from the actual value of monthly wind speeds with the range of 8.57% and 17.05%. On the other hand, the MAPE values of ANNs (RP) method ranged from 7.82% to 10.88% differ from the actual value of monthly wind speed. However, the maximum MAPE was found to be 17.05% for Antakya meteorological station in the MLR model, while

ANNs (RP) method provided that the best result was found to be 7.82% for Mersin meteorological station, the maximum correlation coefficient between the target value and output value was 0.96 for Antakya meteorological station. On the other hand, MLR model provided that the minimum correlation coefficient was found as 0.38 for Samandağ meteorological station which is expected, because of the low rate of correlation coefficient between the wind speed and other meteorological variables. As seen in this table, the performance values of the ANNs method are better than the performance values of the MLR model. Moreover, another significant point in this table, because of the high rate of correlation coefficient between the wind speed and other meteorological variables, the performance values of Antakya and Mersin meteorological stations are better than the performance values of Samandağ meteorological station.

Table 4.25. Performance values of prediction results for all stations

Station	MLR method		ANN method					
			RP algorithm		SCG algorithm		LM algorithm	
	MAPE	R	MAPE	R	MAPE	R	MAPE	R
Antakya	17.05	0.92	10.88	0.96	11.00	0.96	11.70	0.95
Mersin	8.57	0.89	7.82	0.92	8.47	0.90	8.75	0.89
Samandağ	12.61	0.38	10.10	0.71	10.04	0.66	11.36	0.62

The aim of the present work is to try to predict wind speed using monthly meteorological variables, and establish a model between these variables. For this purposes, methods of multiple linear regression analysis and artificial neural network were used. Results of these methods were compared to each other. In order to improve the accuracy of predictions a few independent parameters or initial parameters were used and related independent parameters were only included to the model. Between monthly wind speed and meteorological variables such as atmospheric temperature and pressure a good relations were obtained for Antakya and Mersin meteorological stations, and hence using ANN and MLR methods provide acceptable wind speeds for both stations. On the other hand, since there was no a satisfactory relations between wind speed and independent variables such as atmospheric temperature and pressure, these methods did not provide a predicted results with an acceptable error in it for Samandağ meteorological station.

It was concluded that if there is good relations between wind speed and other meteorological variables such as atmospheric temperature and pressure, wind speed with these meteorological variables can be predicted with acceptable accuracy using ANN and MLR methods.

4.7. Daily, Weekly and Monthly Wind Speed Predictions of Target Station Using Artificial Neural Networks

4.7.1. Preparation of Input and Output Data

In this study, the ANN method was applied for the prediction of the daily, weekly and monthly wind speed of any target station at a location with no measurement, which is referred to as the target station from the measurements of a set of surrounding stations. This study has been applied for regional wind speed prediction in some parts of the Aegean and Marmara region of Turkey. This wind speed prediction of any pivot station was based on the wind speeds of neighboring measuring stations. In order to estimate a target station, the correlation coefficient was obtained for each pair of wind speed time series of all stations and weighting factors between the pivot station and its surrounding stations were determined by artificial neural network technique.

The data used in this study were collected from Gökçeada, Foca, Gelibolu and Bababurnu stations which have been set up by the General Directorate of Electrical Power Resources Survey Administration (EIE). The map of the region and the location of the stations are presented in Figure 4.78. Geographical coordinates and measurement periods of these stations are given in Table 4.26. Stations extend from latitude $38^0$39'25" to $40^0$26'34" north and longitude $25^0$57'00" to $26^0$46'22" east, while the heights of stations above the sea level vary between 175 meter and 348 meter. These stations located in the Marmara and Aegean region of Turkey supply wind speed and direction every one hour. The Marmara region comes under the influence of the mild Mediterranean climate during the summer months. During the winter time, this region is under the influence of high pressure of Siberia and the Balkan Peninsula and, consequently, northeasterly or westerly winds influence the area with high rainfall amounts in addition to snow every year with cold and wet spells (Öztopal, 2006). In the Aegean region geomorphological features have long valleys that run perpendicular to the coast. These are parallel to the cyclonic movements that originate from the Genoa bay and move towards the east and therefore show strong wind effects at the Aegean coast as well as the moving air which penetrates deep in these valleys (Durak and Şen, 2002).

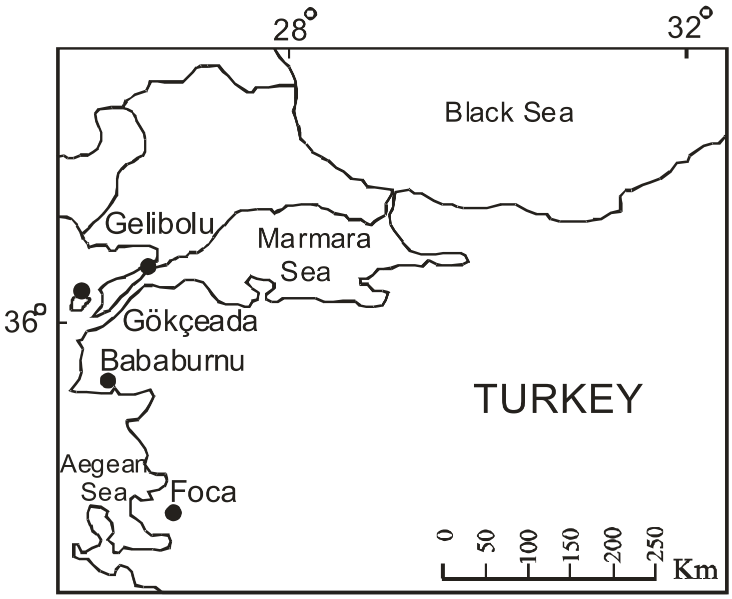

Figure 4.78. The map of the region and the location of the stations

Table 4.26. Geographical coordinates and measurement periods of stations

Station	Latitude	Longitude	Altitude (m)	Period	Anemometer height (m)
Gökçeada	40^0 07' 58" N	25^0 57' 00" E	244	1998-2003	10
Foca	38^0 39' 25" N	26^0 46' 22" E	175	1998-2003	10
Gelibolu	40^0 26' 34" N	26^0 32' 56" E	302	1998-2003	10
Bababurnu	39^0 30' 03" N	26^0 12' 39" E	348	1998-2003	10

The sensors measuring wind speed and direction of all stations are situated 10 m above the ground level. The long-term wind data cover the period from the year 1998 to 2003. The daily, weekly, monthly and annual wind data were obtained using the averages of hourly wind data. The annual average wind speed, energy potential and dominant prevailing wind direction of all stations for the year 2001 are presented in Table 4.27. It is seen from the table that the annual average wind speeds range from a low of 5.7 m/s in Foca station to a high of 7.2 m/s in Gökçeada station. The standard deviation of wind speeds varies mainly from a low level of 2.6826 to a maximum level of 4.3673. These regions are highly suitable for wind power generation. While the highest annual wind energy potential value is determined as 518 W/m^2 in Gökçeada station, the lowest annual wind energy potential value is found as 196 W/m^2 in Foca station. The annual wind energy potential values of Bababurnu and Gelibolu stations are determined as 254 W/m^2 and 406 W/m^2, respectively. As it is mentioned in Table 4.27, the dominant prevailing wind directions for Gökçeada, Foca, Gelibolu and Bababurnu stations are 210^0, 30^0, 90^0 and 30^0, on the other hand the effect of wind that is observed at the lowest degree is in the direction of 90^0, 240^0, 150^0 and 270^0, respectively. The direction of the wind is of decisive significance for the evaluation of the possibilities of utilizing wind power. Scatter diagrams of the monthly average wind speeds of stations for the year 2001 are presented in Figure 4.79. It is interesting to note that the monthly average wind speeds of stations show the same variation according to each other. It is also clear from the figure that the four curves have similar changing trends, but the rate of change is not the same. A dramatic variation in the monthly average wind speed occurs during a year at these stations. The maximum monthly average wind speed occurs in December; on the other hand the minimum monthly average wind speed occurs in April and September for all stations. The monthly average wind speeds range from a low of 4.6 m/s in Bababurnu station to a high of 10.8 m/s in Gökçeada station. The minimum and maximum monthly average wind speeds of Gökçeada station which has the highest value among these stations are 5.3 m/s and 10.8 m/s, respectively.

Table 4.27. The annual average wind speed, energy potential and dominant wind direction of stations in 2001

Station	Mean wind speed (m/s)	Standard deviation	Mean wind energy potential (W/m^2)	Dominant wind direction
Gökçeada	7.2	4.3673	518	SW (210^0)
Foca	5.7	2.6826	196	NE (30^0)
Gelibolu	6.8	3.8692	406	E (90^0)
Bababurnu	6.0	3.1618	254	NE (30^0)

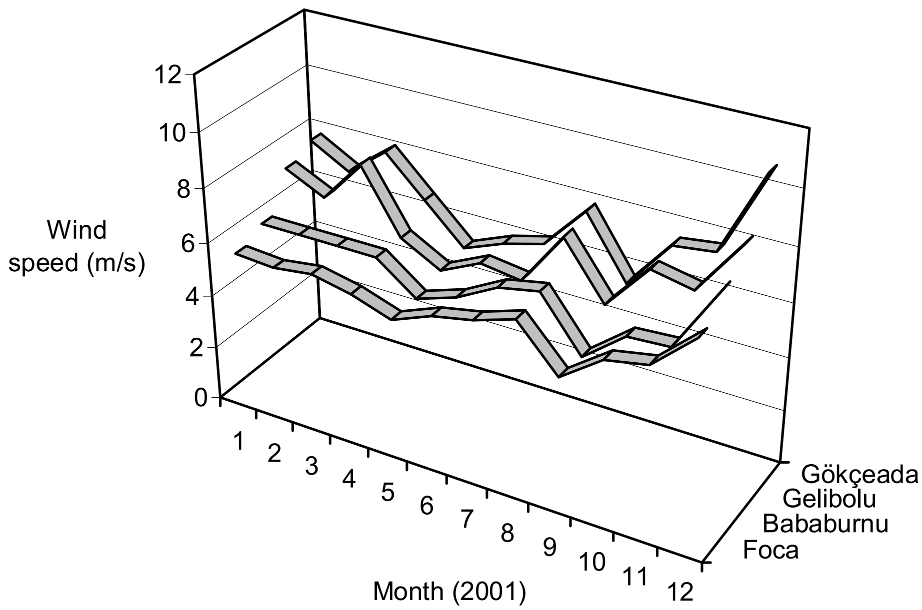

Figure 4.79. Monthly average wind speed of stations

4.7.2. Application

Artificial neural network architecture used in this study is shown in Figure 4.80. It can be seen from the figure that three station wind speeds (Foca, Gelibolu and Bababurnu) were used as input neurons in the ANN architecture, while target station wind speed (Gökçeada) was used as output neuron in the ANN architecture. Similar to this architecture, input and output neurons in the ANN architecture can be changed according to the selection of the target station. This network consists of an input layer, a hidden layer and an output layer. Resilient propagation (RP), scaled conjugate gradient (SCG) and Levenberg-Marquardt (LM) learning algorithms were applied in the present simulation. Neurons in the input layer have no transfer function. Logistic sigmoid transfer function (logsig) and linear transfer function were used in the hidden layers and output layer of the network as an activation function, respectively. Simulations were performed to predict the daily, weekly and monthly average wind speed of target station using reference stations data.

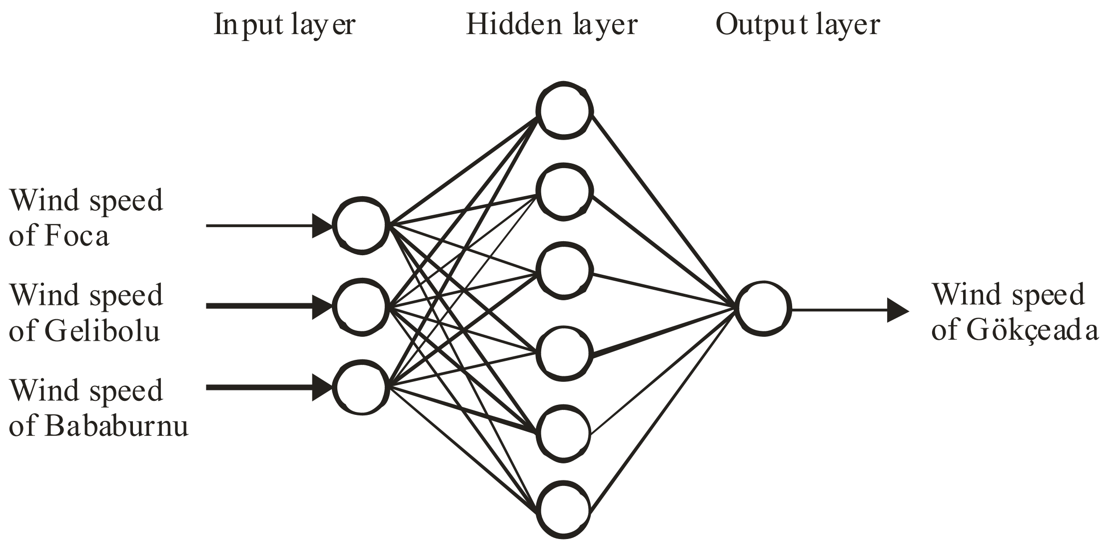

Figure 4.80. Artificial Neural Network architecture

4.7.2.1. Daily Prediction

Here, a model was developed to predict the daily wind speed of any pivot station utilizing wind speeds of the reference measuring stations. The wind speed data used in this study was measured between January 1 and December 31 for the year 2001. Firstly, the daily average wind speed data was obtained using the averages of hourly wind data. Then, in order to designate relationship amongst stations, the daily average wind speeds of all stations were compared with each other and the correlation coefficients between them two by two were determined. The accuracy of the results is basically depended on the cross-correlation level between the two stations' wind speed, which is related to the morphology of the surrounding area (Bechrakis et al., 2004). The correlation coefficients of daily wind speeds amongst stations are presented in Table 4.28. It is also clear from the table that there is a high rate of correlation coefficient between the daily wind speeds. These correlation coefficients range from a low level of 0.65445 between Gelibolu and Foca stations to a high level of 0.91782 between Gelibolu and Gökçeada stations.

Table 4.28. Correlation coefficients of daily wind speeds between stations

Station	Gökçeada	Foca	Gelibolu	Bababurnu
Gökçeada	1	0.72372	0.91782	0.78539
Foca	0.72372	1	0.65445	0.82579
Gelibolu	0.91782	0.65445	1	0.7092
Bababurnu	0.78539	0.82579	0.7092	1

The total available daily average wind speed data for each station (365 days) was divided into two parts. The first part of the data (334 days) was used for training process, while the second part of the data which covers the days between October 1 and October 31 (31 days) was used for testing process. Training data is used to design the model, while the testing data is used to predict the performance of the network. Three station wind speeds were used as input neurons in the ANN architecture, while target station wind speed was used as an output neuron in the ANN architecture. The scatter diagrams of the network predictions against the actual values were drawn for all stations in order to indicate the performance of the ANN method. It can be seen from Figures 4.81-84 that the results of prediction have fairly close agreement with the corresponding measurements for all stations. The daily average wind speed varies rapidly from day to day, though the prediction of ANN for most of the days agrees well with the actual values.

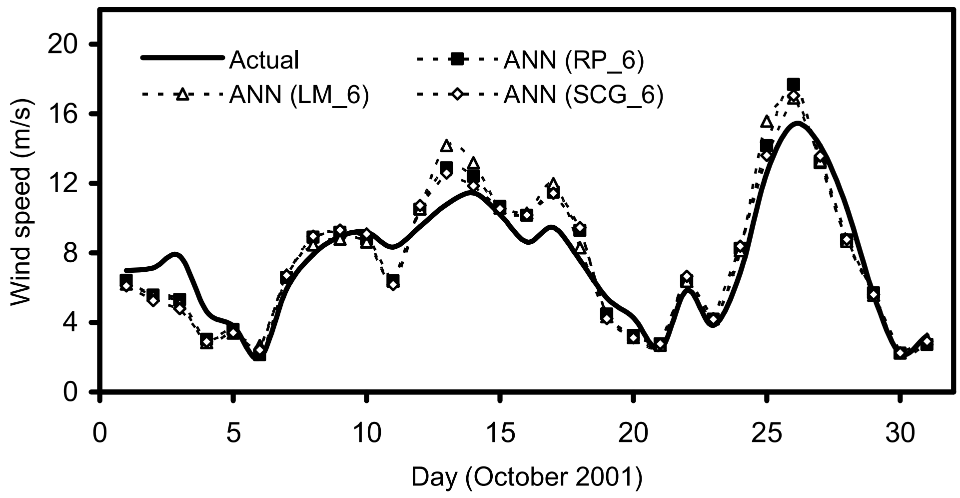

Figure 4.81. Comparison between predictions of ANN and daily measured wind speeds for Gökçeada station

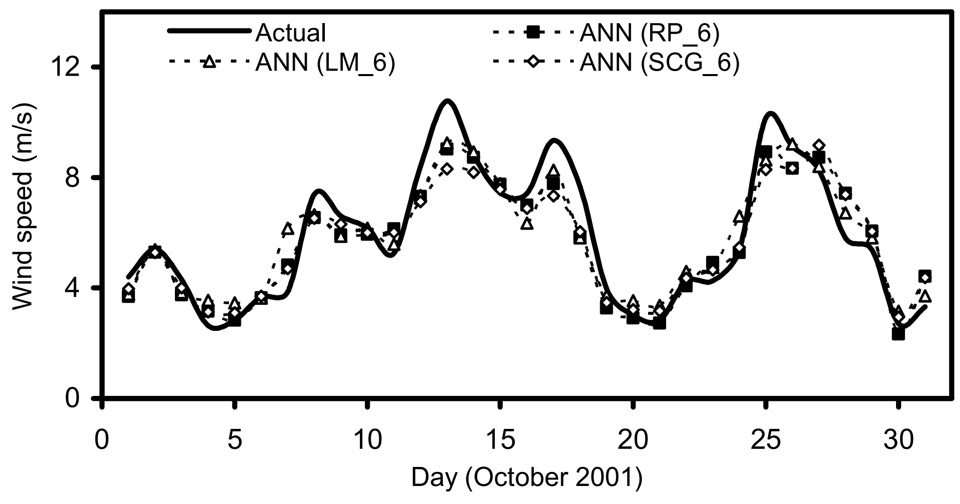

Figure 4.82. Comparison between predictions of ANN and daily measured wind speeds for Foca station

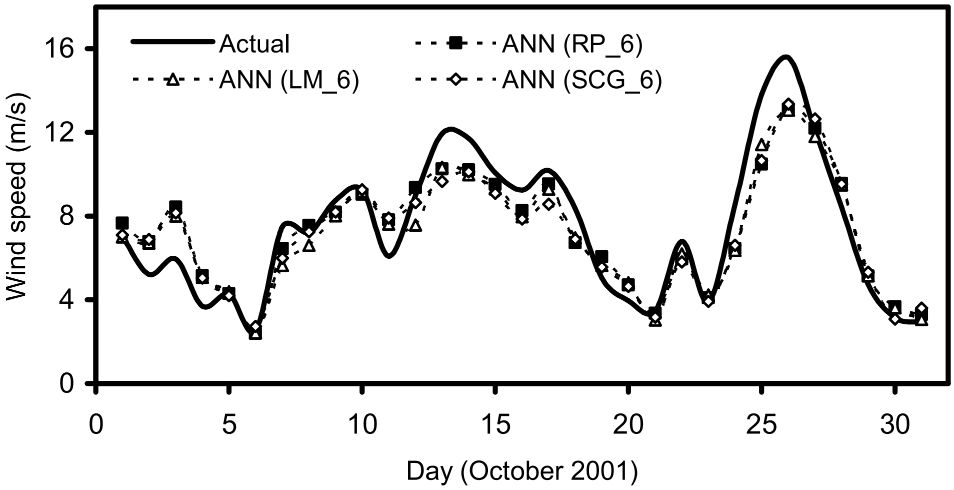

Figure 4.83. Comparison between predictions of ANN and daily measured wind speeds for Gelibolu station

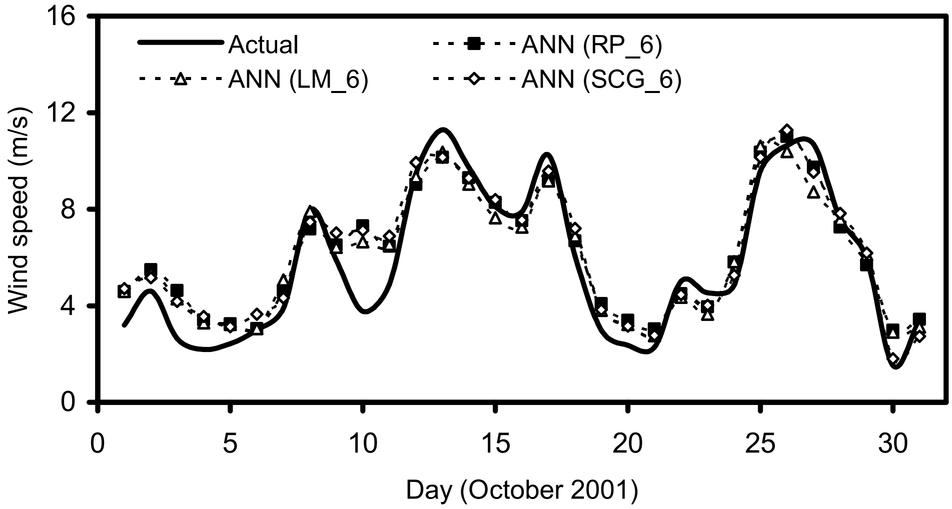

Figure 4.84. Comparison between predictions of ANN and daily measured wind speeds for Bababurnu station

4.7.2.2. Weekly Prediction

The wind speed data used in this study was measured between January 1 and December 31 for the year 2001. The weekly average wind speed data was obtained using the averages of hourly wind data. The correlation coefficients of weekly wind speeds amongst stations are presented in Table 4.29. It is also clear from the table that there is a high rate of correlation coefficient between the weekly wind speeds. These correlation coefficients range from a low level of 0.65191 between Gelibolu and Foca stations to a high level of 0.92717 between Gelibolu and Gökçeada stations.

Table 4.29. Correlation coefficients of weekly wind speeds between stations

Station	Gökçeada	Foca	Gelibolu	Bababurnu
Gökçeada	1	0.7792	0.92717	0.82427
Foca	0.7792	1	0.65191	0.9006
Gelibolu	0.92717	0.65191	1	0.73252
Bababurnu	0.82427	0.9006	0.73252	1

The total available weekly average wind speed data for each station (52 weeks) was divided into two parts. The first part of the data (40 weeks) was used for training process, while the second part of the data which covers the weeks between July 16 and October 7 (12 weeks) was used for testing process. The scatter diagrams of the network predictions against the actual values were drawn for all stations in order to indicate the performance of the ANN method. Figures 4.85-88 reveal that predictions of ANN follow the variation of experimentally measured data exactly.

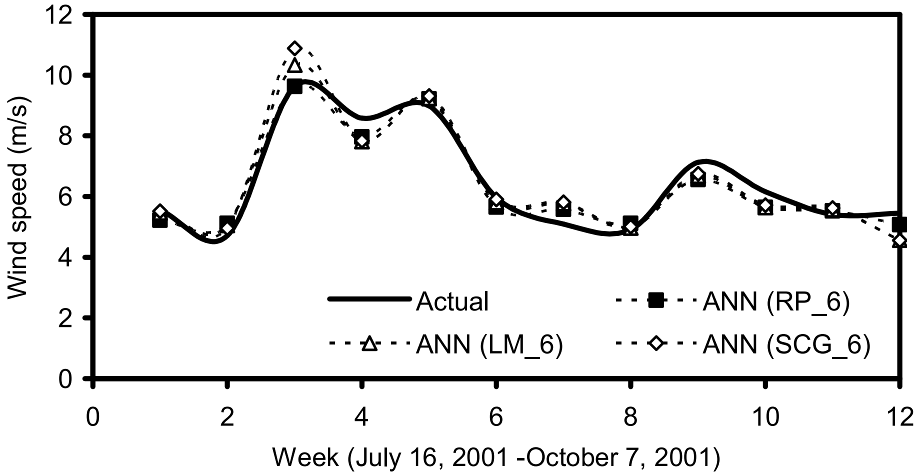

Figure 4.85. Comparison between predictions of ANN and weekly measured wind speeds for Gökçeada station

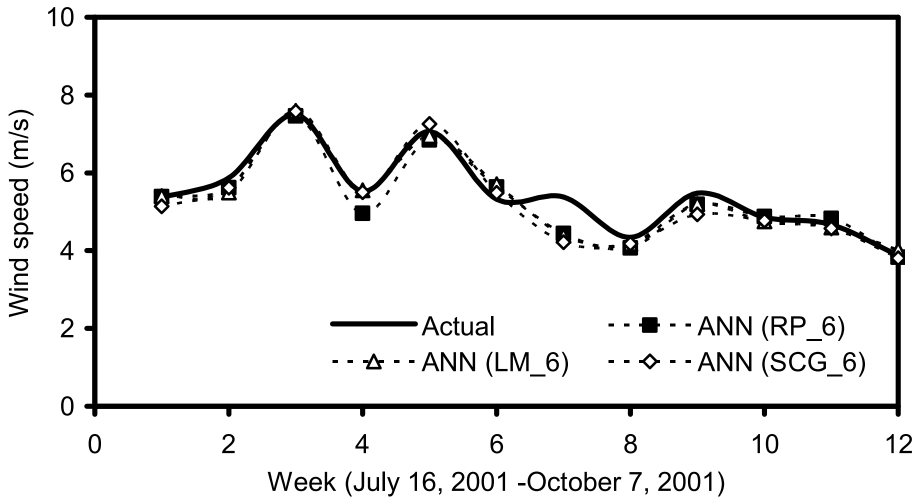

Figure 4.86. Comparison between predictions of ANN and weekly measured wind speeds for Foca station

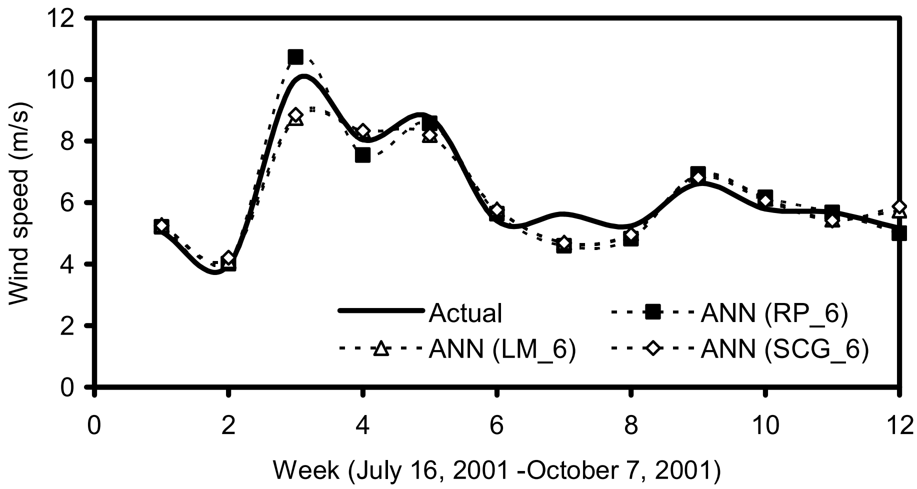

Figure 4.87. Comparison between predictions of ANN and weekly measured wind speeds for Gelibolu station

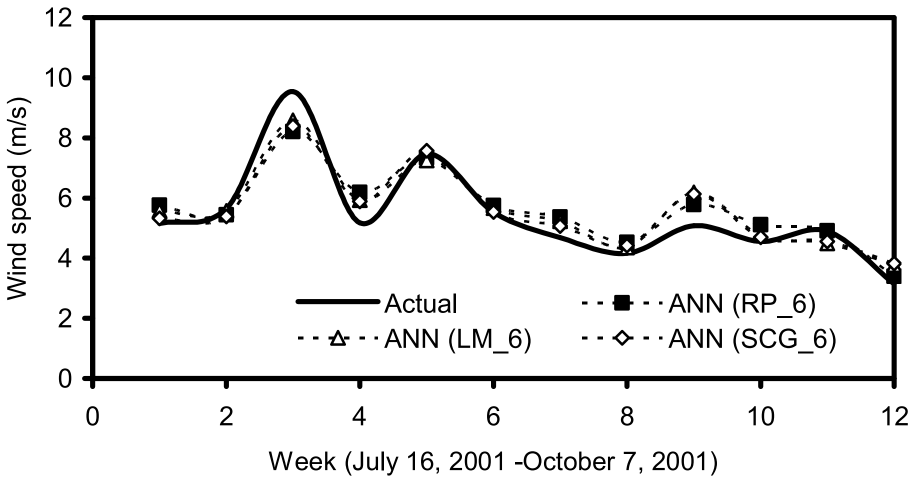

Figure 4.88. Comparison between predictions of ANN and weekly measured wind speeds for Bababurnu station

4.7.2.3. Monthly Prediction

The wind speed data used in this study was experimentally measured between the years 1998 and 2003. The correlation coefficients of monthly wind speeds amongst stations are presented in Table 4.30. These correlation coefficients range from a low level of 0.64429 between Gökçeada and Foca stations to a high level of 0.87082 between Bababurnu and Foca stations. There are missing data for some months due to faulty operation of the anemometer.

Table 4.30. Correlation coefficients of monthly wind speeds between stations

Station	Gökçeada	Foca	Gelibolu	Bababurnu
Gökçeada	1	0.64429	0.79538	0.64774
Foca	0.64429	1	0.81797	0.87082
Gelibolu	0.79538	0.81797	1	0.73022
Bababurnu	0.64774	0.87082	0.73022	1

The total available monthly average wind speed data for each station (47 months) was divided into two parts. The first part of the data (35 months) was used for training process, while the second part of the data which covers the months in the year of 2001 (12 months) was used for testing process. The scatter diagrams of the network predictions against the experimentally measured values were presented for all stations in order to indicate the performance of the ANN method. As seen in Figures 4.89-92 that the results of prediction have fairly close agreement with the corresponding experimentally measured wind speed data for all stations.

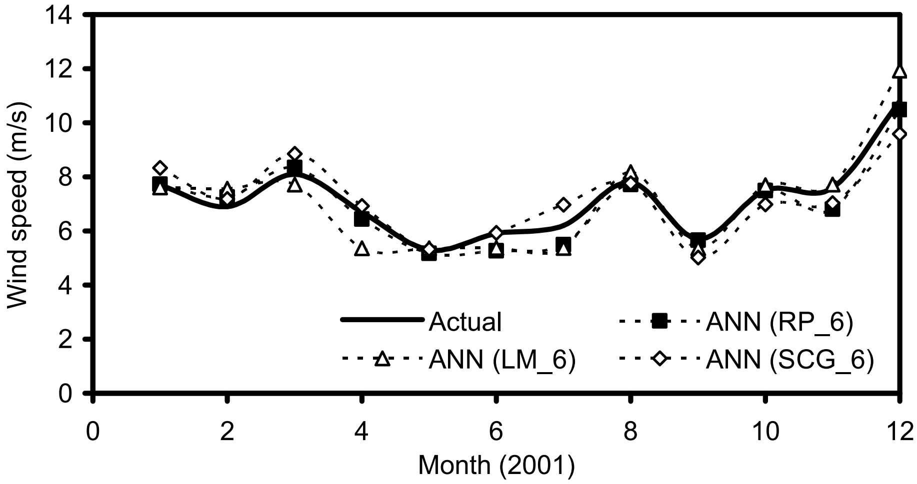

Figure 4.89. Comparison between predictions of ANN and monthly measured wind speeds for Gökçeada station

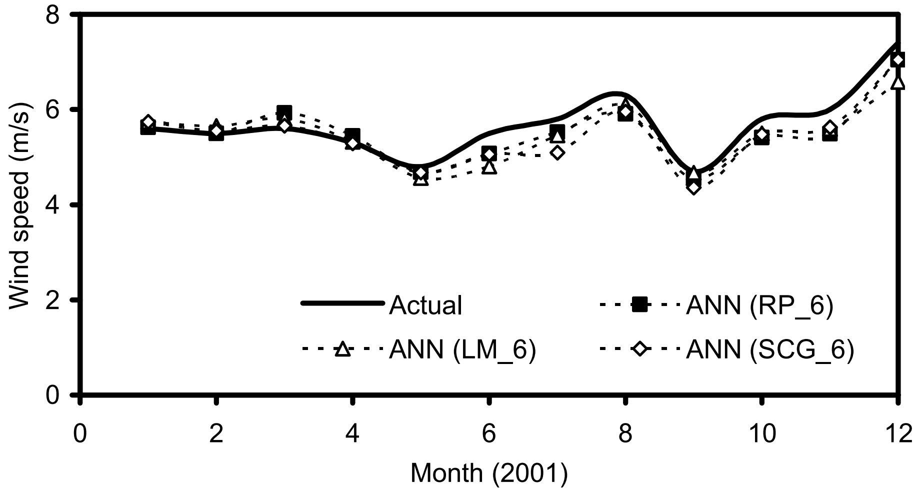

Figure 4.90. Comparison between predictions of ANN and monthly measured wind speeds for Foca station

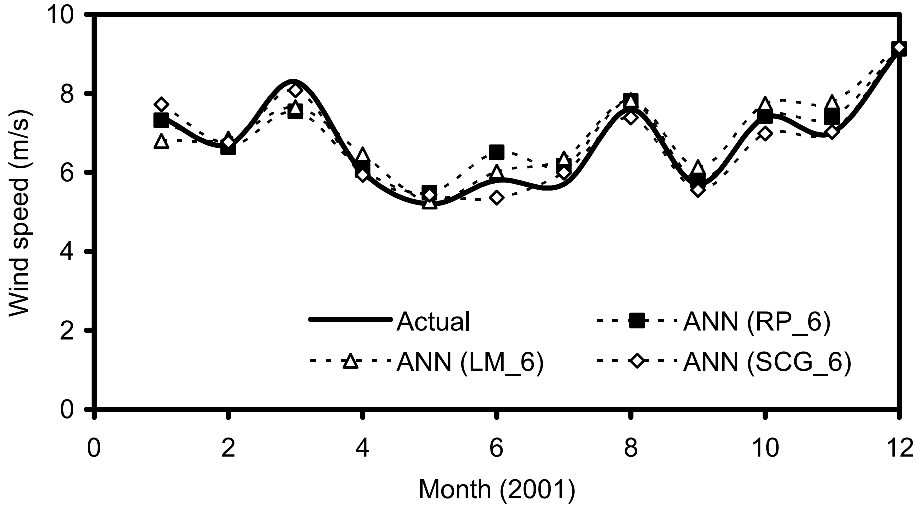

Figure 4.91. Comparison between predictions of ANN and monthly measured wind speeds for Gelibolu station

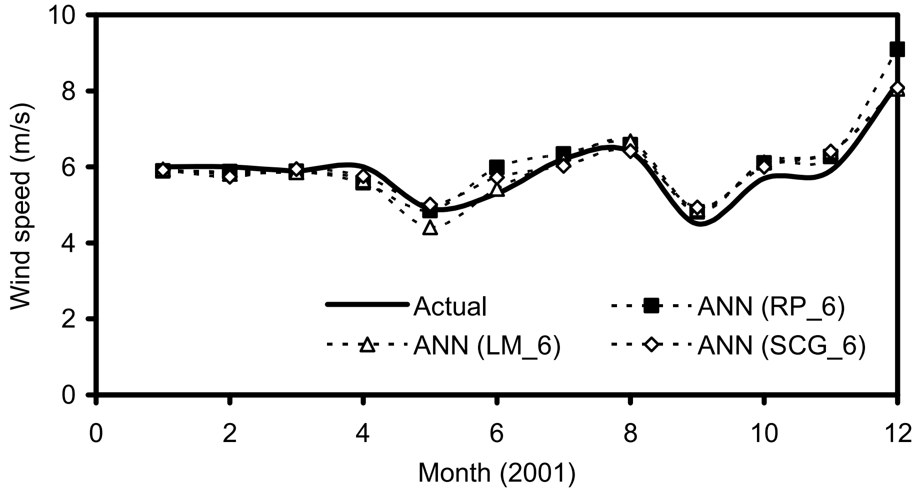

Figure 4.92. Comparison between predictions of ANN and monthly measured wind speeds for Bababurnu station

4.7.3. Results and Discussion

In the present study, it is realized that artificial neural network is convenient method to apply for the prediction of the wind speed. The mean absolute percentage error (MAPE) and correlation coefficient (R) were used to see the convergence between the target value and the output value. Firstly, training process is applied to design the model. Then, testing process is applied to evaluate the performance of the network. The performance values such as MAPE and R for learning and testing process are given in Table 4.31. In the result of testing process, it can be seen from the table that, the MAPE values ranged from 11.6909% to 16.7572% differ from the actual value for daily wind speeds, while the MAPE values ranged from 4.7970% to 8.6794% and from 3.2376% to 7.5701% differ from the actual value for weekly and monthly wind speeds, respectively. The maximum MAPE was found to be 16.7572% for daily wind speeds in Gökçeada station. On the other hand, the best result was found to be 3.2376% for monthly wind speeds in Gelibolu station. It is seen from the table that the performance values of monthly wind speed prediction are better than the performance values of weekly and daily wind speed prediction. Another significant point in this table, the performance values of the learning process are in general better than the performance values of the testing process. The maximum correlation coefficient between the experimentally measured and predicted value was found to be 0.9769 for monthly wind speeds of Gelibolu station in the SCG learning algorithm. On the other hand, the minimum correlation coefficient was found as 0.8856 for monthly wind speeds of Foca station in the LM learning algorithm.

Table 4.31. The performance values for learning and testing process
a) For daily wind speeds

Station	Learning process						Testing process					
	RP_6		LM_6		SCG_6		RP_6		LM_6		SCG_6	
	MAPE	R	MAPE	R	MAPE	R	MAPE	R	MAPE	R	MAPE	R
Gökçeada	15.514	0.946	15.249	0.944	15.340	0.950	15.130	0.952	16.593	0.941	16.757	0.946
Foca	13.362	0.871	13.976	0.857	13.788	0.861	11.691	0.941	12.279	0.937	11.842	0.933
Gelibolu	16.695	0.925	15.708	0.928	16.682	0.923	13.401	0.934	13.986	0.945	13.870	0.932
Bababurnu	15.942	0.885	14.966	0.901	15.057	0.902	16.628	0.949	16.693	0.951	15.741	0.951

Table 4.31. (Continued) The performance values for learning and testing process
b) For weekly wind speeds

Station	Learning process						Testing process					
	RP_6		LM_6		SCG_6		RP_6		LM_6		SCG_6	
	MAPE	R	MAPE	R	MAPE	R	MAPE	R	MAPE	R	MAPE	R
Gökçeada	5.234	0.975	5.551	0.975	5.658	0.971	5.885	0.973	6.847	0.957	6.875	0.952
Foca	5.204	0.924	5.715	0.925	4.700	0.952	5.319	0.949	4.797	0.948	5.360	0.951
Gelibolu	6.055	0.959	7.346	0.943	7.254	0.944	5.760	0.972	7.222	0.950	7.420	0.951
Bababurnu	5.581	0.954	4.175	0.973	2.945	0.987	8.679	0.948	8.447	0.953	7.884	0.950

Table 4.31. (Continued) The performance values for learning and testing process
c) For monthly wind speeds

Station	Learning process						Testing process					
	RP_6		LM_6		SCG_6		RP_6		LM_6		SCG_6	
	MAPE	R	MAPE	R	MAPE	R	MAPE	R	MAPE	R	MAPE	R
Gökçeada	8.662	0.837	8.800	0.869	7.686	0.888	4.712	0.972	7.570	0.961	6.441	0.906
Foca	2.553	0.966	2.556	0.958	2.776	0.964	4.684	0.929	5.370	0.886	5.075	0.934
Gelibolu	5.361	0.942	3.396	0.968	3.722	0.966	3.893	0.958	5.612	0.931	3.238	0.977
Bababurnu	3.774	0.936	1.807	0.979	3.322	0.954	4.836	0.947	4.433	0.947	3.906	0.956

4.8. Prediction of Long Term Monthly Temperature and Rainfall in Turkey Using Artificial Neural Networks

4.8.1. Data Analysis and Climate of Turkey

The climate is one of the most important parameters for energy efficiency of buildings. It is not possible to design an energy efficient building without having the temperature, the solar radiation, the wind velocity data, etc. Bulut et al. (2003) reported that the design of heating, ventilating and air-conditioning (HVAC) and solar energy systems, the energy analysis of buildings and the calculation of cooling and heating loads depend on the weather data.

One of the most important meteorological parameters is the air temperature. That is the reason the air temperature is recorded regularly in a meteorological stations worldwide. Guan et al. (2007) stated that it is also widely known that there is a relationship between air temperature and other meteorological parameters such as solar radiation, air humidity, atmospheric pressure and wind speed. Because of the source of heat energy supplied to the Earth's surface and the atmosphere comes predominantly from the Sun, the variation in solar radiations has a major impact on the weather conditions on the Earth which leads the air temperature to fluctuate. This air temperature variations cause variations in the level of water evaporation and air saturation, leading the air humidity to change. Furthermore, the air temperature differences between different zones also cause an air pressure difference, which in turn produces air movement.

Nowadays it is possible to predict the weather forecasting in terms of the application of science and technology for a future time and a given location or any region on the Earth. Guan et al. (2007) and, Maqsood and Abraham (2007) stated that the weather forecasting is essential for the resource of many subjects, such as the performance of buildings, agricultural production and critical information about future weather. Estimating the properties of the weather helps to safeguard life and properties, and play a crucial role in planning the activities of government, industry and the public. Maqsood and Abraham (2007) reported that the weather phenomena of a complex nature have a direct impact on the safety and/or economic stability.

Accurate weather forecast models are important to the regions, where the entire agricultural depends upon weather, in particular at the present time. In addition, Kalogirou et al. (1999) stated that the predicted variations of meteorological parameters such as wind speed, relative humidity, solar radiation, air temperature, rainfall etc. are needed in the industry of renewable energy for design purposes, performance analysis and running cost estimation of renewable energy systems.

The experimental data used in this study were measured by the Turkish State Meteorological Service (TSMS) at 76 measuring stations of Turkey. The long-term monthly temperature and rainfall cover the period from the year 1975 to 2006. Locations of the measuring stations are presented in Figure 4.93. As seen in this figure, meteorological stations cover almost all parts of the country. Sixty-nine stations are selected for training data, while seventeen stations in the different regions of Turkey are used for testing data. Geographical coordinates of these stations are indicated in Tables 4.32 and 33. Stations extend from latitude 36.12^0 to 42.02^0 north and longitude 26.24^0 to 44.03^0 east, while the heights of stations above the sea level vary between 3.4 meter and 1869 meter. These stations supply meteorological variables such as temperatures and rainfalls in seven different regions of Turkey. Scattering diagram of the long term monthly temperatures and rainfalls in Turkey is presented in Figure 4.94. These data were obtained using average values of temperatures and rainfalls taken from 76 measuring stations. It is also clear from Figure 4.94 that the two curves present different changing trends according to each other. A dramatic variation in the long term monthly temperature and rainfall in Turkey occurs during a year. The long term monthly temperature ranges from a low level of 2.09 ^{0}C in January to a high level of 24.39 ^{0}C in July. Where as, the long term monthly rainfall ranges from a low level of 3.77 day in August to a high level of 12.46 day in December.

Turkey is situated in a large Mediterranean geographical region where climatic conditions have a quite high temperate, diverse nature of the landscape, and the existence of the mountains that run parallel to the Mediterranean and Black Sea costs and perpendicular to the Aegean Sea cost which result in significant differences in climatic conditions from one region to the other. In conclusion, Turkey's diverse regions have different climates because of irregular topography (TSMS, 2007).

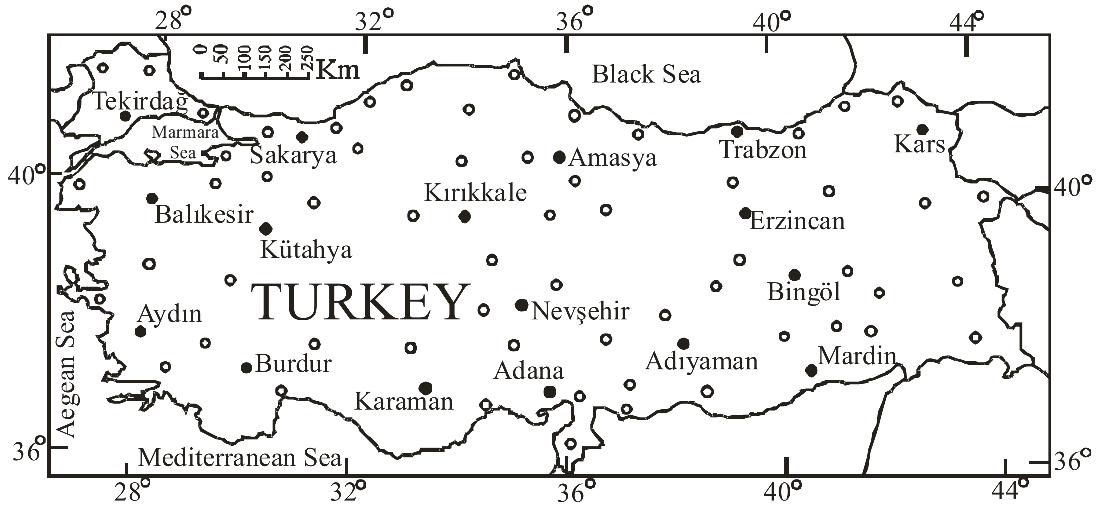

Figure 4.93. Locations of the measuring stations (○: stations used in training, ●: stations used in testing)

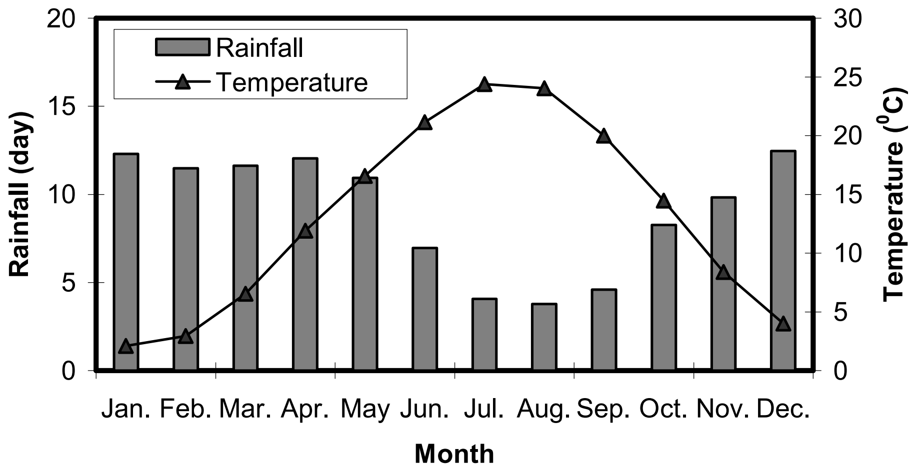

Figure 4.94. Long term monthly temperature and rainfall of Turkey

Table 4.32. Geographical coordinates of the stations selected for training data

Station	Latitude (^{0})	Longitude (^{0})	Altitude (m)
Ağrı	39.43	43.03	1632
Aksaray	38.23	34.03	960.77
Ankara	39.57	32.53	890.52
Antalya	36.52	30.42	47.328
Ardahan	41.07	42.43	1829
Artvin	41.11	41.49	628.35
Bartın	41.38	32.20	32.52
Batman	37.35	41.07	610
Bilecik	40.09	29.59	539.19
Bitlis	38.22	42.06	1573
Bolu	40.44	31.56	742.92
Bursa	40.13	29.00	100.32
Çanakkale	40.08	26.24	5.5
Çankırı	40.37	33.37	751
Çorum	40.33	34.58	775.91
Denizli	37.47	29.05	425.29
Diyarbakır	37.54	40.14	649
Düzce	40.50	31.10	145.67
Edirne	41.41	26.33	51.19
Elazığ	38.39	39.15	989.75
Erzurum	39.54	41.17	1869
Eskişehir	39.46	30.33	801
Gaziantep	37.03	37.21	854
Gümüşhane	40.28	39.28	1219
Hakkari	37.34	43.44	1727.74
Hatay	36.12	36.10	100
Iğdır	39.55	44.03’	858
Isparta	37.45	30.33’	996.88

Table 4.32. (Continued) Geographical coordinates of the stations selected for training data

Station	Latitude (^{0})	Longitude (^{0})	Altitude (m)
İstanbul	40.58	29.05’	32.98
İzmir	38.23	27.04’	28.55
Kahramanmaraş	37.36	36.56	572.13
Kastamonu	41.22	33.47	799.91
Kayseri	38.43	35.29	1092
Kırklareli	41.44	27.13	231.5
Kırşehir	39.09	34.10	1007.17
Kilis	36.42	37.06	650
Kocaeli	40.46	29.56	76
Konya	37.52	32.28	1028.59
Malatya	38.21	38.13	947.87
Manisa	38.37	27.26	71
Mersin	36.48	34.38	3.4
Muğla	37.13	28.22	646.07
Muş	38.41	41.29	1322.76
Niğde	37.58	34.41	1210.5
Ordu	40.59	37.54	4.13
Osmaniye	37.06	36.15	99
Rize	41.02	40.30	8.6
Samsun	41.21	36.15	4
Siirt	37.55	41.57	895.54
Sinop	42.02	35.10	32
Sivas	39.45	37.01	1285
Şanlıurfa	37.09	38.47	547.187
Tokat	40.18	36.34	607.6
Tunceli	39.07	39.33	980.914
Uşak	38.41	29.24	919.22

Table 4.32. (Continued) Geographical coordinates of the stations selected for training data

Station	Latitude (^{0})	Longitude (^{0})	Altitude (m)
Van	38.28	43.41	1670.52
Yalova	40.40	29.17	3.81
Yozgat	39.49	34.48	1298.43
Zonguldak	41.27	31.48	135.35

Table 4.33. Geographical coordinates of the stations selected for testing data

Station	Latitude (^{0})	Longitude (^{0})	Altitude (m)
Adana	37.03	35.21	27
Adıyaman	37.45	38.17	672
Amasya	40.39	35.51	411.69
Aydın	37.51	27.51	56.3
Balıkesir	39.39	27.52	153
Bingöl	38.52	40.30	1177
Burdur	37.43	30.18	957
Erzincan	39.45	39.30	1218.22
Karaman	37.12	33.13	1023.05
Kars	40.37	43.06	1775
Kırıkkale	39.51	33.31	750.889
Kütahya	39.25	29.58	969.28
Mardin	37.18	40.44	1050
Nevşehir	38.37	34.42	1259.54
Sakarya	40.46	30.24	30.43
Tekirdağ	40.59	27.30	3.6
Trabzon	40.59	39.45	30

The Marmara region of Turkey comes under the influence of the mild Mediterranean climate during the summer months. During the winter time, this region is under the influence of high pressure of Siberia and the Balkan Peninsula and, consequently, northeasterly or westerly winds influence the area with high rainfall amounts in addition to snow every year with cold and wet spells (Öztopal, 2006).

In the Aegean region of Turkey geomorphologic features have long valleys that run perpendicular to the coast. These are parallel to the cyclonic movements that originate from the Genoa bay and move towards the east and therefore show strong wind effects at the Aegean coast as well as the moving air which penetrates deep in these valleys (Durak and Şen, 2002). The Aegean and Mediterranean coasts have cool, rainy winters and hot, moderately dry summers.

In Eastern Anatolia and South-Eastern Anatolia there is a long winter, and snow remains on the ground from November until the end of April. The climate in the Black Sea area is wet, and humid. The Black Sea coast receives the greatest amount of rainfall. The eastern part of that receives 2,200 millimeters annually and is the only region of Turkey that receives rainfall throughout the year (TSMS, 2007).

4.8.2. Artificial Neural Network Architecture

In order to get the results in the best overall performance, several network architectures were investigated. At the end of this analysis, the network architecture used in this study was generated eventually. As seen in Figure 4.95, this network architecture has one hidden layer with 32 neurons. Four neurons which receive input signals of latitude, longitude, altitude and month were used in the input layer of the network. Two neurons which produce corresponding output signals of the long term monthly temperature and rainfall were utilized in the output layer of the network. In order to train the neural network, meteorological and geographical data taken from 76 measuring stations were used as a training (59 stations) and testing (17 stations) data. A total of 912 data sets (76 stations x 12 months) were divided into two parts. From this set 708 data sets (59 stations x 12 months) were used for training procedure of the network, while the remaining 204 data sets (17 stations x 12 months) were selected to be used as the testing procedure of the network. The stations used for training and testing procedure are presented in Figure 4.93. The stations used for the testing procedure are Adana, Adıyaman, Amasya, Aydın, Balıkesir, Bingöl, Burdur, Erzincan, Karaman, Kars, Kırıkkale, Kütahya, Mardin, Nevşehir, Sakarya, Tekirdağ and Trabzon. Training data is used to design the model, while the testing data is used to predict the performance of the network. Levenberg-Marquardt (LM-32) learning algorithm was applied in the present simulation. Logistic sigmoid transfer function (logsig) and linear transfer function (purelin) were used in the hidden layers and output layer of the network as an activation function, respectively. Simulations were performed to predict the long term monthly temperature and rainfall at any specific point of region of Turkey.

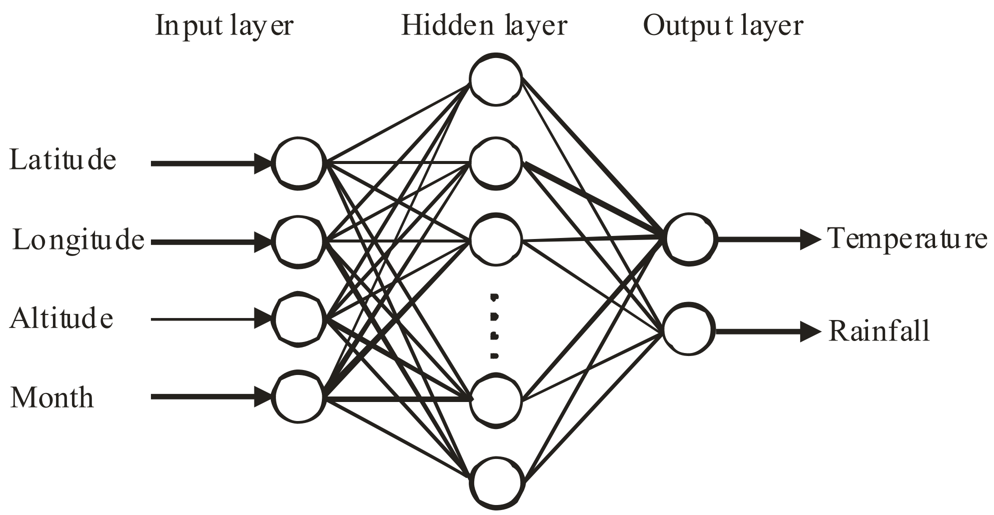

Figure 4.95. ANN architecture

As seen in Figure 4.95, every neuron in each layer of the network is connected to a neuron of adjacent layer having different weights and, each neuron receives signals from the neurons of the previous layer weighted by the interconnect values between neurons except input layer. Neurons then produce an output signal by passing the summed signal through an activation function. In order to perform functional input/output mappings, the weights of the connections between neurons are adjusted during the training procedure. This procedure goes on until the difference between the actual output of the network and the desired output is equal with a specified remainder value. Here, the criterion is put forward as the network output which should be closer to the value of desired output.

4.8.3. Results and Discussion

It is believed that global warming has attracted considerable attentions of scientists in recent years. Global warming related with an average increase in the temperature Earth's surface and lower atmosphere which in turn causes changes in climate. A warmer Earth may lead to changes in rainfall patterns, a rise in sea level, and a wide range of impacts on plants, wildlife, and humans. Due to this reason, the importance of temperature and rainfall predictions has been increased all over the World.

In the present study, it is realized that artificial neural network is convenient method to apply for the prediction of the long term monthly temperature and rainfall at any specific location in Turkey based on geographical variables. The mean absolute error (MAE) and correlation coefficient (R) were used to see the convergence between the target value and the output value. MAE parameter is defined as follows (Valverde Ramirez et al., 2005),

$$MAE = \frac{1}{n}\sum_{i=1}^{n} abs\left|o_i - t_i\right| \tag{4.8.1}$$

Where, t is the target value, o is the output value, n is the total number of months, $\bar{t}$ is the mean of the t_i's, $\bar{o}$ is the mean of o_i's and $\overline{t.o}$ is the mean of the $t_i.o_i$'s.

ANNs have a two-step procedure; these are called training and testing procedure. Firstly, training procedure is applied to design the model. Then, testing procedure is applied to evaluate the performance of the network. The performance values such as MAE and R for learning and testing procedure are given in Table 4.34 and 35, respectively. In the result of testing procedure, it can be seen in Table 4.35

that, the MAE values ranged from 0.5076 ^{0}C to 1.6397 ^{0}C differ from the actual value for the long term monthly temperature, while the MAE values ranged from 0.3604 day to 1.8365 day differ from the actual value for the long term monthly rainfall. For the long term monthly temperature and rainfall, the maximum MAE values were found to be 1.6397 ^{0}C and 1.8365day in Mardin and Erzincan meteorological station. On the other hand, the best results were found to be 0.5076 ^{0}C and 0.3604 day in Sakarya and Burdur meteorological station, respectively. It is seen from the table that in general, the performance values of long term monthly temperature prediction are better than the performance values of the long term monthly rainfall prediction. The maximum correlation coefficients (R) between the experimentally measured and predicted value for the long term monthly temperature and rainfall were found to be 0.9994 and 0.9912 in Bingöl and Burdur meteorological station, respectively. On the other hand, the minimum correlation coefficients (R) were found as 0.9946 and 0.8858 in Kars meteorological station, respectively. Another significant point in this study, as seen in Tables 4.34 and 34, the performance values of the learning procedure are in general better than the performance values of the testing procedure.

The scatter diagrams of the network predictions against the actual values were drawn for all target stations in order to indicate the performance of the ANN method. It can be seen from Figures 4.96-112 that the results of prediction have fairly close agreement with the corresponding measurements for all stations. Errors obtained in these models are well within acceptable limits. It can be concluded that the ANN technique can successfully predict the long term monthly temperature and rainfall of any site at a location with no measurement, which is referred as the target station, based on the use of the neighboring stations data and its geographical variables.

Table 4.34. The performance values for training procedure

Station	For temperature		For rainfall	
	MAE (^{0}C)	R	MAE (day)	R
Ağrı	0.85790	0.99690	0.64907	0.98273
Aksaray	0.40617	0.99891	0.83280	0.98640
Ankara	0.58454	0.99837	0.76595	0.96715
Antalya	0.75179	0.99551	0.49600	0.99276
Ardahan	0.92025	0.99475	0.87313	0.90126
Artvin	0.77869	0.99224	0.57587	0.95625
Bartın	1.05949	0.98969	0.51656	0.98370
Batman	0.53644	0.99880	0.78094	0.98401
Bilecik	0.57789	0.99930	0.61752	0.98278
Bitlis	0.85891	0.99779	0.89887	0.98357
Bolu	0.67670	0.99899	1.54574	0.98155
Bursa	0.31017	0.99842	0.59125	0.98677
Çanakkale	0.68515	0.99688	0.56586	0.98528
Çankırı	0.73451	0.99854	1.18155	0.92651
Çorum	0.42735	0.99892	0.40605	0.98977
Denizli	0.50870	0.99806	0.52325	0.98422
Diyarbakır	1.23908	0.99795	0.64848	0.98580
Düzce	0.86245	0.99631	0.65983	0.98441
Edirne	0.81007	0.99664	0.95582	0.91148
Elazığ	0.44483	0.99871	0.57255	0.99028
Erzurum	0.72498	0.99877	0.83875	0.95904
Eskişehir	0.95022	0.99875	0.51649	0.97009
Gaziantep	0.50518	0.99808	0.46765	0.99261
Gümüşhane	0.97595	0.99852	0.76658	0.96564
Hakkari	0.43623	0.99880	0.82750	0.97249
Hatay	0.68740	0.99396	1.41150	0.98864
Iğdır	0.66878	0.99601	0.95684	0.92964

Table 4.34. (Continued) The performance values for training procedure

Station	For temperature		For rainfall	
	MAE (^{0}C)	R	MAE (day)	R
Isparta	0.36016	0.99813	0.53755	0.98395
İstanbul	0.31205	0.99840	1.15956	0.98061
İzmir	0.45561	0.99874	0.60573	0.98892
Kahramanmaraş	0.55016	0.99818	0.71788	0.99233
Kastamonu	0.50417	0.99855	0.88118	0.94513
Kayseri	0.49149	0.99803	0.92686	0.97482
Kırklareli	0.27025	0.99922	0.78181	0.95931
Kırşehir	0.35383	0.99865	0.48280	0.99071
Kilis	0.59367	0.99882	0.41584	0.99362
Kocaeli	0.57655	0.99863	0.59130	0.98478
Konya	0.65937	0.99887	1.05350	0.96254
Malatya	0.66893	0.99909	0.73059	0.98033
Manisa	0.56290	0.99849	0.42555	0.98908
Mersin	0.37141	0.99746	0.74675	0.97680
Muğla	0.55237	0.99721	0.82290	0.98594
Muş	1.21710	0.99835	0.59702	0.98958
Niğde	0.43550	0.99791	0.76883	0.96816
Ordu	0.66695	0.99587	0.55931	0.94105
Osmaniye	0.46524	0.99722	1.02079	0.96735
Rize	0.47730	0.99549	0.60141	0.59572
Samsun	0.43578	0.99786	0.76149	0.96040
Siirt	0.67301	0.99820	0.77996	0.98873
Sinop	0.84511	0.99263	0.79329	0.96316
Sivas	0.41058	0.99929	0.57656	0.98624
Şanlıurfa	0.85246	0.99933	0.55994	0.98849
Tokat	0.70871	0.99613	0.82171	0.96861
Tunceli	0.63544	0.99911	0.79245	0.98274

Table 4.34. (Continued) The performance values for training procedure

Station	For temperature		For rainfall	
	MAE (^{0}C)	R	MAE (day)	R
Uşak	0.60614	0.99843	0.60153	0.98570
Van	1.32466	0.99861	0.77740	0.98617
Yalova	0.35975	0.99846	0.60195	0.98762
Yozgat	0.51111	0.99884	0.64503	0.98767
Zonguldak	0.60545	0.99633	0.65170	0.97689

Table 4.35. The performance values for testing procedure

Station	For temperature		For rainfall	
	MAE (^{0}C)	R	MAE (day)	R
Adana	0.56150	0.99646	0.51150	0.98488
Adıyaman	1.16931	0.99876	0.51560	0.99101
Amasya	0.97591	0.99860	0.82164	0.98076
Aydın	0.56030	0.99649	0.63586	0.97934
Balıkesir	0.67376	0.99802	1.42774	0.98738
Bingöl	0.89545	0.99938	0.71023	0.98403
Burdur	0.57537	0.99882	0.36037	0.99117
Erzincan	0.79563	0.99828	1.83648	0.93239
Karaman	0.61426	0.99742	1.66395	0.96600
Kars	1.18908	0.99463	1.17491	0.88579
Kırıkkale	0.85787	0.99833	0.64226	0.98553
Kütahya	0.60989	0.99810	1.37921	0.97877
Mardin	1.63967	0.99812	1.45350	0.98530
Nevşehir	0.83241	0.99806	0.68138	0.98253
Sakarya	0.50762	0.99620	0.61540	0.98777
Tekirdağ	0.55056	0.99887	1.01069	0.95329
Trabzon	0.66850	0.99586	1.44191	0.93851

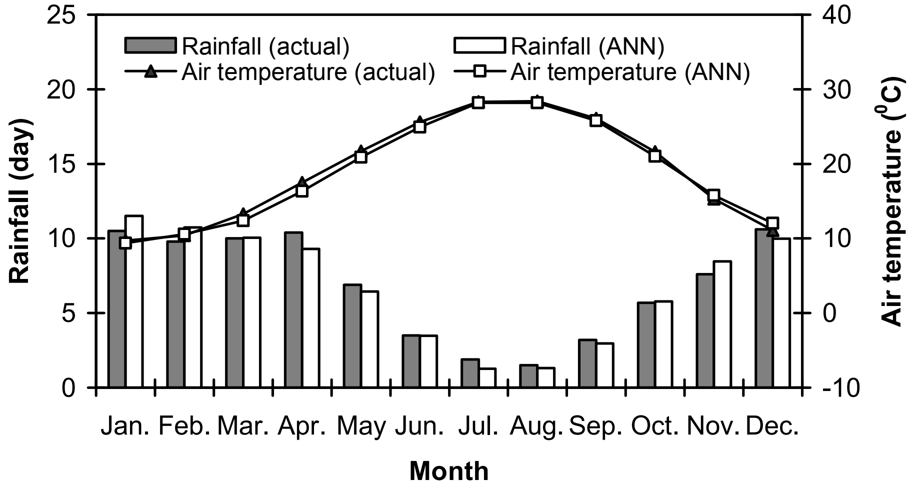

Figure 4.96. Comparison between prediction of ANN and actual results for Adana meteorological station

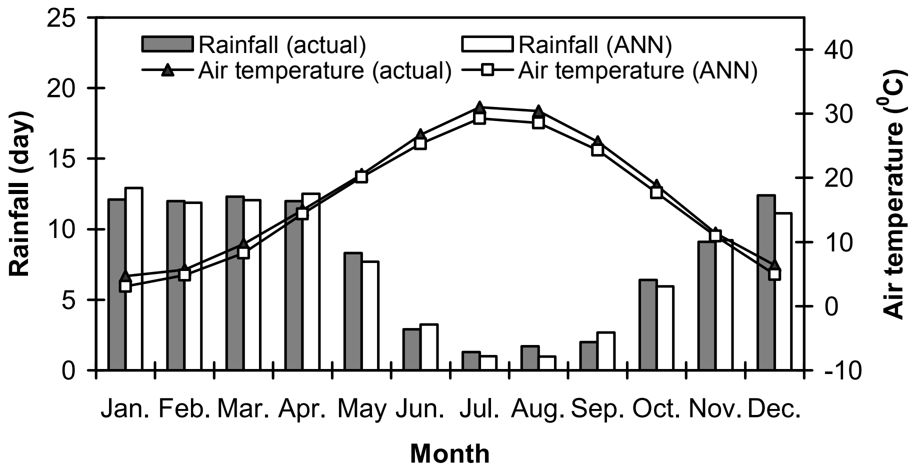

Figure 4.97. Comparison between prediction of ANN and actual results for Adıyaman meteorological station

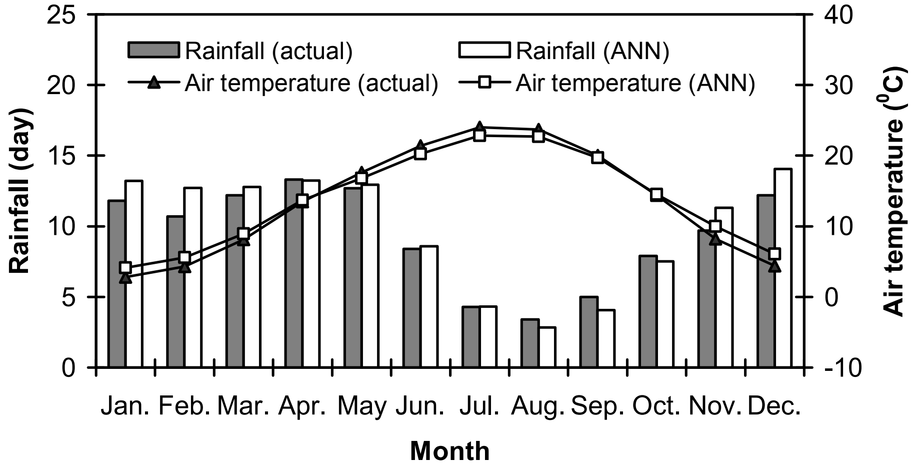

Figure 4.98. Comparison between prediction of ANN and actual results for Amasya meteorological station

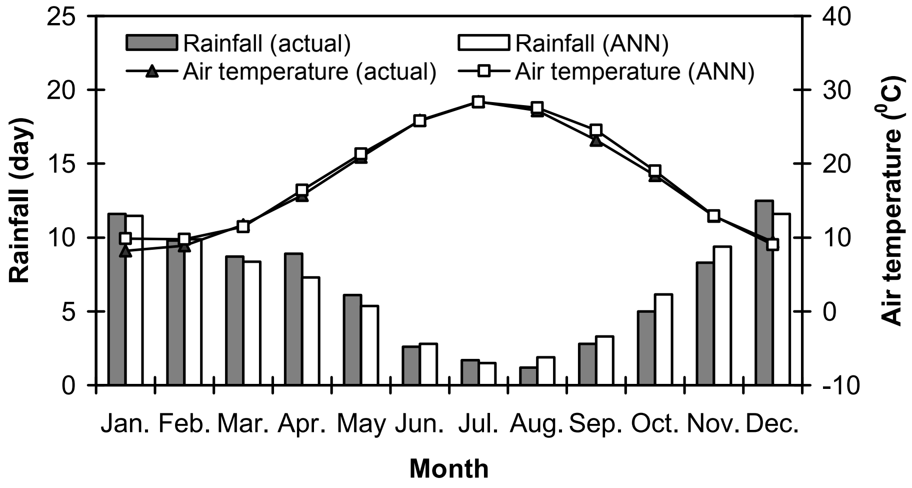

Figure 4.99. Comparison between prediction of ANN and actual results for Aydın meteorological station

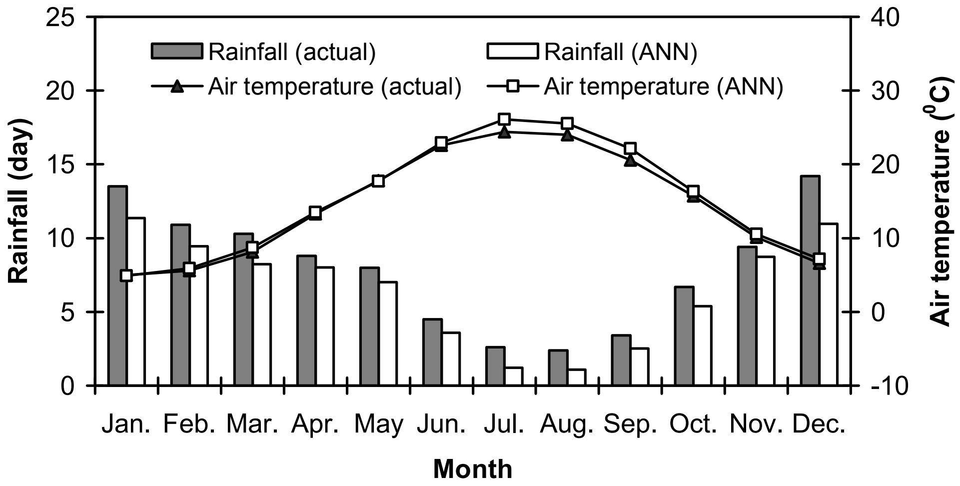

Figure 4.100. Comparison between prediction of ANN and actual results for Balıkesir meteorological station

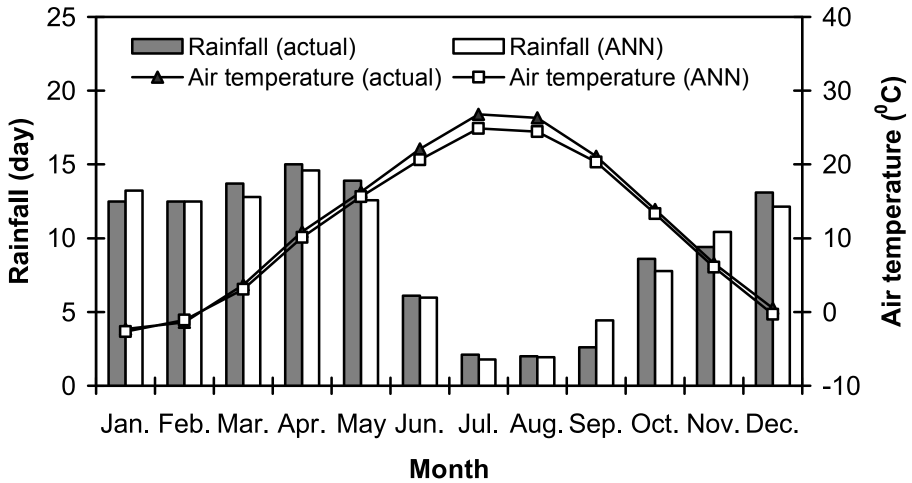

Figure 4.101. Comparison between prediction of ANN and actual results for Bingöl meteorological station

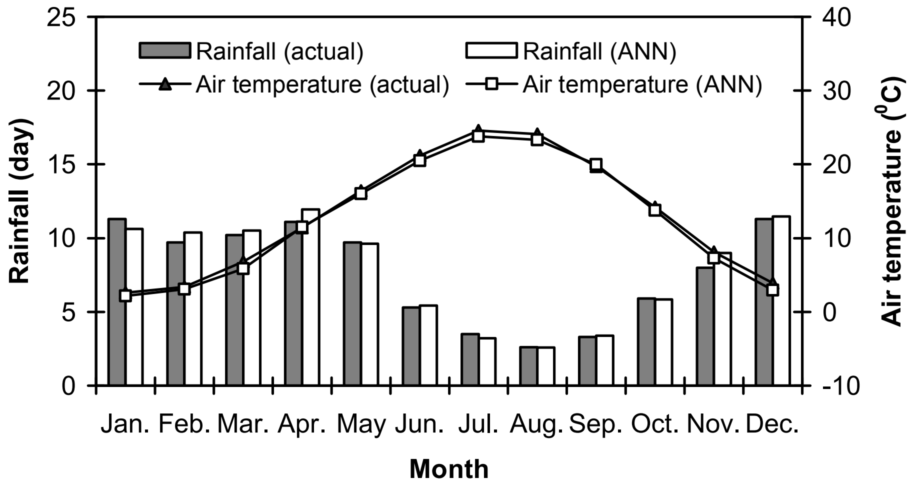

Figure 4.102. Comparison between prediction of ANN and actual results for Burdur meteorological station

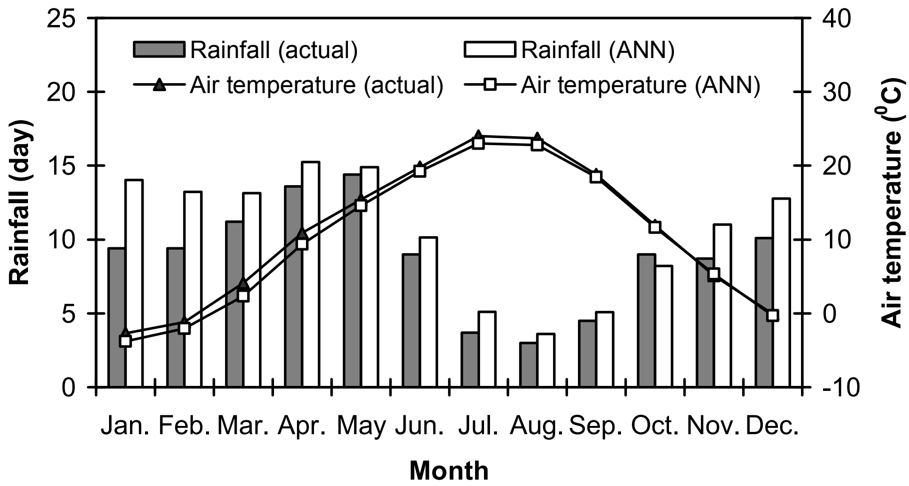

Figure 4.103. Comparison between prediction of ANN and actual results for Erzincan meteorological station

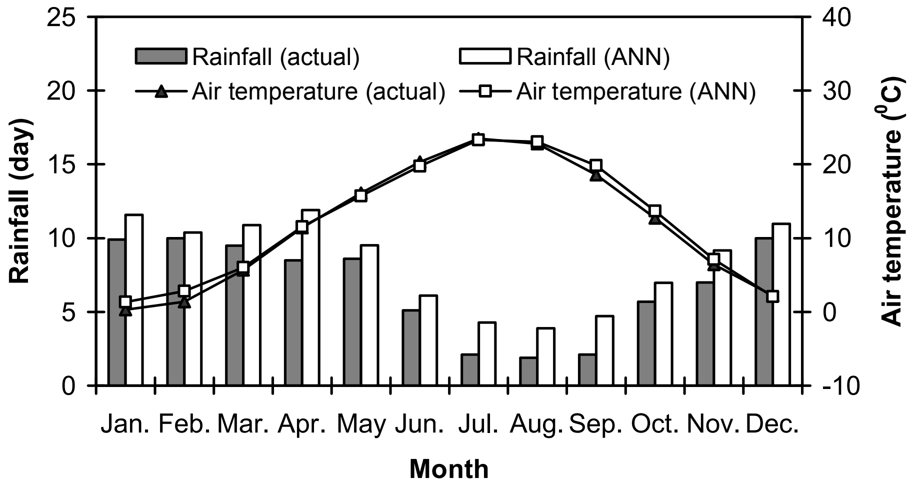

Figure 4.104. Comparison between prediction of ANN and actual results for Karaman meteorological station

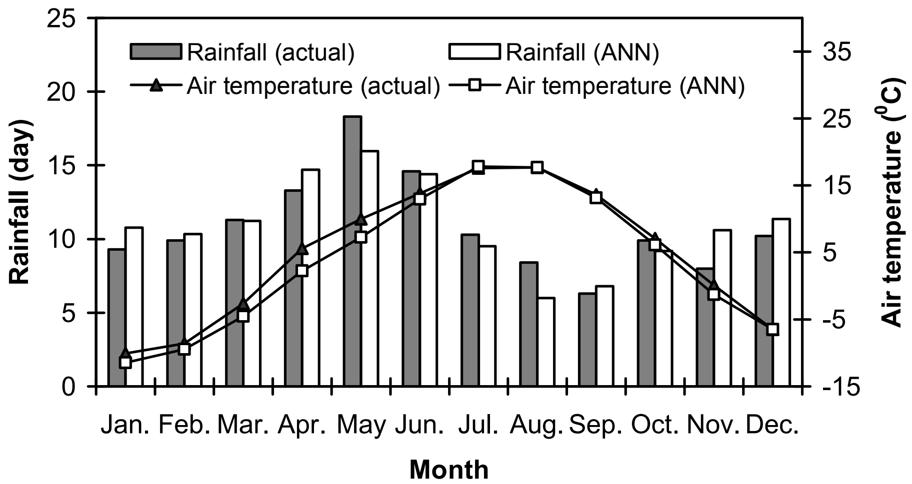

Figure 4.105. Comparison between prediction of ANN and actual results for Kars meteorological station

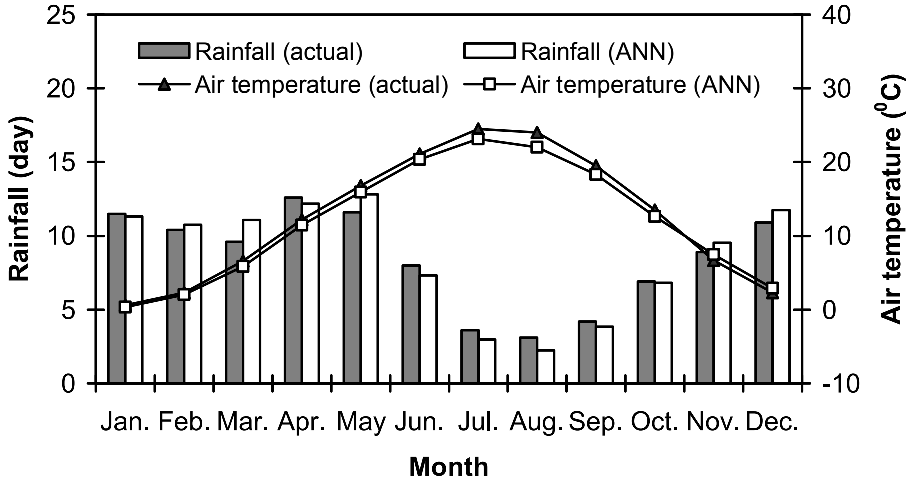

Figure 4.106. Comparison between prediction of ANN and actual results for Kırıkkale meteorological station

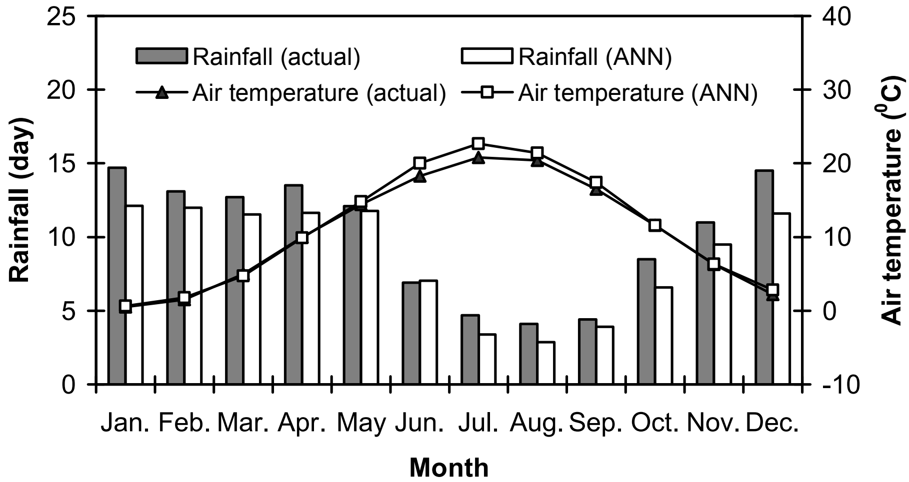

Figure 4.107. Comparison between prediction of ANN and actual results for Kütahya meteorological station

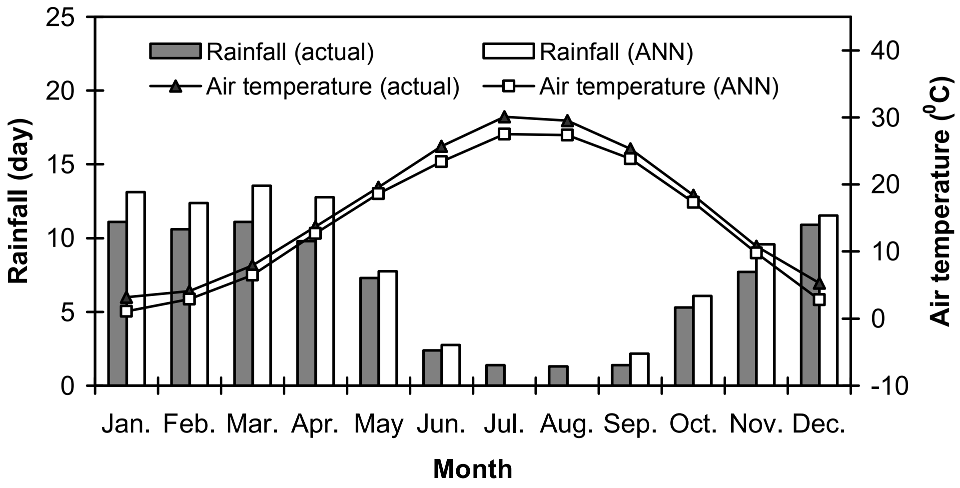

Figure 4.108. Comparison between prediction of ANN and actual results for Mardin meteorological station

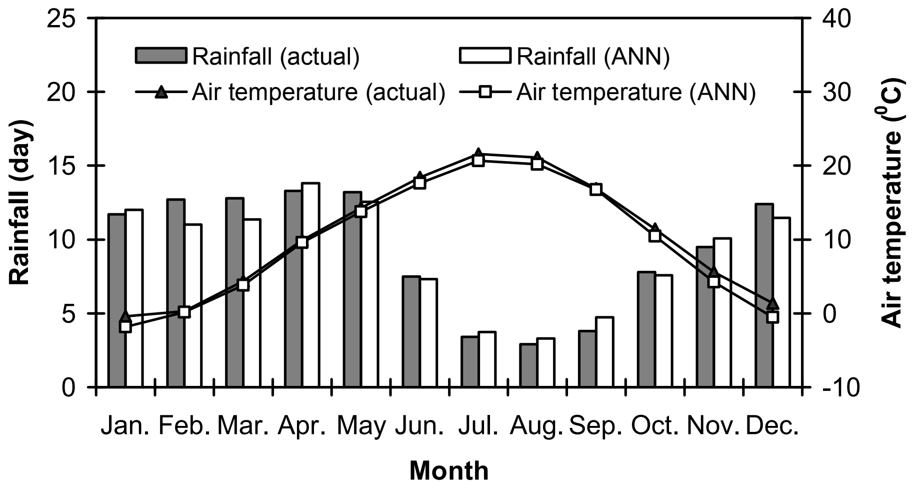

Figure 4.109. Comparison between prediction of ANN and actual results for Nevşehir meteorological station

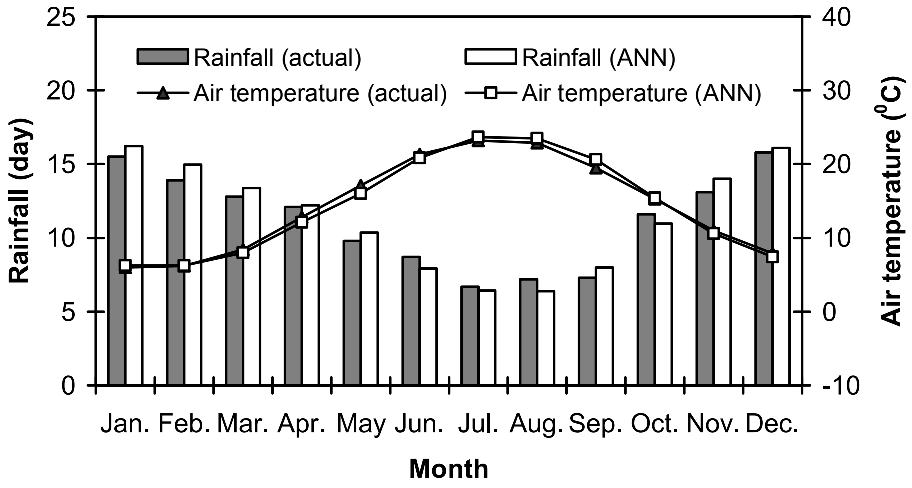

Figure 4.110. Comparison between prediction of ANN and actual results for Sakarya meteorological station

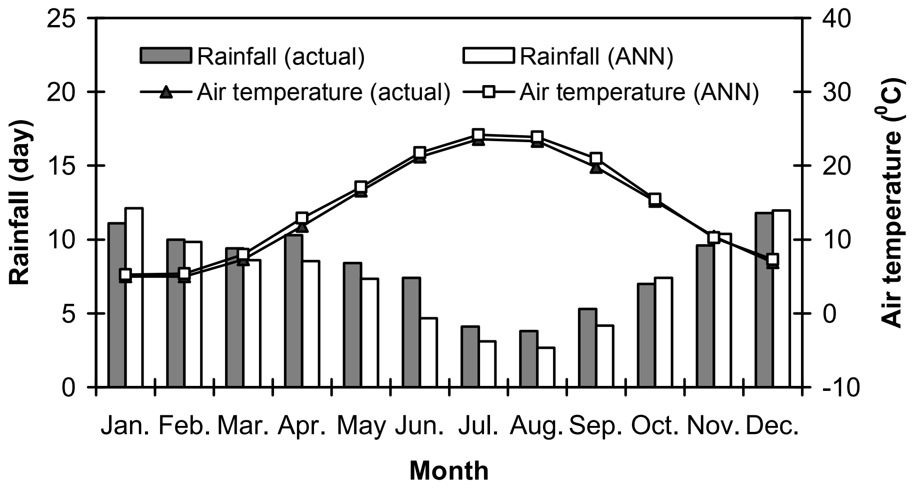

Figure 4.111. Comparison between prediction of ANN and actual results for Tekirdağ meteorological station

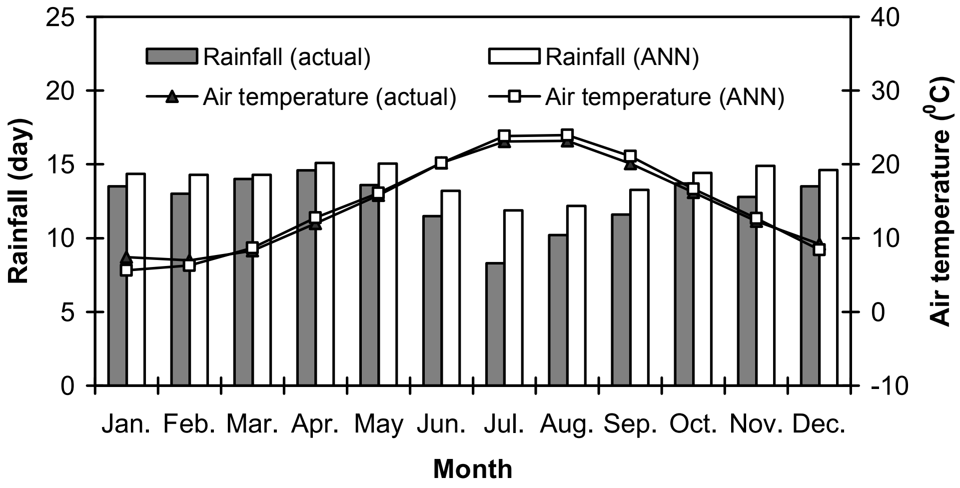

Figure 4.112. Comparison between prediction of ANN and actual results for Trabzon meteorological station

5. CONCLUSIONS AND RECOMMENDATIONS

1) The objective of the present study is to quantify the wind energy potential of the Marmara, Aegean and Mediterranean regions of Turkey and specify the locations where considerable potentials are available. It can be concluded that, present regions are suitable for the plantation of wind energy turbines. It is known that there is no wind turbine placed in these regions yet for the electricity production. These regions are most industrialized and highly populated regions and there is a high rate of demands for electricity. The present results suggest that it can be profitable to establish a wind farm in the present regions. In these regions, there is very large land available for constructing wind energy farms. However, their suitability and availability for these applications are acceptable in terms of other aspects such as being in close proximity to the electrical grid lines, land ownership, road network infrastructure, etc. From the examinations of nine different sites, it can be concluded that in all these regions electricity generation using wind power can be economical. But Gökçeada Gelibolu and Belen stations are most promising and convenient for the production of the electricity from the wind power. It can be concluded that, present regions are suitable for the plantation of wind energy turbines. Several locations can quite reasonably be considered favorable for the production of wind energy. It is known that there is no wind turbine placed in the region of Belen-Hatay yet for the electricity production. The present results suggest that it can be profitable to establish a wind farm in the present regions. At 10 m height above the ground level, mean wind speed and power potential of the site are 7.0 m/s and 378 W/m^2, respectively. The hourly wind speeds are higher than 5 m/s in about 70% of occasions. The monthly mean wind speeds are higher than 5 m/s during 9 months of the year; on the other hand the monthly mean wind power potentials are higher than 200 W/m^2 during 8 months of the year. In this provision, there is very large land available for constructing wind energy farms. However, their suitability and availability for these applications are acceptable in terms of other aspects such as being in close proximity to the electrical grid lines, land ownership, road network infrastructure, etc.

2) Application of ANN increases rapidly in particular in the engineering problems. In the present work, wind power potential for 4 different districts was predicted and obtained results were compared with the prediction of WAsP program. It was concluded the learning algorithm provided best predictions for all regions. The results obtained by WAsP agree well with the prediction of ANN for the period of 24 months covered the year from 2000 to 2001. Predicted results indicate that ANN method appears to be convenient method for the prediction of wind energy potential. It can be concluded that ANN method can be applied to predict wind speed of other years providing that related data of previous years must be given as an input value for learning and testing processes. Furthermore, by giving meteorological data such as pressure, density, temperature and humidity it is possible to predict the wind speed and finally wind potential of the examined districts.

3) In order to improve the accuracy of the simulations of ANN method one must select wind speed measuring stations having similarity correlation factors of 0.59. According to this statement, there is no good relation amongst the relative stations for Dörtyol meteorological station, because of the fact that the biggest correlation coefficient is 0.25 between Dörtyol and Mersin meteorological station. On the other hand, selecting Antakya meteorological station as a target station, it seems that İskenderun and Mersin meteorological stations should be chosen as a reference stations due to the high rate of correlation coefficient between the target and reference stations. That is to say, the value of the mean monthly wind speed of İskenderun and Mersin meteorological stations can be utilized to estimate the mean monthly wind speed of Antakya meteorological station. Similarly, selecting Samandağ meteorological station as a target station, it seems that Karataş, İskenderun and Yumurtalık stations should be chosen as a reference stations due to the high rate of correlation coefficient between the target and reference stations. In addition, İskenderun, Yumurtalık, Adana and Samandağ stations were chosen as a reference stations to predict the mean monthly wind speed of Karataş meteorlogical station as a target station. Yumurtalık, Mersin, Atakya, Samandağ and Karataş stations can be used to estimate wind speed of İskenderun meteorological station, on the other hand, İskenderun and Antakya stations can be used to predict wind speed of Mersin meteorological station. It can be concluded that the ANN method seems a powerful tool in predicting the missing wind speed of target station depending on the correlation between target and reference stations. The advantage of this model is that as long as having the required wind speed data of the reference stations, the future wind speed of target station can also be predicted straightaway and satisfactorily without the use of any topographical details or other meteorological data.

4) The aim of the present work is to try to predict wind speed using monthly meteorological variables, and establish a model between these variables. For this purposes, methods of multiple linear regression analysis and artificial neural network were used. Results of these methods were compared to each other. In order to improve the accuracy of predictions a few independent parameters or initial parameters were used and related independent parameters were only included to the model. Between monthly wind speed and meteorological variables such as atmospheric temperature and pressure a good relations were obtained for Antakya and Mersin meteorological stations, and hence using ANN and MLR methods provide acceptable wind speeds for both stations. On the other hand, since there was no a satisfactory relations between wind speed and independent variables such as atmospheric temperature and pressure, these methods did not provide a predicted results with an acceptable error in it for Samandağ meteorological station. It was concluded that if there is good relations between wind speed and other meteorological variables such as atmospheric temperature and pressure, wind speed with these meteorological variables can be predicted with acceptable accuracy using ANN and MLR methods.

5) In this paper, artificial neural network has been applied to predict daily, weekly and monthly wind speed of target station using reference stations data. Topographical details or other meteorological data have not been used for this approach. This prediction model has been applied to 4 measuring stations located in the Aegean and Marmara region of Turkey. Wind data characteristics have been presented for all of measuring stations. A reasonable cross-correlation coefficient of the wind speed between the stations has been found. Different network learning algorithms such as RP, LM and SCG have been tried. The wind speed prediction results have been compared with experimentally measured values at a target station. Comparisons have shown that there is a good agreement between predicted and measured data. Errors obtained in these models are well within acceptable limits. The best result has been found to be 3.2376% for monthly wind speeds in Gelibolu station. In addition, it has been found that the performance values of monthly wind speed prediction are better than the performance values of weekly and daily wind speed prediction. The advantage of this model is that having the required wind speed data of the reference stations, the wind speed of target station can be predicted quickly and satisfactorily without the use of any topographical details or other meteorological data. It can be concluded that the ANN looks promising in predicting the wind speed of a pivot station depending on the selection of the reference measuring stations.

6) In this paper, artificial neural networks were applied to predict the long term monthly temperature and rainfall at any specific location in Turkey. Geographical variables (latitude, longitude and altitude) and time were used as an input data for this approach. This prediction model was applied to 76 measuring stations located in 7 regions of Turkey. Different network architectures were tried in order to get the best approach. The long term monthly temperature and monthly rainfall predicted results were compared with experimentally measured values at a target station. Comparisons have shown that there was a good agreement between predicted and measured data. Errors obtained in these models are well within acceptable limits. The maximum mean absolute errors (MAE) for the long term monthly temperature and rainfall were found to be 1.6397 ^{0}C and 1.8365 day for Mardin and Erzincan meteorological station in the testing process, respectively, while the best results were found to be 0.5076 ^{0}C and 0.3604day for Sakarya and Burdur meteorological station, respectively. It can be concluded that the ANN method seems a powerful tool in predicting the long term monthly temperature and rainfall of any specific point with no measurement depending on its geographical variables. The advantage of this model is that as long as having the required latitude, longitude and altitude of any target point, the long term monthly temperature and rainfall of this specific point can also be predicted straightaway and satisfactorily without the use of other meteorological data.

ACKNOWLEDGEMENT

The authors wish to thank the Turkish State Meteorological Service (TSMS) for the supply of long term monthly temperature and rainfall data, and the office of Scientific Research Projects of Cukurova University for funding this project under contract no. MMF2006D18.

REFERENCES

ABDUL-WAHAB, S. A., BAKHEİT, C. S., AL-ALAWI, S. M., 2005. Principle component and multiple regression analysis in modeling of ground-level ozone and factors affecting its concentrations. Environmental Modeling and Software, 20: 1263-1271.

AKPİNAR, E. K., AKPİNAR, S., 2004. Determination of the wind energy potential for Maden-Elazığ, Turkey. Energy Conversion and Management, 45: 2901-14.

AKPİNAR, E. K., AKPİNAR, S., 2004. Statistical analysis of wind energy potential on the basis of the Weibull and Rayleigh distributions for Agin-Elazığ, Turkey. Journal of Power and Energy, 218: 557-65.

AKPİNAR, E. K., AKPİNAR, S., 2006. An investigation of wind power potential required in installation of wind energy conversion systems. Journal of Power and Energy, 220: 1-13.

AKPİNAR, E. K., AKPİNAR, S., 2005. A statistical analysis of wind speed data used in installation of wind energy conversion systems. Energy Conversion and Management, 46: 515-32.

AL-SHEHRI, A., 1999. Artificial neural network for forecasting residential electrical energy. International Journal of Energy Research, 23: 649-661.

ANDERSON, D., and MCNEİL, G., 1992. Artificial Neural Networks Technology. Rome Laboratory, http://www.dacs.dtic.mil/techs/neural/neural1.html.

BALAT, M., 2006. Current geothermal energy potential in Turkey and use of geothermal energy. Energy Sources, 1: 55-65.

BARBOUNIS, T. G., and THEOCHARIS, J. B., 2006. Locally recurrent neural networks for long-term wind speed and power prediction. Neurocomputing, 69: 466-496.

BATOR, R., and SIENIUTYCZ, S., 2006. Application of artificial neural network for emission prediction of dust pollutants. International Journal of Energy Research, 30: 1023-1036.

BECHRAKİS, D. A., and SPARİS, P. D., 2004. Correlation of wind speed between neighboring measuring stations. IEEE Transactions on Energy Conversion, 19(2): 400-406.

BECHRAKİS, D. A., DEANE, J. P., and MCKEOGH, E. J., 2004. Wind resource assessment of an area using short term data correlated to a long term data set. Solar Energy, 76: 725-32.

BİLGİLİ M., ŞAHİN, B. and KAHRAMAN, A., 2004. Wind energy potential in Antakya and İskenderun regions, Turkey. Renewable Energy, 29: 1733-45.

BİLGİLİ, M., SAHİN, B., and YASAR, A., 2007. Application of artificial neural networks for the wind speed prediction of target station using reference stations data. Renewable Energy, 32: 2350-2360.

BULUT, H., BÜYÜKALACA, O., and YILMAZ, T., 2003. New outdoor heating design data for Turkey. Energy, 28: 1133-1150.

CELİK, A. N., 2003. A statistical analysis of wind power density based on the Weibull and Rayleigh models at the southern region of Turkey. Renewable Energy, 29: 593-604.

CELİK, A. N., 2004. On the distributional parameters used in assessment of the suitability of wind speed probability density functions. Energy Conversion and Management, 45: 1735-47.

CHAPRA, S. C., CANALE, R. P., 1985. Numerical methods for engineers. Singapore, McGraw-Hill, Inc, pp. 351-352.

CİCEK, A., and KOPARAL, A. S., 2006. Assessment of environmental effects of the coal used in the Seyitömer thermal power plant (Turkey) on white willow. Communications in Soil Science and Plant Analysis, 37: 1795-1804.

ÇAM, E., ARCAKLIOĞLU, E., ÇAVUŞOĞLU, A., and AKBIYIK, B., 2005. A classification mechanism for determining average wind speed and power in several regions of Turkey using artificial neural networks. Renewable Energy, 30: 227-239.

DEMİRBAŞ, A., 2002. Sustainable developments of hydropower energy in Turkey. Energy Sources, 24: 27-40.

DEMİRBAŞ, A., ŞAHİN-DEMİRBAŞ, A., and DEMİRBAŞ A. H., 2004. Turkey's natural gas, Hydropower, and geothermal energy policies. Energy Sources, 26: 237-248.

DEMİRBAŞ, A., and BAKIŞ, R., 2004. Electricity from thermal and Hydropower Sources in Turkey: Status and future direction. Energy Sources, 26: 453-461.

DEMUTH, H., and BEALE, M., 1992. Neural Network Toolbox, For Use with MATLAB. The MathWorks, Inc, Natick, MA.

DURAK, M., ŞEN, Z., 2002. Wind power potential in Turkey and Akhisar case study. Renewable Energy; 25: 463-72.

EIE, General Directorate of Electrical Power Resources Survey and Development Administration, 2007. Hydroelectric studies. http://www.eie.gov.tr.

EPDK, Energy Market Regulatory Authority, 2007. Electricity market. http://www.epdk.gov.tr.

EROL, O., 1999. Genel Klimatoloji. İstanbul, Inc, 116 pp.

ETEMOGLU, A. B., and CAN, M., 2007. Classification of geothermal resources in Turkey by exergy analysis. Renewable and Sustainable Energy Reviews, 11: 1596-1606.

EUAS, Electricity Generation Company, 2005. EUAS annual report 2005. http://www.euas.gov.tr/.

FLORES, P., TAPİA, A., and TAPİA, G., 2005. Application of a control algorithm for wind speed prediction and active power generation. Renewable Energy, 30: 523-536.

GENC, A., ERİSOĞLU, M., PEKGOR, A., OTURANC, G., HEPBASLİ, A., 2005. Estimation of wind power potential using Weibull distribution. Energy Sources, 27: 809-22.

GÖKÇEK, M., BAYÜLKEN, A., BEKDEMİR, Ş., 2007. Investigation of wind characteristics and wind energy potential in Kirklareli, Turkey. Renewable Energy, 32: 1739-52.

GUAN, L., YANG, J. and BELL, J. M., 2007. Cross-correlation between weather variables in Australia. Building and Environment, 42: 1054-1070.

HAMZAÇEBİ, C., 2007. Forecasting of Turkey's net electricity energy consumption on sectoral bases. Energy Policy, 35: 2009-2016.

HAYKİN, S., 1994. Neural networks, a comprehensive foundation. New Jersey: Prentice-Hall, Inc.

HEPBASLİ, A., and OZGENER, O., 2004. A review on the development of wind energy in Turkey. Renewable and Sustainable Energy Reviews, 8: 257-276.

IEA, International Energy Agency, 2001. Energy policies of IEA countries, Turkey 2001 review. http://www.iea.org/textbase/nppdf/free/2000/turkey2001.pdf.

IEA, International Energy Agency, 2005. Energy policies of IEA countries, Turkey 2005 review. http://www.iea.org/textbase/nppdf/free/2005/turkey2005.pdf.

INCECIK, S., ERDOĞMUŞ, F., 1995. An investigation of the wind power potential on the western coast of Anatolia. Renewable Energy, 6(7): 863-65.

KALOGİROU, S. A., 2001. Artificial neural networks in renewable energy systems applications: a review. Renewable and Sustainable Energy Reviews, 5: 373-401.

KALOGİROU, S. A., NEOCLEOUS, C., PASCHİARDİS, S., and SCHİZAS, C., 1999. Wind speed prediction using artificial neural networks. European Symp. on Intelligent Techniques ESIT'99, Crete (Greece).

KARSLİ, V. M., GEÇİT, C., 2003. An investigation on wind power potential of Nurdağı-Gaziantep, Turkey. Renewable Energy, 28: 823-30.

KAYA, D., 2006. Renewable energy policies in Turkey. Renewable and Sustainable Energy Reviews, 10: 152-163.

KENİSARİN, M., KARSLI, V. M., and ÇAĞLAR, M., 2006. Wind power engineering in the world and perspectives of its development in Turkey. Renewable and Sustainable Energy Reviews, 10: 341-369.

KINCAY, O., and OZTURK, R., 2003. Thermal power plants in Turkey. Energy Sources, 25: 135-151.

KRAUSS, G., KİNDANGEN, J. I., DEPECKER, P., 1997. Using artificial neural networks to predict interior velocity coefficients. Building and Environment, 32 (4): 295-303.

Lİ, S., WUNSCH, D. C., O'HAİR, E., GİESSELMANN, M. G., 2001. Comparative analysis of regression and artificial neural network models for wind turbine power curve estimation. Journal of Solar Energy Engineering, 123(4): 327-332.

MAQSOOD, I., and ABRAHAM, A., 2007. Weather analysis using ensemble of connectionist learning paradigms. Applied Soft Computing, 7, 995-1004.

MAQSOOD, I., KHAN, M. R., HUANG, G. H., and ABDALLA, R., 2005. Application of soft computing models to hourly weather analysis in southern Saskatchewan, Canada. Engineering Applications of Artificial Intelligence, 18: 115-125.

MATSUİ, M., İSHİHARA, T., and HİBİ, K., 2002. Directional characteristics of probability distribution of extreme wind speeds by typhoon simulation. Journal of Wind Engineering and Industrial Aerodynamics, 90: 1541-53.

MELESSE, A. M., and HANLEY, R. S., 2005. Artificial neural network application for multi-ecosystem carbon flux simulation. Ecological Modeling, 189: 305-314.

MOHANDES, M. A., HALAWANİ, T. O., REHMAN, S., and HUSSAİN, A. A., 2004. Support vector machines for wind speed prediction. Renewable Energy, 29: 939-947.

MOHANDES, M. A., REHMAN, S., and HALAWANI, T. O., 1998. A neural networks approach for wind speed prediction. Renewable Energy, 13(3): 345-54.

MORE, A., and DEO, M. C., 2003. Forecasting wind with neural networks. Marine Structures, 16: 35-49.

MORTENSEN, N. G., HEATHFİELD D. N., LANDBERG, L., RATHMANN, O., TROEN, I., and PETERSEN, E. L., 2001. Getting started with WAsP 7, Riso National Laboratory, Roskilde, Denmark.

OCAK, M., OCAK, Z., BİLGEN, S., KELEŞ, S., and KAYGUSUZ, K., 2004. Energy utilization, environmental pollution and renewable energy sources in Turkey. Energy Conversion and Management, 45: 845-864.

ÖZTOPAL, A., 2006. Artificial neural network approach to spatial estimation of wind velocity data. Energy Conversion and Management, 47: 395-406.

PASHARDES, S., and CHRİSTOFİDES C., 1995. Statistical analysis of wind speed and direction in Cyprus. Solar Energy, 55(5): 405-14.

PEREZ-LLERA, C., FERNANDEZ-BAIZAN, M. C., FEİTO, J. L., and GONZALEZ, V., 2002. Local short-term prediction of wind speed: a neural network analysis. Proceedings of the iEMSs, 2: 124-129.

RAJPAL, P. S., SHİSHODİA, K. S., and SEKHON, G. S., 2006. An artificial neural network for modeling reliability, availability and maintainability of a repairable system. Reliability Engineering and System Safety, 91: 809-819.

SAHİN, B., BİLGİLİ, M., and AKILLI H., 2005. The wind power potential of the eastern Mediterranean region of Turkey. Journal of Wind Engineering and Industrial Aerodynamics, 93: 171-83.

SAHİNLER, S., 2000. En küçük kareler yöntemi ile doğrusal regresyon modeli oluşturmanin temel prensipleri. MKÜ Ziraat Fakültesi Dergisi, 5(1-2): 57-73.

SEGORO, J. V., LAMBERT, T. W., 2000. Modern estimation of the parameters of the Weibull wind speed distribution for wind energy analysis. Journal of Wind Engineering and Industrial Aerodynamics, 85: 75-84.

SFETSOS, A., 2000. A comparison of various forecasting techniques applied to mean hourly wind speed time series. Renewable Energy, 21: 23-35.

SFETSOS, A., 2002. A novel approach for the forecasting of mean hourly wind speed time series. Renewable Energy, 27: 163-74.

SÖZEN, A., ARCAKLİOĞLU, E., ÖZALP, M., and KANİT, E. G., 2005. Solar-energy potential in Turkey. Applied Energy, 80: 367-81.

SÖZEN, A, ARCAKLIOĞLU, E., ÖZALP, M., and ÇAĞLAR, N., 2005. Forecasting based on neural network approach of solar potential in Turkey. Renewable Energy, 30: 1075-1090.

SÖZEN, A., and ARCAKLIOĞLU, E., 2007. Prospects for future projections of the basic energy sources in Turkey. Energy Sources, 2: 183-201.

SUNAR, M., 1999. Artificial neural networks for thermopiezoelectric systems. International Journal of Energy Research, 23: 1123-1131.

TEIAS, Turkish Electricity Transmission Company, 2005. Electricity statistics of Turkey. http://www.teias.gov.tr/istatistik2005/index.htm.

TORRES, J. L., GARCİA, A., PRİETO, E., and FRANCİSCO, A. D., 1999. Characterization of wind speed data according to wind direction. Solar Energy, 66(1): 57-64.

TSMS, 2007: Turkish State Meteorological Service. Climate of Turkey. http://www.meteor.gov.tr.

VALVERDE RAMİREZ, M. C., DE CAMPOS VELHO, H. F., and FERREİRA, N. J., 2005. Artificial neural network technique for rainfall forecasting applied to the Sao Paulo region. Journal of Hydrology, 301: 146-162.

YALCINTAS, M., and AKKURT, S., 2005. Artificial neural networks applications in building energy predictions and a case study for tropical climates. International Journal of Energy Research, 29: 891-901.

YALCINTAS, M., 2006. An energy benchmarking model based on artificial neural network method with a case example for tropical climates. International Journal of Energy Research, 30: 1158-1174.

YILMAZ, A. O., and USLU, T., 2007. Energy policies of Turkey during the period 1923-2003. Energy Policy, 35: 258-264.

YUKSEK, O., KOMURCU, M. I., YUKSEL, I., and KAYGUSUZ, K., 2006. The role of hydropower in meeting Turkey's electric energy demand. Energy Policy, 34: 3093-3103.

CIRRICULUM VITAE

Mehmet Bilgili was born in December 14, 1971 in Adana, Turkey. In 1988, he graduated from High School, and enrolled at Çukurova University to study mechanical engineering. In 1992, he graduated from the Department of Mechanical Engineering. He worked as a mechanical engineer at Adana Police Directorate between 1992 and 2004. He started his MSc studies in 2001 at the Department of Mechanical Engineering of Çukurova University. He obtained MSc degree from the same department on March 5, 2003. He started the studies leading to degree of PhD in 2004 at the Department of Mechanical Engineering of Çukurova University. He has been working as a Lecturer at Adana Vocational School of Çukurova University since 2004. He is married and has two children.